THE UNIVERSITY
of EDINBURGH

Regulation Studies on Human Pyruvate Kinases

by

Yiyuan Chen

Thesis Presented for the Degree of Doctor of Philosophy

School of Biological Sciences

University of Edinburgh

Edinburgh, UK

2017

Abstract

Human pyruvate kinase performs the last step in glucose glycolysis in all cells and organisms and can be a key regulator of glycolytic flux. Pyruvate produced by PYK is transported into the mitochondria to fuel the TCA cycle, which enables the production of ATP; the main energy source of the cell. Human PYK contains four isoforms: M1 (found in muscle, heart and brain), M2 (in foetal cells and tumours), L (liver), and R (red blood cells) PYK. M2PYK plays a crucial role in tumour cell proliferation; by down-regulating metabolic flux, upstream metabolites can be used for protein and DNA synthesis. Reprogramming the metabolism of fast proliferating cells is called the 'Warburg effect'. The biological relevance of the different isoform activities is also discussed. For example， RPYK in red blood cells is exposed to slowly altering metabolite concentrations, especially after intestinal absorption in plasma and RBCs uptake some of the metabolites.

This thesis describes biochemical and biophysical studies of human M1PYK, M2PYK, LPYK, and RPYK. PYK is allosterically regulated by a range of metabolites. A comparative enzyme kinetics study of the four isoforms was performed to examine the mechanisms of activation and inhibition of these small molecule regulators, including all 20 amino acids and the thyroid hormone T3. The redox state of the environment was also found to be an important regulator of PYK activity. All four PYK isoforms were successfully expressed and purified. Interestingly, only M2PYK and RPYK were strongly regulated by amino acids and metabolites. We also found that the redox state regulates the activity of all four PYK isoforms as well as the sensitivity of M2PYK in response to natural regulators. These studies also confirmed the dissociation of tetrameric PYK into inactive monomers as an important mechanism of regulation, particularly for M2PYK activity. Nuclear magnetic resonance (NMR) and Small-angle X-ray scattering (SAXS) studies were performed to investigate the conformational behaviour of PYK isoforms in solution and to compare the effects of ligand binding. NMR data of all four isoforms reveal a conserved binding mechanism between isoforms and specific amino acids. SAXS data of all four isoforms demonstrate that ligands affect tetramerisation of PYK isoforms.

Lay Summary

In each human cell, pyruvate kinase catalyses the last step of glycolytic pathway. Many diseases and cell functions correlate with the activity of pyruvate kinase. For example, in fast proliferating cells like cancer cells the regulation of pyruvate kinase may be involved in the metabolic flux from energy production to amino acids, lipid, nucleotides biosynthesis. Some natural effectors have been identified to regulate the enzyme allosterically including amino acids and other metabolites.

It is, therefore, important to further study the interaction between those metabolites and human pyruvate kinases. We screened four human pyruvate kinases with metabolites including amino acids using a combination of biochemical and biophysical assays and revealed that there is a universal binding between human pyruvate kinases and amino acids but only some of them act as up- or down- enzymatic regulators. We also revealed that the redox environment plays an important role in the regulation of enzyme activity

Declaration

I hereby declare the work presented in this thesis is the original work of the author. This thesis has been composed by the author and has not been submitted in whole or in part for any other degree.

Signature

Yiyuan Chen

Acknowledgments

First, I would like to thank my supervisor, Professor Malcolm D. Walkinshaw, for his support and encouragement throughout my studies. His kindness, patience, and understanding have played a large part in helping me to complete this degree.

In addition, I would like to thank all the members of the Structural Biochemistry Group, past and present, for their help and assistance throughout my period of study. I am especially grateful for the help, support, and encouragement of Dr. Hugh Morgan, whose joy and enthusiasm for his research was contagious and hugely motivational during the earlier years of my studies. I also very grateful for the help I received from Sandra Bruce, Dr. Martin Weir, Dr. Liz Blackburn, Dr. Iain McNae, Dr. Jacqueline Dornan, Dr. Paul Taylor, Dr. Linda Gilmore, and Dr. Matthew Nowicki.

I would also like to thank my colleges Dr. Meng Yuan, Dr. Willie Yen, Miss Jia Ning for their kindly help in the past several years.

Finally, I would like to extend my gratitude to my parents, without their support nothing would be possible for me at this stage.

List of abbreviations

ADP	adenosine diphosphate
1,3-BPG	1,3-Bisphosphoglyceric acid
2,3-BPG	2,3-Bisphosphoglyceric acid
3PGA	3-phosphoglycerate
6PGL	6-phosphogluconolactone
AcCoA	acetyl-CoA
ACL	ATP citrate lyase
ADP	Adenosine diphosphate
Akg	α-ketoglutarate
Ala	Alanine
AMP	Adenosine monophosphate
Arg	Arginine
Asn	Asparagine
Asp	Aspartic acid
ATP	Adenosine triphosphate
CH+-Thf	5-methylenetetrahydrofolate
CH2-Thf,	5,10-methylenetetrahydrofolate
Cit	citrate
CV	Column volume
Cys	Cysteine
DLS	Dynamic Light Scattering
DNA	Deoxyribonucleic acid
DTT	Dithiothreitol
F-1,6-BP	Fructose 1,6-bisphosphate
F-2,6-BP	fructose 2,6-bisphosphate
FFA	fatty acids
G6P	glucose 6-phosphate
GA3P	glyceraldehyde 3-phosphate
Glc	glucose
Gln	Glutamine
Glu	Glutamic acid
Gly	Glycine
GOT	glutamic-oxaloacetic transaminase
GSH	glutathione (reduced)
GSSG	Glutathione disulfide
Hgb	haemoglobin
His	Histidine

IC_{50}	The half maximal inhibitory concentration
IMAC	metal ion affinity chromatography
IPTG	Isopropyl-β-D-thiogalactopyranoside
Ile	Isoleucine
Lac	lactate
LB	Luria-Bertani broth
LDH	lactate dehydrogenase
Leu	Leucine
LmPYK	*Leishmania mexicana* pyruvate kinase
LMW-PTP	low molecule weight protein tyrosine phosphatase
LPYK	liver pyruvate kinase
Lys	Lysine
M1PYK	muscle pyruvate kinase M1
M2PYK	muscle pyruvate kinase M2
MDH 1	malate dehydrogenase
Met	Methionine
NADH	nicotinamide adenine dinucleotide
$NADP^+$	nicotinamide adenine dinucleotide phosphate
NADPH	nicotinamide adenine dinucleotide phosphate
NEAA	non-essential amino acids
NMR	Nuclear magnetic resonance
Oaa	oxaloacetate
P-Pyr	3-phosphohydroxypyruvate
PBS-CM	phosphate buffered saline without calcium or magnesium
PDB	protein data bank
PEP	phosphoenolpyruvate
PFK	phosphofructokinase
Phe	Phenylalanine
PPP	pentose phosphate pathway
Pro	Proline
PTMs	post-translational modifications
PYK	pyruvate kinase
Pyr	pyruvate
QELS	Quasi-elastic light scattering
R5P	ribose 5-phosphate
RBC	Red blood cell
RNA	Ribonucleic acid
ROS	reactive oxygen species
RPYK	erythrocyte pyruvate kinase
SAICAR	succinyl-5- aminoimidazole-4-carboxamide-1-ribose-59-phosphate

SAXS	Small-angle X-ray scattering
SDS-PAGE	sodium dodecyl sulfate – polyacrylamide gel electrophoresis
Ser	Serine
STD-NMR	Saturation-Transfer Difference Nuclear magnetic resonance
T3	triiodothyronine
T4	thyroxine
TCA	Tricarboxylic acid
Thr	Threonine
Trp	Tryptophan
TY	Tryptone Yeast
Tyr	Tyrosine
Val	Valine

Table of Contents

List of Figures

List of Table

CHAPTER 1. Introduction

1.1 Pyruvate kinase is an important enzyme in glycolysis pathway

1.1.1 The role of pyruvate kinase in cellular metabolism, flux control and gene regulation

Glycolysis converts one molecule of glucose into two molecules of pyruvate and releases two ATP (Adenosine triphosphate). Despite the level of free energy released, the intermediates are also directly useful in other metabolic pathways, including pentose phosphate pathway (the parallel pathway), TCA cycle (the following energy releasing reactions), amino acids synthesis, fatty acids synthesis, etc.

As shown in Figure 1-1, Pyruvate kinase catalyses the last step in the glycolytic pathway and converts phosphoenolpyruvate to pyruvate while phosphorylating adenosine diphosphate (ADP) to adenosine triphosphate (ATP) (Chaneton & Gottlieb, 2012; Mazurek, 2011). The reaction is important in the control of the lower part of the whole glycolysis pathway. Its substrate PEP (phosphoenolpyruvate) and the product pyruvate are both crucial in a variety of metabolic pathways. Pyruvate feeds into the TCA (the tricarboxylic acid) cycle in mitochondria (for most eukaryotes)，releasing more free energy in the form of NADH (Nicotinamide adenine dinucleotide). Cells then use another metabolic pathway, oxidative phosphorylation, to generate more ATP. In terms of amino acid synthesis, the α-ketoglutarate family of amino acid synthesis (glutamate, glutamine, proline and arginine) and the oxaloacetate/aspartate family (lysine, asparagine, methionine, threonine, and isoleucine) are derived from TCA cycle intermediates α-ketoglutarate and oxaloacetate. The aromatic amino acids (phenylalanine, tyrosine, and tryptophan) are synthesized from PEP and Erythrose 4-

phosphate, which are intermediates from the pentose phosphate pathway. Another pentose phosphate pathway middle metabolite, ribose 5-phosphate, leads to histidine synthesis, while the Pentose phosphate pathway leads to nucleotide biosynthesis. Serine is produced from 3-phosphoglycerate and then it is modified to generate cysteine and glycine. In human cells, nine amino acids (phenylalanine, valine, threonine, tryptophan, methionine, leucine, isoleucine, lysine, and histidine) cannot be synthesized as there are mutated enzymes in the pathway. The ten enzymes of the glycolysis pathway and other related branches are shown in Figure 1-1.

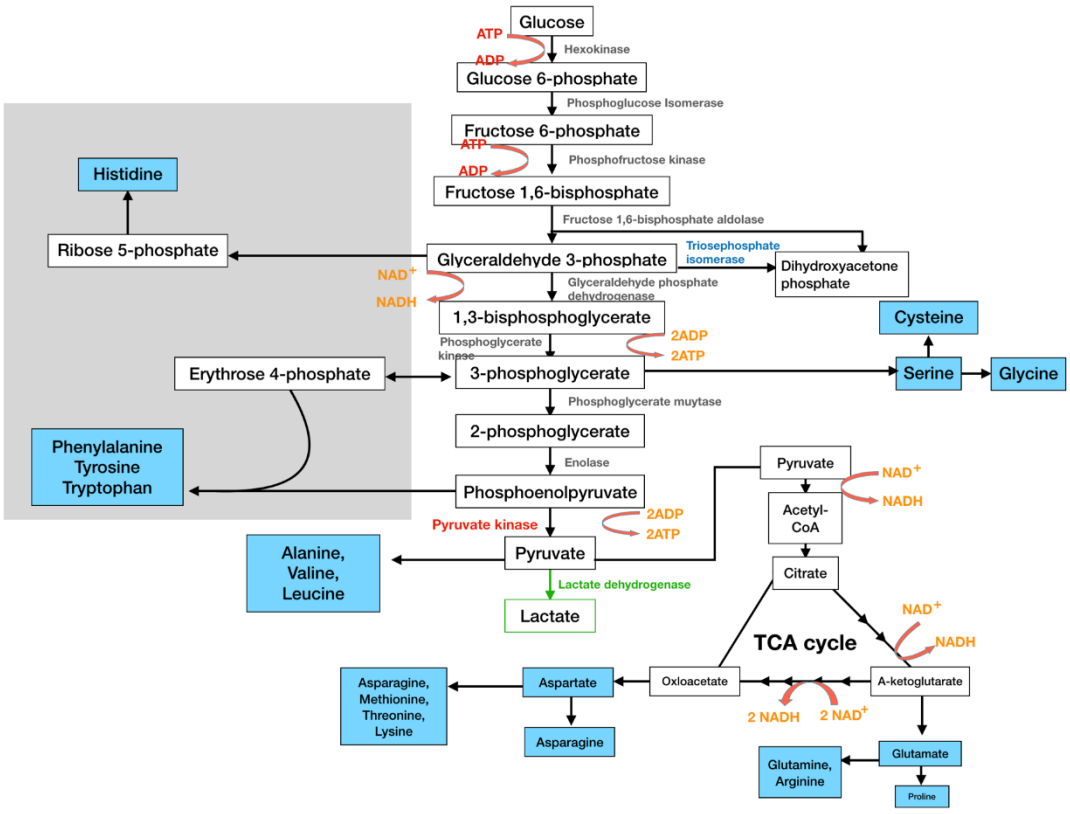

Figure 1-1. Glycolysis pathway from glucose to pyruvate consumes 2 ATP and produces 4 ATP for each glucose molecule. Pyruvate feeds into TCA cycle to release

more energy. The pentose phosphate pathway is shown in grey. All the amino acids are shown in blue.

1.1.2 Four PYK isoforms in human cells

Pyruvate kinases in mammalian tissues were first identified as two types in research from the mid 1960's (Tanaka, Harano, Morimura, & Mori, 1965). There were two major types of pyruvate kinases identified from rabbit tissues, L type and M type. Type M was isolated from muscle, heart, liver, brain, kidney, fat pads, and leucocytes while type L was only found in liver and erythrocytes. In 1987, cDNA clones of rat pyruvate kinases L type and R type were isolated (Noguchi, Yamada, Inoue, Matsuda, & Tanaka, 1987) and in this work it was found that L type PYK and R type PYK are produced from a single gene PKLR by splicing with tissue-specific promoters, resulting in exon 1 in RPYK and exon 2 in LPYK, as shown in Figure 1-2.

In 1986, it was reported that M1PYK and M2PYK are also made from the same gene by alternative RNA splicing (Noguchi, Inoue, & Tanaka, 1986). The alternative splicing of PYKM was regulated by heterogeneous nuclear ribonucleoproteins (hnRNPs) A1 and A2 and polypyrimidine-tract binding (PTB) protein. M1PYK and M2PYK generation depends on the inclusion of exon 9 or exon 10 respectively, as shown in (David, Chen, Assanah, Canoll, & Manley, 2010).

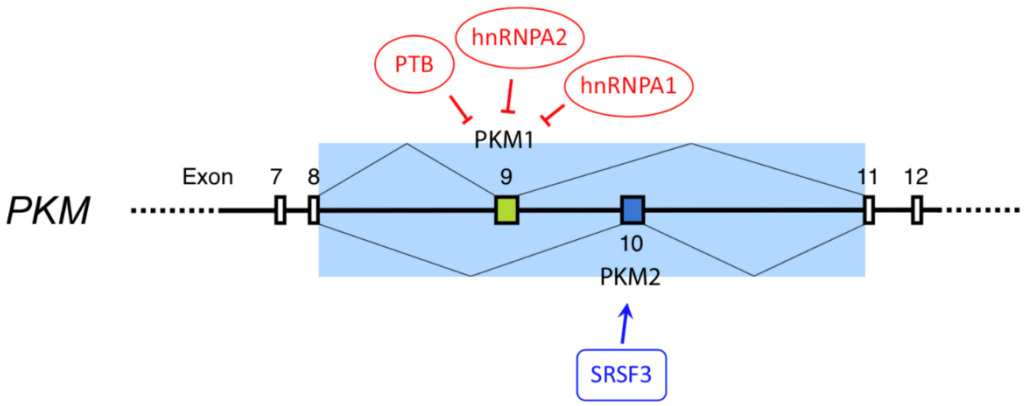

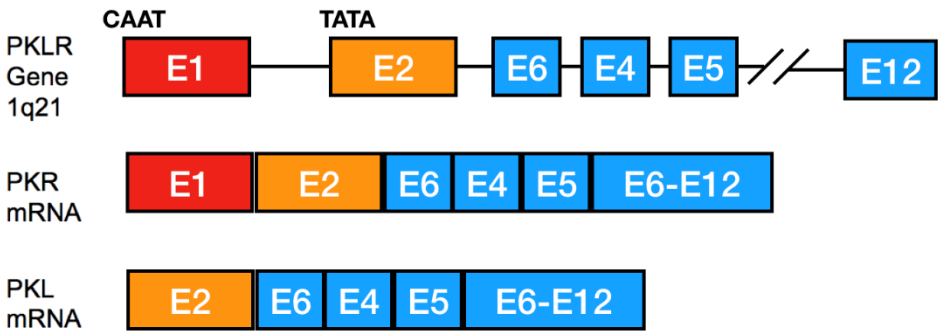

Figure 1-2. Upper figure: Alternative splicing of M1PYK and M2PYK by splicing factors PTB, hnRNPA2, hnRNPA1 and SRSF3. M1PYK contains exon 9 and M2PYK contains exon 10. The picture is from William J's article (Israelsen & Vander Heiden, 2015). Bottom figure: L type PYK and R type PYK are produced from a single gene PKLR by splicing with tissue-specific promoters.

The comparison of four human PYK sequences are shown in Table 1. The sequence identity between LPYK and RPYK is 94.3%, and sequence identity between M1PYK and M2PYK is 95.9%.

Gene	Isoform	Tissue expressed in	Sequence identity (%)			
			L	R	M1	M2
PKLR	L	liver	100	94.3	68	69.2
	R	red blood cell	94.3	100	64.3	70.8
PKM	M1	tissues with high catabolic demand	68	64.3	100	95.9
	M2	most adult tissues, especially proliferating cells	69.2	70.8	95.9	100

Table 1. Sequence identity of human pyruvate kinase isoforms. The pairwise sequence identities are calculated with EMBOSS Needle.

1.1.3 Protein structure of M1PYK and M2PYK

Human pyruvate kinase is a tetrameric enzyme with identical subunits. The architecture of human pyruvate kinase M2 is shown in Figure 1-3. M2PYK is a homotetramer with each of the four chains comprising an A-domain, B-domain, C-domain, and a small N-terminal domain. The A domain is the largest domain and forms

the main body of the monomer with the B domain and C domain at the sides. The active site is located at a cleft between A domain and B domain. The B domain is flexible, and it covers on the A domain when the substrate complex (ADP and Mg^{2+}) binds to the enzyme (Larsen, Laughlin, Holden, Rayment, & Reed, 1994). The C domain is on the other side and binds the natural allosteric activator FBP. When the protein is fully assembled as a tetramer, the C domain forms the C-C interface. The spliced exon that is alternatively expressed in M1PYK and M2PYK is located in the C domain as shown in bottom picture coloured magenta (Jurica et al., 1998). It shows that M2PYK specific exon 10 forms major part of the C-C interface and part of the F-1,6-BP binding pocket.

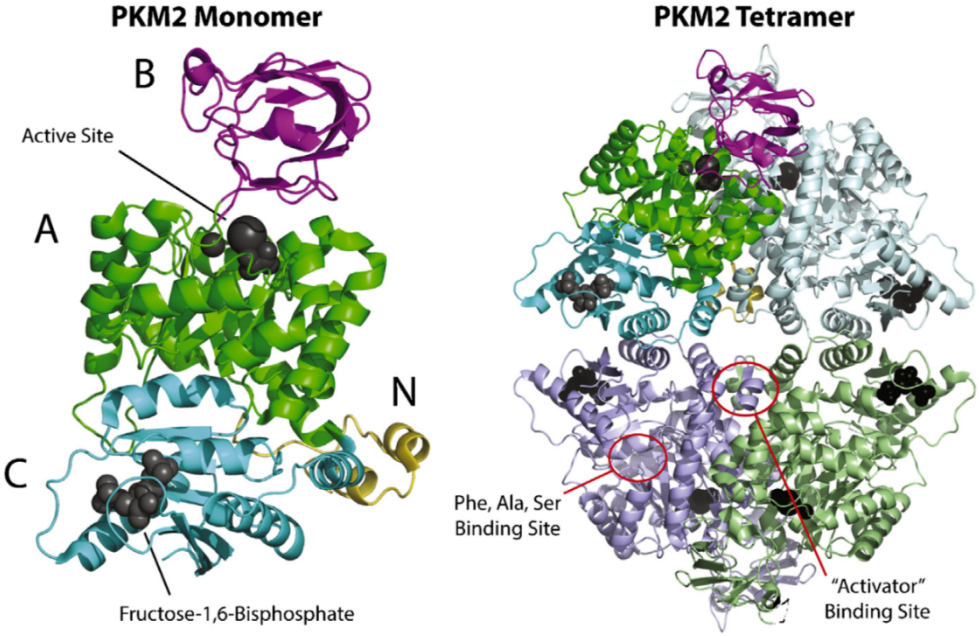

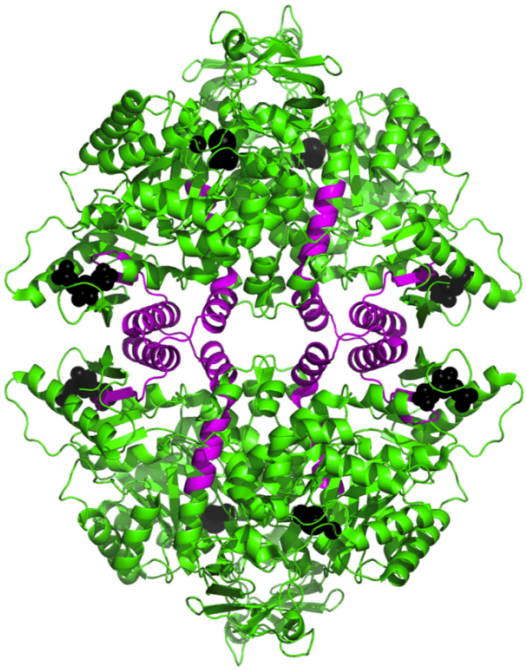

Figure 1-3. Upper left: the ribbon structure of monomer M2PYK is shown, with the A, B, and C domains are depicted in green, magenta, cyan, and N-terminal in yellow green, respectively. A group of molecules of K^{+}, Mg^{2+} and oxalate (a PEP analogue) binds to the active site, shown as black spheres. Similarly, FPB binds to the effector pocket. Upper right: tetrameric M2PYK (PDB 3BJF, (Christofk, Vander Heiden, Wu, Asara, & Cantley, 2008)). The activator side for F-1,6-BP and amino acids binding site are indicated. Bottom: the ribbon structure of tetramer M2PYK with exon 10 shown as magenta.

The sequence alignment of human pyruvate kinases is show in Figure 1-4. Sequence length of wild types of M1PYK, M2PYK, RPYK, LPYK are 531, 531, 574, and 543. The F-1,6-BP binding site related residues are indicated in red. Similarities of residue between isoforms are indicated by symbols. All isoforms have resolved structures available in PDB (RCSB Protein Data Bank), wild type for M1PYK, M2PYK, point mutant for LPYK, and truncated mutant for RPYK. The N-terminal tail of RPYK (indicated as strikethrough) was truncated in this structure (Giovanna Valentini et al., 2002). The protein sequence alignment was performed using Clustal Omega (https://www.ebi.ac.uk/Tools/msa/clustalo/).

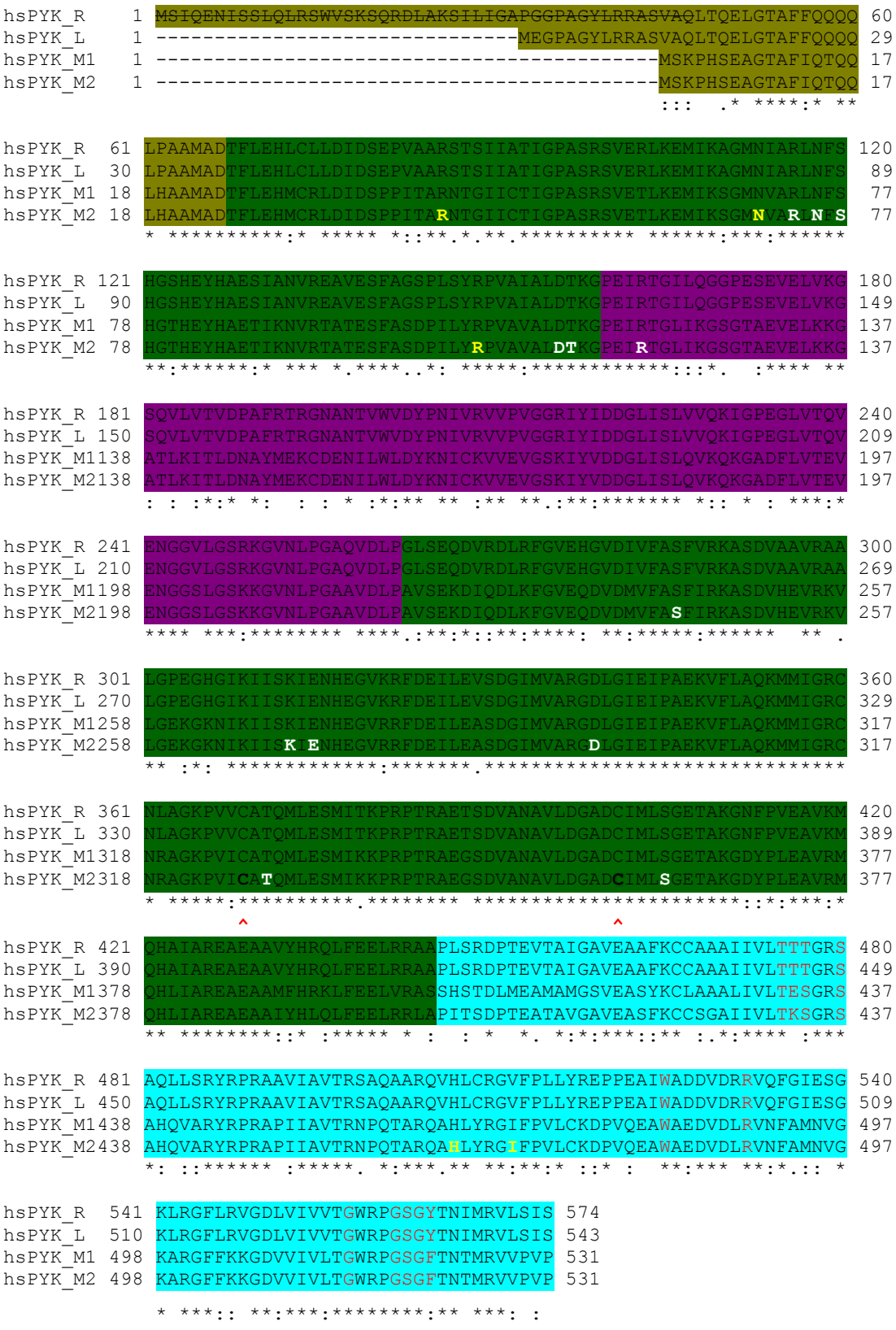

Figure 1-4. Sequence alignment of human pyruvate kinase isoforms ((PKM Uniprot No.: P14618; PKLR Uniprot No.: P30613).). Identical residues, strongly similar residues, and weakly similar residues are indicated by symbols as “*”, “:”, “.”

respectively. Residues in the F-1,6-BP binding pocket are indicated as red; residues involved in the amino acid binding pocket are indicated in yellow; residues involved in the active site are indicated in white. Cysteine 358 and Cysteine 326 on M2PYK is indicated by a red colour and bolded. The colour scheme is the same as figure 1-3, A domain (residues 25-116), B domain (residues 117-219), and C domain (residues 403-531) are depicted in green, magenta, cyan, and N-terminal (residues 1-24) in yellow green, respectively.

1.1.4 M2PYK regulation on gene expression level in cancer cells

In 1927, Otto Warburg observed the metabolic difference between normal differentiated cells and cancer cells (Warburg, Wind, & Negelein, 1927). Cancer cells utilize the aerobic glycolysis pathway which is a relatively less efficient way to produce ATP (adenosine 5'-triphosphate) compared with the mitochondrial oxidative phosphorylation (Heiden, Cantley, & Thompson, 2009). The Warburg effect argued that cancer cells lose their cellular respiratory capacity. But Crabtree suggested that some tumours have high respiration rates (Crabtree, 1929). 1980, Eigenbrodt demonstrated that on one hand, M2PYK was phosphorylated and inactivated by protein kinases showing that the enzyme is related to cancer signalling; on the other hand, M2PYK enzymatic activity inhibition step is important in nucleotide biosynthesis, showing that the enzyme is connected to cancer metabolism (Eigenbrodt, Reinacher, Scheefers-Borchel, Scheefers, & Friis, 1992; Mazurek, 2011).

The expression of M2PYK is regulated at multiple levels including DNA methylation, transcription factors, pre-mRNA slicing of PKM gene, PKM2-specific microRNAs and post-translational modifications of the PKM2 proteins (Israelsen & Vander Heiden, 2015). One important mechanism was revealed indicating that epigenetic regulation by DNA methylation was found in PKM transcription across multiple cancers (Desai et al., 2013). Several transcriptional factors were found to regulate the promotor activity of PKM (Discher, Bishopric, Wu, Peterson, & Webster, 1998; Yamada, Tanaka, Miyamoto, & Noguchi, 2000; Yang & Lu, 2013). At the transcription level, activity can be upregulated by oncogenic transcription factors. Heterogeneous nuclear ribonucleoproteins (hnRNPs) bind to splicing signals that flank PKM exon 9 and then upregulate M2PYK expression (David et al., 2010). miRNA, which function by specifically binding to target mRNAs to hinder the translation, was also found to

regulate expression of M2PYK. Activity was reduced by PKM transcript targeted miRNA to overexpressed M2PYK (Wong et al., 2008) or by targeting the splicing factors PTB, hnRNPs to switch the gene expression from M1PYK to M2PYK, consequently leading to lower cancer cell growth (Sun, Zhao, Zhou, & Hu, 2012). Finally, the acetylation of M2PYK also provides a regulation route to degrade the enzyme, which in turn promotes cell proliferation and tumorigenesis (Lv et al., 2011). Further evidence also indicates that expression of M2PYK is not necessary for growth of some human tumour cell lines in mice, including liver tumours, leukaemia, xenograft tumours or breast tumours (Dayton et al., 2016; Israelsen & Vander Heiden, 2015). Although the loss of M2PYK leads to cancer growth in some tumours and activation of M2PYK can impair some tumour growth, in some reports M2PYK is not viewed as a good therapeutic target in many cancers, which are able to tolerate loss of pyruvate kinase expression (Israelsen & Vander Heiden, 2015).

1.1.5 Regulation of the enzymatic activity and metabolic functions of M2PYK

M2PYK activity can be regulated by glycolytic intermediates. Fructose 1,6-bisphosphate (F-1,6-BP) activates the protein by improving its tetramerization, as the dimers and monomers have very low activities (Christofk et al., 2008). The phosphorylated tyrosine binding leads to a reverse effect by disruption of tetramerization. Human M2PYK mutants H391Y and K422R found in Bloom syndrome patients shows that these missense mutations reduce M2PYK activity. The reduction subsequently leads to accumulation of glycolytic intermediates, cell proliferation, polyploidy and tumour growth (Gupta & Bamezai, 2010; Iqbal et al., 2013). Deactivated M2PYK was reported to result in PEP-dependent histidine phosphorylation and activation of phosphoglycerate mutase, which catalyse the 8th step of glycolysis, as well as less ATP production. This means that deactivated M2PYK in cancer cells promotes aerobic glycolysis with increased glucose consumption and contribute to anabolic metabolism (Vander Heiden, Locasale, et al., 2010). Furthermore, gene knockout experiment showed that absence of M2PYK in primary mouse embryonic fibroblasts results in reduced DNA synthesis level and impaired cell cycle progress. M2PYK is crucial for normal cell proliferation (Lunt et al., 2015).

Serine was found to be another allosteric activator of M2PYK (Chaneton et al., 2012). When serine is sufficient, M2PYK is fully activated, allowing a high glycolytic rate to consume glucose. When serine is not abundant, M2PYK is deactivated, leading to carbon flux to serine biosynthesis (Chaneton et al., 2012). Another intermediate succinyl-5-aminoimidazole-4-carboxamide-1-ribose-59-phosphate (SAICAR) is another allosteric regulator. It activates M2PYK to raise glucose consumption rates (Keller, Tan, & Lee, 2012).

M2PYK can also be regulated by post-translational modifications including phosphorylation. Phosphorylation on Y105 deactivated M2PYK by promoting dimerization of the enzyme, this was shown to result in cell proliferation and tumorigenesis (Hitosugi et al., 2009). Oxidation on C358, induced by ROS (reactive oxygen species), diamide (a thiol-oxidizing compound) or hypoxia deactivates M2PYK, leading to diversion of glucose flux into the pentose phosphate pathway to generate a reducing potential to balance the oxidative environment and cell proliferation (Anastasiou et al., 2011).

1.1.6 Hyperglycaemia and LPYK as drug target

Allosteric activators of LPYK have been identified through high-throughput screening as a potential therapy for hyperglycaemia. The mechanism is to activate LPYK enzyme activity to create a glycolytic/gluconeogenic futile cycle (Fenton, 2012). The activation of the drug target enzyme LPYK is to increase the glycolysis pathway efficiency and consuming more glucose to counteract hyperglycaemia.

1.1.7 Erythrocyte pyruvate kinase (RPYK) deficiency

Pyruvate kinase deficiency is caused by the PKLR gene mutations or genetic variations (Fermo et al., 2005). As the glycolysis pathway is the only energy source in RBC (red blood cell), decreased enzyme activity leads to anaemia (van Zwieten et al., 2015). In literature, people affected by pyruvate kinase mutations are estimated at 1 in 20,000 and more than 158 mutations of PKLR gene have been identified (Zanella & Bianchi,

2000). However, pyruvate kinase deficiency is a protective effect in against malaria as it prevents the parasites replicating in red blood cells (Ayi et al., 2008).

1.2 Natural regulation of human PYKs

1.2.1 Allosteric effects

In 1903, haemoglobin research by C. Bohr revealed that ligand binding of a multimeric protein could lead to affinity changes of another ligand. The phenomenon is called cooperativity, which could be either homotropic, where the binding affinity of one ligand is changed by the binding of a same ligand, or heterotropic, where the binding affinity of one molecule is changed by the binding of a different molecule on the polymeric protein. In 1965, the MWC (Monod-Wyman-Changeux) allosteric model was conceived to explain cooperativity of such allosteric effects in homo-tetrameric complexes (Monod, Wyman, & Changeux, 1965). The phenomenon explains that equilibrium of tensed (T state) and relaxed (R state) protein depends on the binding of a ligand to an allosteric site. All four units of a tetrameric protein are in same state at any time, there are two pre-existing quaternary states (T state and R state) (Changeux, 2012). That is to say the binding of the substrate to one subunit alters the affinity of all other subunits by T-R transition. And the model holds further that when there is no ligand binding, the equilibrium favours one of the conformational states. The equilibrium can be changed by binding in a pocket different from the active site. In this case, the ligand is defined as an allosteric effector and the pocket is the allosteric site. In 1966, the Koshland, Nemethy and Filmer (KNF) model suggested that in a given tetramer, both R state and T state units exist (Koshland, Nemethy, & Filmer, 1966). The model is also named the sequential model. The binding of one subunit leads to the tertiary T-R transition and any of other subunits can exist in a different state. The binding only slightly changes the structure of other subunits so that their binding pocket are more receptive to the substrate.

Pyruvate kinase is an example of allosterically regulated enzyme. This is a conserved property of this enzyme with E. coli pyruvate kinase, yeast pyruvate kinase, and human M2PYK, all allosterically activated by F-1,6-BP, which is a product of the PFK

(phosphofructokinase) reaction (Jurica et al., 1998). F-1,6-BP activates both RPYK and LPYK allosterically however M1PYK is regarded as a non-allosteric enzyme and shows constitutively full activity (Prasannan, Tang, & Fenton, 2012; G Valentini et al., 2000). In human cells, M2PYK, LPYK, and RPYK are upregulated by PEP in a homotropic cooperative way and by F-1,6-BP in a heterotropic cooperative way (Gupta & Bamezai, 2010). PEP is the substrate of PYKs however this is not an allosteric effect as it affects the affinity on the same pocket. F-1,6-BP is an allosteric effector to PYKs as its binding to the protein leads to higher affinity to substrate binding. M2PYK is also allosterically inhibited by the thyroid hormone 3,3',5-triiodo-L-thyronine (T3). T3 prevents tetramerization and stabilizes monomer M2PYK (Kato, Fukuda, Parkison, McPhie, & Cheng, 1989).

There is growing literature showing that amino acids act as another family of allosteric regulators for human PYKs. Published amino acid activators of human pyruvate kinase are summarized in Chapter 4.1.1. Some amino acids are activators and while others are inhibitors. Amino acids are as important as F-1,6-BP in the regulation of PYK activity and glycolytic flux control. For example, serine as a natural allosteric activator of M2PYK and may regulate the serine biosynthesis pathway, which is crucial for cancer cell proliferation (Chaneton et al., 2012). It was described as a rheostat-like mechanistic system as shown in Figure 1-5. When the overall PYK activity is low via the preferential expression of M2PYK, which has low basal enzymatic activity compared with M1PYK, the intermediates related to serine biosynthesis accumulate including 3PGA (3-phosphoglycerate) and PEP. When serine is abundant, M2PYK is fully activated and the carbon flux used through glycolysis as shown in the righthand figure in Figure 1-5. However, when the serine concentration drops, the enzymatic activity of M2PYK cannot be maintained, the intermediates, 3PGA and PEP, will accumulate and the carbon flux is redirected to serine biosynthesis pathway to compensate for the shortfall of serine and other related amino acids.

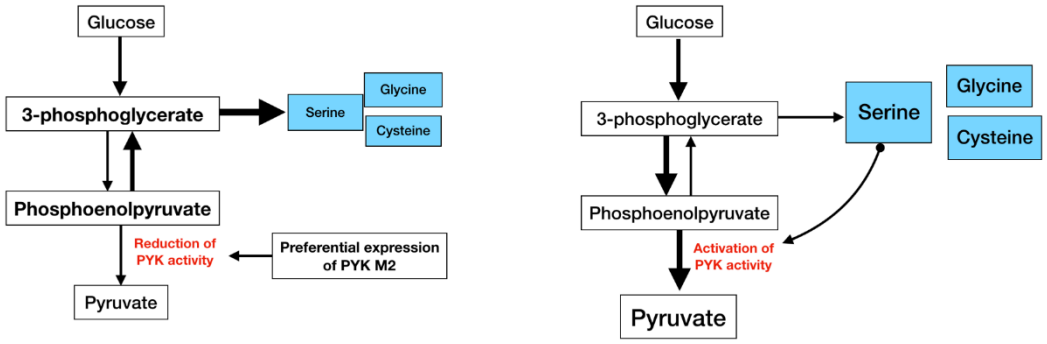

Figure 1-5. Illustration of the rheostat-like mechanistic system of serine biosynthesis pathway and the M2PYK activity.

The amino acid binding pockets of human PYKs are conserved as shown in Figure 1-6. In the left figure, four structures show almost the same pocket. In the right, the pocket of M2PYK (white) co-crystalized with phenylalanine (red) in its pocket.

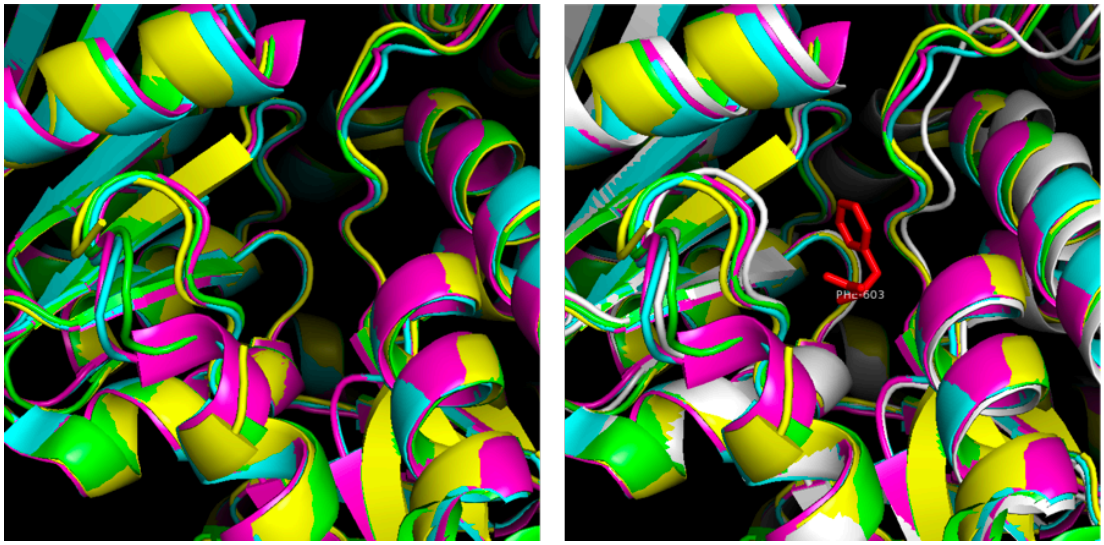

Figure 1-6. The left figure shows the amino acid pocket area of a series of aligned human pyruvate kinase crystal structures. The four structure are Apo enzymes. The right figure is the alignment of four isoforms with a M2PYK co-crystalized with phenylalanine. The structure of M1PYK (3SRF), M2PYK (4FXJ), LPYK (4IP7) and RPYK (2VGB) are coloured in yellow, blue, green, and purple respectively. The white structure in the right figure is the M2PYK (4FXF) co-crystalized with phenylalanine (red).

It is highly possible that phenylalanine or other amino acids could bind to these pockets. As described in Chapter 4, we screened four human PYK isoforms with a group of amino acids. Surprisingly, many other amino acids were found to be regulators of

M2PYK and RPYK. Further investigation between the binding of human PYKs and amino acids were carried out through STD-NMR, which is shown in Chapter 5. We demonstrated that all amino acids we tested bind to any of the four isoforms. These results might indicate that the conserved amino acid pockets in PYKs bind to amino acids, which are biochemical regulators (some activators and some inhibitors) or non-regulators. As there is no additional ligand-protein structure evidence generated from this research, we don't know if these very different amino acids (large/small; positive/neutral/negative) bind to the same or different pockets.

A rock and lock Allosteric model of PYK

In 2010, a study of *Leishmania mexicana* pyruvate kinase (LmPYK) demonstrated a rock and lock allosteric model of PYK (Hugh P. Morgan et al., 2010). LmPYK could be stabilized by ATP and oxalate or locked by the effector fructose 2,6-bisphosphate (F-2,6-BP) through rigid body rotation of each unit of the protein.

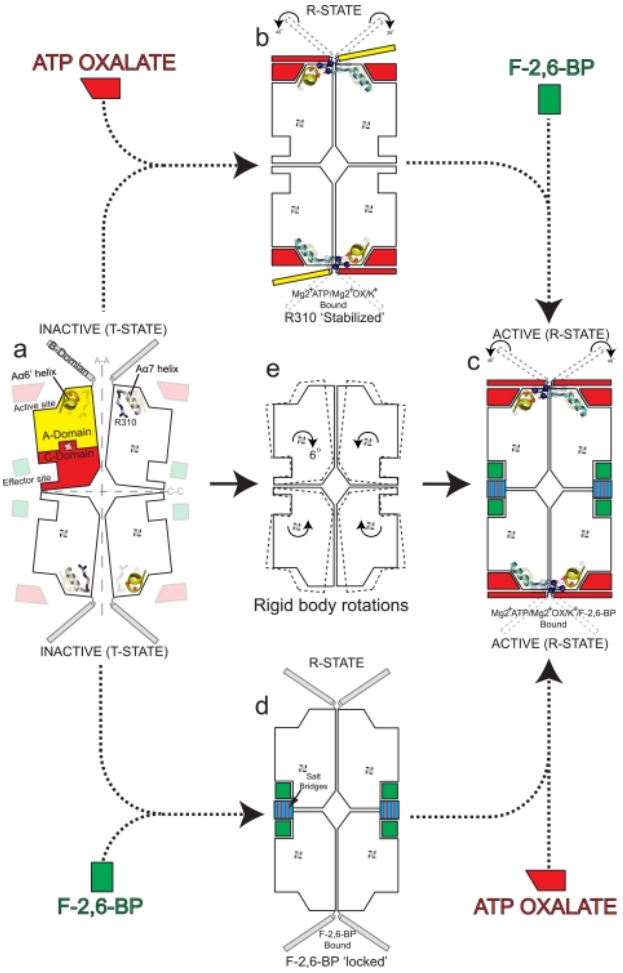

Figure 1-7. The schematic diagram of LmPYK allosteric mechanism: a, representation of inactive T-state, the relative positions of effector and substrate are shown; b, binding of ATP and oxalate to the active R-state of LmPYK; c, active R-state LmPYK binding with ATP, oxalate and F-2,6-BP; d, active R-state locked by F-2,6-BP; e, superposition of inactive T-state and active R-state. The figure is from the study from Morgan's article.

1.2.2 Hormonal control on human PYKs

It has been studied that both known dietary and hormonal regulators of LPYK alter the glycolysis pathway by controlling LPYK at the mRNA level. Glycogen and cyclic AMP (adenosine monophosphate) inhibit the induction of LPYK mRNA. The presence of insulin and dietary carbohydrates activate the mRNA synthesis of LPYK (Munnich et al., 1984; Vaulont, Munnich, Decaux, & Kahn, 1986). Recently research has shown that insulin plays a very important role in the regulation of M2PYK in cancer cells by up-regulation of M2PYK expression but significantly reducing its activity (Iqbal et al., 2013). In this process, glycolytic flux is diverted to biosynthesis and cell growth by insulin.

Thyroid hormone also inhibits LPYK at the transcription level (Munnich et al., 1984). The structures of thyroid hormone T3 (triiodothyronine) and its prohormone T4 (thyroxine) are shown in Figure 1-8.

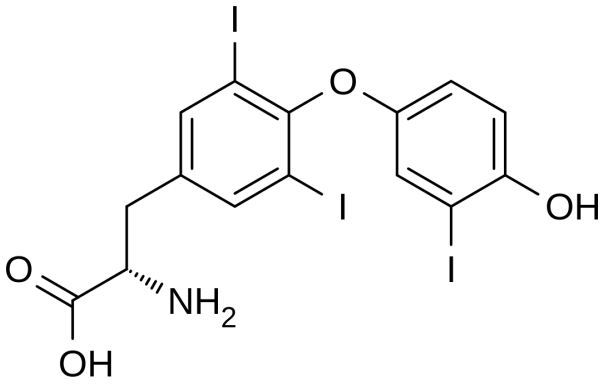

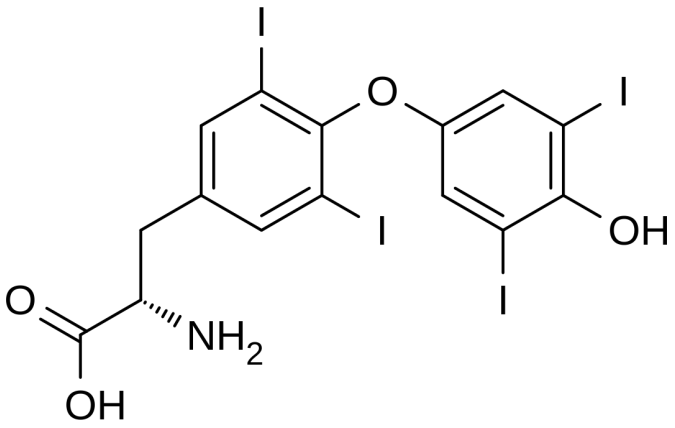

Figure 1-8. The structural formula of thyroid hormone. The upper figure is triiodothyronine (T3), the bottom figure is thyroxine (T4).

It was reported that when red blood cells are incubated with thyroid hormone, the level of 2,3-BPG (2,3-bisphosphoglyceric acid increases) (Snyder & Reddy, 1970). In 1967, Reinhold and Ruth Benesch found that in red blood cells, 2,3-BPG acts as an allosteric effector of haemoglobin to decrease its affinity of oxygen (Benesch & Benesch, 1967). In addition, it was also found that in the blood of hyperthyroid patient, 2,3-BPG level increased (Zaroulis, Kourides, & Valeri, 1978). The haemoglobin saturation curve is shown in Figure 1-9. 2,3-BPG is a major regulator of the haemoglobin-oxygen affinity. Left and right shifts of the curve represent higher and lower oxygen affinity. But how thyroid hormone affects the 2,3-BPG production is still unclear.

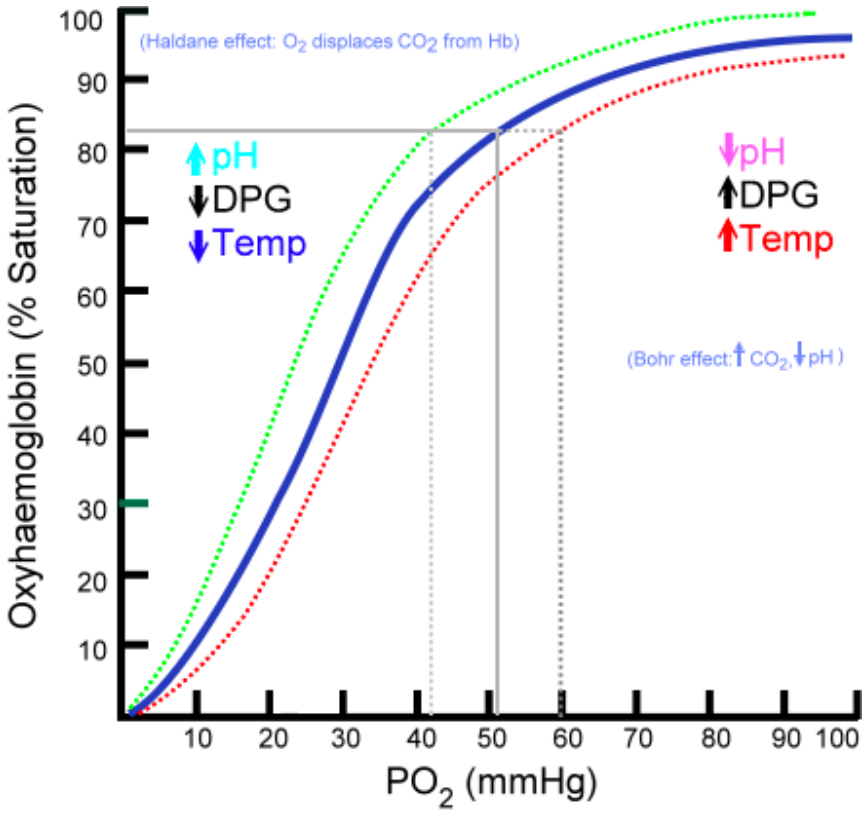

Figure 1-9. The haemoglobin saturation curve of how pH, temperature, and 2,3-BPG (shown as DPG in the figure) affect the affinity of oxygen with haemoglobin. X-axis is the partial pressure of oxygen and y-axis is the oxygen saturation by percentage. When pH goes up, or 2,3-BPG levels decrease, or the temperature goes down, the saturation curve moves to left (blue curve to green one). When these conditions change to the other direction, the curve moves to right (from blue to red).

Interestingly, in our research both thyroid hormone T3 and T4 inhibit RPYK, which is discussed in Chapter 4. It is highly possible that the activity of RPYK in red blood cells is inhibited by increasing thyroid hormone level. Then one of the middle products from the glycolysis pathway as shown in Figure 1-1, 1,3-BPG (1,3-bisphosphoglyceric acid), is accumulated in red blood cells. Bisphosphoglycerate mutase transform 1,3-BPG to 2,3-BPG (2,3-diphosphoglyceric acid). As the Luebering-Rapoport pathway described shown in Figure 1-10, bisphosphoglycerate mutase catalyzes the transfer of a phosphoryl group from C1 to C2 of 1,3-BPG, forming 2,3-BPG. Then, bisphosphoglycerate phosphatase catalyses the reaction from 2,3-BPG to 3-phosphoglycerate. When RPYK is inactivated, upstream intermediates accumulate. The hypothesis is that thyroid hormones regulate RPYK to control the 2,3-BPG

concentration in red blood cells and control the oxygen affinity of haemoglobins. The schematic diagram is shown in **Error! Reference source not found.**.

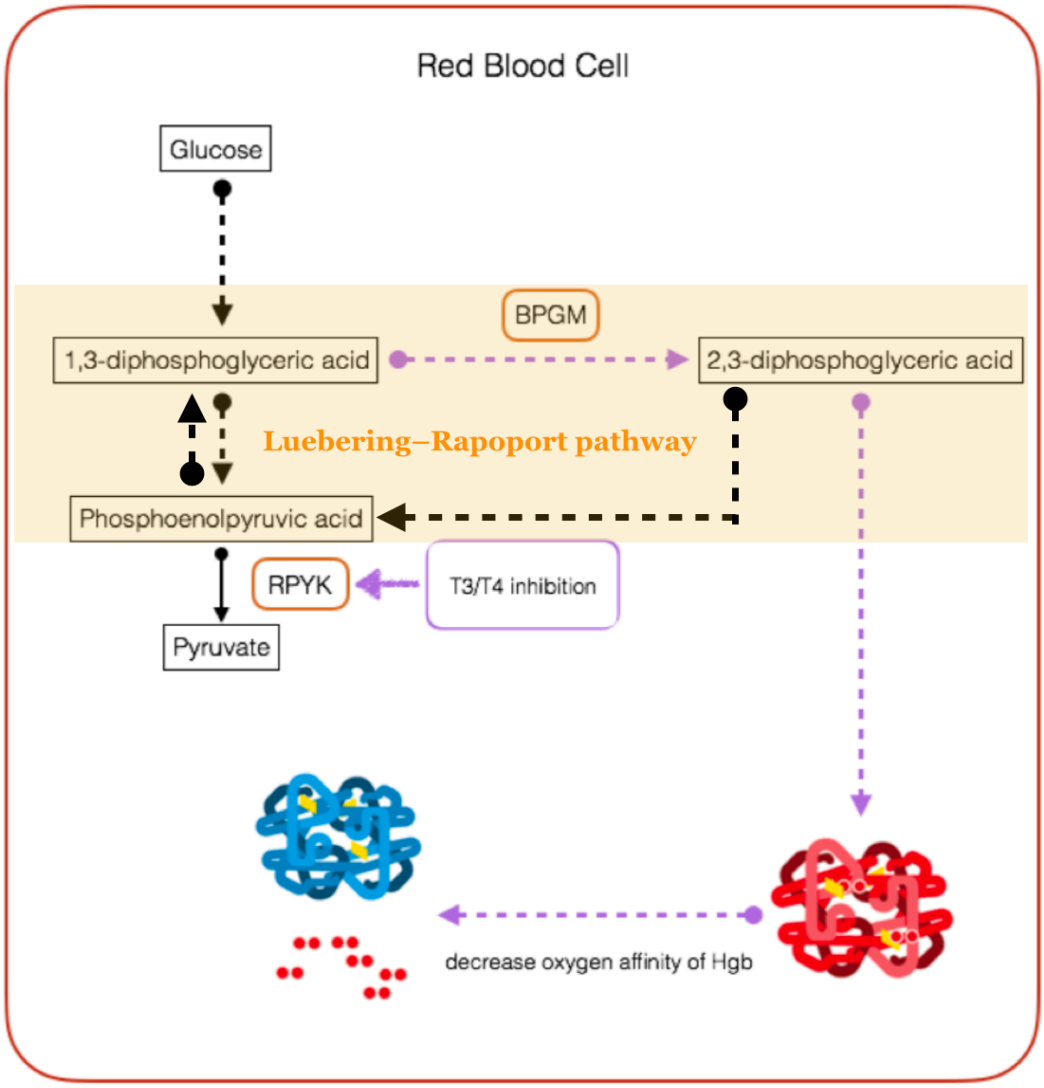

Figure 1-10. The schematic diagram of the hypothesis that thyroid hormones (T3/T4) regulate the affinity of oxygen with haemoglobin (Hgb). RPYK activity is down-regulated by T3/T4 and the glycolysis pathway is altered to accumulate intermediate 1,3-BPG. Then, 1,3-BPG is catalysed by Bisphosphoglycerate mutase (BPGM) to 2,3-BPG, which in turn allosterically regulates the oxygen affinity of Hgb. Black arrows show the energy production direction of the glycolysis pathway. Purple arrows show the hypothesised T3/T4 regulation pathway.

Other research has reported that hyperthyroidism can affect hepatic system and even cause up to 65% hepatic dysfunction (KHEMICHIAN, 2001). Research in Graves' hyperthyroidism also indicates that people with this disease are often observed to suffer hepatic dysfunction (Wang, Tan, Zhang, Zheng, & Li, 2017). The effect of T3

and T4 on LPYK has been tested and shown in Chapter 4. Both thyroid hormones are strong inhibitors for LPYK. It is also possible that excessive thyroid hormone secretion increases the T3/T4 concentration in hepatocytes and inhibition of LPYK by thyroid hormones may lead to poor efficiency of energy production. Our hypothesis is that the regulation of thyroid hormone on LPYK may play an important role in this type of hepatic dysfunction.

1.3 The biochemical environment of human PYKs

In this thesis, we discuss two aspects of the biochemical environment of human PYKs: redox environment and free amino acids concentration. Neither are homogeneous in human tissues and will also vary depending on physical stress affecting the body. For example, redox status and regulation is different between normal cells and cancer cells (Gaascht et al., 2014). Free amino acid concentration changes after a high-protein meal (FRAME, 1958) or exercise (McCormack, Cooke, O'Connor, & Jakeman, 2017). Nutrient availability is also different in various tissues (Canepa et al., 2002). Human PYK isoforms are expressed in various human tissues and work in very different environments, especially RPYK, which is travelling in the human body within red blood cells through all kinds of tissues. It is therefore of interest to test how redox reagents and amino acids regulate human pyruvate kinases. Results from such studies are recorded in Chapter 3 and 4.

1.3.1 ROS regulation on M2PYK

Redox, short for reduction and oxidation reactions, is often described as the balance of several chemical pairs, GSH (Glutathione) /GSSG (Glutathione disulfide), NAD^+ (oxidized nicotinamide adenine dinucleotide) /NADH (reduced nicotinamide adenine dinucleotide) and $NADP^+$ (nicotinamide adenine dinucleotide phosphate) /NADPH (reduced nicotinamide adenine dinucleotide phosphate).

In lung cells, ROS (reactive oxygen species) regulation of M2PYK is crucial for detoxification of ROS. When intracellular ROS concentration increases and oxidative stress builds up, Cys^{358} on M2PYK is oxidized and the metabolic flux changes to the pentose phosphate pathway, this generates enough reducing reagents to detoxify the

oxidized environment (Anastasiou et al., 2011). Not only human PYK but also its orthologues in other species, from bacteria to mammalian cells, can be inhibited by ROS (Butterfield & Sultana, 2007; Cumming et al., 2004; Maeba & Sanwal, 1968). A study in this area suggested that ROS contributes to the development of the severe disease Pulmonary Arterial Hypertension by decreasing M2PYK activity. Activators of M2PYK might be a potential treatment for this disease (D. Guo et al., 2016).

1.3.2 Amino acid regulation in cancer cells

Amino acids are building blocks in protein synthesis but they are also important signalling and regulatory metabolites in a number of cellular pathways. Fast proliferation in tumours require cancer cells to alter their metabolic flux to increase biomass production (Hanahan & Weinberg, 2011). Cancer metabolism has been heavily explored, some drug development programmes target glycolysis and oxidative phosphorylation. A metabolic starvation therapy removing or limiting the availability of some metabolites including amino acids was studied (Changou et al., 2014). It was thought this might be a more efficacious method as it is less toxic than chemotherapy or radiation. In these programmes, nonessential amino acids are important as potential starvation inducing metabolites. Normally they can be synthesized in cells but some nonessential amino acids become essential in cancer cells due to their altered metabolism, as demonstrated in breast cancer cells (Geck & Toker, 2016). The amino acid concentration in saliva from patients with breast cancer was shown to be changed significantly compared with healthy controls (Cheng, Wang, Huang, Duan, & Wang, 2015).

Of all amino acids, glutamine is the most consumed amino acid in cancer cells (Jain et al., 2012). Although consumed in nucleotide and lipid biosynthesis, glutamate is produced from glutamine via glutaminolysis, which is often increased in cancer cells (Erickson & Cerione, 2010). Apart from glucose, glutamine (as the most abundant amino acid in the bloodstream) plays one of the most important roles as building blocks for growth by two processes: glycolysis and glutamine utilization by reductive carboxylation. All other NEAAs (non-essential amino acids), including serine, glycine, cysteine, tyrosine, alanine, aspartic acid, asparagine, arginine, proline, are derived from glutamine utilization in cancer cells (Alberghina & Gaglio, 2014; Thiele et al.,

2013). A schematic representation is shown in Figure 1-11 A. Some amino acids, about 50% of the amino acids required for protein synthetic activity of cancer cells, are derived from glycolysis pathway intermediates: serine, glycine and cysteine derived from 3PGA (3-Phosphoglycerate); tyrosine from PEP; alanine from pyruvate (Pyr in the figure). While the other 50% of the required amino acids in cancer metabolism rewiring, including asparagine, arginine, proline, aspartic acid, are derived from glutamine metabolism.

The metabolic pathways have been rewired to support biosynthesis of proteins, nucleotides, glycans, and lipids, as well as production of energy and NADPH. A concept map from Alberghina's article is shown in Figure 1-11 B (Alberghina & Gaglio, 2014) . Glycolysis is identified as yellow arrows. Glutamine metabolism is represented by blue arrows. Pentose phosphate pathway is shown in green arrows. Bright lilac arrows are the pathway of serine/glycine and folate metabolism. The red arrows identify an NAD(P)H electron transfer flux (ETF). Both glutamine and glucose are transferred within cancer cells to support the altered metabolism. Glycolysis pathway provides free energy to support the energetics in cancer cells; provides the carbon skeleton to half of amino acid biosynthesis; provides 3PGA to fuel serine biosynthesis pathway. Pentose phosphate pathway provides NADPH to support amino acids biosynthesis, lipid biosynthesis, and redox balance. Glutamine metabolism pathway supplies α-ketoglutarate to fuel TCA cycle and TCA cycle produces oxaloacetate and citrate which are used in amino acid biosynthesis and lipid biosynthesis.

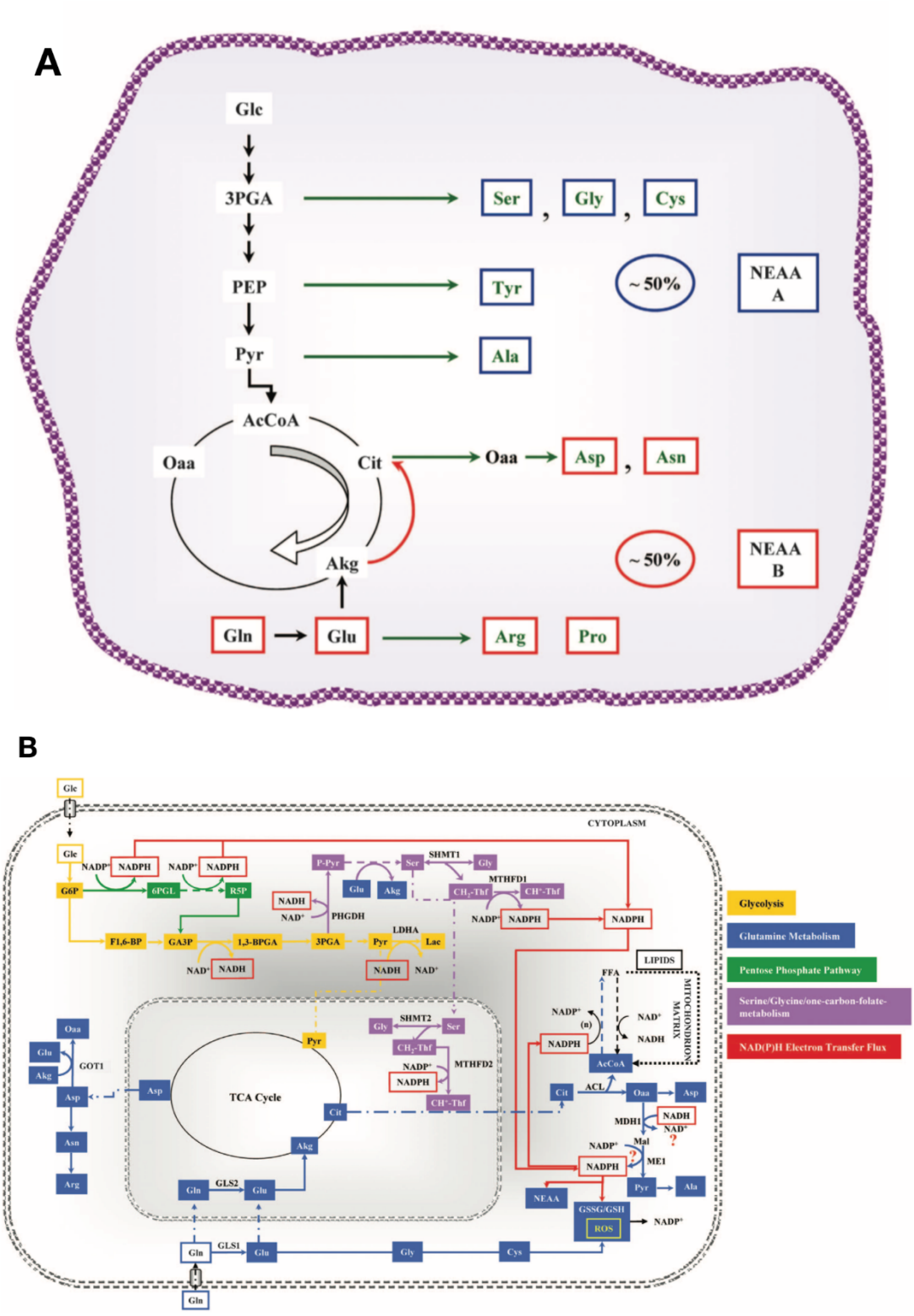

Figure 1-11. A: NEAA biosynthesis pathways. B: Concept map of the cancer metabolic rewiring. Abbreviations: 1,3BPGA, 1,3-bisphosphoglycerate; 3PGA, 3-phosphoglycerate; 6PGL, 6-phosphogluconolactone; AcCoA, acetyl-CoA; ACL, ATP citrate lyase; Akg, α-ketoglutarate; Ala, alanine; Arg, arginine; Asn, asparagine;

Asp, aspartate; CH+-Thf, 5-methylenetetrahydrofolate; CH2-Thf, 5,10-methylenetetrahydrofolate; Cit, citrate; Cys, cysteine; F-1,6-BP, fructose 1,6 bisphosphate; FFA, fatty acids; G6P, glucose 6-phosphate; GA3P, glyceraldehyde 3-phosphate; Glc, glucose; Gln, glutamine; Glu, glutamate; Gly, glycine; GOT, glutamic-oxaloacetic transaminase; GSH, glutathione reduced; GSSG, glutathione oxidized; Lac, lactate; LDHA, lactate dehydrogenase; MDH 1, malate dehydrogenase; ME, malic enzyme; MTHFD1 and 2, methylenetetrahydrofolate dehydrogenase ($NADP^+$ dependent); NEAA, non-essential amino acids; Oaa, oxaloacetate; PPP, pentose phosphate pathway; P-Pyr, 3-phosphohydroxypyruvate; Pyr, pyruvate; R5P, ribose 5-phosphate; ROS, reactive oxygen species; Ser, serine; SHMT1 and 2, serine hydroxymethyltransferase

Glutamine maintains a relatively high concentration to support glutamine metabolism as both carbon donor and nitrogen donor, with a combination of sources such as dietary uptake, de novo synthesis, and muscle protein catabolism (Zhang, Pavlova, & Thompson, 2017). Another important intermediate metabolite amino acid is serine. As discussed in Chapter 1.2.1, elevated intracellular serine levels cause feedback of M2PYK activation, which leads to serine/glycine biosynthesis(Gravel et al., 2014).

1.3.3 Amino acid concentration in erythrocytes

Amino acid concentration has been widely reported to vary in different tissues. Free intracellular amino acids are crucial for protein synthesis and they accumulate at the site of protein synthesis (Canepa et al., 2002). Skeletal muscles contain most free intracellular amino acids (Bergström, Alvestrand, & Fürst, 1990).

It was reported that erythrocytes play an important amino acids transportation role in the process of post-absorptive state in health humans (Agli, Schaefer, Geny, Piquard, & Haberey, 1998). In this report, oral load of amino acids was used to investigate whether erythrocytes absorb amino acids during the period of intestinal absorption. The result showed that for most amino acids erythrocytes contained higher concentrations than plasma after an oral load. The amino acids concentration test of an oral load experiment lasted 125 minutes and suggested that after a period of 25-50 minutes, amino acid exchange might take place between plasma and erythrocytes. The result from this report is shown below in (Agli et al., 1998). So, RPYK in cytosol of erythrocytes are in an environment with changing amino acids concentrations and the glycolysis rate might change if these amino acids affect the enzymatic activity of

RPYK. This effect might be important as glycolysis is the only pathway in erythrocytes to produce ATP.

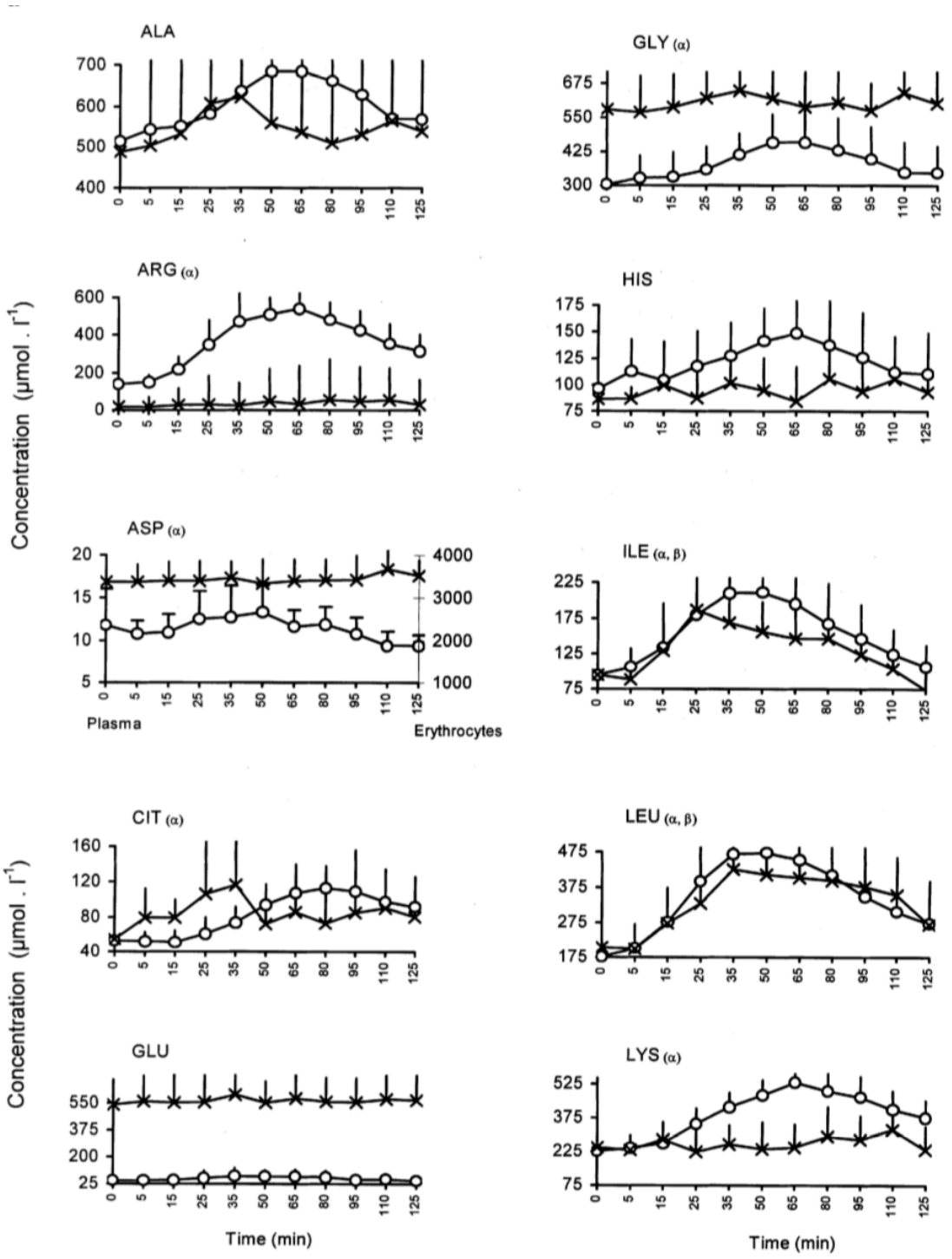

Figure 1-12. The time dependant variations of the mean amino acid concentrations for plasma (o) and erythrocytes (x). The changes in concentration are given by α (plasma) and β (erythrocytes).

1.4 Formulation of the objectives of the research

Firstly, we purified proteins and investigated the biophysical, biochemical properties of all human pyruvate kinase forms. During the study, we discovered that the activities of pyruvate kinases are affected significantly by a couple of experimental operations, which are not recorded in other reports in this area, these include the pre-incubation time after protein been diluted from stock to the start of the enzymatic reaction and the redox environment. It is therefore difficult to compare the enzymatic results from different literatures about pyruvate kinases. We verified the experimental methods to determine the optimum way to study pyruvate kinase activity and how its activity is affected by pre-incubation time, redox environment and the protein concentration itself. This provides stable protein activity data and allows the results from different batches of protein or sets of experiments to be compared.

Secondly, the metabolism in proliferating cells is rewired and metabolites including glycolysis intermediate products, amino acids, TCA cycle middle products in these cells are redirected to feed other energetic or biosynthetic pathways. The concentrations of these metabolites is changed, however in this changing environment, metabolic regulation of this sensitive enzyme pyruvate kinase M2 involving amino acids is not fully understood. It is necessary therefore to study how various amino acids regulate M2PYK.

Thirdly, as the concentrations of amino acids in erythrocyte change after intestinal absorption, it will be quite important to investigate how these amino acids specifically affect erythrocyte metabolism especially involving reactions with pyruvate kinase R type. Pyruvate kinases have been shown to be regulated by amino acids, but the effects of amino acids on RPYK activity is still unknown.

In this study, we screened all amino acids with all four human pyruvate kinases in order to investigate the regulations between them.

CHAPTER 2. Biophysical, Biochemical and kinetics characterization of pyruvate kinase isoforms

2.1 Gene expression, protein purification

2.1.1 Expression of His-tagged M1PYK, His-tagged M2PYK, His-tagged LPYK and His-tagged RPYK

All four proteins (His-tagged M1PYK, His-tagged M2PYK, His-tagged LPYK and His-tagged RPYK) used in this thesis were expressed in *E. coli.* The proteins are N-terminally His_6-tagged with a cleavage site (MGSSHHHHHHSSGLVPRGSH). It was reported in literatures of using a His-tagged pyruvate kinase in both enzymatic assays and crystallization (Chen et al., 2011; Dombrauckas, Santarsiero, & Mesecar, 2005; Vander Heiden, Christofk, et al., 2010). The His-tag helps to yield high purity protein and didn't show much influence on enzyme structure and enzymatic activity.

Transformation step: Chemically competent cells (BL21_DE3 *Escherichia. coli* Novagen) were transformed with plasmids encoding human pyruvate kinases (hPYKs) (pET28A_M1PYK, pET28A_M2PYK, pET28A_LPYK or pET28A_RPYK) separately. The four recombinant clones were prepared by Dr Hugh Morgan in house using GENSCRIT DNA synthesis service. The process of transformation is as follow. About 100 ng of each plasmid was added into a tube of 20 µl *E. coli* cells. The tube was incubated on ice for 30 min, then it was treated with heat shock at 42 ^{o}C for 45 s. The sample was put on ice for another 2-min incubation. Afterwards, 250 µl of 37 ^{o}C SOC (super optimal broth) was added into each tube. Then, each sample was incubated at 37 ^{o}C for 60 min in a shaker at 250 rpm. Then, the bacteria in each tube were streaked onto agar plates (lysogeny broth with 50 µg/ml kanamycin), which were pre-incubated at 37 ^{o}C for 10 min. The plates were incubated at 37 ^{o}C for 12-16 hours.

Expression step: Single colonies of transformed cells containing the target gene structures were picked from LB (lysogeny-broth) plate (containing 50 µg/ml kanamycin) and used to inoculate 50 ml of 2xTY media（containing 50 µg/ml kanamycin）separately, then incubated 18 hours at 37 ^{o}C with agitation. 20 ml of each overnight cultures were used to inoculate one litre of 2xTY media containing 50 µg per ml kanamycin. Cultures were grown at 37 ^{o}C with agitation an OD 600 of 0.8-1.0 and then incubated in cold room at 4 ^{o}C for 40 minutes. 1 mM IPTG (isopropyl-β-D-thiogalactopyranoside) was added in cultures to induce protein expression. Cultures were incubated at 20 ^{o}C for 18 hours with shaking. Cells were frozen freshly in liquid nitrogen after been harvested at 8,000 rpm for 40 minutes using a JLA-9,1000 rotor at 10 ^{o}C. Cell pellets were weighted and stored at -80 ^{o}C.

Cell culture medium recipes (1 L medium) used in the process are as follow: lysogeny broth (10 g Tryptone, 5 g yeast extract, and 10 g NaCl, pH 7.2); lysogeny broth agar (15 g agar, 10 g Tryptone, 5 g yeast extract, and 10 g NaCl, pH 7.2); 2x TY (Tryptone Yeast) (16 g Tryptone, 10 g yeast extract, and 5 g NaCl, pH 7.4); super optimal broth (20 g Bacto^{TM} Tryptone, 5 g Oxoid^{TM} yeast extract, 0.58 g NaCl, 0.188 g KCl, 2.47 g $MgSO_4$, 2.03 g $MgCl_2$, and 3.60 g glucose)

2.1.2 Preparation of cell lysates for His6-hPYKs

Cell pellets of the four isoforms were placed on ice to thaw and resuspended in lysis-buffer (30 ml buffer/5g cells). Lysis-buffer consists of 50 ml of buffer A (50mM NaH_2PO_4, 300 mM NaCl, 20 mM imidazole, pH 8.0) supplemented with one tablet of EDTA free protease inhibitors (Roche). A constant disruption system (Constant System Disruptor TS Series Benchtop instrument) was used to lyse the resuspended 19 cells with pressure set to 22 KPSI instrument reading (equivalent to 152 MPa). The

cell lysate was centrifuged at 23,000 rpm for 50 min at 10 ^{o}C using a JA-25,50 rotor. Cellular debris was removed and the supernatant was collected on ice and filtered using a 0.2 μm syringe filter.

2.1.3 Purification of prokaryotic expressed His6-hPYKs

First step IMAC: All steps were processed at 4 ^{o}C. Clarified cell lysates containing His_6-hPYKs were loaded onto a 5 ml IMAC HiTrap HP Sepharose column (pre-charged with cobalt and pre-equilibrated with buffer A; column was purchased from GE Healthcare) at 2 ml/min. The flow through of the column was maintained at a constant rate of 2 ml/min throughout the affinity chromatography step. After the PYK samples were loaded, the column was washed with 10 column volumes (CV) of buffer A (20 mM imidazole, 50 mM NaH_2PO_4, 300 mM NaCl, pH8.0) to wash out contaminating proteins and change buffer in the column, followed by an additional wash step with 15 CVs of 80% buffer A and 20% buffer B (250 mM imidazole, 50 mM NaH_2PO_4, 300 mM NaCl, pH 8.0) to wash off non-specific binding proteins. The His_6-hPYK proteins were eluted using 5 CVs of 100% buffer B. Samples were concentrated with Vivaspin® tubes with cut-off molecular mass 30 kDa to 2 ml for next step.

Second step: A Superdex 200 26/60 XK size-exclusion column was pre-equilibrated with 5 CVs of PBS-CM (Dulbecco's phosphate buffered saline without calcium and magnesium [Sigma Cat. No. D5652]) and used to load eluted fractions pooled from the affinity step at a flow rate of 2.5 ml/min throughout the size-exclusion step. Eluted fractions were pooled and concentrated to 10 mg/ml using a Vivaspin® tube with a molecular weight cut-off of 30 kDa. The concentrations of the proteins were measured using a Nanodrop® 2000 spectrophotometer. The concentration measurement and the

protein purity was checked by SDS-PAGE. All proteins were frozen using liquid nitrogen and stored at -80 ^{o}C.

The two purification steps for each isoform are recorded in Figure 2-1 to Figure 2-4.

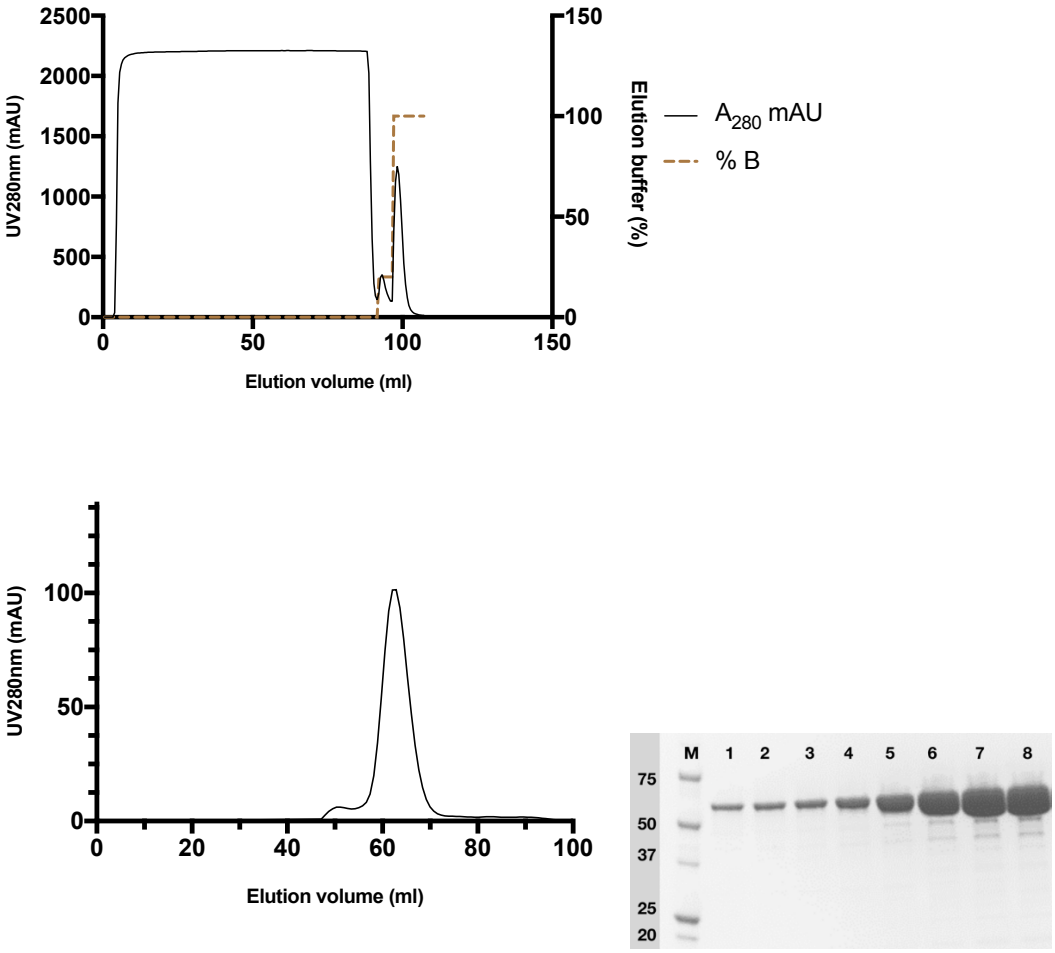

Figure 2-1. Upper part: IMAC of M1PYK, the elution of proteins was monitored by a UV spectrometer at 280 nm (represented by the solid line) and dashed line shows the percentage of Buffer B used for the IMAC purification. Bottom part: gel-filtration purification of M1PYK and figure of SDS-PAGE, showing the purity of the protein, M represents protein marker with unit (kDa).

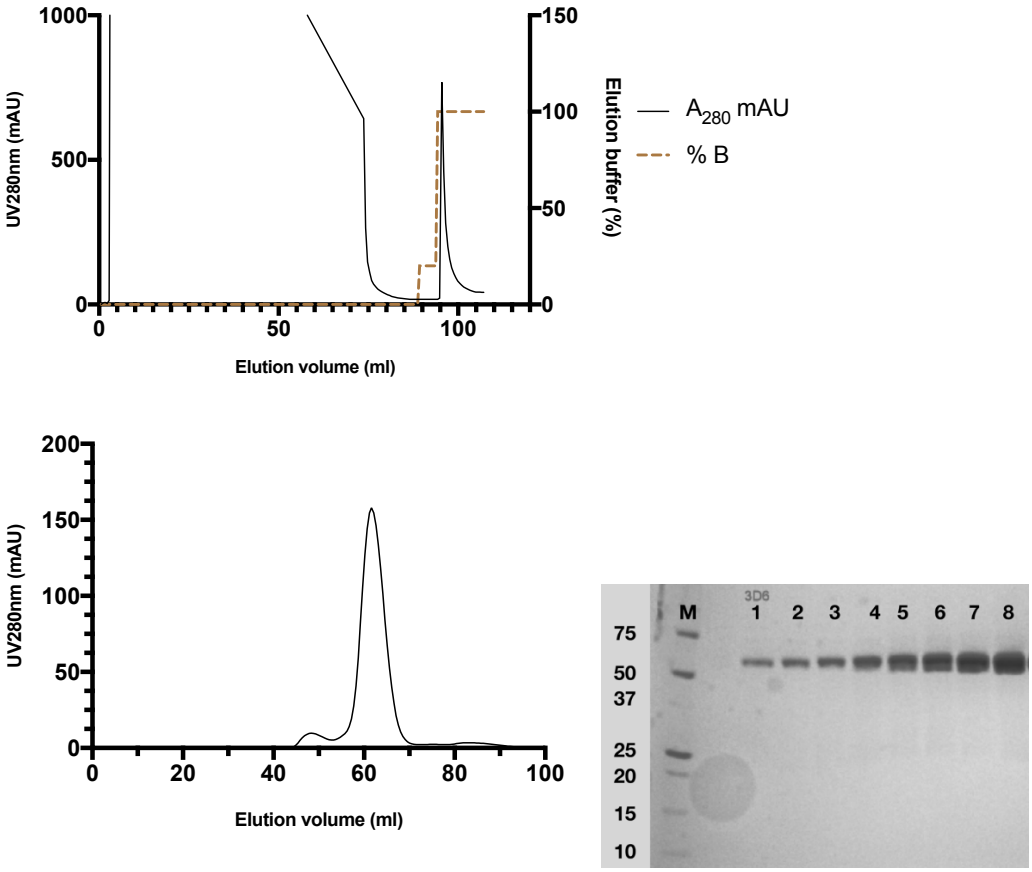

Figure 2-2. Upper part: IMAC of M2PYK, the elution of proteins was monitored by a UV spectrometer at 280 nm (represented by the solid line) and dashed line shows the percentage of Buffer B used for the IMAC purification. Bottom part: gel-filtration purification of M2PYK and figure of SDS-PAGE, showing the purity of the protein, M represents protein marker with unit (kDa).

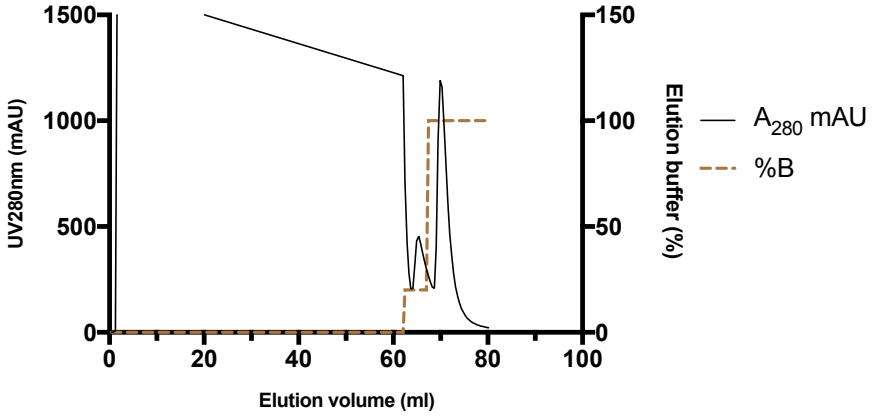

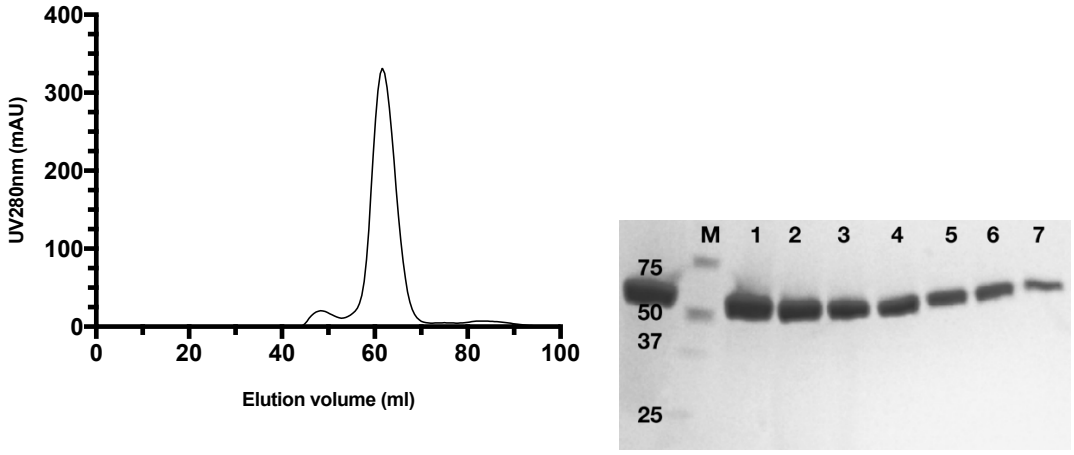

Figure 2-3. Upper part: IMAC of LPYK, the elution of proteins was monitored by a UV spectrometer at 280 nm (represented by the solid line) and dashed line shows the percentage of Buffer B used for the IMAC purification. Bottom part: gel-filtration purification of LPYK and figure of SDS-PAGE, showing the purity of the protein, M represents protein marker with unit (kDa).

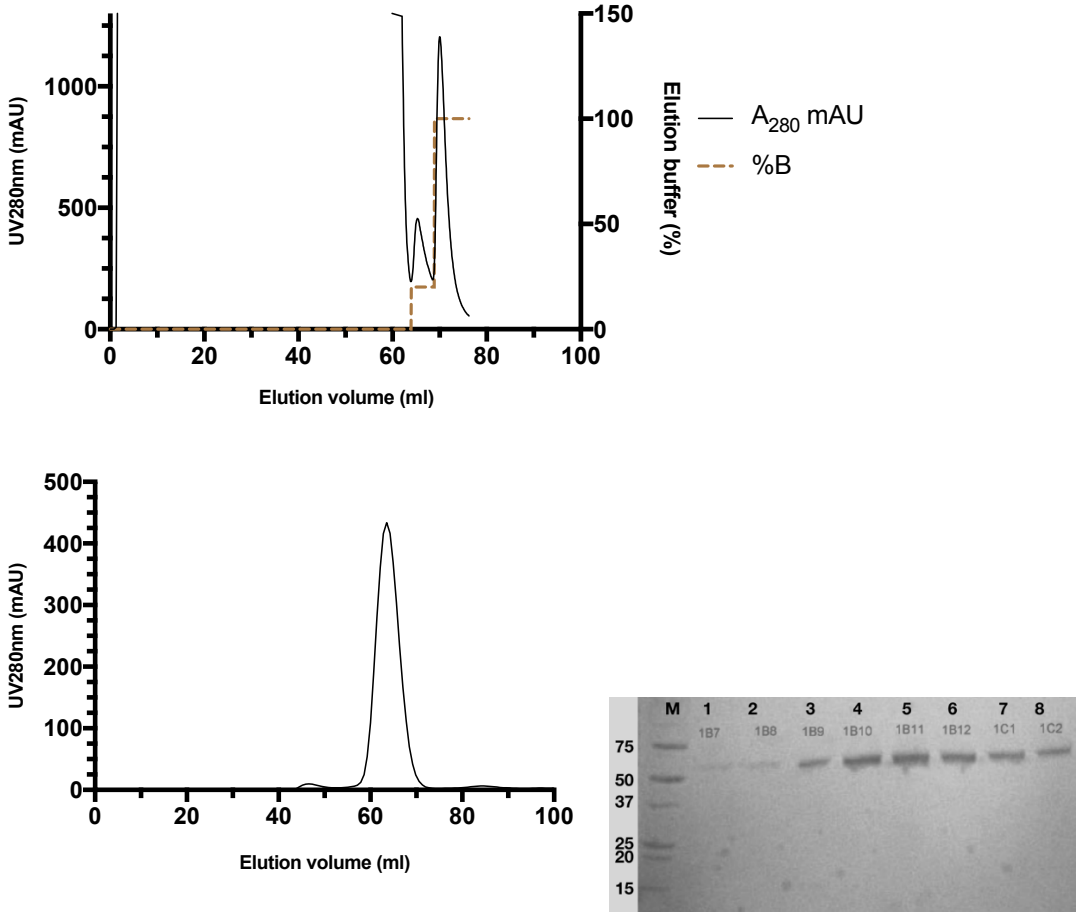

Figure 2-4. Upper part: IMAC of RPYK, the elution of proteins was monitored by a UV spectrometer at 280 nm (represented by the solid line) and dashed line shows the percentage of Buffer B used for the IMAC purification. Bottom part: gel-filtration

purification of RPYK and figure of SDS-PAGE, showing the purity of the protein, M represents protein marker with unit (kDa).

2.1.4 Measurement of protein concentration

Protein concentration was determined by measurement of the absorbance at 280nm using a Nanodrop spectrophotometer and the Beer-Lambert law: $A = \varepsilon * c * l$ (A, absorbance; ε, molar absorbance coefficient, l, path length; c, protein concentration). The theoretical molar absorption coefficient and molecular weight of PYK isoforms, which are estimated by http://web.expasy.org/protparam/, are shown in **Error! Reference source not found.**. Estimated molecule weight His-tagged M2PYK, His-tagged M1PYK, His-tagged LPYK and His-tagged RPYK of 60.1 kDa, 60.2 kDa, 60.7 kDa, and 64.0 kDa. Protein solutions were diluted to ensure the absorbance reading was always between 0.l and 1. Protein concentrations were measured 3 times to ensure consistency and a mean value calculated. Accuracy of concentration measurements was checked by SDS-PAGE.

	M2PYK	M1PYK	LPYK	RPYK
Number of amino acids	551	551	563	594
Molecular weight	60100.21	60225.39	60685.65	63993.49
Tetramer MW	240.4kDa	240.9kDa	242.7kDa	256.0kDa
Theoretical pI	8.22	8.01	6.8	8.12
Ext. coefficient	29910	29910	29910	35410

Table 2. Molecular parameters of human pyruvate isoforms.

2.2 Dynamic Light Scattering

2.2.1 Introduction

To study the stability of hPYKs, we used Dynamic Light Scattering (DLS) to confirm the protein status in solution. DLS, also known as Photon Correlation Spectroscopy (PCS) or Quasi-elastic light scattering (QELS), is a technique used for measuring the

hydrodynamic size distribution of particles, polydispersities, and aggregation effects in solution. A laser beam is introduced into the solution. The protein molecules fluctuate in solution as Brownian motion, which scatters particles. The scattering intensity is recorded, allowing for calculation of the molecular size using the Stokes-Einstein relationship.

2.2.2 Results

DLS assays were carried out on all hPYK isoforms after storage at -80 ^{o}C. Samples were thawed on ice and centrifuged at 12000 rpm at 4 ^{o}C for 15 min to remove any precipitates. PBS-CM was used as a blank reference, which is the same buffer used during the final purification step. Fifty µl of each sample (1 mg/ml) was loaded into the well and measured three times.

Figure 2-5 shows the size distribution data. The "size distribution by volume" graphs show that single peaks from each graph present at 10 nm and the estimated protein molecular weights for M1PYK, M2PYK, LPYK, and RPYK are 228.0 kDa, 242.0 kDa, 254.1 kDa, and 236.7 kDa, respectively. The molecular weights of M1PYK, M2PYK, RPYK and LPYK are shown Figure 2-5. Absence of multiple peaks at a higher hydrodynamic radius indicates that there is no aggregation in the solution.

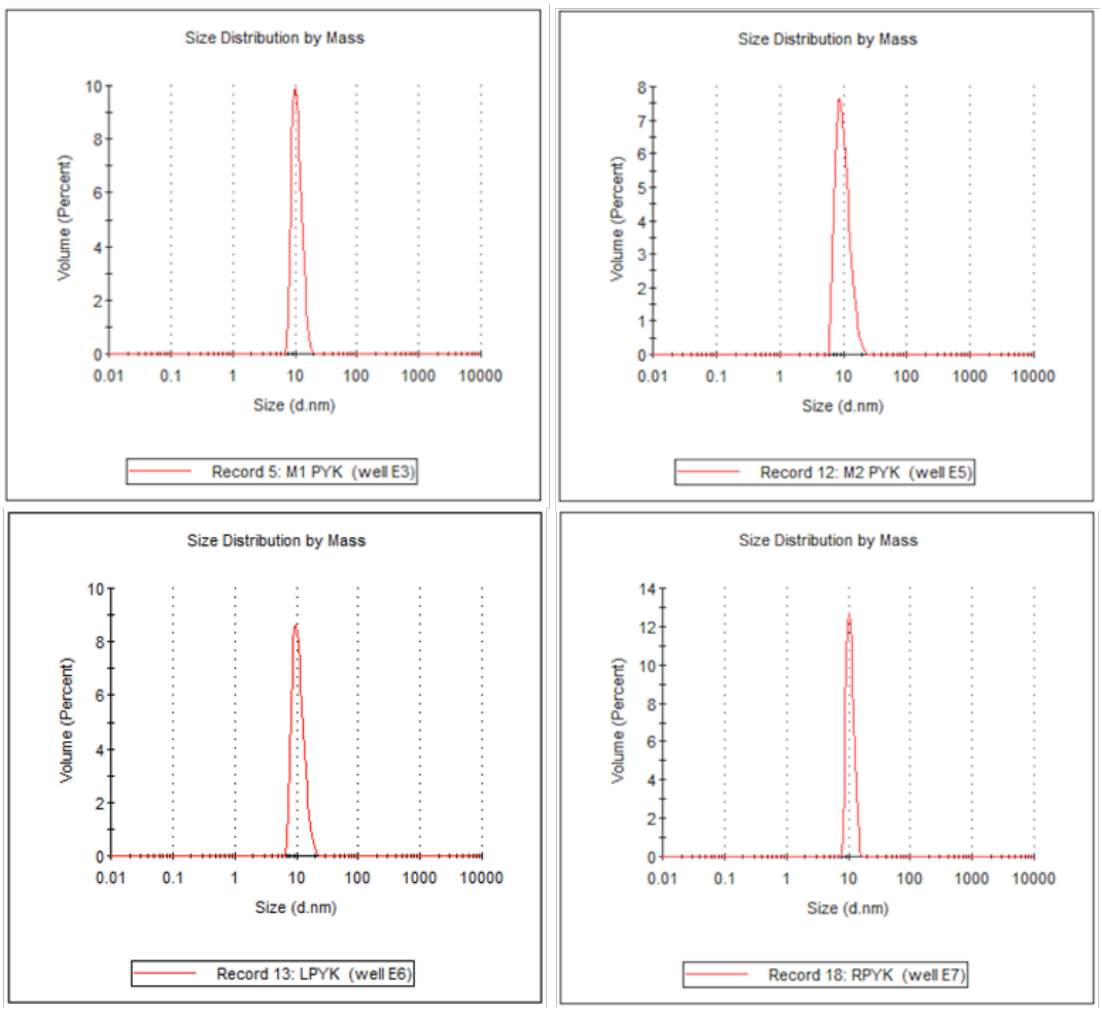

	Mean ± SD (nm)	Est. MW (KDa) (Mean ± SD)	% Intensity	% Mass	Peak Polydispersity
M1PYK	12.12 ± **2.304**	228.0 ± **43.3**	94.1	100.0	Polydisperse
M2PYK	12.43 ± **3.490**	242.0 ± **67.7**	100.0	100.0	Polydisperse
LPYK	12.69 ± **3.029**	254.1 ± **60.0**	100.0	100.0	Polydisperse
RPYK	11.38 ± **1.574**	236.7 ± **44.2**	95.01	100.0	Polydisperse

Figure 2-5. Dynamic light scattering analysis of human PYK isoforms shows that all are stable and pure after storing at -80 ºC in PBS-CM. The molecular weights are estimated by the DLS software and are based on empirical mass vs. size calibration curve.

2.3 Thermal shift assay

2.3.1 Introduction

The thermal shift assay tracks the fluorescence signal change of SYPRO Orange dye. The increasing temperature unfolds the protein. When the protein is unfolding in the

solution, the hydrophobic surface exposes and contacts with the dye, which has an excitation wavelength and the fluorescence signal is recorded through the whole process. The protein melting temperature is the temperature point when the protein 50% unfolds.

The SYPRO Orange was ordered from Invitrogen (catalogue number s6650) and was diluted 5000x with 10 mM PBS just before use. Five µl of the diluted SYPRO Orange dye solution was added to 45 µl of 0.55 mg/ml protein solution or protein diluted in ligand solution in a 96-well PCR plate. The samples were mixed, sealed with Bio-Rad optical quality tape, and centrifuged to make sure the protein fully mixed with the dye. An i-Cycler iQ5 Real-Time PCR Detection System (Bio-Rad) recorded the fluorescence change from 20 to 80 ^{o}C in increments of 1 ^{o}C using an excitation wavelength of 485 nm and an emission wavelength of 575 nm.

2.3.2 Results

Figure 2-6 – Figure 2-9 demonstrate that the melting temperature for the four PYK isoforms are 62 ^{o}C (M1PYK), 48 ^{o}C (M2PYK), 62 ^{o}C (RPYK), and 66 ^{o}C (LPYK). The melting temperature for M2PYK was previously reported to be 48 ºC, which is same as in this study.

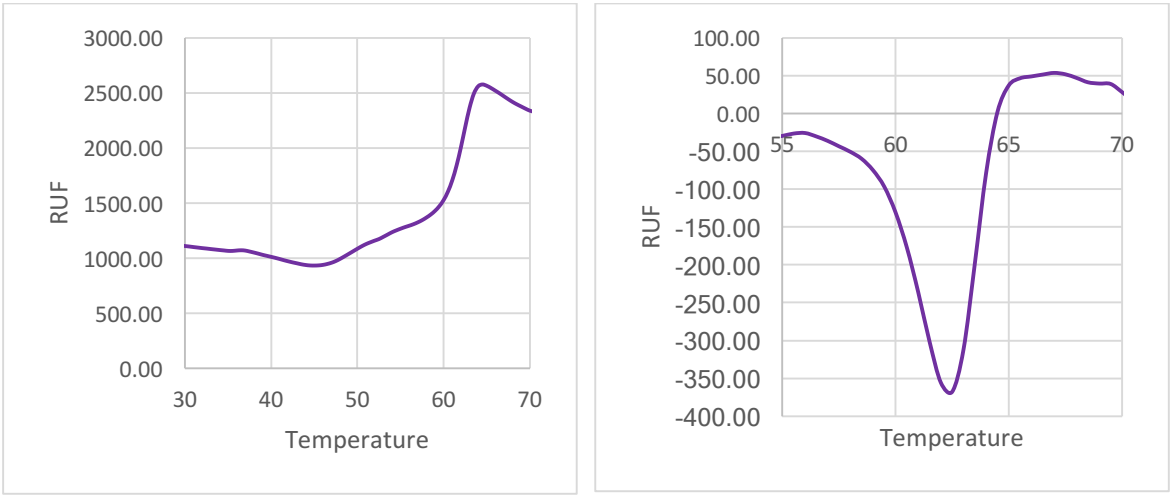

Figure 2-6. Thermal stability of M1PYK. The left figure is the fluorescence readings. The right panel shows the derivative of the left –hand curve. The melting temperature is about 62 ºC.

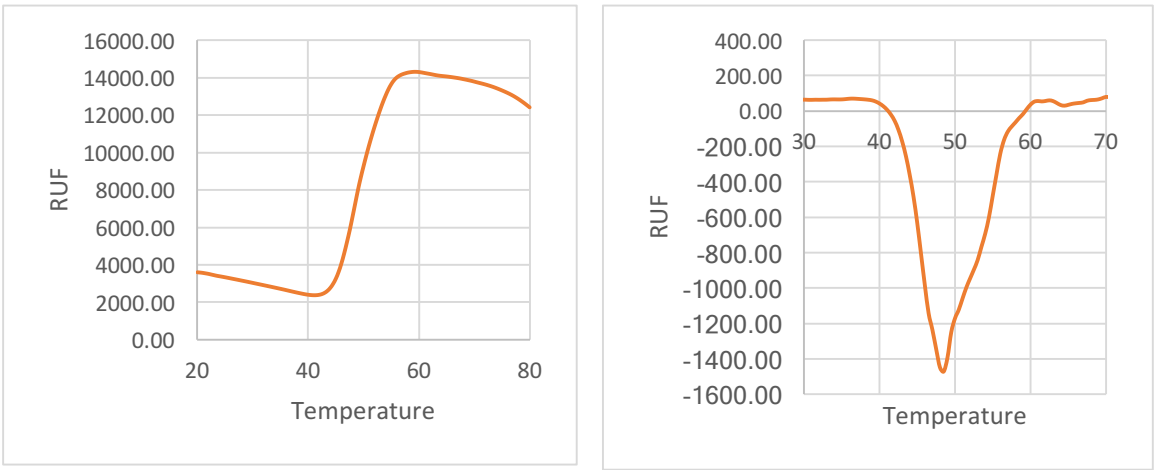

Figure 2-7. Thermal stability of M2PYK. The left figure is the fluorescence readings. The right panel shows the derivative of the left –hand curve. The melting temperature is about 48 ºC.

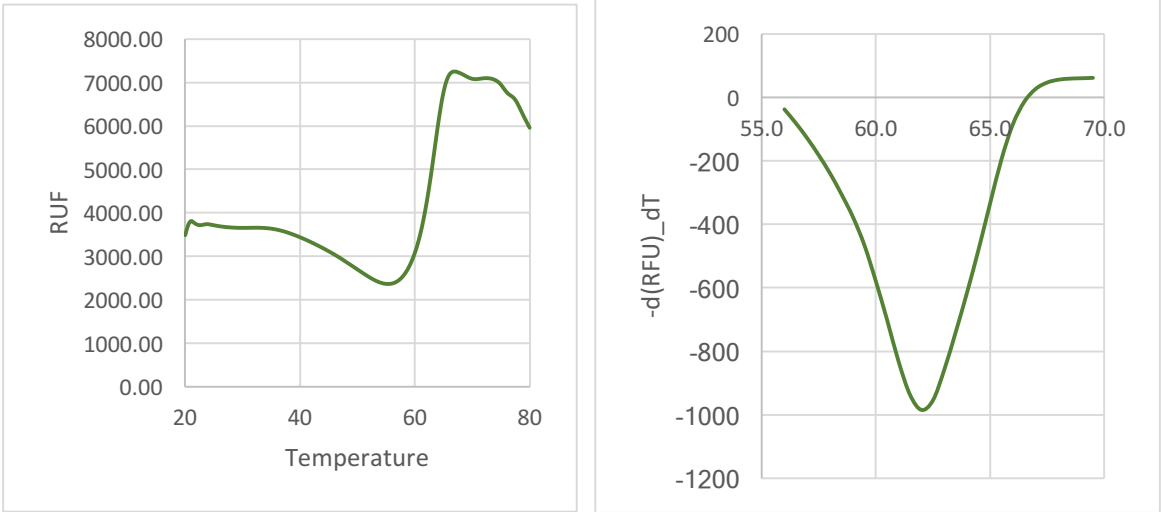

Figure 2-8. Thermal stability of RPYK. The left figure is the fluorescence reading. The right panel shows the derivative of the left –hand curve. The melting temperature is about 62 ºC.

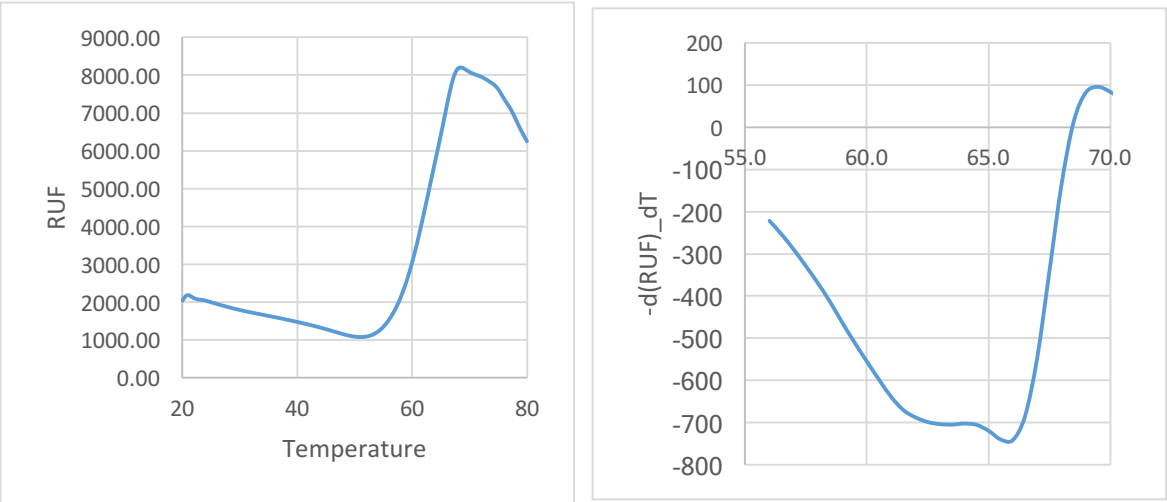

Figure 2-9. Thermal stability of LPYK. The left figure is the fluorescence reading. The right panel shows the derivative of the left –hand curve. The melting temperature is about 66 ^{o}C. LPYK melting curve shows two peaks. This might suggest that LPYK has two unfolding steps.

The melting temperatures of LPYK and RPYK in the following studies in chapter 3 changes from batch to batch by up to 3 ^{o}C. The reason of this inconstancy might be the protein contamination from cell culture step in each batch of protein is different.

2.4 Analytical size exclusion chromatography

2.4.1 Introduction

Analytical size-exclusion chromatography performed as described by (Hugh P Morgan et al., 2013). hPYKs were diluted to 0.1 mg/ml and incubated overnight (18 hours) at room temperature before been loaded independently onto a Superdex 200 PC 3.2/30 gel filtration column pre-equilibrated in PBS-CM at room temperature. A 25µl loop was used and 50 µl was injected at a rate of 0.1 ml/min. The column flow rate was maintained at 0.1 ml/min. UV absorbance was monitored at both 280nm and 214nm.

2.4.2 Results

As shown in Figure 2-10, M1PYK, RPYK, and LPYK demonstrate single peaks, which are believed to be tetramers. There are two peaks in the gel filtration result of M2PYK. Obviously, there exists an equilibrium between the tetrameric and monomeric form. This results suggested that regulation of M2PYK could be due to the effect on the equilibrium, since tetramers are active and monomers are inactive. Regulation of the other isoforms might not be the same mechanism.

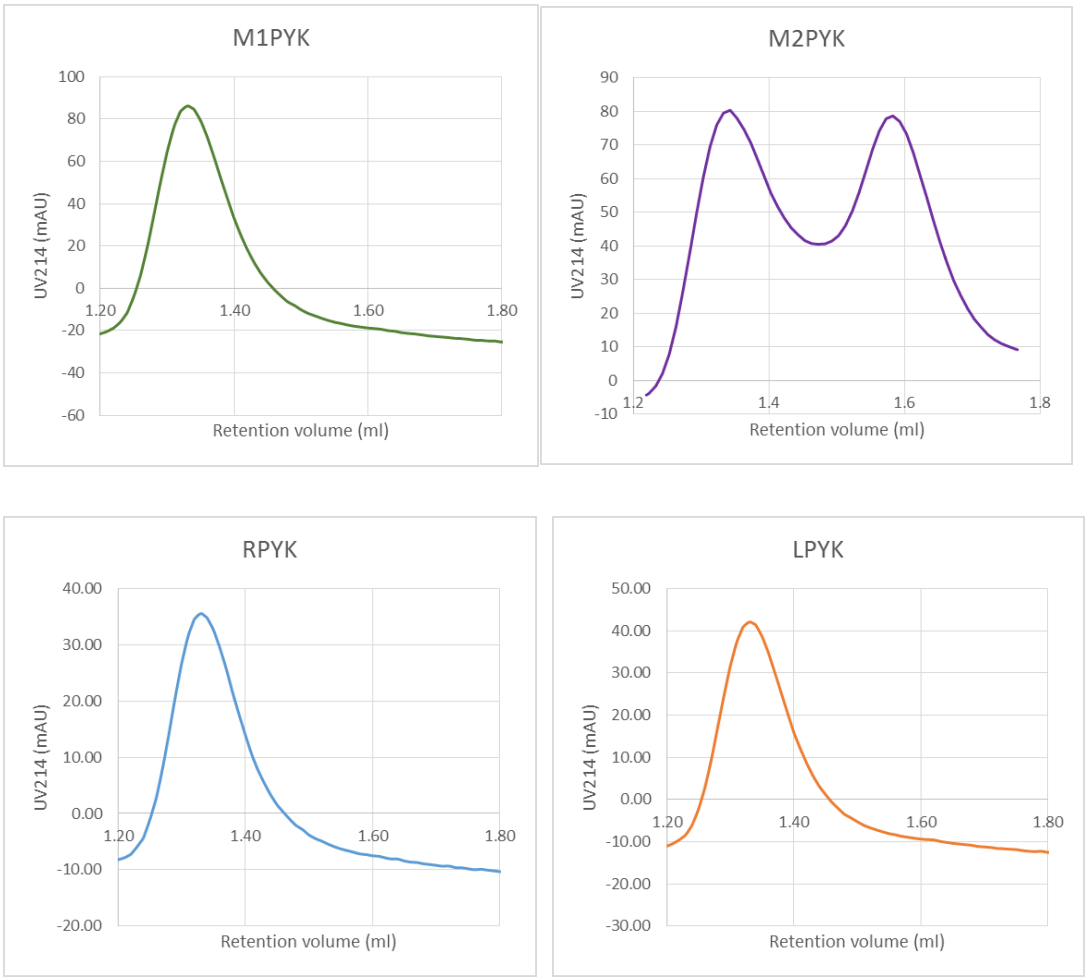

Figure 2-10. Effects of low concentration (0.1 mg/ml) and long-time pre-incubation (18 hours) on the oligomerisation state of all four human PYKs.

2.5 Crystallisation trials

2.5.1 Introduction

Both M1PYK and M2PYK have its wild type structures (PDB: 3SRF and 4FXF) solved (Morgan et al., 2013a). Wild type structures of LPYK and RPYK are still not available. Only truncated or point mutated structures are solved (Holyoak et al., 2013, Valentini et al., 2002). So, we tried to crystalize wild type LPYK and RPYK, M2PYK with several ligands, which are tested to be natural regulators of these isoforms.

Purified M2PYK, RPYK and LPYK samples that had been stored at -80ºC were used for the crystallization trials. Protein samples were thawed on ice and then mixed with ligand buffers to make protein incubated with 50 µM T3, 50 µM T4, 5 mM serine, 5 mM phenylalanine, 5 mM cysteine, or 5 mM F-1,6-BP. Vapour diffusion method was used in the crystallization experiments. The hanging drop technique was carried in stable temperature room at 18 ºC.

The drops were set up by mixing 1.5 µl of well solution with 1.5 µl of 10 mg/ml protein sample containing 5mM of each ligand. The well solution consisted of 6-16% PEG 3350 or PEG 8000, 100mM sodium cacodylate (pH 6), 20 mM triethanolamine-HCl (TEA) buffer (pH 7.2), 50 mM $MgCl_2$, 100mM KCl. Error! Reference source not found. shows the procedure for setting up the well solutions**.** The drops were equilibrated against 1ml of well solution.

Stock solutions	**Final concentration of PEG 3350 or PEG 8000 (%)**					
	6	**8**	**10**	**12**	**14**	**16**
40% PEG 3350/8000	150 µl	200 µl	250 µl	300 µl	350 µl	400 µl
1M Sodium cacodylate pH6.0	100 µl	100 µl	100 µl	100 µl	100 µl	100 µl
1x metals buffer	100 µl	100 µl	100 µl	100 µl	100 µl	100 µl
H_2O	650 µl	600 µl	550 µl	500 µl	450 µl	400 µl
Total volume	1 ml	1 ml	1 ml	1 ml	1 ml	1 ml

Table 3. Procedure for preparation of well solutions used for crystallization. 1x metals buffer was prepared from a 10x metals buffer stock: 200mM TEA, pH 7.2,

500mM $MgCl_2$, 1M KCl. All solutions were filtered using a 0.2µm syringe filter before use.

2.5.2 Results

A summary of crystals generated from conditions above are show in Figure 2-11. These crystals present to be pure and colourless in different shape. X-ray intensity data were collected at Diamond Light Source. Unfortunately, none of these crystals could create enough resolution diffraction intensity images to solve the structure.

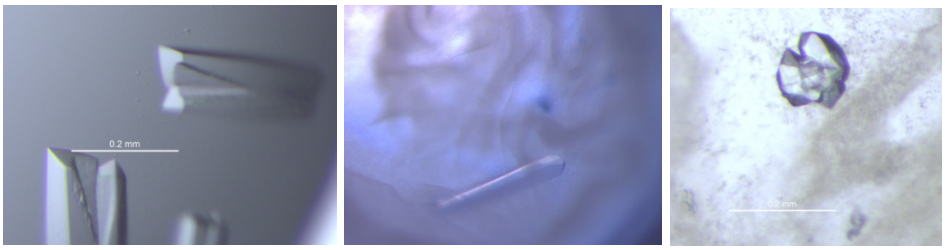

a b c

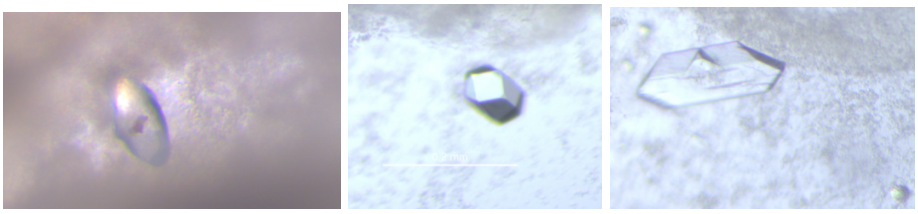

d e f

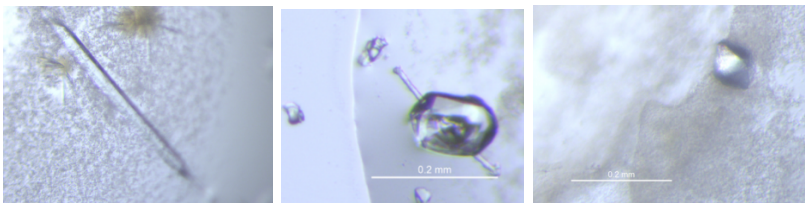

g h i

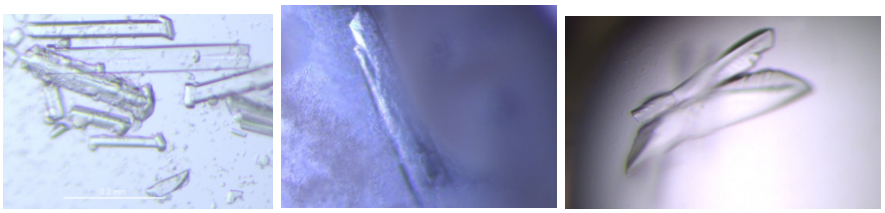

j k l

Figure 2-11. Photos of T3, T4, or amino acids co-crystallized crystals with human PYK isoforms: a, M2PYK with T3; b, LPYK with T3; c, RPYK with T3; d, LPYK with T4. Amino acids co-crystalized with human PYK isoforms: e, RPYK with 0.01mM Cys; f, RPYK with 1mM Cys; g, RPYK with 2mM Phe; h, RPYK with 2mM Ser; i, LPYK with 1mM Cys; j, Human PYK isoforms with natural effectors F-1,6-BP: k, LPYK with 1mM F-1,6-BP; l, RPYK with 1mM F-1,6-BP.

2.6 Enzymatic assays and optimization of pH

2.6.1 Introduction

An LDH coupled enzyme assay has been used widely in the detection of PYKs activity by monitoring the reaction rate (Morgan et al., 2013a, Sun et al., 2011). There are two assumptions made for the assay: 1) reaction 1 is zero order and irreversible. 2) reaction 2 is first order and irreversible (McClure, 1969). A model of one auxiliary enzyme is used to present the model schematically Figure 2-12.

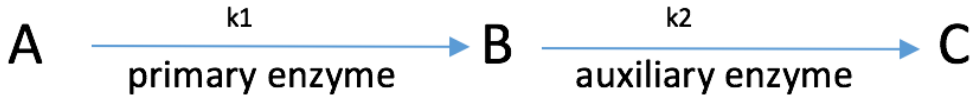

Figure 2-12 Coupled enzyme assay model. Product B is removed by auxiliary enzyme.

The mechanism of the LDH coupled assay is shown in Figure 2-13. In this assay, PYK catalyses the dephosphorylation reaction to generate pyruvate, which is then consumed and transformed to lactate by the next step. Both LDH and NADH were at saturating and the reaction rate of the enzymatic activity assay was measured by the monitoring of light at 340 nm, which is absorbed by NADH (Morgan et al., 2013a).

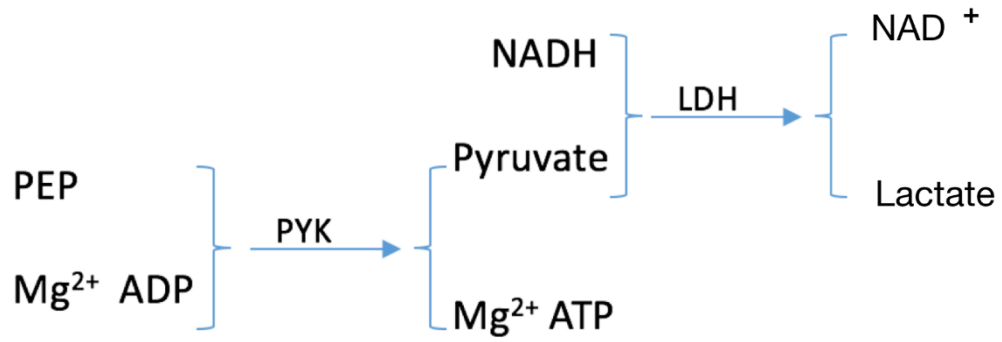

Figure 2-13. LDH-coupled enzyme reactions.

To study the kinetics of PYK with/without effectors, we carried out the assay as follows. The PYK enzyme was sawed on ice for 10 minutes and diluted to 0.002 mg/ml with PBS-CM in the absence/presence of effectors. Five µl of enzyme solution was incubated in each well of a 96-well plate at 37 °C at pH 7.4 for 10 min. Then another 50 µl of assay buffer (PBS-CM supplemented with 20 mM $MgCl_2$, 200 mM KCl, 1 mM NADH, 40 U/ml LDH) of this coupled assay was added and protein solutions of 0.0025mg/ml PYKs were made in PBS-CM with or without addition of additives. The protein solutions were incubated at room temperature for 3 hours to ensure oligomeric equilibrium was reached.

Meanwhile, 25ml 2x assay buffer was made (PBS-CM supplemented with 20mM $MgCl_2$, 200mM KCl, 4mM ADP, 1mM NADH, and 30 U/ml LDH). Five ml of 2x assay buffer was removed and PEP was added to a concentration of 10 mM. Two-fold serial dilutions of PEP were prepared in a 96-well master block (Greiner Bio-one Cat. No. 780270) using 2x assay buffer to yield PEP concentrations ranging from 78 µM to 10 mM (final assay concentrations 39 µM to 5 mM). A multi-channel pipette was used to transfer 50 µl of each PEP dilution to a column of a 96-well plate (Greiner Bio-one Cat. No. 655101).

The reaction (Figure 2.2) was initiated by adding 50 µl of protein solution to the PEP solutions in the 96-well plate using a multi-channel pipette. Final concentrations of reagents were as follows: 0.00125 mg/ml MPYK, 10 mM $MgCl_2$, 100 mM KCl, 2 mM ADP, 15 U/ml LDH, 0.5 mM NADH, and PEP concentrations ranging from 39 µM to 5 mM. Plates were agitated for 10 seconds before measuring the decrease in absorbance at 340 nm for 5 min using a plate reader (SpectraMax M5 multimode plate reader, Molecular Devices). Initial reaction rates were obtained using SoftMax Pro software. Substrate-velocity graphs were plotted using Kaleidograph (Synergy Software).

2.6.2 Results

In this assay, M1PYK, M2PYK, LPYK and RPYK were diluted to 0.001 mg/ml from 23 mg/ml, 19 mg/ml, 16 mg/ml and 8.1 mg/ml, respectively. (a) K_m for M1PYK is stable from pH 7.5 to 6.0. The V_{max} of M1PYK is about 40% higher at pH 6.5-7.0 than at pH 6.0 and pH 7.5. In (b) (c) (d), K_m (PEP) for M2PYK RPYK and LPYK decrease from 3.7, 2.5, and 1.5 mM to 0.17, 0.16 and 0.15 mM, respectively. We conclude that: 1) Optimised pH for M1PYK, M2PYK, LPYK, and RPYK is between 6.5-7.0. 2) Substrate binding of M2PYK, LPYK, and RPYK is tighter in lower pH buffer. Substrate binding of M1PYK is not influenced by pH.

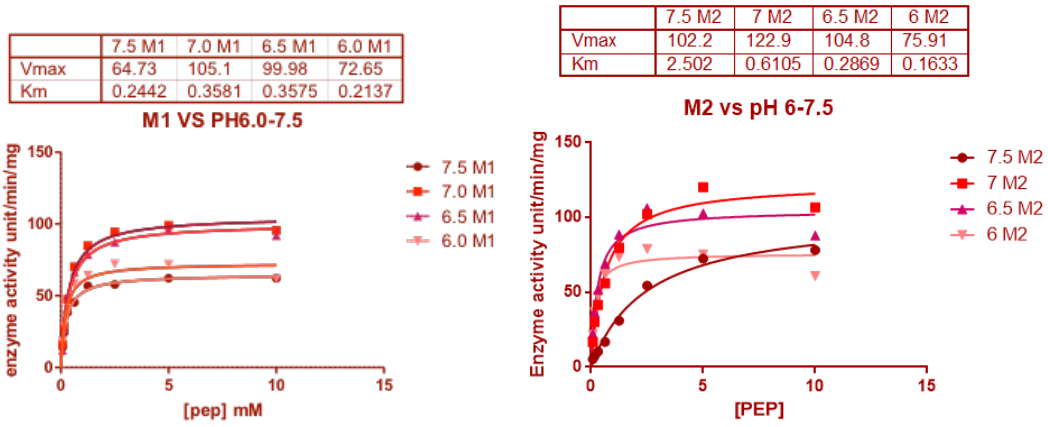

a b

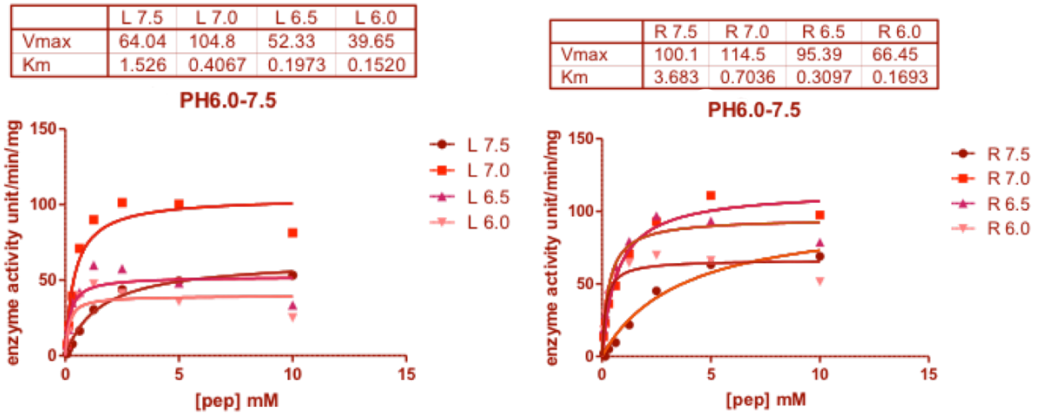

c d

Figure 2-14. The effect of pH on human pyruvate kinases enzyme activity. The unit of V_{max} is unit/mg/ml. One enzyme activity unit will convert 1.0 μmole of PEP to pyruvate per minute at RT at its specific pH. Unit of K_m is mM.

(a) The effect of pH changing influenced the V_{max} of M1PYK. The maximum V_{max} was 105.1 and 99.98 when pH was 7.0 and 6.5, respectively. When pH was 7.5 or 6.0, V_{max} decreased to 64.72 and 72.65.

(b) The effect of pH changing influenced the V_{max} of M2PYK. The maximum V_{max} was 122.9 when pH was 7.0. When pH was 6.0, V_{max} decreased to 75.91.

(c) The effect of pH changing influenced the V_{max} of LPYK. The maximum V_{max} was 104.8 when pH was 7.0. When pH was lower or higher, V_{max} decreased to 64.04, 52.33 and 39.65. The K_m of PEP decreased from 1.5 to 0.15 from pH 7.5 to pH 6.0.

(d) The effect of pH changing influenced the V_{max} of RPYK. The maximum V_{max} was 114.5 and 95.39 when pH was 7.0 and 6.5, respectively. When the pH was 7.5 or 6.0, V_{max} decreased to 64.72 and 72.65. The K_m of PEP decreased from 3.7 to 0.17 from pH 7.5 to pH 6.0.

2.7 Conclusion

All four His_6-tagged human pyruvate isoforms were successfully expressed and purified. The yield is around 12 mg/L and purity is > 95%. The proteins are stable in the storage condition (-80 °C). The protein was used to carry out crystallization trials and a group of crystals were produced, but unfortunately none of them diffract to beyond 5 Å resolution and no structural information has been obtained.

CHAPTER 3. Redox and time dependant regulation on PYK isoforms

3.1 Introduction

Redox status plays an important role in regulation of cell survival. Moderate levels of reducing and oxidative molecules ensure redox homeostasis, which differs significantly between various tissues (Trachootham, Lu, Ogasawara, Nilsa, & Huang, 2008). Redox status affects both signalling protein functions and enzyme activity. More recent works show that redox status regulates enzyme activity significantly. For example, LMW-PTP (low molecule weight protein tyrosine phosphatase) could be oxidized by H_2O_2 (hydrogen peroxide) or nitric oxide which leads to irreversible enzyme activity loss (Chiarugi et al., 2001).

3.1.1 Redox status of cell microenvironment has a profound effect on tumorigenesis

Redox status, the balance between reduced state and oxidized state in the cell microenvironment, is one of the three basic states that need to be altered in fast dividing normal cells and tumour cells (Cairns, Harris, & Mak, 2011). The other two are ATP generation and macromolecule synthesis. Because redox status is important in cancer cell survival (Anastasiou et al., 2011) and is different with normal cells, it is reasonable to suggest that activity of enzymes in the glycolytic pathway might be regulated by redox environment.

3.1.2 Redox influences on cancer cells

In human lung cancer cells, the intracellular concentration of ROS (reactive oxygen species) inhibits M2PYK activity and then promotes metabolic flux to meet the requirement of cell proliferation (Anastasiou et al., 2011). It was also reported that redox state regulates the enzymatic activity and oligomerisation state of M2PYK (Brimacombe et al., 2010).

3.1.3 Redox influences red blood cells

In red blood cells (RBCs), the glycolytic pathway is the only ATP generating path as RBCs do not contain mitochondria. In red blood cells, RPYK catalyses PEP to pyruvate reaction, which generates one molecule of ATP as cofactor and one molecule of pyruvate. Then, the conversion of pyruvate to lactate is catalysed by lactate dehydrogenase. Lactate is secreted as the final product of erythrocyte glycolysis. We know that ATP is a vasodilatory signalling molecule and in response to the increased shear stress will help arteries and capillaries to expand in order to speed up circulation and further regulate human body blood pressure (Wan, Ristenpart, & Stone, 2008).

The canonical role of red blood cells is oxygen and carbon dioxide transportation. They are also equipped with a redox buffer systems (Kuhn et al., 2017). The system contains antioxidant molecules and redox couples, including reduced and oxidized glutathione (GSH/GSSG), ascorbate/dehydroascorbate (vitamin C), and α-tocopherol (vitamin E); and reducing equivalents including NADH and NADPH; and many antioxidant enzymes. This system is very important to maintain haemoglobin in a reduced form and keep alive. It is reported that redox dysfunction is related to anaemia. During the anaemia, the ATP production from glycolysis pathway might change in red blood cells if the redox environment change.

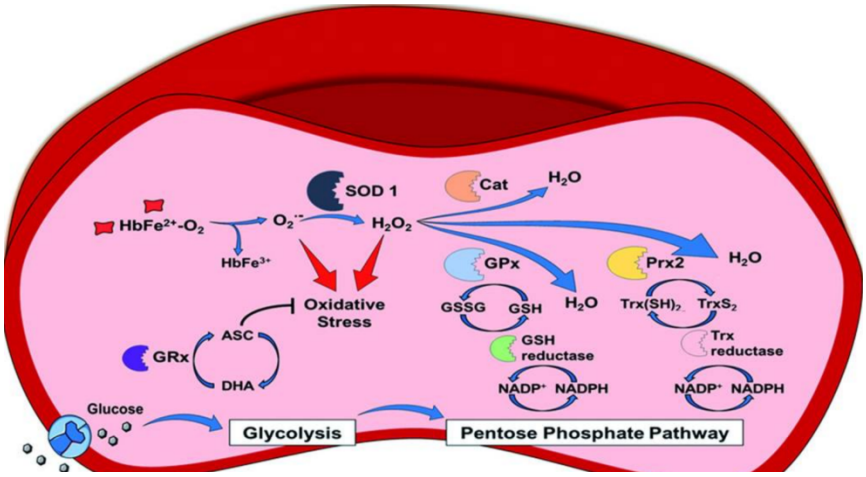

Figure 3-1. Redox regulation in red blood cell from Kuhn's article (Kuhn et al., 2017). Superoxide dismutase (SOD), catalase (Cat), glutathione peroxidase (GPx), and peroxiredoxin 2 (Prx2). oxidized glutathione (GSH/GSSG).

3.1.4 Redox influences liver cells

The redox status of the liver is strictly controlled in hepatocytes by the balance of oxidant and antioxidant molecules. During pathogenic events caused by metabolic and proliferative disorders, oxidative stress is the major cause of liver damage (Cesaratto, Vascotto, Calligaris, & Tell, 2004). Several enzymatic markers and non-enzyme markers related to redox status are used to detect and monitor the level of liver damage. It has also been shown that the rate of ATP generation is related to hypoxia (Z. F. Jiang, Wang, Xu, & Ning, 2017). This suggests that ATP generation is relevant to the redox environment.

To investigate the role of oxidation on PYK and its possible effect on liver damage, we investigated RPYK activity changes under various redox states by adding different amounts of the reductant DTT and the oxidant H_2O_2 to the enzyme assay. The allosteric activator F-1,6-BP was used as a positive control.

3.1.5 Pre-incubation time control is important in enzymatic assays

To explain the strictly controlled pre-incubation time, a diagrammatic drawing of the relationship between pre-incubation time and enzyme activity is shown in Figure 3-2. The enzymatic activity drops gradually during our experiment especially in the enzymatic assay of M2PYK. At different periods of pre-incubation, the difference between the activated, control and inhibited specific enzymatic activity also enlarges by time. It was very important to keep the same pre-incubation time in all experiments performed in the following study. We chose 10 min pre-incubation time to give enough time for protein in solution to reach equilibrium (from the initial oligomeric state to regulated state) and to avoid the inaccuracy by fast pipetting especially when we screen a long list of compounds and at the same time to maintain most enzymatic activity. The pre-incubation time is different from the assay time (usually lasting 200-300 s), in which the 340-nm absorbance was recorded. The assay time always starts when the protein solution (enzyme or enzyme with ligand) was added into the PEP solution (PEP, ADP, $MgCl_2$, KCl, LDH, NADH).

The only exception about pre-incubation time in this study is the time-dependant assay. For example, in Chapter 3.4.2 the pre-incubation time is from 0 min to 150 min, and in Chapter 3.5 the pre-incubation time is from 0 min to 20 min.

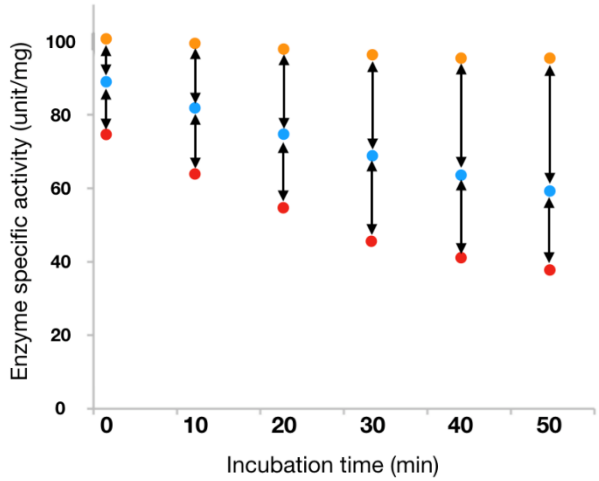

Figure 3-2. Diagrammatic drawing of the relationship between pre-incubation time and enzyme activity. Orange dots represent enzymatic activity of M2PYK with activator; blue dots are M2PYK alone; red dots are M2PYK with inhibitor.

3.2 Regulation of four human isoforms of PYK by reducing reagent

Four human PYKs work in various reducing environments and with natural regulators. To compare the effects of reducing reagent on these isoforms, we tested all four isoforms of hPYK via a series of enzymatic assays by adding 1 mM DTT and 1 mM F-1,6-BP. DTT (dithiothreitol) is a common reducing reagent used in protein assays to prevent oxidation and disulphide bond formation between cysteine groups in proteins. All experiments were carried out under sub-saturating substrate concentrations with an incubation time of 10 min.

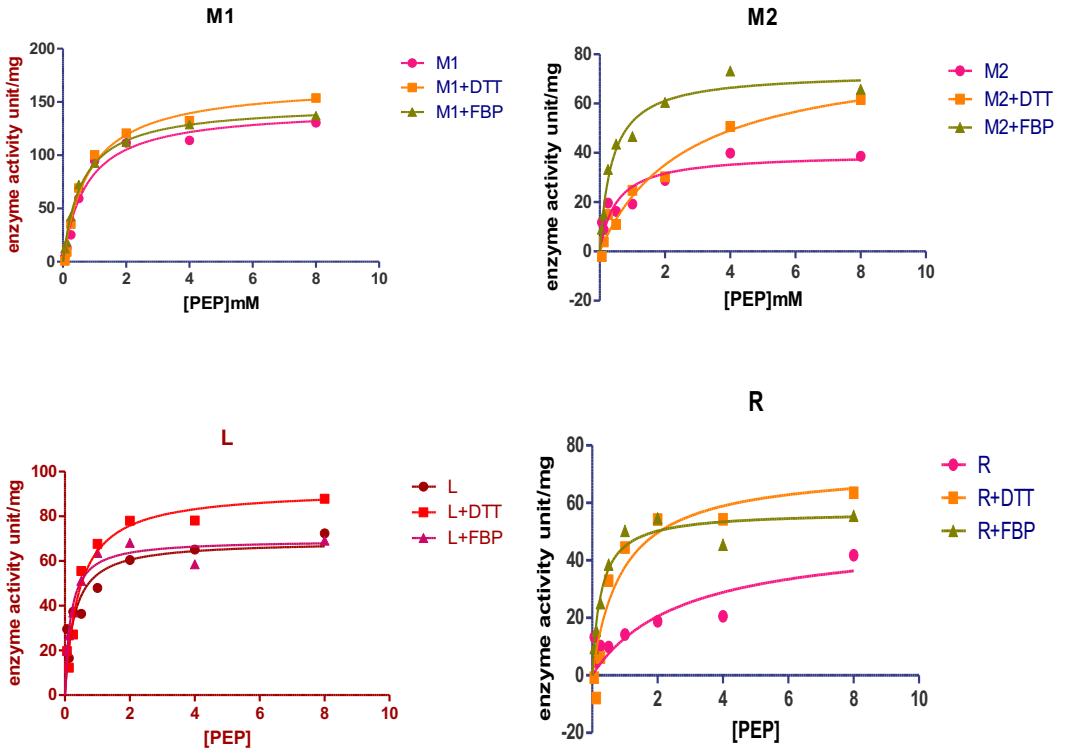

Figure 3-3. Four isoforms of human PYK enzyme activity data in addition of 1mM DTT, 1mM and control (protein alone). Assay condition is that 2mM ADP, 100mM KCl, 10mM $MgCl_2$, in PBS-CM, pH 7.4, at room temperature. The pre-incubation time with ligands after dilution was 10 minutes. One enzyme activity unit will convert 1.0 μmole of PEP to pyruvate per minute at pH 7.6 at RT.

		M1PYK	M2PYK	LPYK	RPYK
control	V_{max} (unit/mg)	144.3	39.67	68.9	48.88
	Km (mM)	0.74	0.51	0.28	2.8
DTT	V_{max} (unit/mg)	168.1	81.75	92.16	72.56
	Km (mM)	0.82	2.66	0.43	0.93
F-1,6-BP	V_{max} (unit/mg)	148	72.7	69.45	57.02
	Km (mM)	0.61	0.38	0.18	0.27

Table 4. A table of four isoforms K_m and V_{max} values.

From the above assay, we could conclude that DTT seems to up regulate all PYKs even V_{max} for M1PYK is increased by 10% even though it is the most stable isoform

and is constitutively active. To exclude the effect of DTT on LDH, we tested 2mM DTT with LDH and found out that DTT did not change the activity of LDH. Another observation is that the effector molecule F-1,6-BP activates M2PYK, RPYK and LPYK but not M1PYK, confirming earlier reports (Carminatti, Jiménez de Asúa, Leiderman, & Rozengurt, 1971; Jurica et al., 1998; Giovanna Valentini et al., 2002).

3.3 The effect of redox on activity of RPYK

Redox regulation may play a particularly important role in blood given the high oxygen concentrations. Glycolysis may also play a different role in red blood cells as they share the same characteristic as blood-stream form trypanosomes in that they do not have a functioning mitochondrion and they rely on glycolysis to produce ATP rather than oxidative phosphorylation (Bakker, Michels, Opperdoes, & Westerhoff, 1997; Tilton, Seaman, Carriero, & Piomelli, 1991). To investigate the potentially unique regulation of RPYK, we studied enzyme activities in a range of reducing and oxidized conditions, and compared them with the effect of the allosteric activator F-1,6-BP.

The first experiment was to measure the effect of reducing agent dithiothreitol (DTT) on the activity of RPYK. DTT ($HSCH_2CH(OH)CH(OH)CH_2SH$) is a common reducing reagent used in protein assays to prevent oxidation and disulphide bond formation between cysteine groups in proteins.

As described in chapter 2, the enzyme activity assay was set up at room temperature (25ºC) and performed in a multi-plate reader at 37ºC.

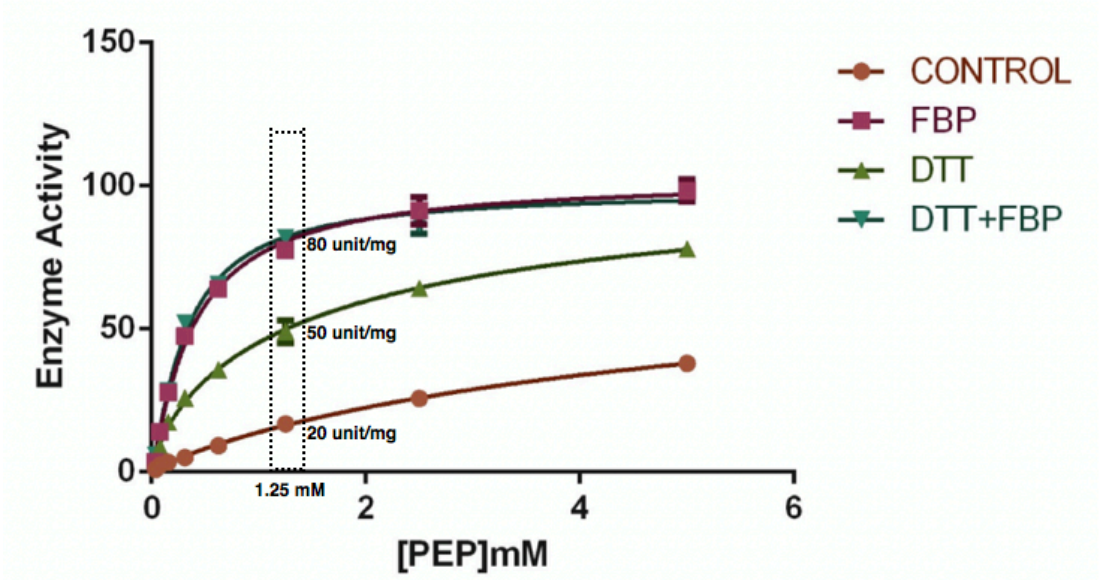

	RPYK	RPYK+FBP	RPYK+DTT	RPYK+DTT+FBP
V_{max} (unit/mg)	84.6	102.5	110.5	98.4
Km (mM)	6.3	0.39	1.6	0.33

Figure 3-4. Enzyme activity assay with PEP titration shows that both F-1,6-BP and DTT could activate RPYK. Assay conditions are pH 8.0, 25 ºC, 2mM ADP (saturating). Unit definition is that one unit will convert 1 µmol of PEP to pyruvate per min at pH 8.0 at 25 ºC. The pre-incubation time with ligands after dilution was 10 minutes.

DTT (2mM) on its own can also activate RPYK, activity at 1.25 mM PEP (sub-saturating) from about 20 unit/mg to 50 unit/mg and at the same time, K_m of RPYK reduced from 6.338 mM to 1.62 mM. Compared with natural activator F-1,6-BP, DTT seems to be a weaker activator. F-1,6-BP activates RPYK from 20 unit/mg to around 80 mg/ml as shown in Figure 3-4. When DTT and F-1,6-BP are added together, there is no additional effect over that of F-1,6-BP alone.

Can oxidation affect RPYK activity?

Firstly, we tested whether dissolved oxygen in buffer might provide an oxidizing environment. RPYK protein in degassed buffer shows marginal activation compared

with non-degassed buffer as the K_m (PEP) increased from 3 mM to 14.71 mM in the more oxidising environment. The V_{max} of the non-degassed buffer could not be accurately determined because of poor curve fitting.

Secondly, we test the effect of reducing agent on RPYK activity. Changing DTT concentration from 2mM to 1mM results in a drop of V_{max} from 92.06 unit/mg to 62.96 unit/mg and Km increases four-fold from 0.37 mM to 1.37 mM.

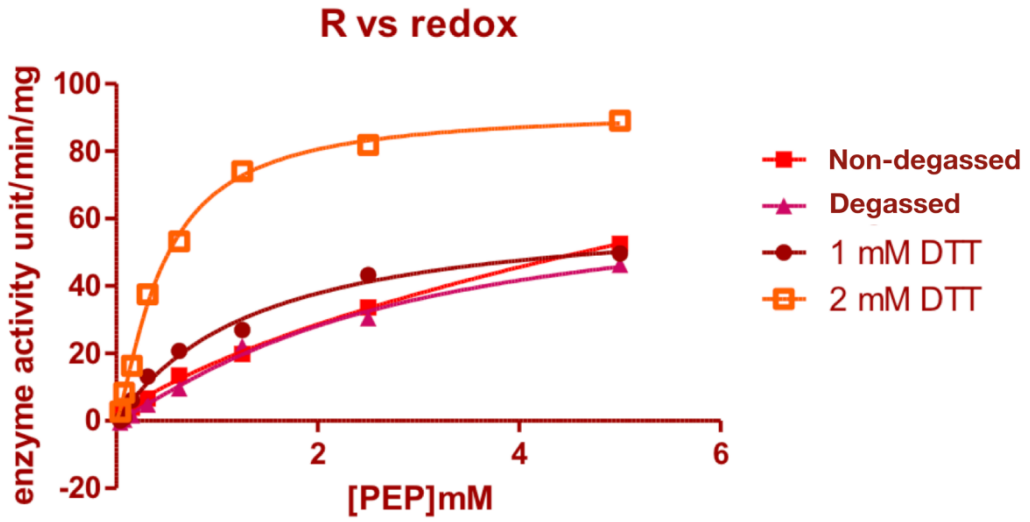

		Non-degassed	Degassed	Degassed +1mM DTT	Degassed +2mM DTT
control	V_{max} (unit/mg)	Fitting failure	67.1	63.0	92.1
	K_m (mM)	14.7	3.1	1.4	0.36

Figure 3-5. Enzymatic assay of RPYK with reducing reagent DTT. Assay condition are pH 8.0, 25 ºC, 2mM ADP (saturating). Unit definition is that one unit will convert one µmol of PEP to pyruvate per min at pH 8.0 at 25 ºC. The pre-incubation time with ligands after dilution was 10 minutes.

These results show that the enzymatic activity of RPYK is much higher in the reduced state (K_m (non-degassed)>K_m (degassed) >K_m (1mM DTT) >K_m (2mM)). A likely explanation for these observations might be that cysteine oxidation in RPYK results in low enzymatic activity.

3.3.1 How do Redox reagents affect thermal stability of RPYK and LPYK?

Thermal denaturation assay results show that DTT increases melting temperatures of RPYK and LPYK. In the presence of 1mM DTT the melting temperatures of RPYK and LPYK are increased by 1.5ºC and 3ºC respectively indicating that DTT has a stabilising effect on the structure of the enzyme as demonstrated in Figure 3-5 b. On the other hand, the melting temperatures of protein with 1 mM H_2O_2 for both RPYK and LPYK showed almost the same melting temperature compared with the control in Figure 3-4 and Figure 3-5. In addition, as a positive control experiment, enzyme with 1mM F-1,6-BP increased the melting temperature of RPYK and LPYK by 2ºC and 1ºC, respectively.

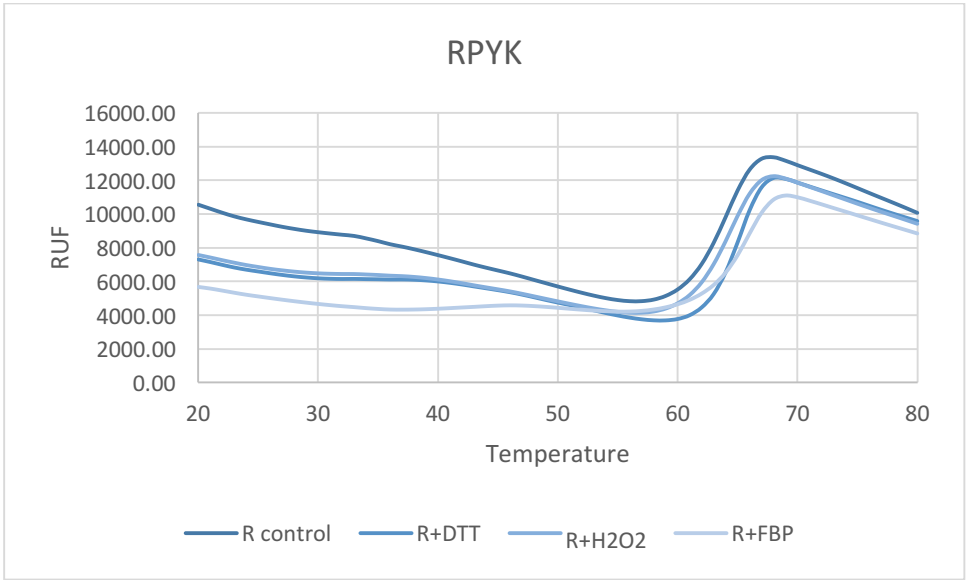

(a)

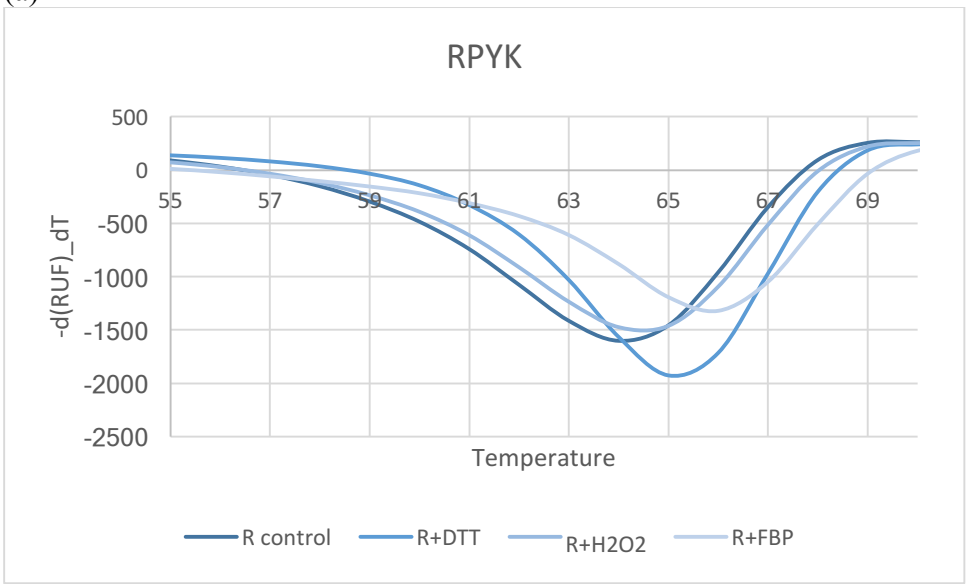

(b)

Figure 3-6. Thermal denaturation data for RPYK and in the presence of 1mM DTT, 1mM H_2O_2, 1mM F-1,6-BP or with no additives. The upper figure shows the change in fluorescence on increasing temperature. The bottom panel is the rate of change of fluorescence with respect to temperature. The melting temperature is 64 ºC (R control), 65 ºC (R+H_2O_2), 64.5 ºC (R+DTT), and 66 ºC (R+F-1,6-BP).

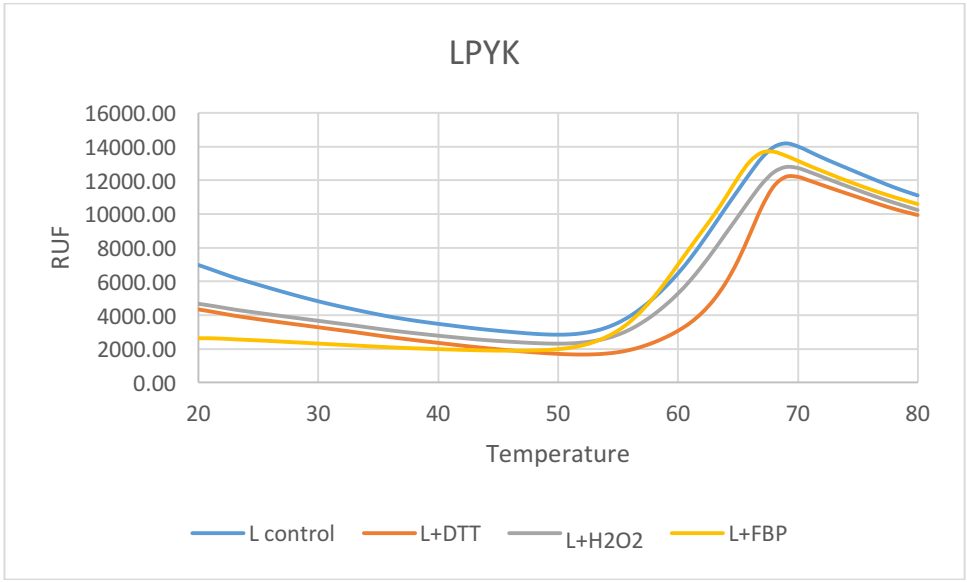

(a)

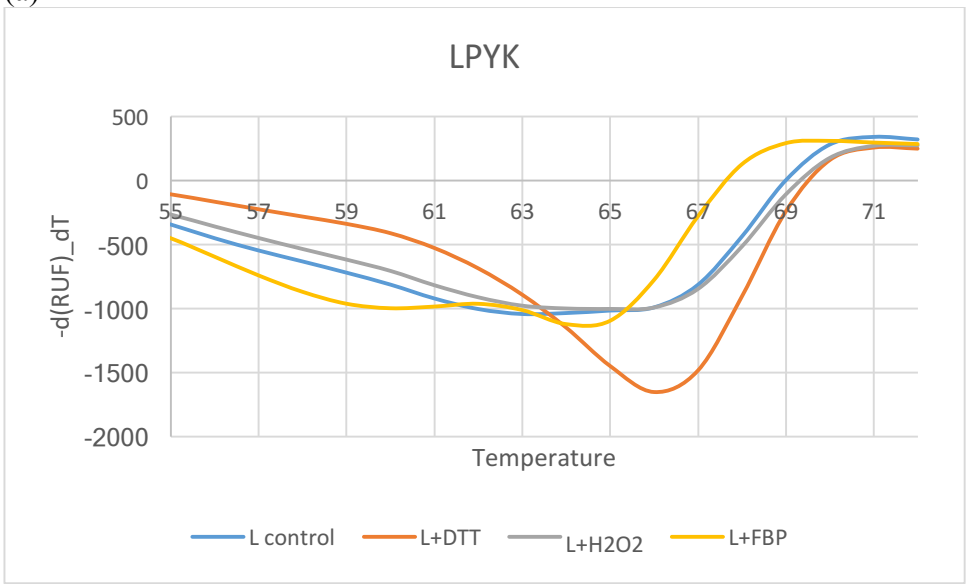

(b)

Figure 3-7. Thermal denaturation data for RPYK and in the presence of 1mM DTT, 1mM H_2O_2, 1mM F-1,6-BP or with no additives. The upper figure shows the change in fluorescence on increasing temperature. The bottom panel is the rate of change of fluorescence with respect to temperature. The melting temperature is at about 66 ºC (L control), 66 ºC (L+DTT), 66 ºC (L+H_2O_2), and 64.5 ºC (L+F-1,6-BP).

Melting temperature of both LPYK and RPYK were not influenced much by H_2O_2 but both DTT and F-1,6-BP show measurable effects with increased stability correlating with increased enzyme activity. To further investigate how reducing reagent, stabilise

PYKs, we studied three concentrations (0.1mM, 1mM, 10mM) to find out whether the strength of reducing reagent would affect the protein stability.

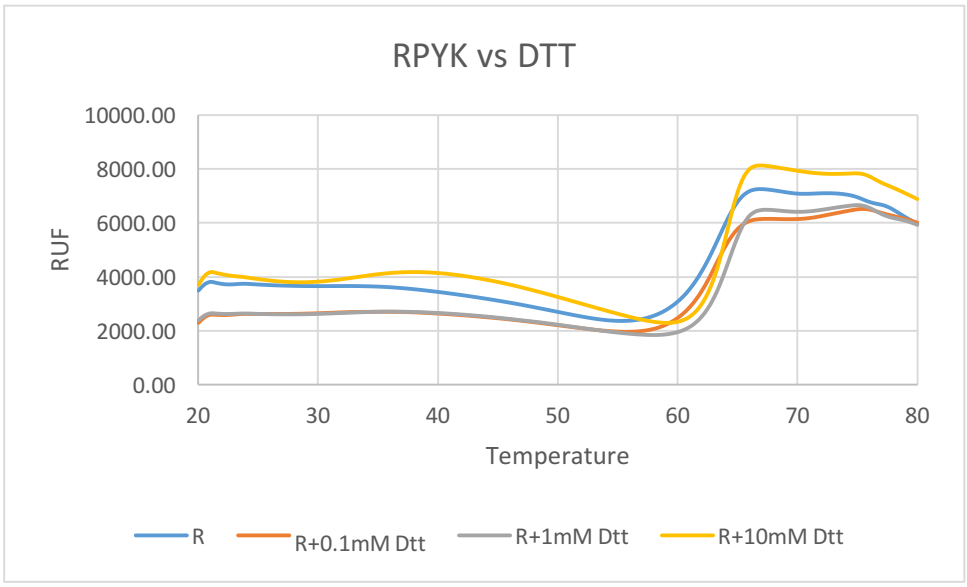

(a)

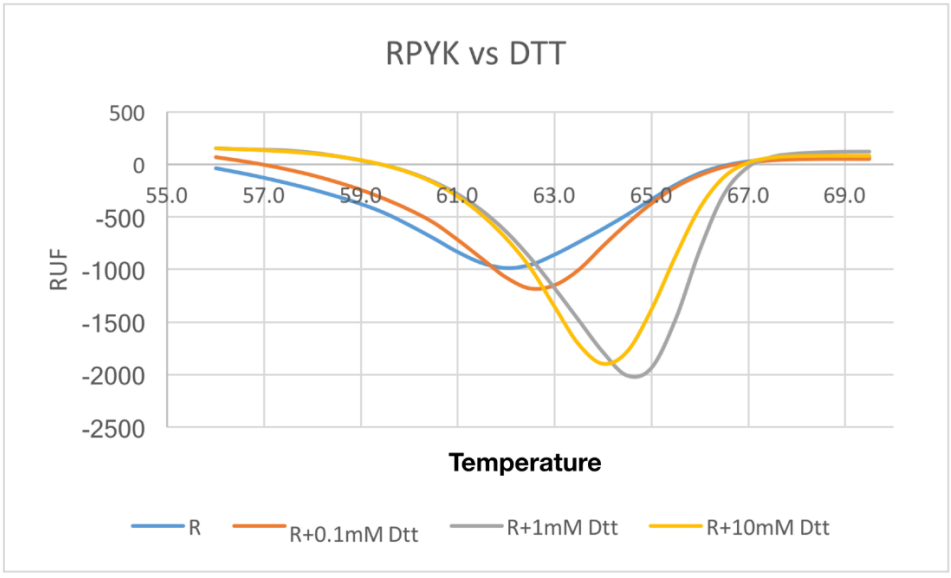

(b)

Figure 3-8. Thermal denaturation data for RPYK and in the presence of 0.1mM DTT, 1mM DTT, 10mM DTT or with no additives. The upper figure shows the change in fluorescence on increasing temperature. The bottom panel is the rate of change of fluorescence with respect to temperature. The melting temperature is at about 62 ºC (R control), 62.5 ºC (R+0.1mM DTT), 64.5 ºC (R+1mM DTT), and 64 ºC (R+10mM DTT).

Figure 3-8 shows clearly that increasing reducing reagent concentration increases RPYK stability. By adding 0.1mM DTT, 1mM DTT and 10mM, melting temperature was increased by 0.5 ºC, 2.5 ºC and 2 ºC. We could also conclude that around 1mM is the concentration that gives maximum effect on melting temperature. It is not clear why higher concentrations (10mM) of DTT should have a lesser effect. The reason might be the saturation of DTT is just 1 mM but to confirm this phenomenon we need to repeat to show reproducibility.

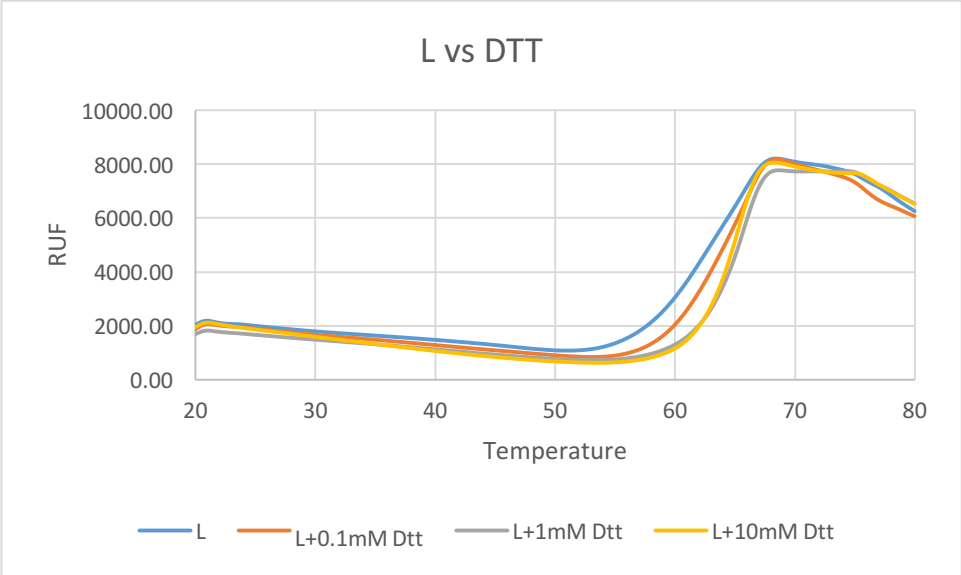

(a)

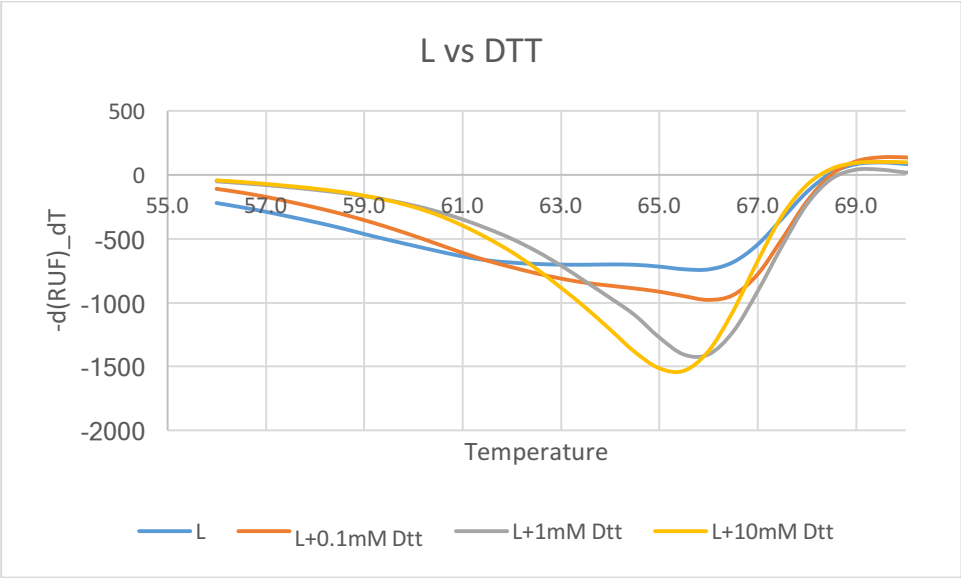

(b)

Figure 3-9. Thermal denaturation data for LPYK and in the presence of 0.1mM DTT, 1mM DTT, 10mM DTT or with no additives. The upper figure shows the change in fluorescence on increasing temperature. The bottom panel is the rate of change of fluorescence with respect to temperature. The melting temperature is at about 66ºC (L control), 66 ºC (L+0.1mM DTT), 65.5 ºC (L+1mM DTT), and 65.5 ºC (L+10mM DTT).

Figure 3-9 shows that the melting temperature of LPYK seems to be stable and not affected by DTT much (control 66 ºC, + 0.1 mM DTT 66 ºC, + 1 mM DTT 65.5 ºC, + 10 mM DTT 65.5 ºC). In addition, the melting temperature of protein alone is about 66 ºC, which is much higher than 63 ºC in the Figure 4-4. This might cause by different batch protein contains different protein contaminations, which might affect melting temperature. However, we still could see the trend that the curve goes deep as the DTT concentration increased from 0mM to 1mM. 1mM and 10mM DTT shows almost the same effect on LPYK.

3.4 Time dependant regulation

An important observation made over the course of running these various enzyme activity experiments was that activity was significantly dependent on the pre-

incubation time after diluting the protein and longer pre-incubation times could significantly reduce enzyme activity. To explore this phenomenon, we carried out a series of time dependant enzyme assays to test how pre-incubation time regulates the enzyme activities of human pyruvate kinase. In particular, it is important to understand the mechanism of this time-dependent change which could be the result of a slow dissociation (or conformational change) of the active tetrameric form in a more dilute environment. Alternatively, it may be an oxidation effect or perhaps gradual denaturation of the protein. To explore these possibilities, we set out to answer the following questions.

- Do all human PYK isoforms activity change over time?
- Do reducing reagent and natural activator affect the time-dependant activity change?
- Is the time-dependant activity changing reversible?

3.4.1 Single point assay shows that PYKs loose enzyme activity after dilution

To examine this phenomenon more carefully, we have studied enzymatic activity at a series of pre-incubation times. All four isoforms were studied using the coupled enzyme assay described in chapter 2. After dilution from high storage concentration (23mg/ml to 0.001mg/ml), M1PYK activity maintained at about 160 unit/mg. However, the other three isoforms, M2PYK, LPYK and RPYK, which were stored at 13.0mg/ml, 16mg/ml and 8.1mg/ml, respectively, lost most of their activity after dilution. Decreasing protein activity is much higher in the first 50 minutes during

which time half of the activity is lost; another 300 minutes is required to decrease activity to near zero.

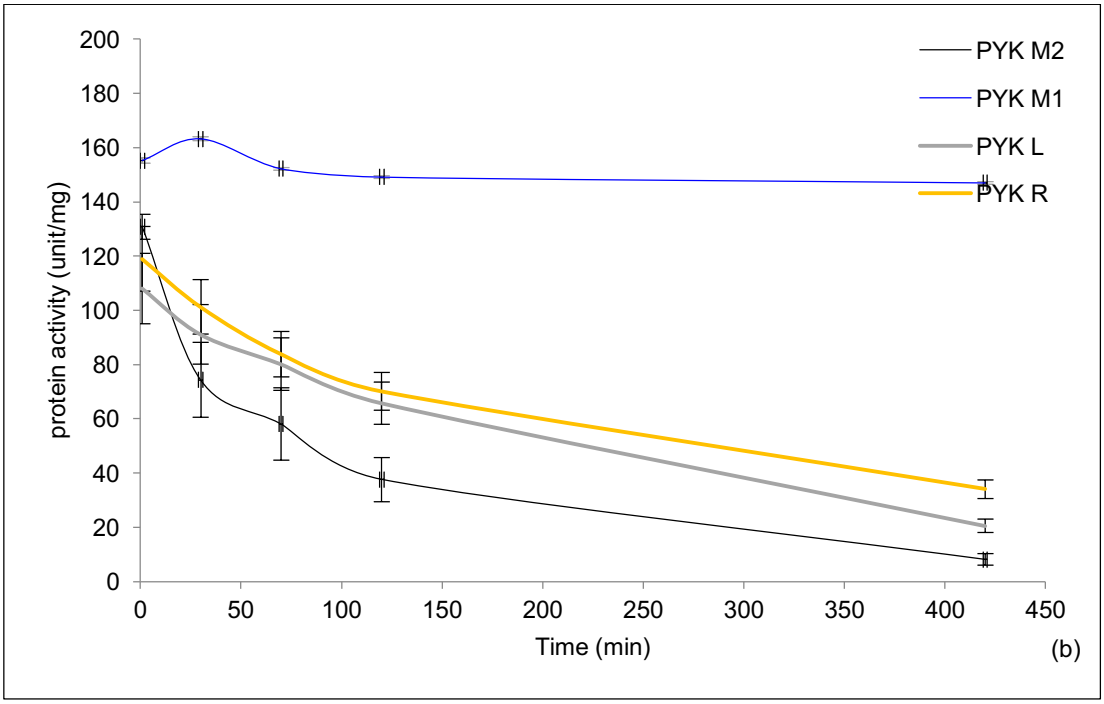

Figure 3-10. The horizontal axial represents pre-incubation time from 0 min to 420 min. M1PYK (blue) shows steady activity; all other three isoforms activity decreases after dilution immediately. Assay condition are pH 8.0, 25 ºC, 1mM ADP (sub saturating). Unit definition is that one unit will convert one µmol of PEP to pyruvate per min at pH 8.0 at 25 ºC.

We can see from Figure 3-8 that the only isoform that maintains enzyme activity is M1PYK. Even after 150 minutes, M1PYK was still fully active. The other 3 isoforms lost their activity rapidly; the half-lives of M2PYK, RPYK and LPYK activities are 30 minutes, 200 minutes and 150 minutes, respectively.

The most likely reasons for the differences in behaviour of the four human isoforms are:

- Constitutively active M1PYK is most stable and least prone to dissociation on dilution
- Cysteines especially in RPYK are more prone to oxidation

To investigate these possibilities, a series of further experiments were carried out.

3.4.2 Reducing reagent and/or activator slows down loss of activity

In the previous Chapter 3.3.1, we showed the effect of reducing reagent DTT and F-1,6-BP on activities of all four human PYK isoforms. To further study the time-dependent activity loss of RPYK, a matrix of conditions was designed to study the effect of DTT and F-1,6-BP over time (outlined in Table 5). A key parameter in the activity assay is the time taken from diluting the protein from its stock concentration (> 10 mg/ml) to the concentration used to measure rate of reaction (< 0.01 mg/ml). This 'pre-incubation time' was studied over a wide time range from 0 minute to 150 minutes.

	M1PYK	M2PYK	LPYK	RPYK
0 min	+FBP/+DTT -FBP/+DTT +FBP/-DTT -FBP/-DTT	+FBP/+DTT -FBP/+DTT +FBP/-DTT -FBP/-DTT	+FBP/+DTT -FBP/+DTT +FBP/-DTT -FBP/-DTT	+FBP/+DTT -FBP/+DTT +FBP/-DTT -FBP/-DTT
10 mins	+FBP/+DTT -FBP/+DTT +FBP/-DTT -FBP/-DTT	+FBP/+DTT -FBP/+DTT +FBP/-DTT -FBP/-DTT	+FBP/+DTT -FBP/+DTT +FBP/-DTT -FBP/-DTT	+FBP/+DTT -FBP/+DTT +FBP/-DTT -FBP/-DTT
15 mins	+FBP/+DTT -FBP/+DTT +FBP/-DTT -FBP/-DTT	+FBP/+DTT -FBP/+DTT +FBP/-DTT -FBP/-DTT	+FBP/+DTT -FBP/+DTT +FBP/-DTT -FBP/-DTT	+FBP/+DTT -FBP/+DTT +FBP/-DTT -FBP/-DTT
60 mins	+FBP/+DTT -FBP/+DTT +FBP/-DTT -FBP/-DTT	+FBP/+DTT -FBP/+DTT +FBP/-DTT -FBP/-DTT	+FBP/+DTT -FBP/+DTT +FBP/-DTT -FBP/-DTT	+FBP/+DTT -FBP/+DTT +FBP/-DTT -FBP/-DTT
150 mins	+FBP/+DTT -FBP/+DTT +FBP/-DTT -FBP/-DTT	+FBP/+DTT -FBP/+DTT +FBP/-DTT -FBP/-DTT	+FBP/+DTT -FBP/+DTT +FBP/-DTT -FBP/-DTT	+FBP/+DTT -FBP/+DTT +FBP/-DTT -FBP/-DTT

Table 5. All four isoforms of human PYKs were tested at 0.001mg/ml with varying pre-incubation times (from 0 min to 150 mins) in four sets of PBS buffer (+F-1,6-BP/+DTT, -F-1,6-BP/+DTT, +F-1,6-BP/-DTT, -F-1,6-BP/-DTT). LPYK, RPYK, M1PYK and M2PYK protein were diluted to 0.001mg/ml from 16mg/ml, 8.1mg/ml, 23mg/ml and 13mg/ml, respectively. Assay condition are pH 8.0, 25 ºC, 2mM ADP (saturating). Unit definition is that one unit will convert one µmol of PEP to pyruvate per min at pH 8.0 at 25 ºC.

For each enzyme, four complete sets of enzymatic curves were measured. The effector F-1,6-BP has been found to stabilise the tetramer form of M2PYK (Morgan et al., 2013a). We hypothesised that one reason of loss activity over time especially at dilute concentrations would be the dissociation of active tetramers into inactive monomers. Therefore, the enzyme activity was measured with and without F-1,6-BP with pre-incubation time from 0 to 150 minutes. Similarly, the effect of reducing agent incubated over the same period was tested at the same time.

In the following sets of experiments, each condition for each isoform was carried out in triplicate in two completely independent studies. For all experiments, the results were highly consistent between two independent runs. Graphs for only one of the sets of experiments are shown below.

Enzyme assay results for M1PYK

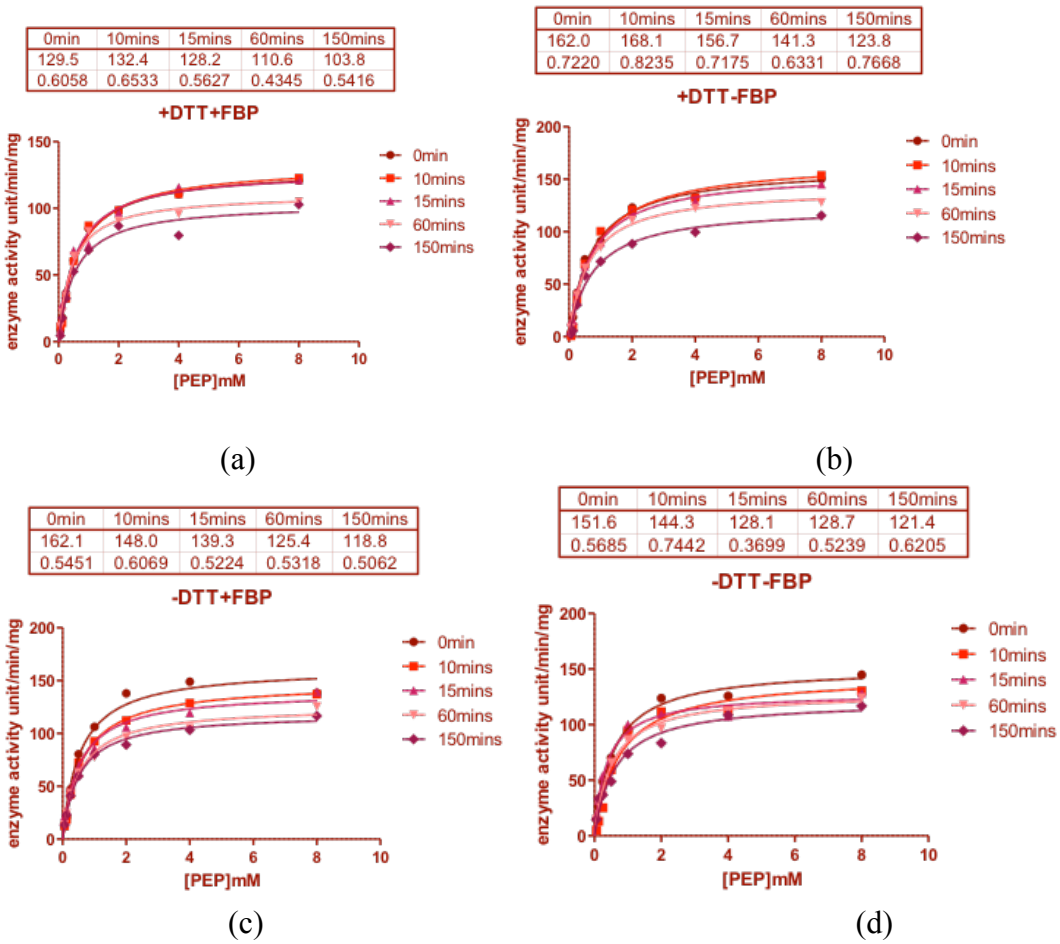

Figure 3-11. The effect of pre-incubation time, DTT and F-1,6-BP on M1PYK enzymatic activity. The first line of the boxes gives the V_{max}, the second line K_m values. (a)The effect of dilution reduced V_{max} from 129.5 to 103.8 in 150 minutes with 1mM DTT and 1mM F-1,6-BP in solution, (b) reduced V_{max} from 162.0 to 123.8 in 150 minutes with 1mM DTT in solution. K_m of PEP was stable, (c) reduced V_{max} from 162.1 to 118.8 in 150 minutes with 1mM F-1,6-BP in solution, and (d) reduced V_{max} from 151.6 to 121.4 in 150 minutes in PBS solution.

Figure 3-11 shows that at time zero point, V_{max} for M1PYK is 150 unit/mg compares to V_{max} (160 unit/mg) of M1PYK when F-1,6-BP was added. This 10% difference in activity is not significant and fits with the published literature which shows no significant increase in activity of M1PYK on addition of F-1,6-BP (Iovine et al.). Similarly, addition of 1 mM DTT does not significantly affect V_{max} (160 unit/mg) of M1PYK. However, when DTT and F-1,6-BP are added together, V_{max} decreases by 20% compared with the other three conditions. Therefore, the question is whether there

is a genuine inactivating effect on adding both DTT and F-1,6-BP together. However, this is difficult to reconcile with the observation that individually DTT and F-1,6-BP slightly activate the enzyme.

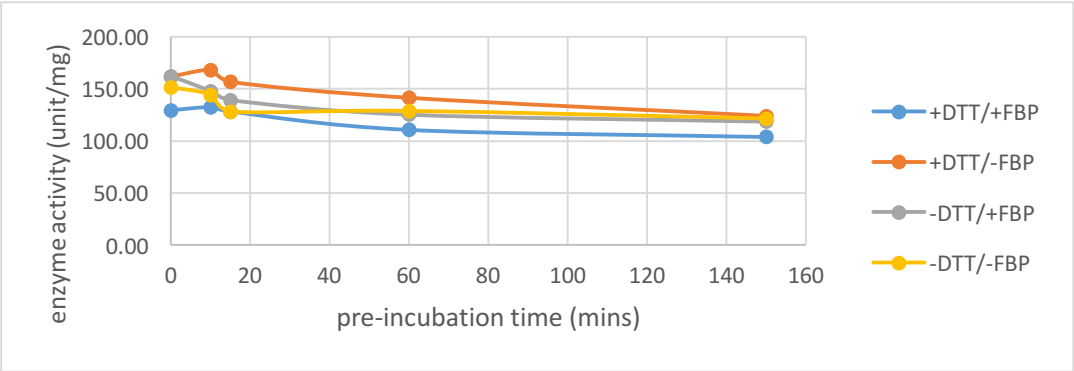

Figure 3-12. V_{max} of M1PYK in 150 minutes pre-incubation in four conditions.

Figure above shows that V_{max} is not strong affected by addition of F-1,6-BP and DTT. The time dependant enzyme activity loss was not obvious for M1PYK. Half-life of protein activity was longer than 150 minutes in all four conditions as after 150 minutes' pre-incubation protein activities are above 100 unit/mg. According to stable K_m data (range from 0.5 mM to 0.7 mM), substrate binding was not affect by pre-incubation, F-1,6-BP or reducing agent.

The effect of DTT, F-1,6-BP, and pre-incubation time on the V_{max} of M2PYK

0 min	10mins	30mins	60mins	150 mins
82.45	69.40	60.36	55.17	38.35
0.3866	0.2491	0.1818	0.2159	0.3941

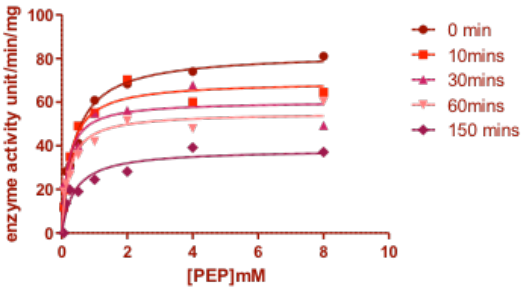

(a)

0 min	10mins	30mins	60mins	150 mins
89.41	81.75	47.89	27.03	23.17
1.225	2.655	1.000	1.424	0.7130

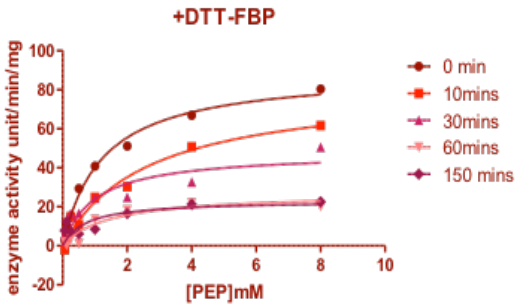

(b)

0 min	10mins	30mins	60mins	150 mins
84.93	72.70	54.16	35.98	27.13
0.2437	0.3808	0.1559	1.067	0.2063

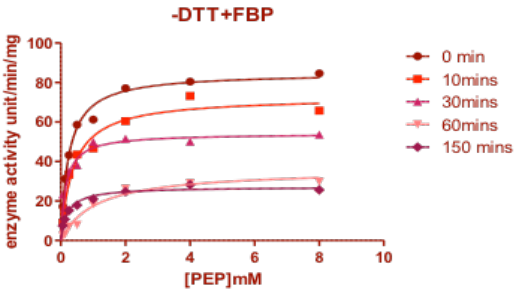

(c)

0 min	10mins	30mins	60mins	150 mins
103.0	39.67	19.86	4.703	11.63
1.774	0.5109	0.04187	2.607e-013	0.2804

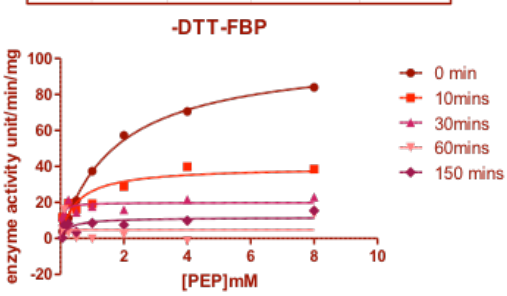

(d)

Figure 3-13. The effect of pre-incubation time, DTT and F-1,6-BP on M2PYK enzymatic activity (a) The effect of dilution reduced V_{max} from 82.5 to 38.4 in 150 minutes with 1mM DTT and 1mM F-1,6-BP in solution, (b) reduced V_{max} from 89.4 to 23.17 in 150 minutes with 1mM F-1,6-BP in solution, (c) reduced V_{max} from 89.9 to 27.13 in 150 minutes with 1mM F-1,6-BP in solution, and (d) reduced V_{max} from 103.0 to 11.62 in 150 minutes with 1mM F-1,6-BP in solution. V_{max} of all M2PYK assays were plotted in the figure below to show how enzyme activity related to pre-incubation time.

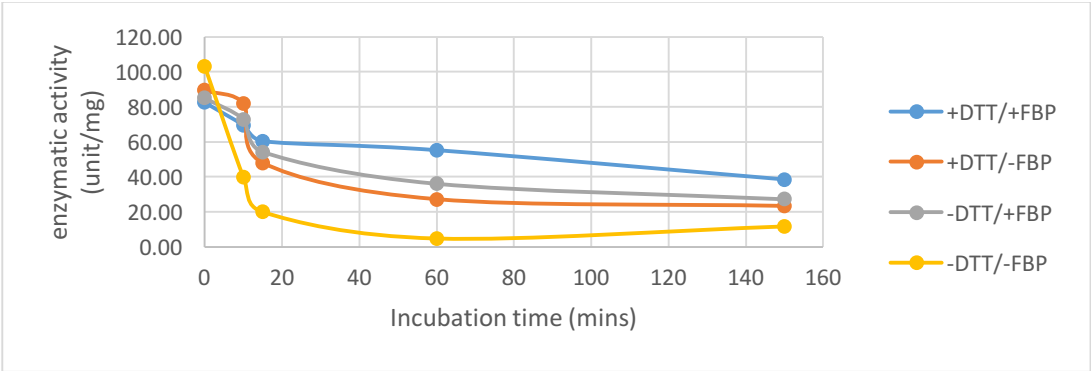

Figure 3-14. Variation of V_{max} of M2PYK over 150 minutes pre-incubation time in the presence or absence of DTT and F-1,6-BP.

Figure 3-11 shows calculated V_{max} values suggesting that the addition of the activators (DTT or F-1,6-BP) individually or in combination result in a slightly lower M2PYK enzymatic activity of 80 unit/mg compared with the M2PYK on its own which has an activity of over 100 unit/mg. However, the curves in Figure 1-11 clearly show that both DTT and F-1,6-BP activate the enzyme at lower more physiologically relevant concentrations of PEP substrate. In keeping with that, M2PYK alone shows the most sigmoidal shaped activity curves at 0 minute as shown in Figure 3-13 while addition of F-1,6-BP results in more hyperbolic shaped curves. We could conclude that F-1,6-BP helps M2PYK to reach higher activity at low PEP concentration as K_m (-DTT/-F-1,6-BP) > K_m (+DTT/-F-1,6-BP) > K_m (+DTT/+F-1,6-BP) > K_m (-DTT/+F-1,6-BP). DTT is however a much weaker activator at low PEP concentrations suggesting that F-1,6-BP increases the protein-substrate binding but this effect is reduced in the presence of DTT.

In Figure 3-12, DTT (Canault et al.) or F-1,6-BP (Cheng et al.) or DTT & F-1,6-BP (blue) in PBS solution all slow down the time dependant enzymatic activity loss compared to protein alone (yellow). Half-life increased from 10 minutes to 15 min (DTT), 60 min (F-1,6-BP) and 150 min (DTT & F-1,6-BP), respectively.

The phenomenon of the biphasic loss of activity is interesting compared with the relative results in this Chapter of other isoforms. There are two possible explanations: The oxidation of the cysteine residues on the surface of the protein leads to activity loss and then the dissociation from tetramer to monomer leads to more activity loss; or the dissociation itself occurs in two steps: tetramer-dimers, dimers-monomers with dimers still having some activity.

The effect of DTT, F-1,6-BP, and pre-incubation time on the V_{max} of LPYK

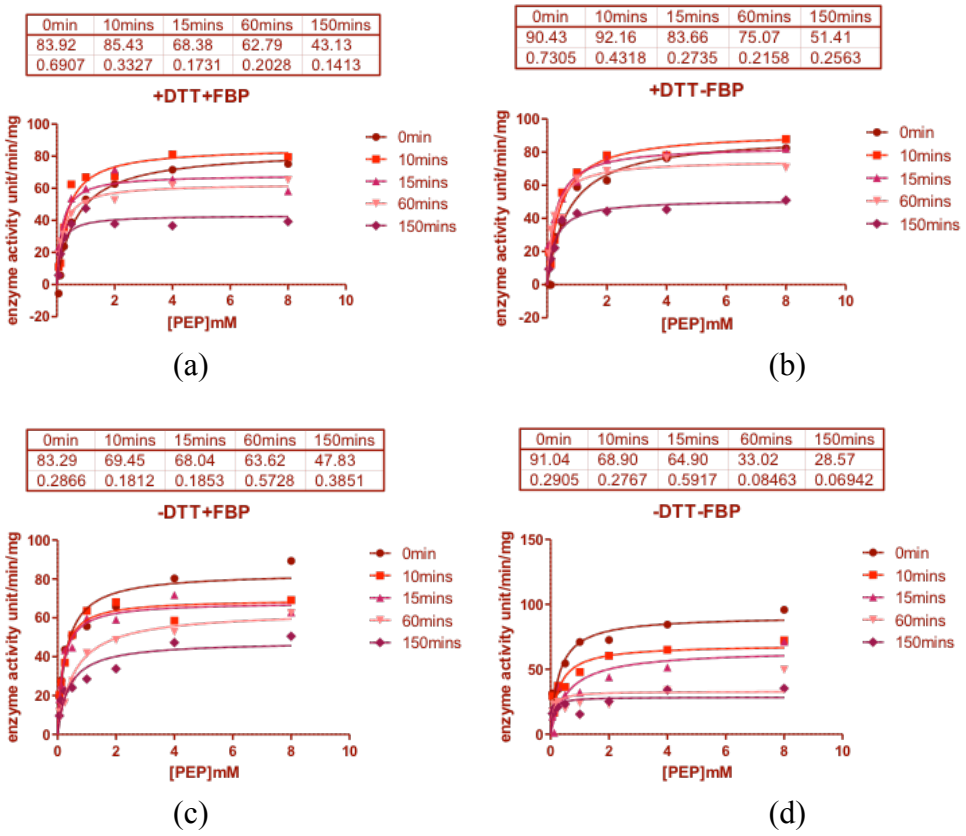

Figure 3-15. The effect of pre-incubation time, DTT and F-1,6-BP on LPYK enzymatic activity (a) The effect of dilution reduced V_{max} from 83.9 to 43.13 in 150 minutes with 1mM DTT and 1mM F-1,6-BP in solution. But the binding of substrates increased. K_m of PEP decreased from 0.69mM to 0.014mM in 150 minutes. (b) The effect of dilution reduced V_{max} from 90.43 to 51.41 in 150 minutes with 1mM DTT in solution. But the binding of substrates increased. K_m of PEP decreased from 0.73mM to 0.26mM in 150 minutes. (c) The effect of dilution reduced V_{max} from 83.3 to 47.8 in 150 minutes without DTT but with 1mM F-1,6-BP in solution. However, the binding of substrates increased in 15 minutes but decreased after longer pre-incubation. (d) The effect of dilution reduced V_{max} of LPYK from 91.0 to 28.6 in 150 minutes in PBS only.

Strangely, the affinity decreased and V_{max} increased when DTT or/and F-1,6-BP were added. This is similar to the RPYK results in the following assays. The reason might be the misuse of software (Prism Version 7.0b) in the data analysis. To further investigate this phenomenon, more repeats need to be performed. If it is reproducable, structure information of M2PYK co-crystallised with F-1,6-BP will be required.

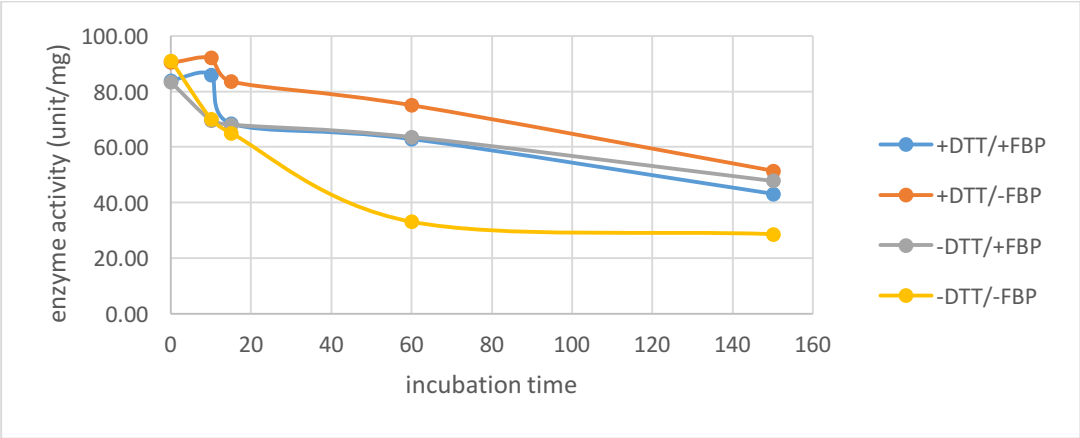

Figure 3-16. V_{max} of LPYK over 150 minutes pre-incubation time in the presence or absence of DTT and F-1,6-BP.

At start point (0 minute), enzymatic activities of LPYK in four conditions are around 85 unit/mg at a PEP concentration was of 8mM. It seems therefore that adding DTT, F-1,6-BP or DTT & F-1,6-BP gives no immediate activation effect. However, DTT, F-1,6-BP or DTT & F-1,6-BP do significantly slow down the time dependant enzymatic activity loss, suggesting that after a pre-incubation period, the protein in PBS solution with DTT or F-1,6-BP or DTT & F-1,6-BP maintained higher enzyme activities than protein alone.

Interestingly, protein with DTT or DTT & F-1,6-BP shows a higher K_m, which means DTT might weaken the substrate binding at low PEP concentrations and this is consistent with the results found for M2PYK in the previous section though for LPYK F-1,6-BP does not appear to increase the protein substrate binding.

The effect of DTT, F-1,6-BP, and pre-incubation time on the V_{max} of RPYK

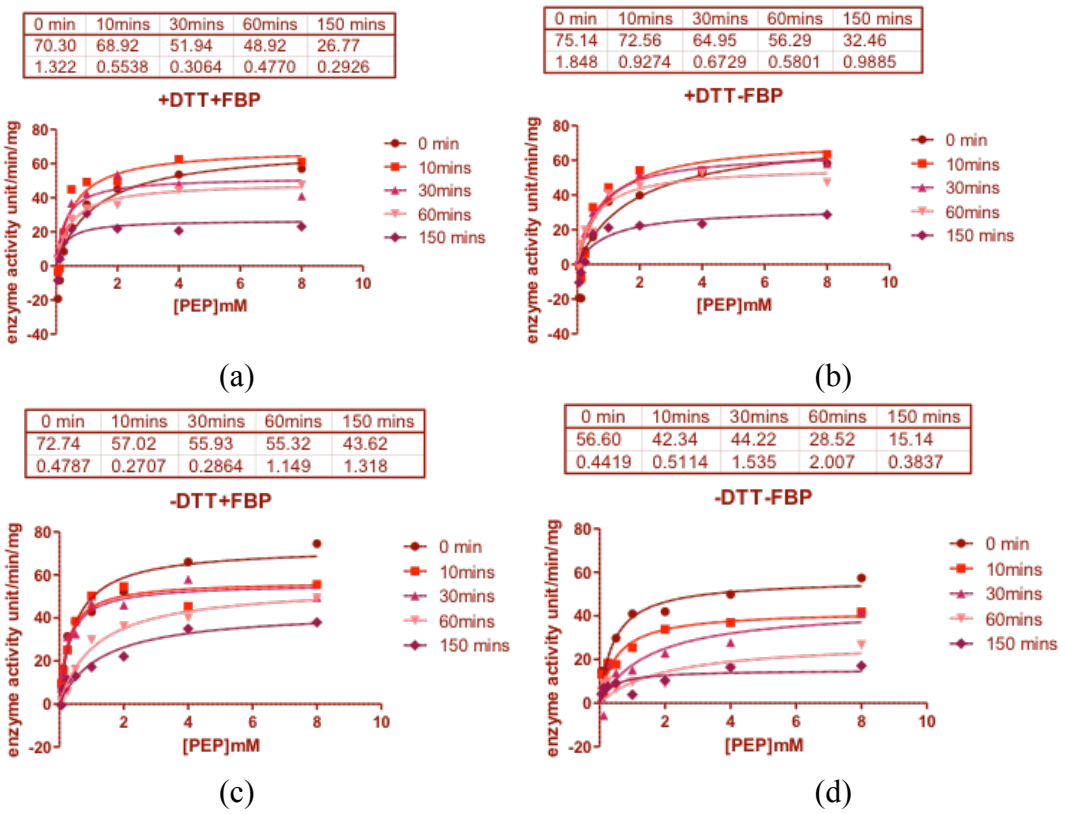

Figure 3-17. The effect of pre-incubation time, DTT and F-1,6-BP on RPYK enzymatic activity (a) The effect of dilution reduced V_{max} from 70.3 to 43.13 in 150 minutes with 1mM DTT and 1mM F-1,6-BP in solution. But the binding of substrates increased. K_m of PEP decreased from 1.32mM to 0.29mM in 150 minutes. (b) The effect of dilution reduced V_{max} from 75.14 to 32.46 in 150 minutes with 1mM DTT and 1mM F-1,6-BP in solution. But the binding of substrates increased. K_m of PEP decreased from 1.85mM to 0.99mM in 150 minutes. (c) Effect of dilution reduced V_{max} from 72.74 to 43.62 in 150 minutes with 1mM F-1,6-BP in solution. But the binding of substrates was tightest at 30 minutes. (d) The effect of dilution reduced V_{max} from 56.6 to 15.14 in 150 minutes in PBS solution.

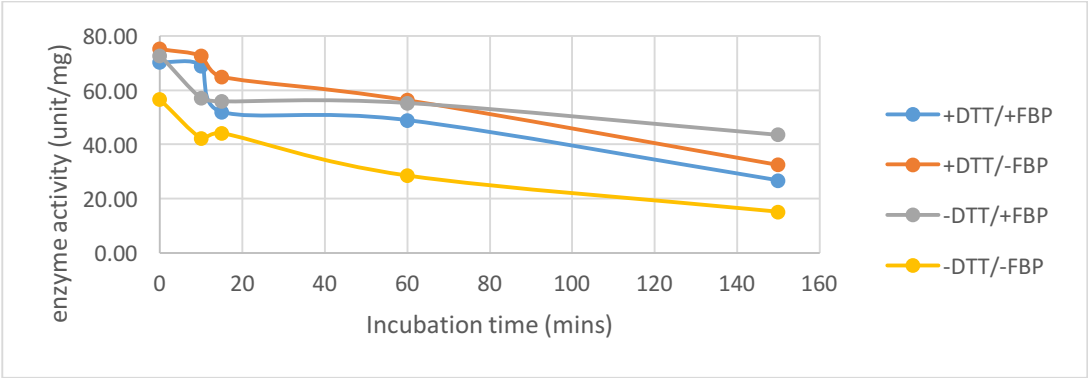

Figure 3-18. V_{max} of RPYK over 150 minutes pre-incubation time in the presence or absence of DTT and FBP.

Figure 3-18 shows that with very short pre-incubation times (immediately after the enzyme is diluted from the higher concentration stock solutions) RPYK activity was increased from 55 unit/mg to about 75 unit/mg by DTT, F-1,6-BP or DTT & F-1,6-BP. Surprisingly, RPYK with DTT or DTT & F-1,6-BP shows lower activity at low PEP concentrations, which means DTT might reduce the PEP-protein binding at low substrate concentrations. We can see from Figure 3-18 that K_m (F-1,6-BP) and K_m (protein alone) are about 0.5 mM but K_m (F-1,6-BP) and K_m (DTT & F-1,6-BP) are 1.3 mM and 1.8 mM, respectively. This is similar to the effect of DTT on LPYK. F-1,6-BP also cannot increase the protein-substrate binding, which is also similar to LPYK.

Conclusion and discussion

M1PYK activity is retained in all conditions as both V_{max} and K_m were not significantly affected by reducing agent or activator. This is in contrast with the enzymatic activities of RPYK, LPYK, and M2PYK for which the activity decreases quickly after dilution in PBS solution. This loss of activity is however considerably slowed by the addition of DTT or F-1,6-BP or a combination of DTT + F-1,6-BP.

The K_m value of four isoforms incubated with/without DTT or F-1,6-BP are summarized in Table 6. For M2PYK addition of F-1,6-BP decreases the K_m of the substrate PEP at low PEP concentrations. The change of K_m for PEP binding by 1,6-BP was not however significant for (PEP) RPYK (from 0.291 mM to 0.287) and LPYK (from 0.442 mM to 0.0.479 mM). DTT decreases the K_m of PEP by decreasing protein substrate binding of RPYK and LPYK. But DTT does not appear to decrease substrate affinity of M2PYK. DTT seems to increase the K_m of LPYK and RPYK.

K_m (PEP) mM	M1PYK	M2PYK	RPYK	LPYK
control	0.57	1.77	0.29	0.44
add 1mM DTT	0.72	1.23	0.73	1.84
add 1mM FBP	0.55	0.38	0.29	0.48

Table 6. K_m values (expressed in mM) of four isoforms incubated with/without DTT or F-1,6-BP.

3.4.3 Reducing reagents help RPYK to maintain activity or recover activity

To find out whether the activity loss is reversible, we tested different time points to add reducing agent through a set of time dependant enzymatic activity assays. Three time points (0 minute, 10 minutes and 180 minutes) after dilution were chosen and DDT was added to test if the enzyme activity was could be recovered.

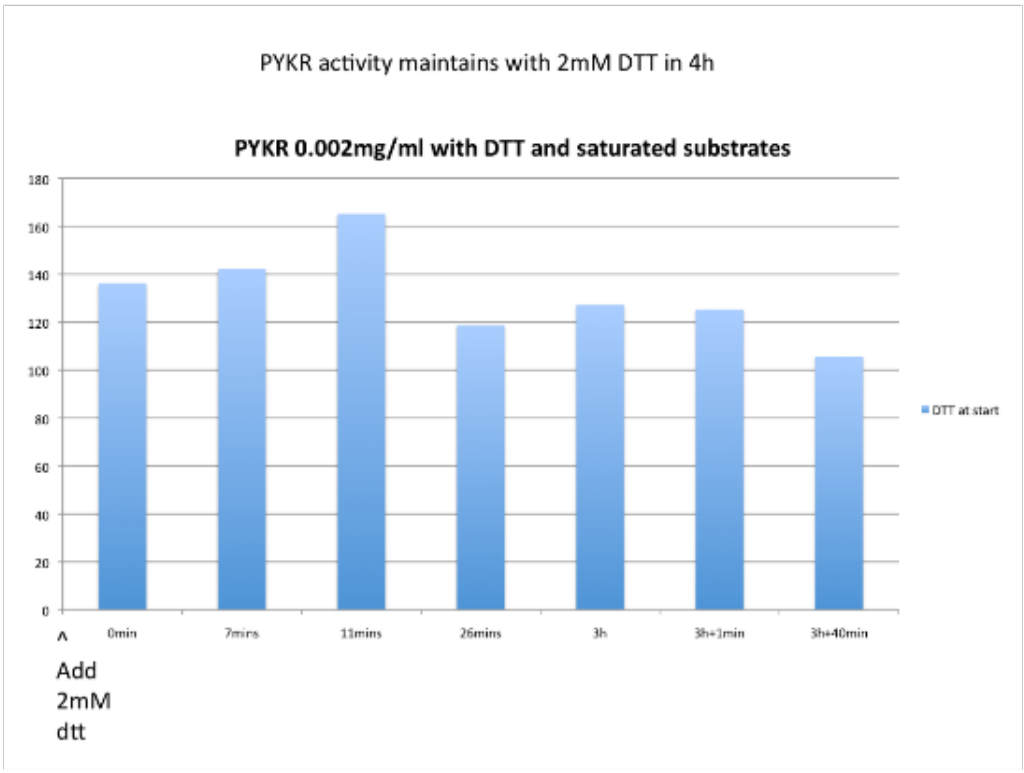
PYKR activity maintains with 2mM DTT in 4h
PYKR 0.002mg/ml with DTT and saturated substrates
180
160
140
120
100
80
60
40
20
0
0min
7mins
11mins
26mins
3h
3h+1min
3h+40min
DTT at start
^
Add
2mM
dtt

(a)

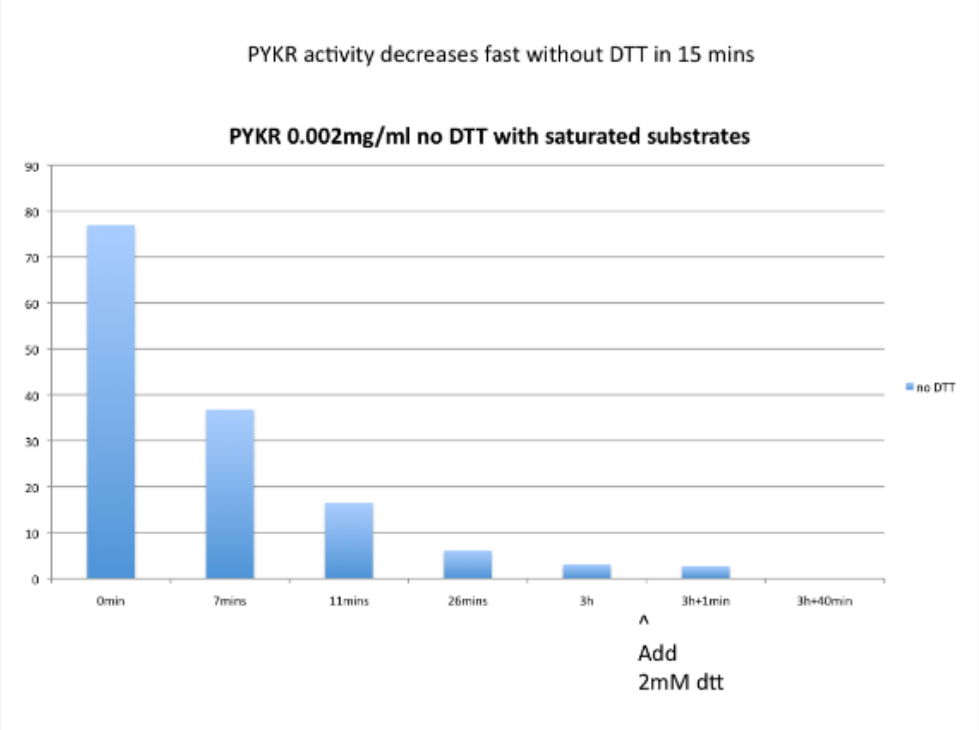
PYKR activity decreases fast without DTT in 15 mins
PYKR 0.002mg/ml no DTT with saturated substrates
90
80
70
60
50
40
30
20
10
0
0min
7mins
11mins
26mins
3h
3h+1min
3h+40min
no DTT
^
Add
2mM dtt

(b)

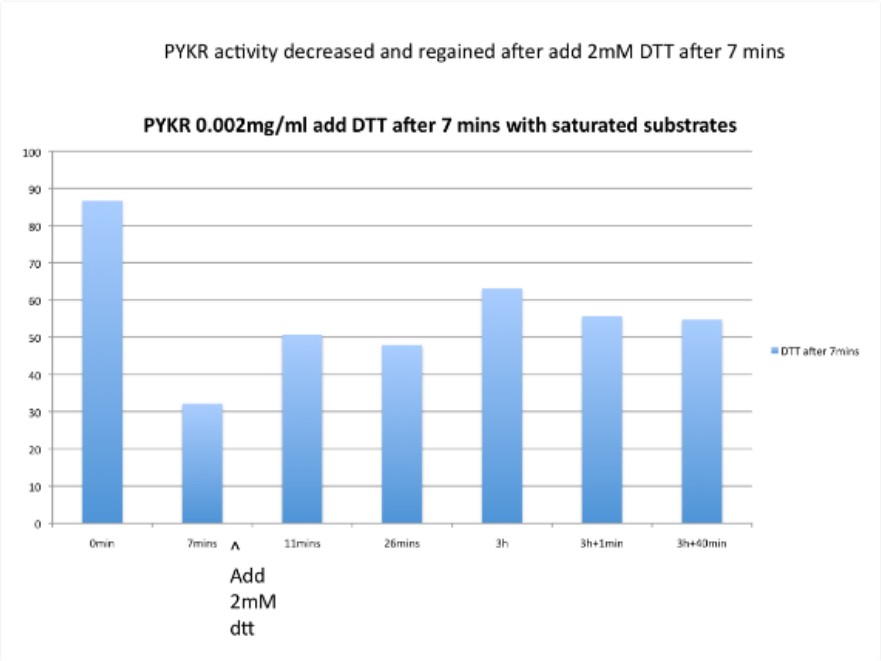

(c)

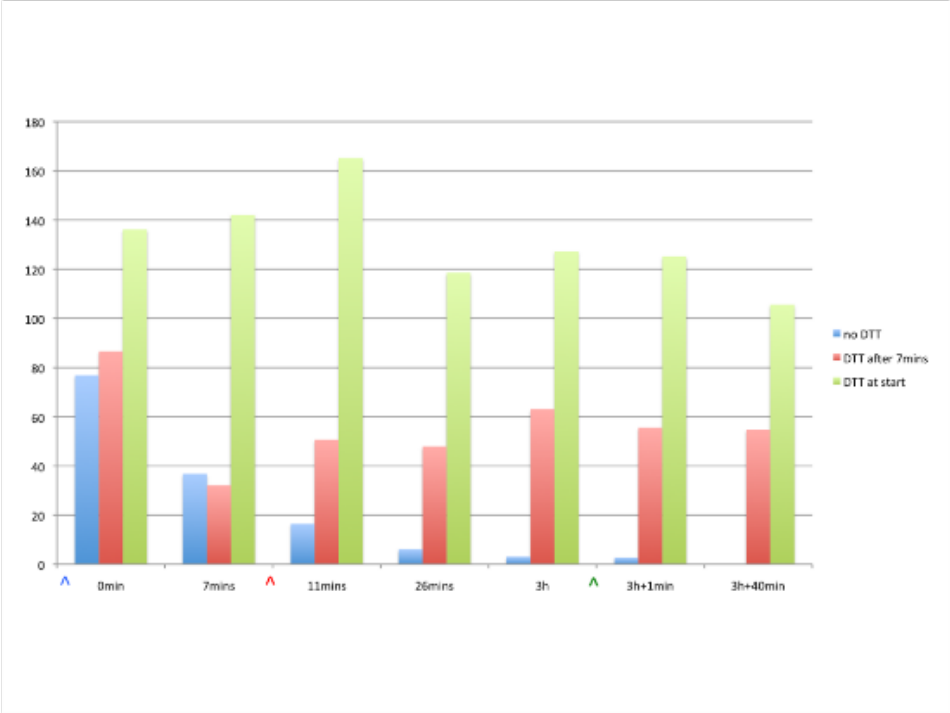

(d)

Figure 3-19. The effect of DTT on recovering the activity of RPYK. RPYK was diluted from 8.1mg/ml to 0.001mg/ml. (a) The protein was diluted in to PBS with 2mM DTT. After dilution, the effect of protein activity decreases slowly from 140 unit/mg to 100 unit/mg in 220 minutes. (b) After 3 hours, 2 mM DTT was added into the protein solution, the enzyme activity could not be recovered. (c) After 7 minutes, 2 mM DTT was added into the protein solution, the enzyme activity was recovered

gradually and maintain a higher activity. (d) Three charts are put together to compare the absolute enzymatic activity values.

The results presented in Figure 3-19. show that the presence of DTT helps to maintain a significant amount of enzyme activity compared with the rapid loss of activity observed for RPYK alone. Importantly, addition of DTT can partially recover enzyme activity suggesting that the mechanism of activity loss is reversible (i.e. activity loss is not caused by protein denaturation or aggregation), but more probably related to oxidation of cysteines and their role in stabilising the active tetrameric form of RPYK.

3.4.1 Both DTT and TCEP maintain RPYK activity over time.

DTT is not a stable reducing agent in aqueous solution and is easily oxidized over time. Another reducing agent TCEP that is more stable was tested with RPYK to rule out the possibility that the decrease of enzyme activity over time was affected by spontaneous oxidation of DTT.

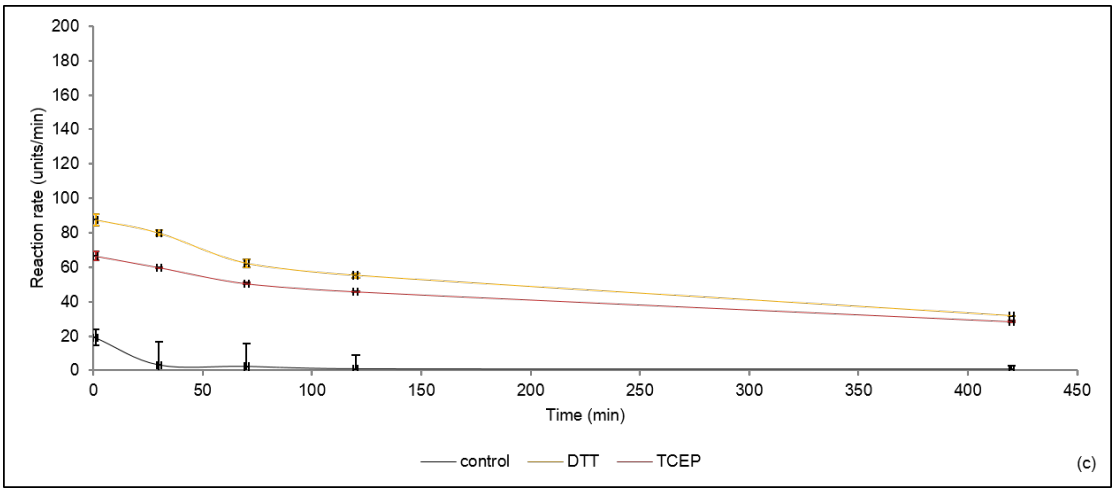

Figure 3-20. Enzyme activity of RPYK alone, with 2 mM DTT or with 2mM TCEP. Both 2 mM DTT and 2 mM TCEP activated RPYK activity. The activity of the protein with both DTT and TCEP decreases gradually over time. In 420 minutes, the protein still has activity: about 40 unit/mg compared with a control of almost 0 activity.

3.4.2 The effect of DTT and GSH on M2PYK

In 2011, it was shown that the oligomerisation state of M2PYK and its enzymatic activity relies on redox state (Anastasiou et al., 2012). The cysteine-containing

tripeptide glutathione (GSH) is one of the major biological redox regulators. Here we compared the effects of the artificial reducing reagent DTT and GSH on enzyme activity of M2PYK.

In this assay, M2PYK was diluted to 0.002 mg/ml and incubated with GSH for 10 min. Then, assays were performed in 100 mM KCl, 10 mM $MgCl_2$, pH 7.4, in PBS-CM, at room temperature (25 ^oC), pre-incubation time 10 min and final protein concentration 0.001 mg/ml.

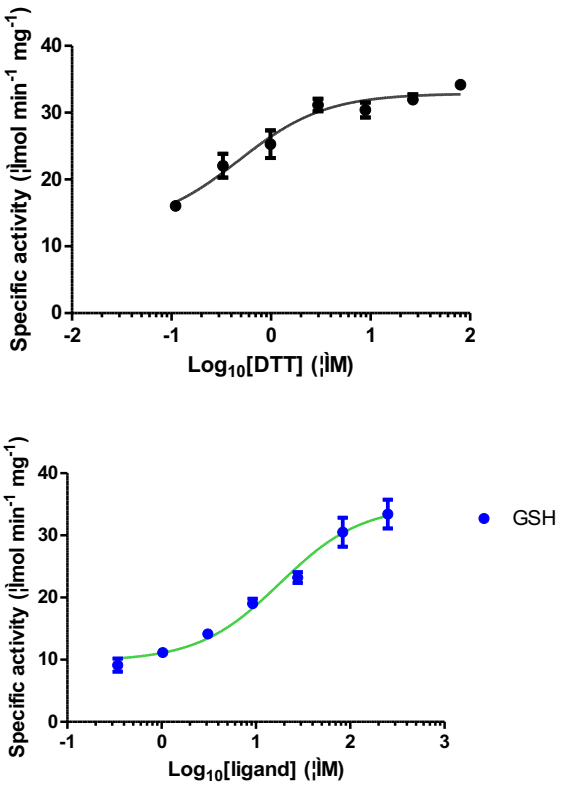

Figure 3-21. Effects of DTT and GSH on enzyme activity of M2PYK. Error bars are derived from three independent repeat experiments.

As shown in Figure 3-21. , M2PYK is upregulated by both reducing reagents from 10 unit/mg to above 30 unit/mg. These effects suggest that M2PYK is sensitive to redox environment. They further suggest that it is a biophysical effect of the reduction potential of GSH and DTT rather than a possible specific binding effect of either of the additive molecules.

3.4.3 Pre-incubation time affects melting temperatures of LPYK and RPYK

As long time pre-incubation affects protein activity, it is important to test what role protein stability plays. We studied the protein stability of RPYK and LPYK after pre-incubation (20 hours) with and without DTT through thermal denaturation assays.

Dilution and pre-incubation not only regulated enzyme activity but also affect the melting temperatures of both RPYK and LPYK.

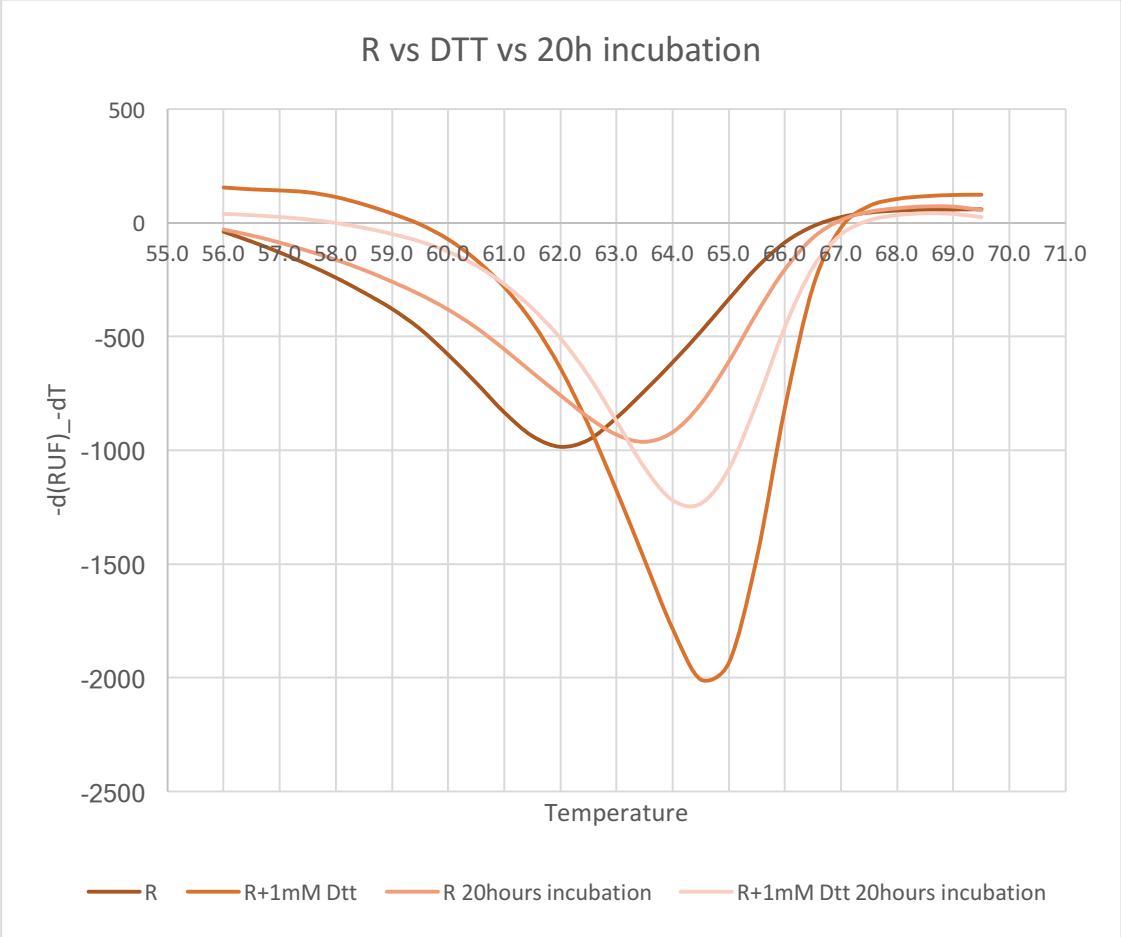

Figure 3-22. RPYK was incubated at room temperature for 20 hours at 0.1mg/ml with or without 1mM DTT. The figure shows derivative calculations of the fluorescence readings. The melting temperature is at about 62 ºC (R control), 64.5 ºC (R + 1mM DTT), 63.5 ºC (R 20 hours of pre-incubation), and 64.5 ºC (R + 1mM DTT + 20 hours of pre-incubation).

As shown above, after 20 hours of pre-incubation, the melting temperature of RPYK alone increased form 62 ºC to 63.5 ºC. However, RPYK with 1mM DTT show stable protein even after 20 hours of pre-incubation. This result is in line with the time dependant enzyme activity assay and suggests a correlation between enzyme stability and enzyme activity.

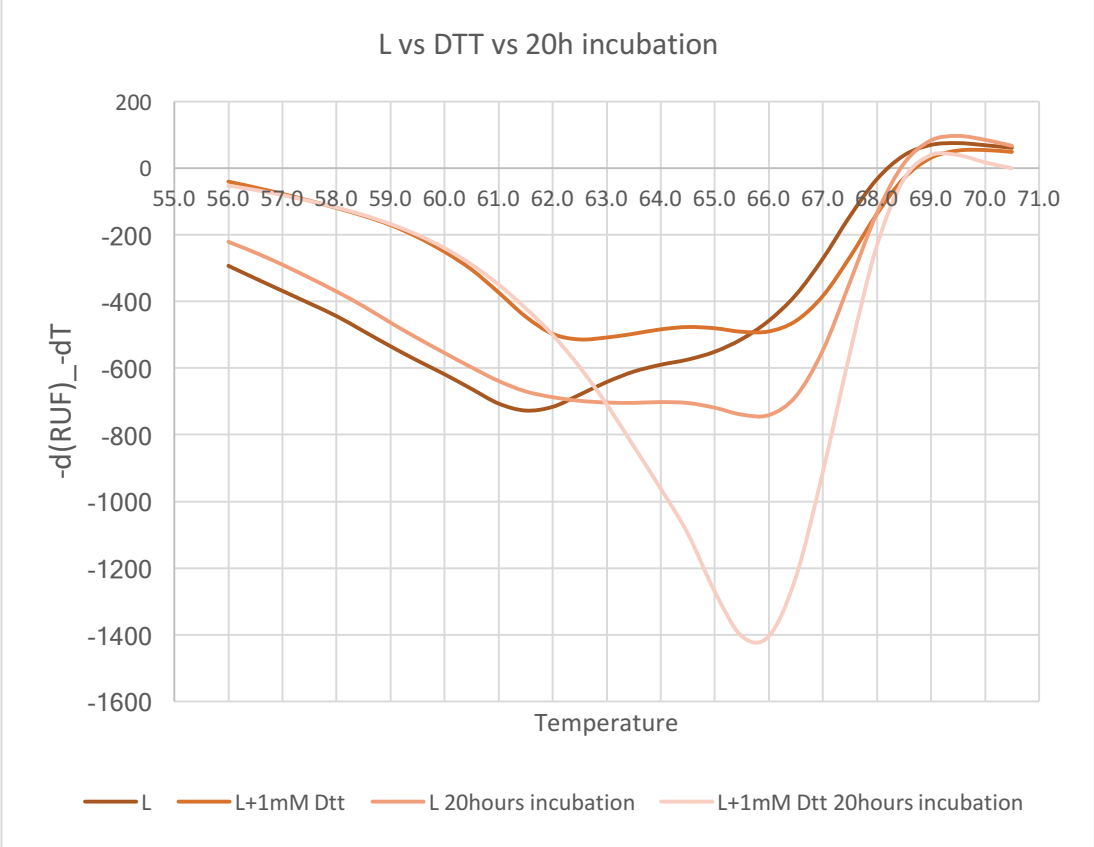

Figure 3-23. LPYK was incubated at room temperature for 20 hours at 0.1mg/ml. The figure shows derivative calculations of the fluorescence readings. The melting temperature is at about 61.5 ºC (L control), 66ºC (L + 1mM DTT), 66 ºC (L 20 hours of pre-incubation), and 66 ºC (L + 1mM DTT + 20 hours of pre-incubation).

3.4.4 Analytical gel filtration shows M2PYK dissociates into monomers

Previous research showed that M2PYK dissociates slowly after dilution from high concentration stocks, changing from tetrameric to monomeric (Morgan et al., 2013a). To investigate the possible dissociation effects on all four isoforms, analytical gel-

filtration was performed. Briefly, 0.5 ml sample of 0.1 mg/ml stock of each protein was incubated in PBS-CM at pH 7.4 at room temperature for 12 hr. The results show clearly that only M2PYK dissociated at 0.1 mg/ml. M1PYK, RPYK and LPYK retained the tetrameric form.

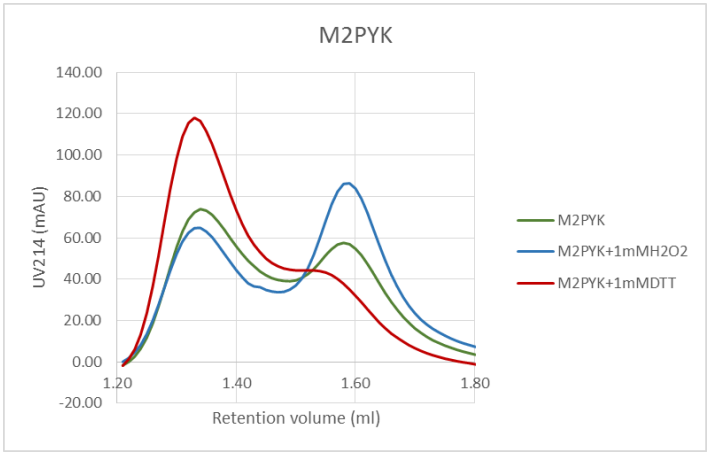

A

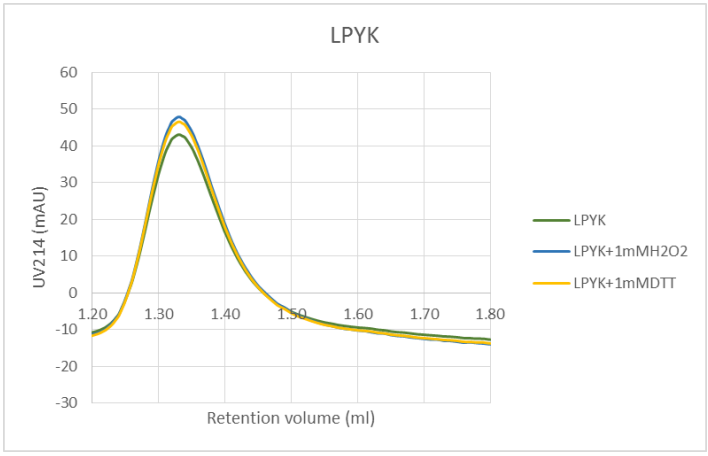

B

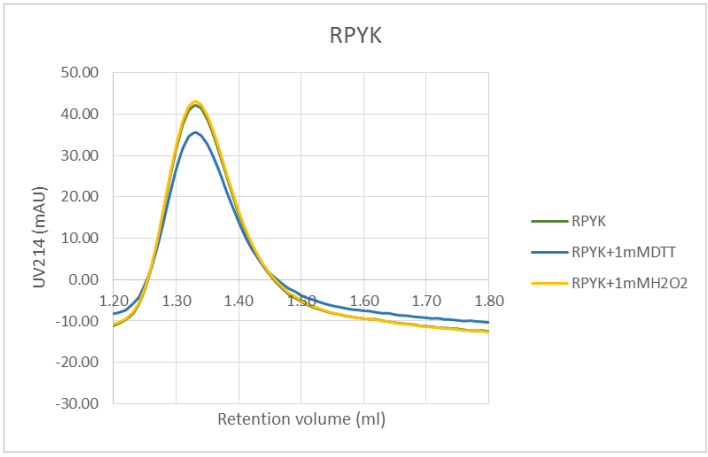

C

Figure 3-24. Effects of DTT and H_2O_2 on the oligomerisation of M2PYK, RPYK and LPYK. Both enzymes were incubated at 0.1 mg/ml with or without 1mM DTT/1mM H_2O_2 in PBS-CM buffer at pH 7.4 at room temperature for 12 hours. Gel filtration traces of M2PYK show two distinct peaks corresponding to tetramer and monomer (Figure 2A). Curve of M2PYK with H_2O_2 shows a bigger monomer peak at about 1.6 ml and curve of M2PYK with DTT shows a bigger tetramer peak around 1.33 ml. In both Figure B and C, LPYK and RPYK show a single peak at 1.33 ml, even with 1 mM DTT or 1 mM H_2O_2.

As shown in Figure 3-24, the ratio of tetramer to monomer is concentration dependent with higher concentrations favouring the tetrameric state. In this experiment, the time-dependent dissociation of M2PYK was measured by diluting a solution of 20 mg/ml M2PYK to 0.1 mg/ml (PBS-CM, pH 7.4) and incubating for 0 h, 1 h, 2 h, 5.5 h, 8 h, and 12 h at room temperature. The results indicate that M2PYK dissociated slowly from tetramer to monomer reaching an equimolar equilibrium of 1 tetramer: monomers after ~8 h A similar experiment was carried out with the M1PYK isoform and showed no dissociation of the tetrameric form (Figure 2B). Gel filtration studies can only provide a reliable signal at relatively high protein concentrations greater than ~0.1 mg/ml.

Several papers have shown that the M2PYK tetramer has higher activity relative to its monomeric/dimeric forms (Ashizawa, McPhie, Lin, & Cheng, 1991; Chaneton et al., 2012; Eigenbrodt et al., 1992; Mazurek, 2011). Here we show loss of enzyme activity correlates with the time dependent dissociation observed in the gel filtration experiments. (Figure 2C). In the enzyme assay (see methods) activities were measured using a stock solution of 20 mg/ml M2PYK which was diluted to a concentration of 0.002 mg/ml in PBS-CM (pH 7.4). Monitoring enzyme activity as a function of time showed a 50% loss of activity of M2PYK in 30 min. The enzyme concentration used to measure the enzyme activity is 50 times more dilute than the solutions studied by gel filtration which explains the more rapid dissociation and loss of activity. In contrast, an identical study with M1PYK showed only 17% loss of M1PYK activity over the 3 h period of the experiment consistent with M1PYK retaining its active tetrameric structure even at very low protein concentration.

3.4.5 Summary of results on the time dependent change in activity of hPYK

From these series of assays, we could show that for M2PYK, LPYK, and RPYK protein, activity decrease gradually to nearly zero after dilution from high concentration stock to low concentration assay solution. Reducing reagents (DTT and TCEP) and the natural activator F-1,6-BP help to maintain protein activities in solution.

We also could show that pre-incubation time at low protein concentration is an important parameter in enzyme activity measurement of PYKs, especially in M2PYK, LPYK and RPYK.

3.5 The effect of protein concentrations on pyruvate kinase activity

Another parameter related to the dilution and pre-incubation time discussed above and that could affect the accuracy of enzyme activity measurement, is protein concentration. We studied LPYK at three concentrations. A series of time dependant assays were designed to find out how protein concentration affects rate of loss of activity after dilution.

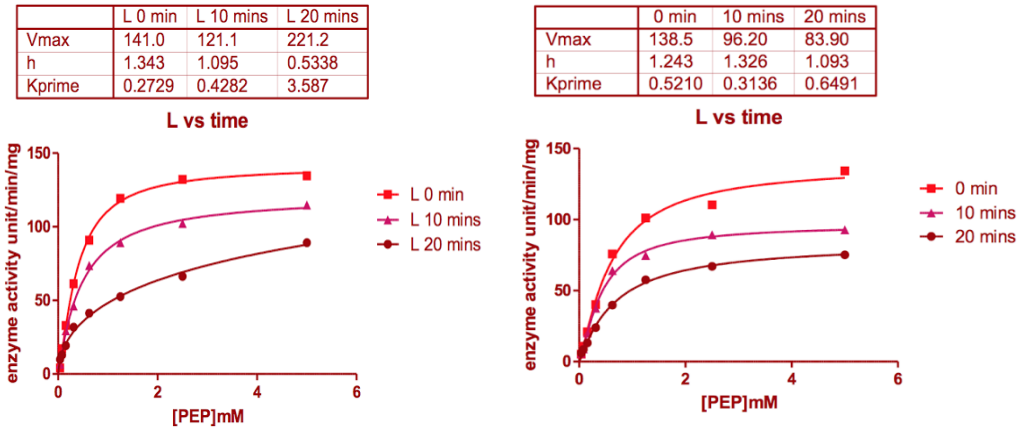

	L 0 min	L 10 mins	L 20 mins
Vmax	141.0	121.1	221.2
h	1.343	1.095	0.5338
Kprime	0.2729	0.4282	3.587

(a)

	0 min	10 mins	20 mins
Vmax	138.5	96.20	83.90
h	1.243	1.326	1.093
Kprime	0.5210	0.3136	0.6491

(b)

	0 min	10 mins	20 mins
Vmax	116.3	92.06	87.98
h	1.717	1.317	1.297
Kprime	0.2563	0.3562	0.4634

(c)

Figure 3-25. LPYK enzyme activity assay with pre-incubation of 0 minutes, 10 minutes, 20 minutes. Assay conditions are 2mM ADP, 100mM KCl, 10mM $MgCl_2$, in PBS-CM, pH 7.4, at room temperature. (a) protein concentration 0.001mg/ml, (b) protein concentration 0.002mg/ml (c) protein concentration 0.004mg/ml

From the above figure, it is apparent that time of incubation affects the lower concentration assays most with the largest drop in V_{max}, shown in Figure 3-23. Kinase activity of LPYK in (a) showed wider gaps between the curves than in (b) and (c). To quantify this effect, we plotted the sub-saturating points of the three figures at 1.25 mM PEP.

	0.001mg/ml	0.002mg/ml	0.004mg/ml
Best-fit values			
Slope	-3.340 ± 0.1900	-2.182 ± 0.2748	-1.781 ± 0.3210

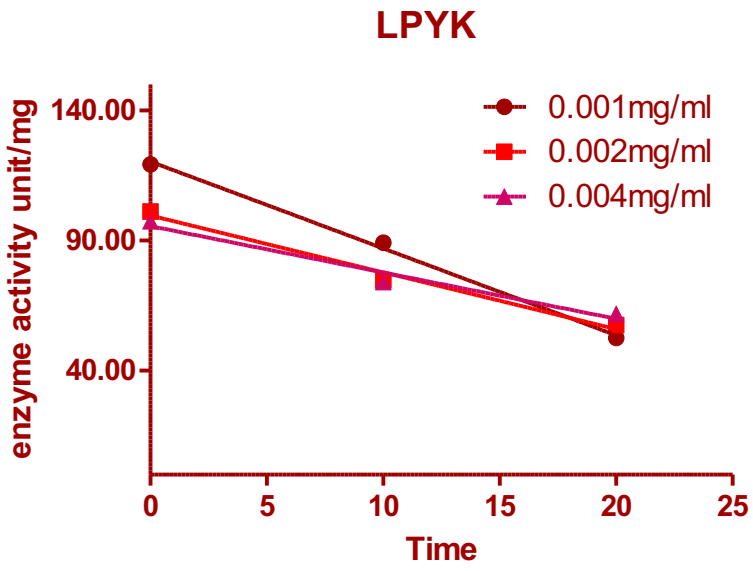

Figure 3-26. LPYK time dependent assay when PEP concentration is at 1.25mM at 0.001mg/ml, 0.002mg/ml, and 0.004mg/ml.

From Figure 3-26, we see that lower protein concentration shows faster activity decrease rate. The decrease slope of activities is -3.3, -2.2, and -1.8 (UNITS) with LPYK at 0.001mg/ml losing activity faster than the higher concentrations.

CHAPTER 4. Activity regulation of human PYKs by natural metabolites

4.1 Introduction

4.1.1 Regulators of PYKs are diverse

A variety of regulators of human PYKs has been discovered from small molecules to hormones and peptides, especially for M2PYK. For example, phosphotyrosine peptides bind directly to M2PYK and inhibit its enzyme activity. This has the effect of diverting metabolic flux from energy production to anabolic processes (Christofk et al., 2008b). Another example is for LPYK which has been shown to be inhibited by alanine and ATP, which raises the K_m and shifts the kinetics of PEP metabolism from hyperbolic to sigmoid (Llorente et al., 1970). Table 7 summarises published data on the wide range of metabolites known to either inhibit or activate the different mammalian PYK isoforms.

Effector	Classification	Effect	Effect mechanism	Effect position	Reference
Phe	metabolite	inhibition of enzyme activity	not shown	amino acid binding site	(Rozengurt et al., 1970)
Ala	metabolite	inhibition of enzyme activity	not shown	amino acid binding site	(Williams et al., 2006)
DAPk	protein-protein interaction	activation of enzyme activity	stabilise tetramer	not shown	(Mor et al., 2012)
MUC1-C	protein-protein interaction	activation of enzyme activity	stabilise tetramer	C474	(Kosugi et al., 2011)
JMJD5	protein-protein interaction	inhibition of enzyme activity	promote dissociation of M2PYK	tetramer interface	(Wang et al., 2014)
phosphotyrosine	protein-protein interaction	inhibition of enzyme activity	reduce F16BP binding	near F-1,6-BP-binding site	(Christofk et al., 2008a)
PML	protein-protein interaction	inhibition of enzyme activity	promote dissociation of M2PYK	not shown	(Shimada et al., 2008)
F16BP	metabolite	activation of enzyme activity	promote association of M2PYK, stabilise R-state	F-1,6-BP site	(Dombrauckas et al., 2005)
SAICAR	metabolite	activation of enzyme activity	not shown	not F-1,6-BP site	(Keller et al., 2012)
serine	metabolite	activation of enzyme activity	promote association of M2PYK, stabilise R-state	amino acid binding site	(Chaneton et al., 2012)
cysteine	metabolite	inhibition of enzyme activity	promote dissociation of M2PYK	not shown	(Nakatsu et al., 2015)
phenylalanine	metabolite	inhibition of enzyme activity	promote association of M2PYK, stabilise T-state	amino acid binding site	(Morgan et al., 2013a)

ATP	metabolite	inhibition of enzyme activity	not show	active site	
T3	hormone	inhibition of enzyme activity	promote dissociation of M2PYK	not shown	(Morgan et al., 2013a)
F16BP	metabolite	activation of enzyme activity	promote allosteric effect	F-1,6-BP site	(Blair and Walker, 1984)
Ala	metabolite	inhibition of enzyme activity	not show	amino acid binding site	(Llorente et al., 1970)
ATP	metabolite	inhibition of enzyme activity	not show	active site	(Fenton and Hutchinson, 2009)
F16BP	metabolite	activation of enzyme activity	promote allosteric effect	F-1,6-BP site	(Pinilla et al., 1987)
ATP	metabolite	inhibition of enzyme activity	not show	active site	(Pinilla et al., 1987)
Ala	metabolite	inhibition of enzyme activity	not show	amino acid binding site	(Marie et al., 1980a)

Table 7. Regulatory factors of PYK isoforms in vivo. (Effects of metabolites, protein-protein interaction, and hormone are highlighted by white, yellow, and blue, respectively)

From this table, we see that F-1,6-BP is the natural activator of M2PYK, LPYK and RPYK and amino acids also play an important role in PYK regulation. As PYKs regulate the final step in the glycolytic pathway controlling the energy flux, it is reasonable to expect that metabolites in the pathway may up-or down-regulate the activity of this important final step. We therefore undertook a broad screen of some of the important metabolites to study their effect against all four human isoforms.

4.1.2 Kinetic properties of the four human pyruvate kinase isoforms

All assays were performed in 100mM KCl, 10mM $MgCl_2$, pH 7.4, in PBS-cm, at room temperature (25 ºC), pre-incubation time 10 minutes and final protein concentration is 0.001mg/ml.

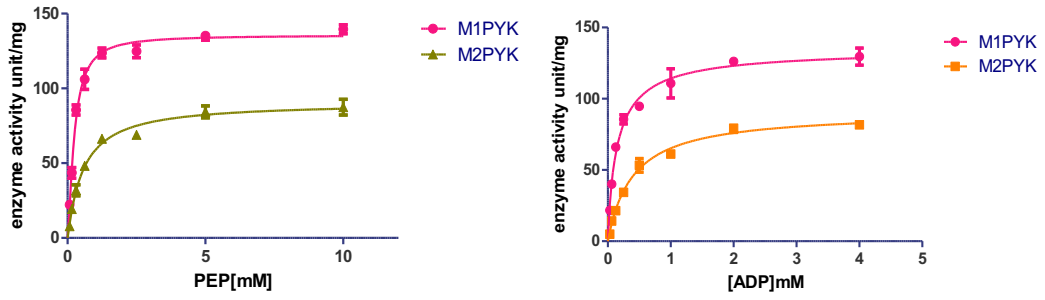

A B

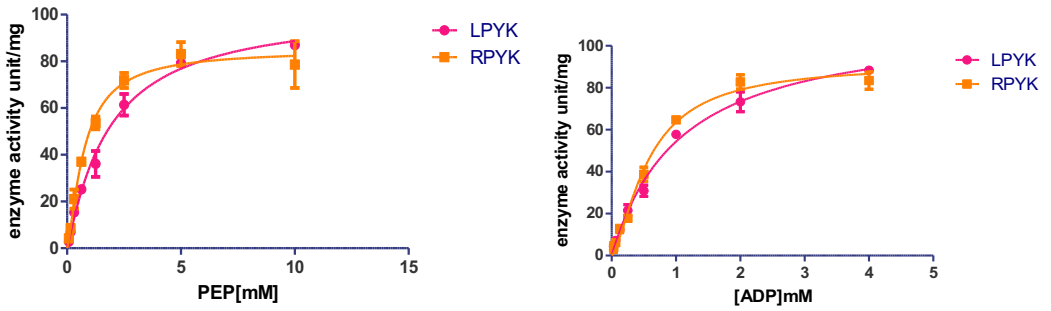

C D

Figure 4-1. Kinetics of M1PYK, M2PYK, LPYK and RPYK. Error bars are derived from three independent repeat experiments.

(A) and (C) The kinetic characterisations of the catalysis of PEP at saturating concentration of ADP (4mM).

(B) and (D) The kinetic characterisations of the catalysis of ADP at saturating concentration of PEP (10mM).

	LPYK	RPYK	M1PYK	M2PYK
V_{max} µmol/min/mg	112.2	91.62	135.5	90.62
K_m[PEP]	1.07	0.44	0.13	0.55
K_m[ADP]	1.94	0.69	0.18	0.40

Table 8. Kinetic properties of M1PYK, M2PYK, LPYK and RPYK

M1PYK shows highest activity (V_{max} = 135.5 µmol/min/mg), compared with M2PYK (V_{max} = 90.62 µmol/min/mg), LPYK (V_{max} = 112.2 µmol/min/mg), and RPYK (V_{max} = 91.62 µmol/min/mg). M1 also shows highest affinity for both PEP (K_m = 0.13mM) and ADP (K_m = 0.18mM), which are lower than data of M2PYK, LPYK and RPYK. These results correlate with previously published reports that M1PYK is a constitutively active enzyme compared with other isoforms (Morgan et al., 2013b).

4.1.3 Amino acids and metabolites screening

An enzymatic assay was carried out to screen human pyruvate kinases and a search was made for enzymatic modulators. M1PYK, M2PYK, LPYK and RPYK were incubated for 10 minutes with 2 mM amino acids (including cysteine, histidine, tryptophan, glutamine, methionine, valine, serine, isoleucine, phenylalanine, alanine, proline, leucine, tyrosine, glycine, threonine, arginine, glutamic acid, and lysine), F-1,6-BP and other metabolites (including F6P, malic acid, alpha-ketoglutarate, succinic acid, citric acid, GMP, AMP, UMP, oxalic acid). F-1,6-BP and oxalic acid were used as a positive control and negative control, respectively. The assay was performed in 10 mM PBS at pH 7.4 at 37 ºC. Substrates were used at sub-saturating concentration at about K_m (PEP) and K_m (ADP) as shown in Chapter 5.1.1. The results of the screen are shown in this chapter in sections 4.2 and 4.5.

4.2 M1PYK

Regulatory effects of amino acids on the constitutively fully active M1PYK have been extensively studied (Carminatti et al., 1971, Consler et al., 1992, Cheng et al., 1996, Lonhienne et al., 2003, Lonhienne and Winzor, 2002, Williams et al., 2006, Herman and Lee, 2009, Urness et al., 2013). The results showed that only phenylalanine moderately regulates M1PYK by inhibition of its enzymatic activity (Carminatti et al., 1971). The other amino acids and metabolites did not show direct regulatory effects on M1PYK. In Chapter 3.2, it was also shown that natural allosteric activator F-1,6-BP could not activate M1PYK much, as it is not an allosteric enzyme.

M1PYK could be inhibited by the product analogue - oxalic acid. In the literature, phenylalanine and alanine are inhibitors of M1PYK (Williams et al., 2006) and they reported phenylalanine inhibited M1PYK by 20% but alanine didn't show any inhibition effect on the activity of the protein. The inhibition ratios are not consistent with Carminatti and Williams' data, probably because the concentration of Ala and Phe in their experiments were much higher. As summarised in Figure 4-2, M1PYK

could not be regulated significantly by any of the amino acids or metabolites tested in the screen.

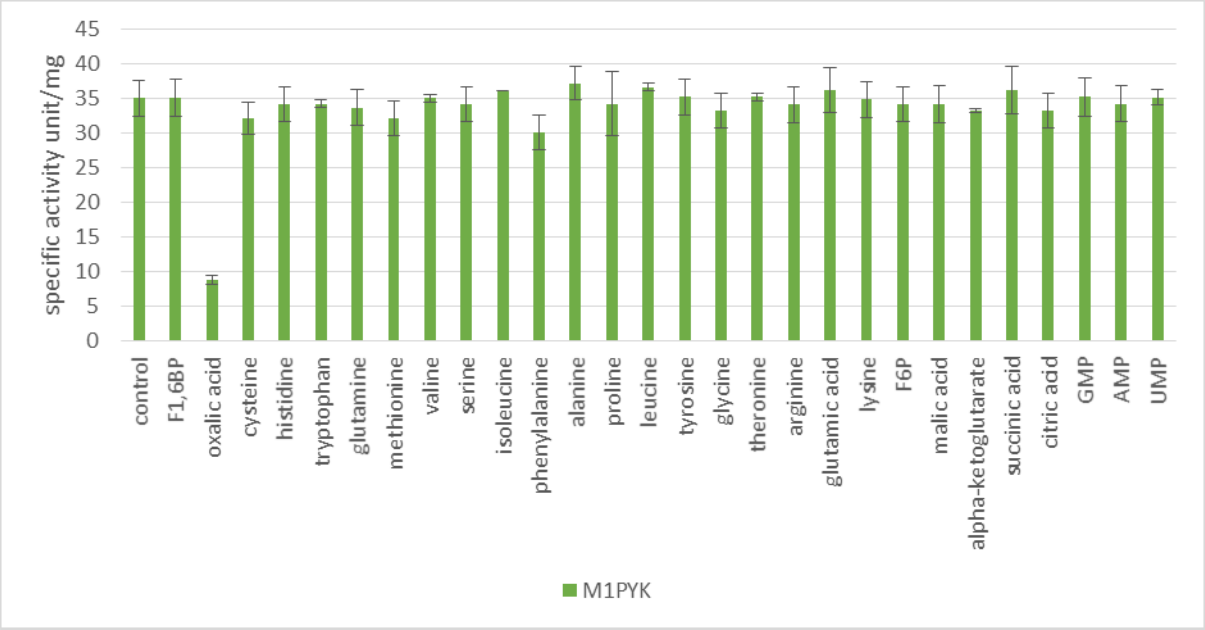

Figure 4-2. Effect of metabolites on the activity of M1PYK activity. Error bars are derived from three independent repeat experiments. The protein concentration is 0.01mg/ml. Buffer conditions are set as follow (sub saturating--substrate at about K_m value): 10 mM PBS-CM, 0.55 mM PEP, 0.4 mM ADP, 100 mM KCl, 10 mM $MgCl_2$, 37 ° C.

4.3 M2PYK

It has been reported that metabolites including activator serine (Chaneton et al., 2012), and inhibitors phenylalanine (Morgan et al., 2013a) and cysteine (Nakatsu et al., 2015) regulate M2PYK allosterically. F-1,6-BP is the natural activator of M2PYK (Dombrauckas et al., 2005).

From the results shown in Figure 4-3, M2PYK is less active than M1PYK at sub-saturating conditions (0.55mM PEP and 0.4 mM ADP). M2PYK enzyme activity (14 unit/mg) was much less active compared with the activity of M1PYK (35 unit/mg). Natural activator F-1,6-BP activates M2PYK to 32 unit/mg, which is almost equal to the activity of fully active isoform M1PYK. Oxalic acid inhibits both M1PYK and M2PYK, providing a stable positive control inhibitor. Surprisingly, not only amino acids like Ser, Phe, Cys, which have been reported previously, showed regulation of M2PYK, but we also found some additional activators and inhibitors from this screen. Gly, Ser, and His activate M2PYK from 14 unit/mg to 22 unit/mg, 30 unit/mg, and 31 unit/mg respectively. The activation by Ser and His are as strong as the natural effector

F-1,6-BP. We also discovered a series of inhibitors (Val, Phe, Ala, Met, Thr, Iso, AMP, Pro, GMP, alpha-ketoglutarate, Cys).

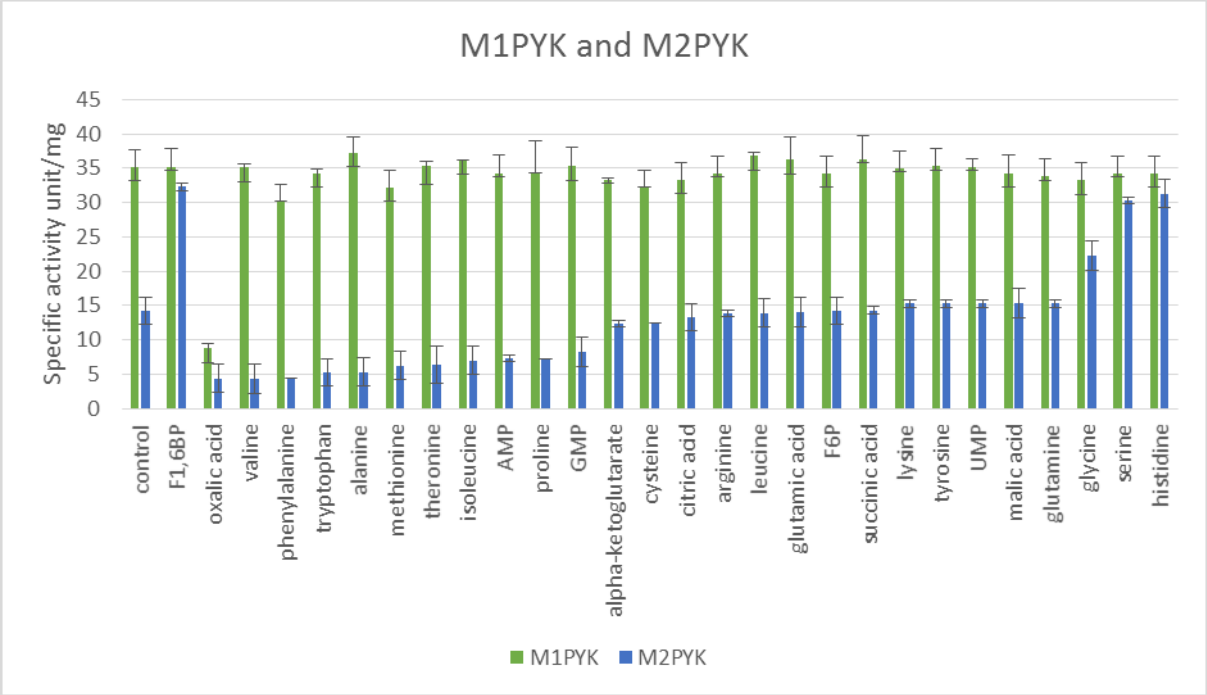

Figure 4-3. Effect of metabolites on activity of M1PYK and M2PYK. Error bars are derived from three independent repeat experiments. The protein concentration is 0.01mg/ml. Buffer conditions are set as follow (sub saturating--substrate at about K_m value): 10 mM PBS-CM, 0.55 mM PEP, 0.4 mM ADP, 100 mM KCl, 10 mM $MgCl_2$, 37 ° C.

In 2012, Chaneton's research show that serine activates M2PYK by 11-fold (Chaneton et al., 2012). Our experiment, showed serine activates M2PYK 2-fold. This large difference between experimental results is probably due to different assay conditions and pre-incubation times resulting in different degrees of M2PYK dissociation from tetramers to monomers at the low concentrations required in the enzyme assays. This dissociation is highly PKM2-concentration-dependant and pre-incubation time dependant. Chaneton et al. used 4 nM M2PYK to incubate with ligand and further incubate for 20 minutes. But in our experiments, we used 126 nM M2PYK and incubated for 10 minutes. So, the protein will dissociate much faster in Chaneton's assay than ours. Furthermore, in Chaneton et al.'s research (Chaneton et al., 2012), all other amino acids are weak activators like Ala and Phe, which according to our results are quite strong inhibitors. To further investigate the amino acids effect on M2PYK

and to study the possible opposing effect of activators and inhibitors of M2PYK, we tested a series of enzymatic assays by ligand competition.

4.3.1 Opposing effects of amino acids on M2PYK are competitive

In human cells, a range of amino acids are present at different concentrations. Both activators and inhibitors coexist in different tissues. It is therefore of interest to find out how ligands with opposing effects regulate M2PYK and whether this regulation could be physiologically important.

4.3.1.1 The opposing effects of serine and alanine on M2PYK

Briefly, the ligand competition assay was performed for the investigation of the effect on enzyme activity when both activator and inhibitor of M2PYK are present. Twenty-five microliters of 0.004 mg/ml of protein in PBS was mixed and incubated with twenty-five microliters of both ligands (activator and inhibitor) at a given concentration with or without 1 mM DTT at 37 ºC at pH 7.4 for 10 minutes. The fifty microliters assay buffer (PBS_CM supplemented with 20 mM $MgCl_2$, 200 mM KCl, 1mM NADH, 40 U/ml LDH, as well as sub-saturating PEP (0.5mM) and ADP (0.4mM)) was added to each well to start the reaction and absorbance read at 340 nm on a multiplate reader.

From the results shown in Figure 4-4 and Figure 4-5, 1.25 mM Ser activates M2PYK by about 10% and 100% with and without DTT respectively when Ala/Phe concentration is 0 mM. We also show in this experiment that the percentage of activation is also affected by reducing environment. These results also suggested that activator serine could decrease the affinity of both inhibitors alanine and phenylalanine.

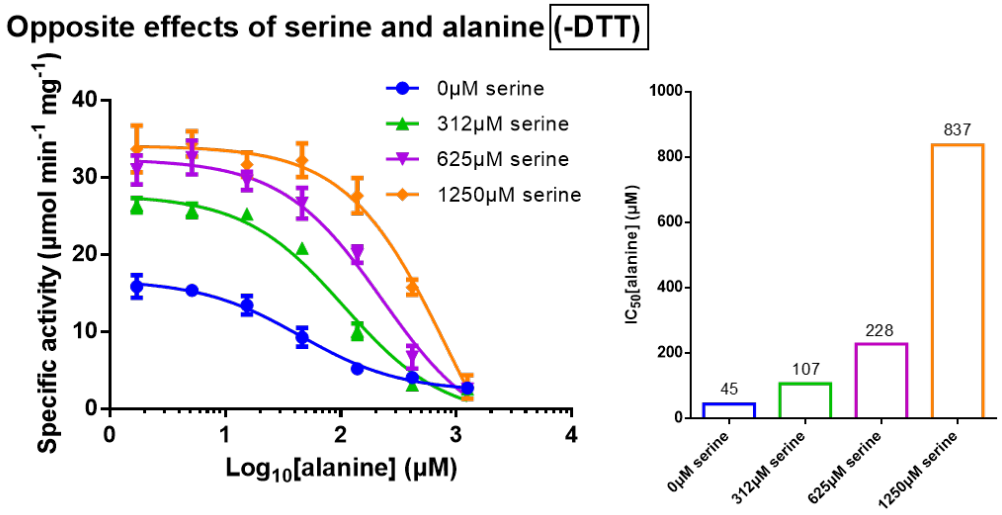

Figure 4-4. Ligand competition of serine and alanine on M2PYK in the absence of DTT. Error bars are derived from three independent repeat experiments.

The blue curve Figure 4-4 shows that activity of enzyme was reduced by alanine from about 16 unit/mg to 2 unit/mg with IC_{50} (alanine) of 45 µM. The enzyme was activated to 34 unit/mg in the presence of 1.25 mM serine.

In a competition experiment in which both ligands are present at the same time, high concentrations of serine (1.25mM) increase the IC_{50} (alanine) by about 20 times to 837 µM Figure 4-5.

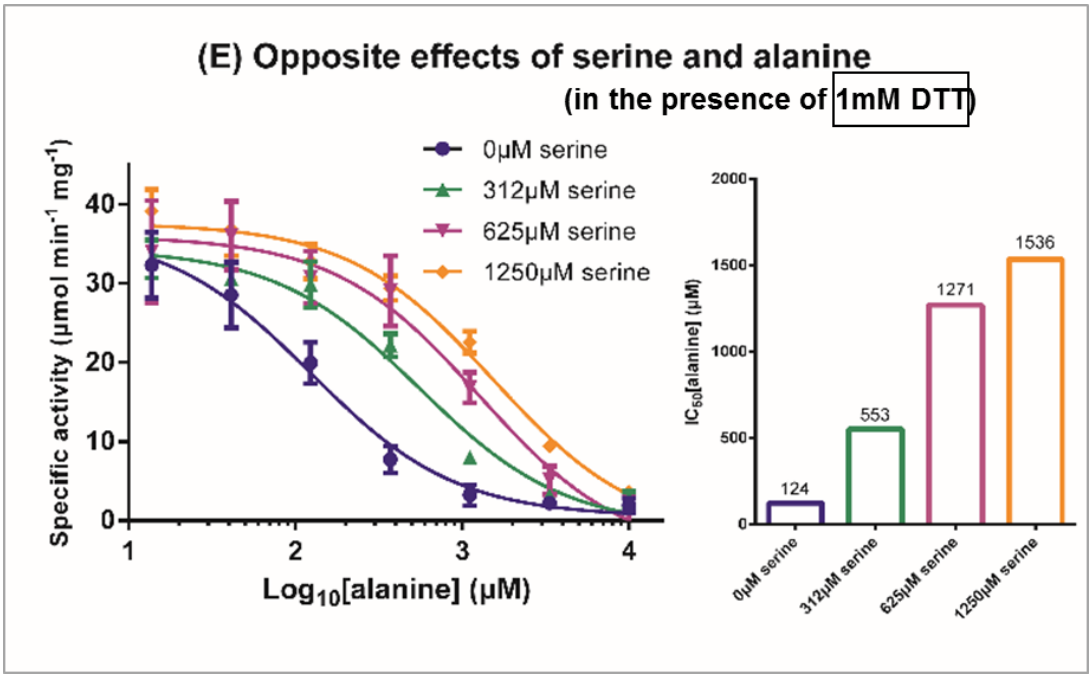

Figure 4-5. Ligand competition of serine and alanine on M2PYK in the presence of 1 mM DTT. Error bars are derived from three independent repeat experiments.

In the presence of DTT, activity of enzyme without alanine or serine increases to 32 unit/mg compared with enzyme without DTT (Figure 4-7). M2PYK with 1.25mM serine was activated to 37 unit/mg from 33 unit/mg. The IC_{50} (alanine) at each concentration of serine was doubled in the presence of DTT compared with Figure 4-4, which also suggested that DTT decreases the affinity of alanine.

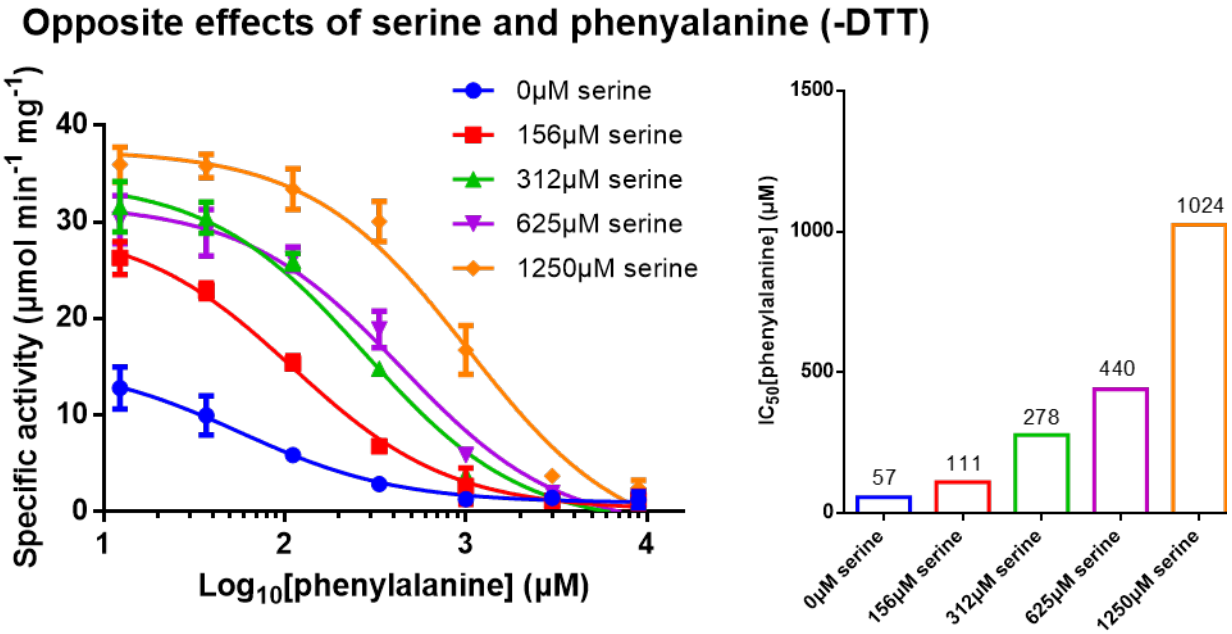

Figure 4-6. Ligand competition of serine and phenylalanine on M2PYK in the presence of 1 mM DTT. Error bars are derived from three independent repeat experiments.

The blue curve in Figure 4-6 shows that phenylalanine inhibits enzyme activity from 14 unit/mg to almost zero (at a concentration of 4mM). The yellow curve suggests that serine activates enzyme to 37 unit/mg. The IC_{50} (phenylalanine) increased by about 20 times to 1024 µM from 57 µM. This suggests that serine decreases the affinity of phenylalanine.

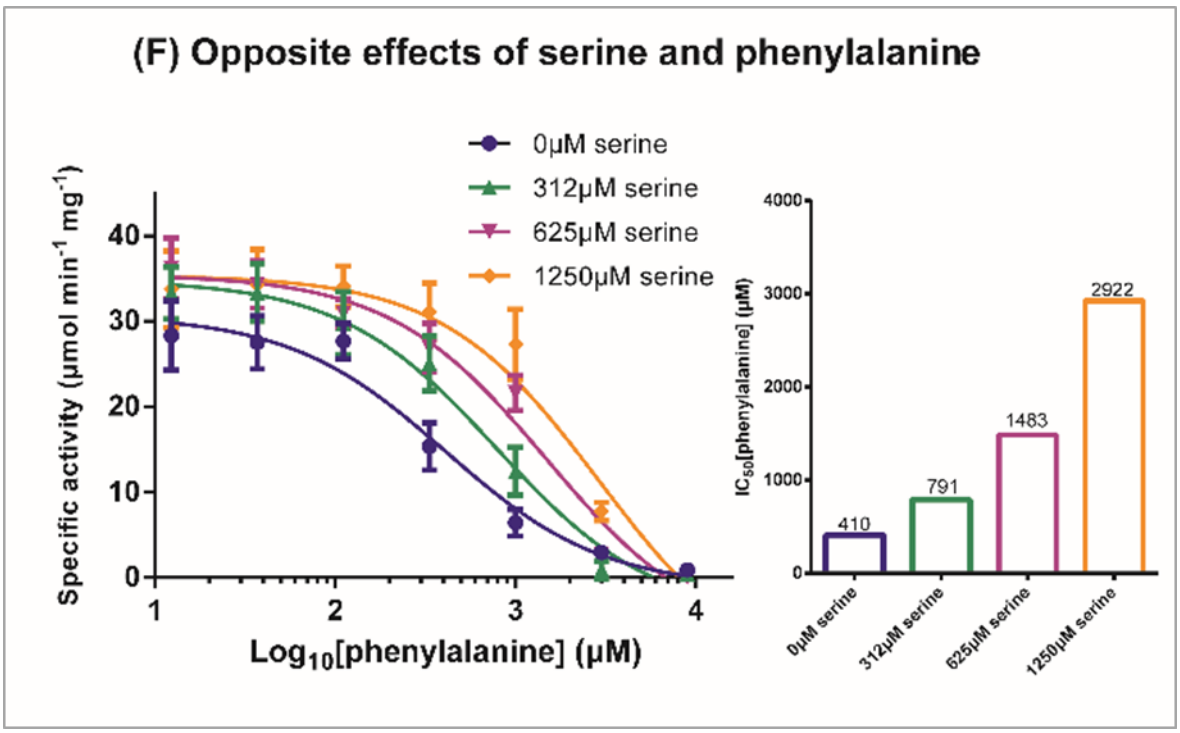

Figure 4-7. Ligand competition of serine and phenylalanine on M2PYK in the absence of DTT. Error bars are derived from three independent repeat experiments.

In the presence of DTT, activity of enzyme without phenylalanine or serine increases to 29 unit/mg compared with enzyme without DTT (Figure 4-9). M2PYK with 1.25mM serine was activated to 35 unit/mg. The IC_{50} (phenylalanine) was increased by 8 times in the presence of DTT and in the absence of serine, which also suggested that DTT decreases the affinity of phenylalanine.

In summary, different concentrations of binary mixtures of serine and alanine (or phenylalanine) were used to show their competing effects on enzyme activity. At a concentration of 1250 μM, serine increases the IC_{50} values of inhibitory amino acids alanine (from 124 μM to 1536 μM) and phenylalanine (from 410 μM to 2922 μM). The measured concentrations of amino acids in normal and cancer tissues is in the high micromolar to low millimolar range (Lefauconnier et al., 1976, Brodzki et al., 2005). With an approximate cellular concentration of alanine of 1 mM, M2PYK is only ~10% active, however in the presence of serine at an intracellular concentration of ~0.6 mM, activity is restored to ~65%. A similar effect has been measured for phenylalanine which at a cellular concentration of ~0.2 mM reduces M2PYK activity to ~ 65% which can be raised to nearly full activity in the presence of 0.6 mM serine.

4.3.1.2 .The effects of histidine/glycine and alanine on M2PYK

	0μM histidine	4.9μM histidine	9.8μM histidine	19.5μM histidine	39μM histidine	78μM histidine	156μM histidine	312μM histidine
IC50	41.62	42.61	55.48	44.35	67.99	54.50	55.10	67.05

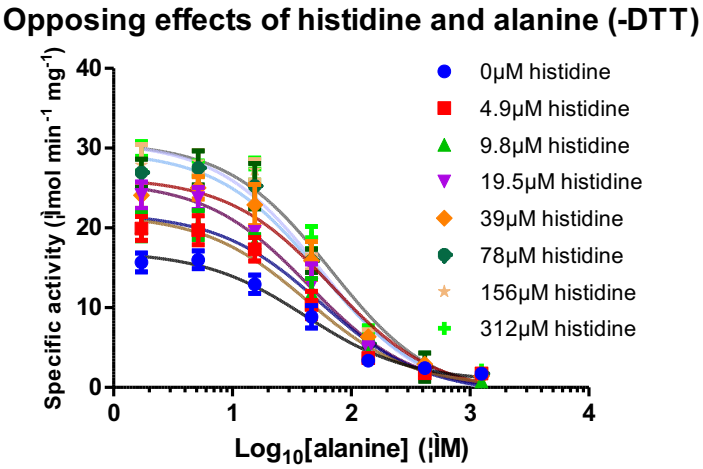

Figure 4-8. Ligand competition of histidine and alanine on M2PYK in the absence of DTT. Error bars are derived from three independent repeat experiments.

Histidine activated the enzyme from 15 unit/mg to 28 unit/mg in the absence of alanine. Alanine inhibited the activity from 15 unit/mg to near zero. But, IC_{50} (alanine) did not increase significantly when higher concentrations of histidine were added.

	His 1.25mM	His 0.625mM	His 0.3125mM	His 0.15625mM	His 0mM
IC50	98.53	82.08	69.24	83.98	119.1

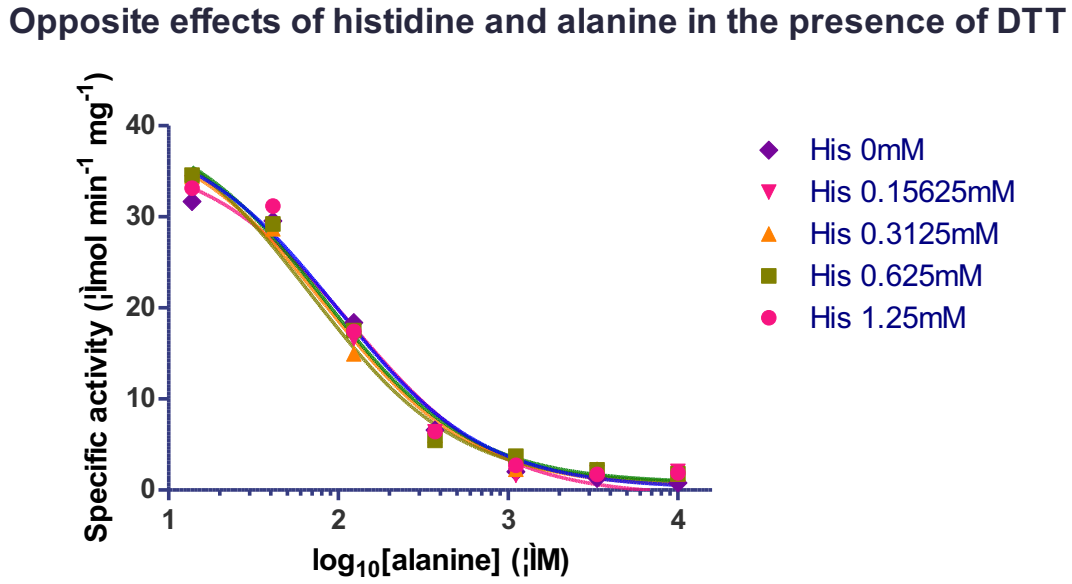

Figure 4-9. Ligand competition of histidine and alanine on M2PYK in the presence of 1 mM DTT. Error bars are derived from three independent repeat experiments.

Interestingly, in the presence of 1 mM DTT, histidine could no longer activate M2PYK at any concentration.

	0μM glycine	312μM glycine	625μM glycine	1250μM glycine	2500μM glycine
IC50	39.63	40.48	38.98	43.21	49.02

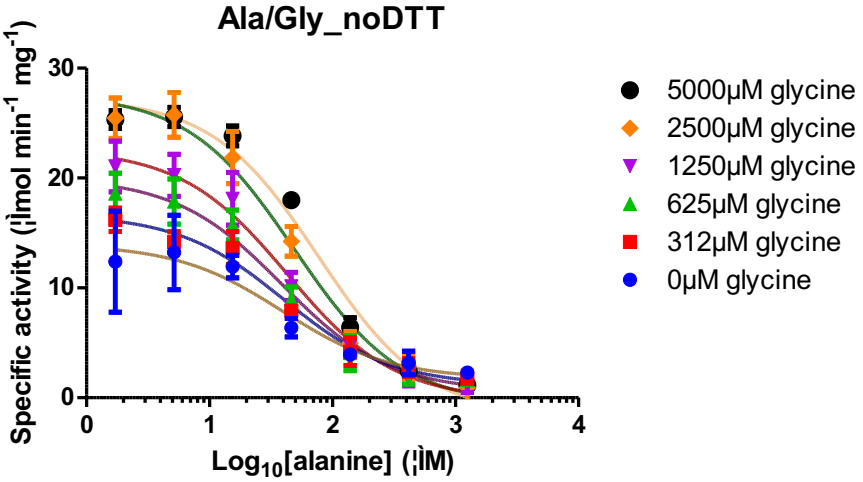

Figure 4-10. Ligand competition of glycine and alanine on M2PYK in the absence of DTT. Error bars are derived from three independent repeat experiments.

Glycine activated the enzyme from 13 unit/mg to 27 unit/mg in the absence of alanine. Alanine inhibited the activity from 13 unit/mg to near zero. As with histidine, the IC_{50} (alanine) did not increase when higher concentration of glycine was added.

	M2+0mM Gly	M2+0.156mM Gly	M2+0.31mM Gly	M2+0.625mM Gly	M2+1.25mM Gly	M2+2.5mM Gly	M2+5mM Gly
IC50	76.36	68.83	80.56	59.29	54.46	71.61	56.70

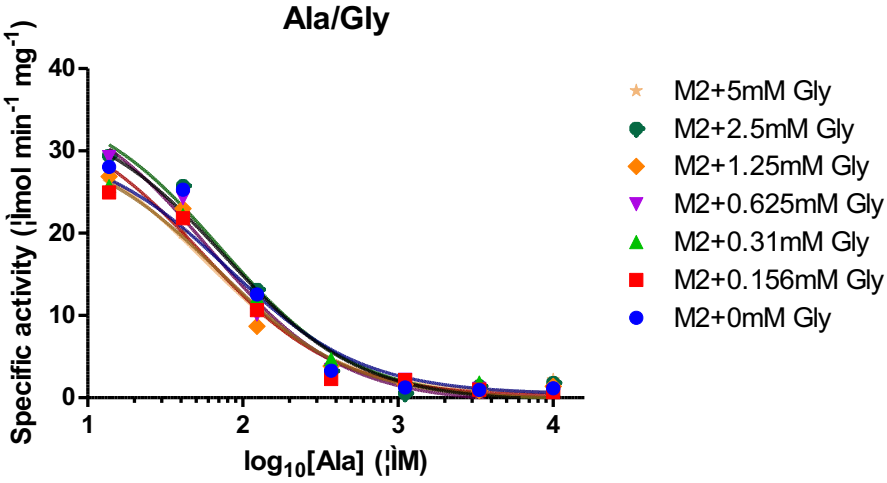

Figure 4-11. Ligand competition of glycine and alanine on M2PYK in the presence of 1 mM DTT. Error bars are derived from three independent repeat experiments.

As with His, in the presence of 1 mM DTT, Gly could no longer activate the activity of M2 at any given concentration. IC_{50} of Ala remained at the same level but 50% higher than M2PYK without DTT. The results from Figure 4-8, Figure 4-9, Figure 4-10, and Figure 4-11 can be summarised as follows:

1. Both His and Gly activate M2PYK on their own
2. Neither Gly nor His significantly increases the IC_{50} of alanine. This result is in contrast with the effect of Ser which also activates M2PYK on its own but decreases affinity of Ala and Phe.
3. DTT decreases the affinity of Ala (and increases the IC_{50}).
4. IC_{50} (Ala) is around 40 µM without DTT and 70 µM with DTT even when His or Gly were added at any given concentration.

4.3.1.3 Conclusion and discussion:

From these experiments, we can conclude two points. Firstly, we have generated strong evidence showing that activator and inhibitor amino acids bind competitively. Furthermore, given that serine increases the affinity of alanine but glycine and histidine do not, we suggest that this regulation may stem from two different mechanisms, which are likely to be important in cellular regulation.

The cellular concentration of alanine and serine (Table 2 Chapter 1) was reported at 0.5 mM and 0.6 mM respectively in normal cells (Iovine et al., 2014). The concentration increased to 5.7 mM (alanine) and 1.5 mM (serine) in cancer cells (Brodzki et al., 2005). From Figure 4-4, we see the activities of M2PYK under these two conditions are about 25 unit/mg and 8 unit/mg, respectively. We have also shown that the amino acid modulation of M2PYK activity is redox-dependent. In other words, reducing environments de-sensitise M2PYK to amino acid inhibition/activation, and vice versa. This observation is particularly interesting for cancer cells because the redox homoeostasis of cancer cells is deregulated.

4.4 LPYK

4.4.1 Amino acids and metabolites screening

In the current literature, only F-1,6-BP and alanine have been reported as regulating LPYK (Llorente et al., 1970). In experiments reported in this thesis we tested 18 amino acids and 10 metabolites to see if LPYK could be regulated. M1PYK was included for comparison. Experimental conditions are described in Chapter 4.1.3. All enzyme activity assays were carried out with a protein concentration at 0.01mg/ml. Buffer conditions are set as follow: 10 mM PBS-CM, 0.55 mM PEP, 0.4 mM ADP, 100 mM KCl, 10 mM $MgCl_2$, 37 ° C.

From the results in Figure 4-12 the specific activity of LPYK is 17 unit/mg. F-1,6-BP is a natural activator of LPYK which activated LPYK to 31 unit/mg. Oxalic acid is a natural inhibitor of LPYK which inhibited the protein to 4 unit/mg. In contrast to these positive and negative controls, none of the amino acids and metabolites were found to have a significant effect on the enzyme activity of LPYK. From our enzyme assay we found that alanine at 2 mM did not show any change of activity to LPYK. This differs

from the Llorente results that showed inhibition of LPYK (50% inhibition by 0.1 mM alanine) (Llorente et al., 1970). The LPYK that Llorente paper used is from mouse liver cells extract, therefore it could be that the mouse LPYK has different activity than our recombinant human LPYK because of post translational modifications. Also, the mouse liver cells extract could contain other PYK isoforms which we have shown are significantly down regulated by alanine.

Initially we hypothesized that cysteine is a reducing agent that could activate LPYK like DTT. Surprisingly, the enzyme data showed that cysteine has no activation nor inhibition to LPYK.

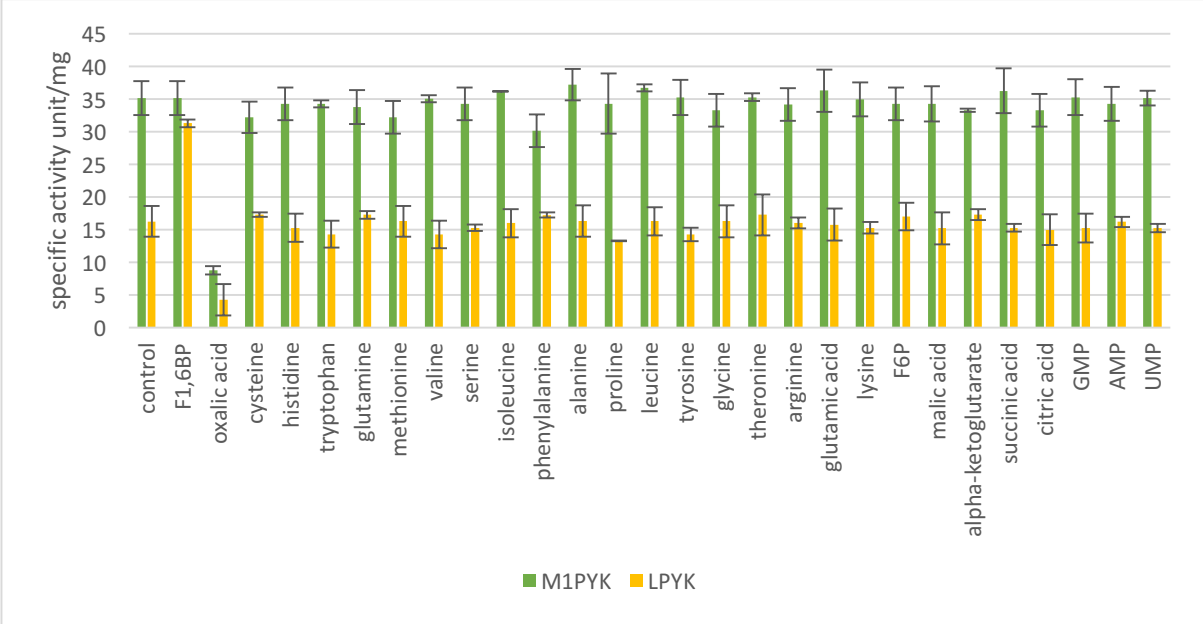

Figure 4-12. Effects of metabolites on activity of LPYK. Error bars are derived from three independent repeat experiments. The protein concentration is 0.01mg/ml. Buffer conditions are set as follow: 10 mM PBS-CM, 0.55 mM PEP, 0.4 mM ADP, 100 mM KCl, 10 Mm $MgCl_2$, 37 ° C.

The enzyme activity of LPYK in Figure 4-12 was not regulated by 2 mM cysteine. However, from the TDA result in Figure 4-13 10 mM cysteine showed an increase in melting temperature from 62 ºC to 66 ºC. This suggests that cysteine binds to LPYK;

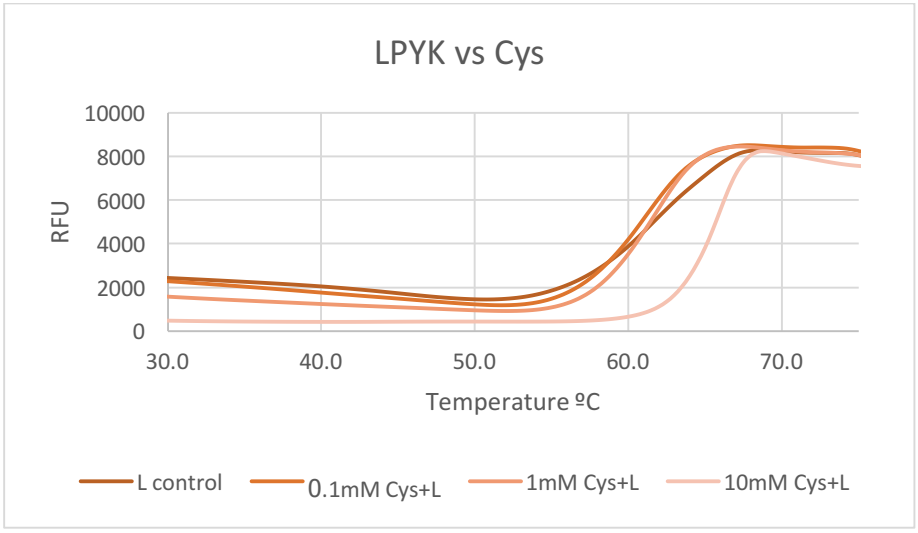

A

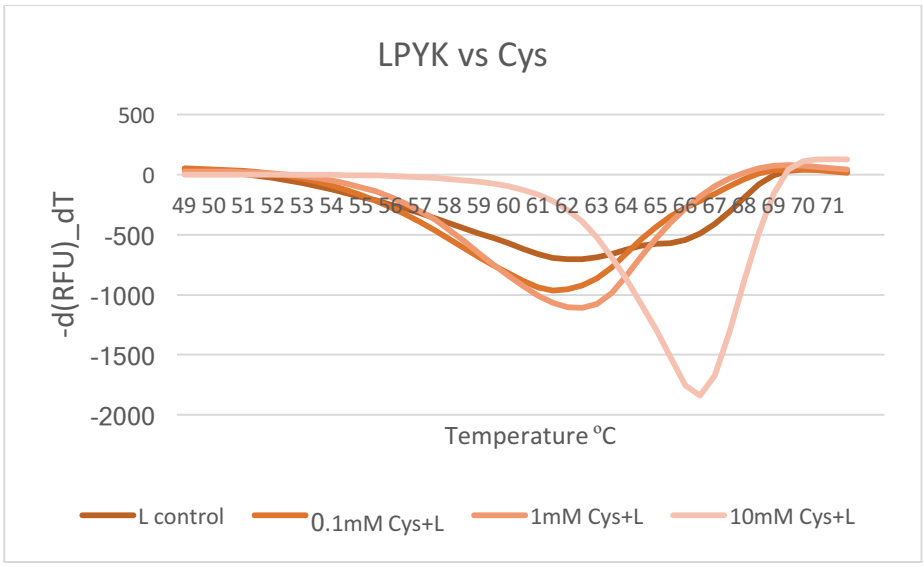

B

Figure 4-13. (A) Raw data of TDA for LPYK incubated with 0.1 mM, 1 mM and 10 mM Cys. (B) Derivative calculations of the fluorescence readings.

4.4.2 T3 is an inhibitor of LPYK

T3 (triiodothyronine) is a hormone in human that is responsible for the regulation of metabolism. From Morgan's paper (Iovine et al.2014). T3 was found to be a strong inhibitor of M2 PYK (Morgan et al., 2013b). To confirm if T3 can also inhibit LPYK an enzymic assay was performed with addition of 20µM T3. The results showed that T3 also inhibits LPYK with 75% inhibition at 20 µM (Figure 4-15).

Previous studies showed that T3 inhibited M2PYK thereby increasing cell proliferation (Morgan et al., 2013b). Therefore, inhibition of LPYK shown here suggests that T3 may also play a role in the regulation of LPYK in cells.

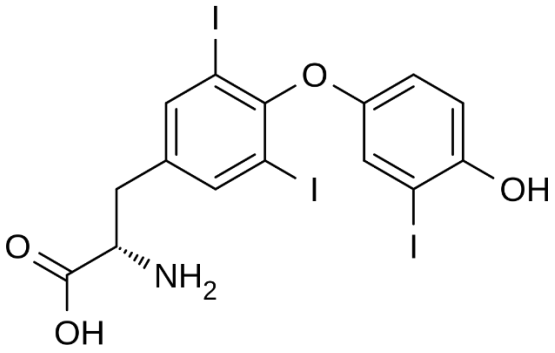

Figure 4-14. Structure of triiodothyronine (T3).

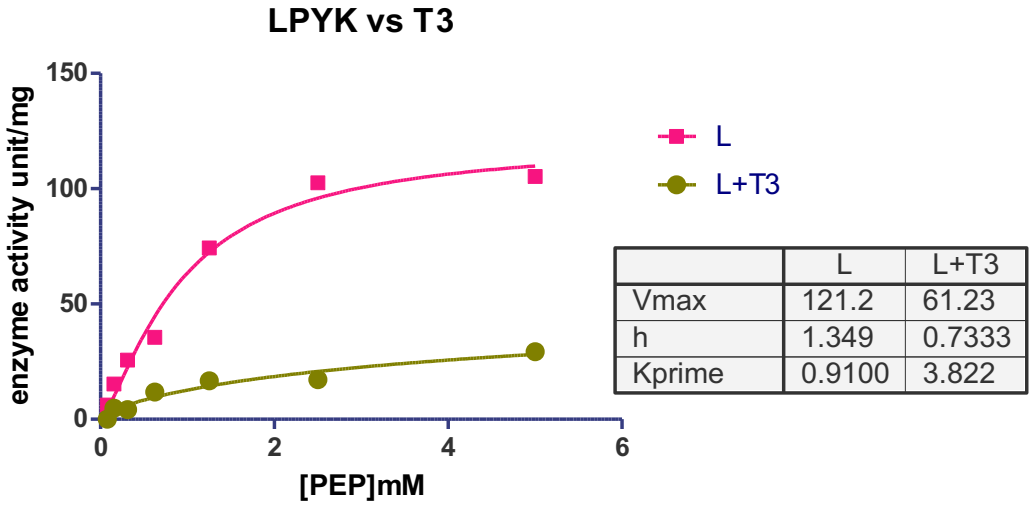

	L	L+T3
Vmax	121.2	61.23
h	1.349	0.7333
Kprime	0.9100	3.822

Figure 4-15. LPYK was diluted to 0.001mg/ml from 16.1mg/ml in to PBS solution and PBS solution with 20μM T3. After 10 minutes room temperature pre-incubation, the V_{max} of RPYK with T3 was reduced from 121.2 unit/mg to 61.23 unit/mg.

4.5 RPYK

In the published reports, from all metabolites tested only alanine has been reported as an inhibitor of RPYK (Marie et al., 1980b). But surprisingly, we show that alanine is a strong activator for RPYK in the assays used in this thesis. This difference may be because the protein used in Marie's assays was extracted from human red cells and may be modified (e.g. phosphorylated) or be bound to other contaminant metabolites.

As summarised in Figure 4-16, our single-point assay showed that RPYK was upregulated by natural activator F-1,6-BP and down regulated by natural inhibitor oxalic acid. Eleven amino acids, further investigated in 4.5.1, enhance RPYK activity by between 1.5-fold and 2-fold.

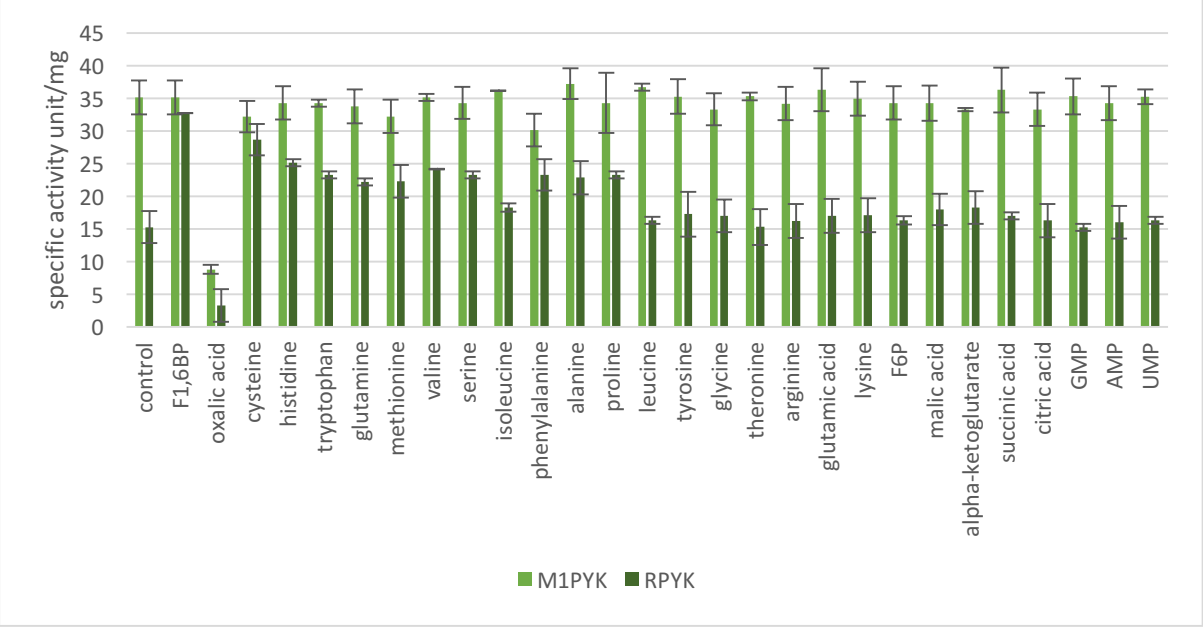

Figure 4-16. Effect of metabolites on activity of RPYK. Error bars are derived from three independent repeat experiments. The protein concentration is 0.01mg/ml. Buffer conditions are set as follow: 10 mM PBS-CM, 0.55 mM PEP, 0.4 mM ADP, 100 mM KCl, 10 mM $MgCl_2$, 37 ° C.

4.5.1 11 amino acids up-regulate RPYK

Interestingly, unlike M2PYK, there is no inhibitor of RPYK found among all the amino acids and metabolites tested, but we have identified several activators. Here we carried out dose response curves on all the activators to investigate the AC_{50}. The assay details are given in section 5.4.2. The results summarised in Figure 4-17 show that 10 amino acids activate RPYK. Interestingly, cysteine is an activator under 1mM concentration but becomes an inhibitor when the concentration is above 1mM.

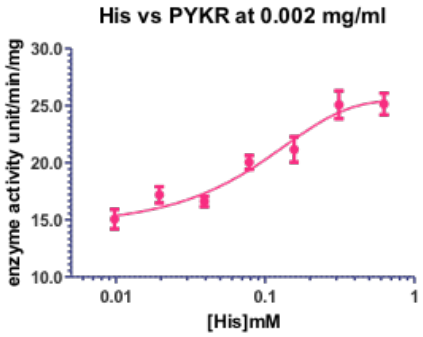
His vs PYKR at 0.002 mg/ml
enzyme activity unit/min/mg
30.0
25.0
20.0
15.0
10.0
0.01
0.1
1
[His]mM

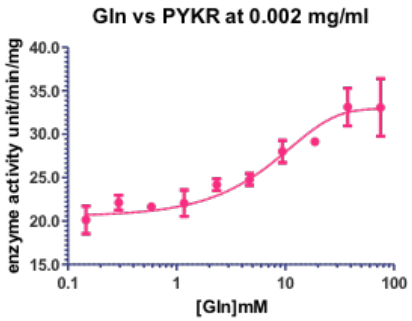
Gln vs PYKR at 0.002 mg/ml
enzyme activity unit/min/mg
40.0
35.0
30.0
25.0
20.0
15.0
0.1
1
10
100
[Gln]mM

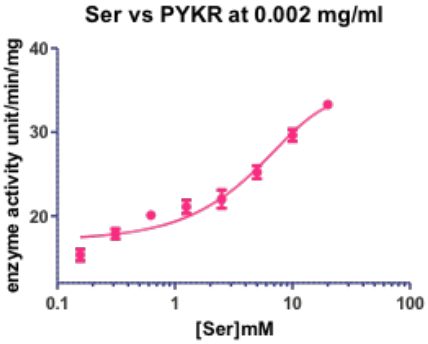
Ser vs PYKR at 0.002 mg/ml
enzyme activity unit/min/mg
40
30
20
0.1
1
10
100
[Ser]mM

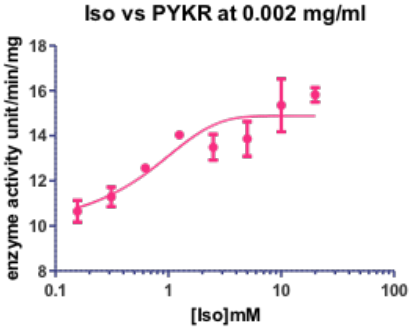
Iso vs PYKR at 0.002 mg/ml
enzyme activity unit/min/mg
18
16
14
12
10
8
0.1
1
10
100
[Iso]mM

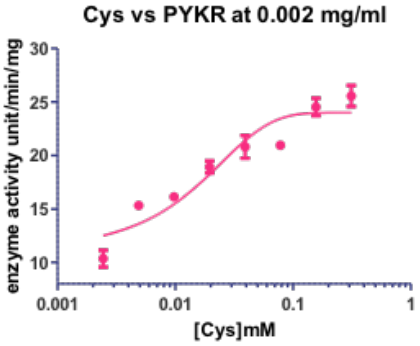
Cys vs PYKR at 0.002 mg/ml
enzyme activity unit/min/mg
30
25
20
15
10
0.001
0.01
0.1
1
[Cys]mM

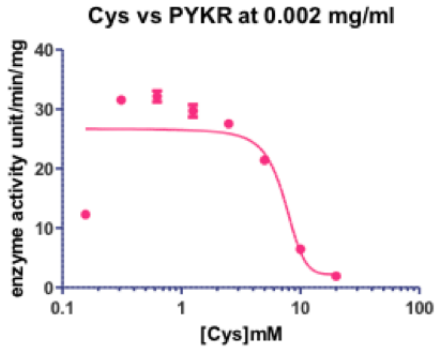
Cys vs PYKR at 0.002 mg/ml
enzyme activity unit/min/mg
40
30
20
10
0
0.1
1
10
100
[Cys]mM

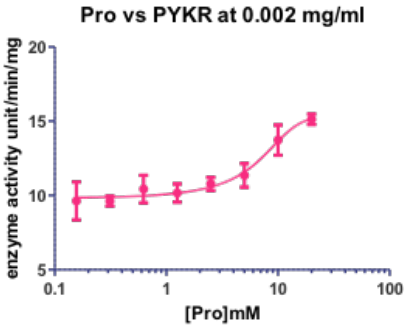
Pro vs PYKR at 0.002 mg/ml
enzyme activity unit/min/mg
20
15
10
5
0.1
1
10
100
[Pro]mM

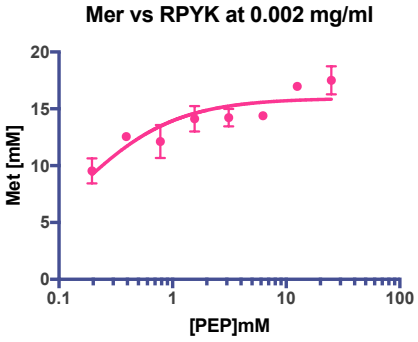
Mer vs RPYK at 0.002 mg/ml
Met [mM]
20
15
10
5
0
0.1
1
10
100
[PEP]mM

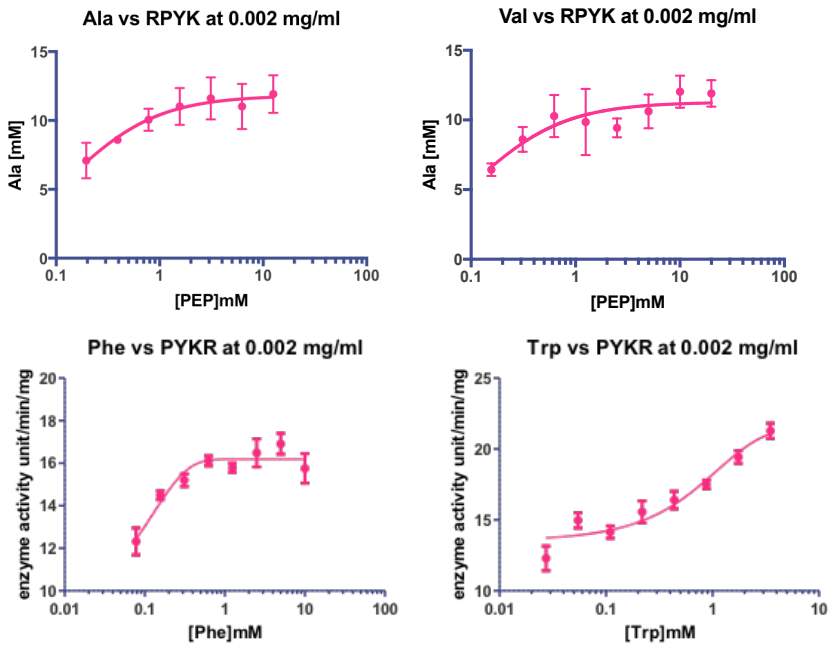

Figure 4-17. Effects of amino acids on enzyme activity of RPYK. Error bars are derived from three independent repeat experiments. The protein concentration is 0.01mg/ml. Buffer conditions are set as follow: 10 mM PBS-CM, 1 mM ADP, 100 mM KCl, 10 mM $MgCl_2$, 37 ° C.

4.5.2 Amino acids influence thermal stability of RPYK

To confirm that the amino acids were binding to RPYK, we investigated amino acid influence on the thermostability of RPYK. Results for histidine (which gives the strongest activating effect on RPYK) thermal stability are shown in Figure 4-18. Addition of 0.1mM, 1mM, or 10mM histidine increases the melting temperature from 62 ºC (unliganded) to 64 ºC, 64 ºC and 64 ºC, respectively. This correlates with the effect found in the enzyme activity assay in which RPYK activity increases from about 16 unit/mg (0 mM His) to 25 unit/mg (1 mM His) over the same concentration range (Figure 4-17).

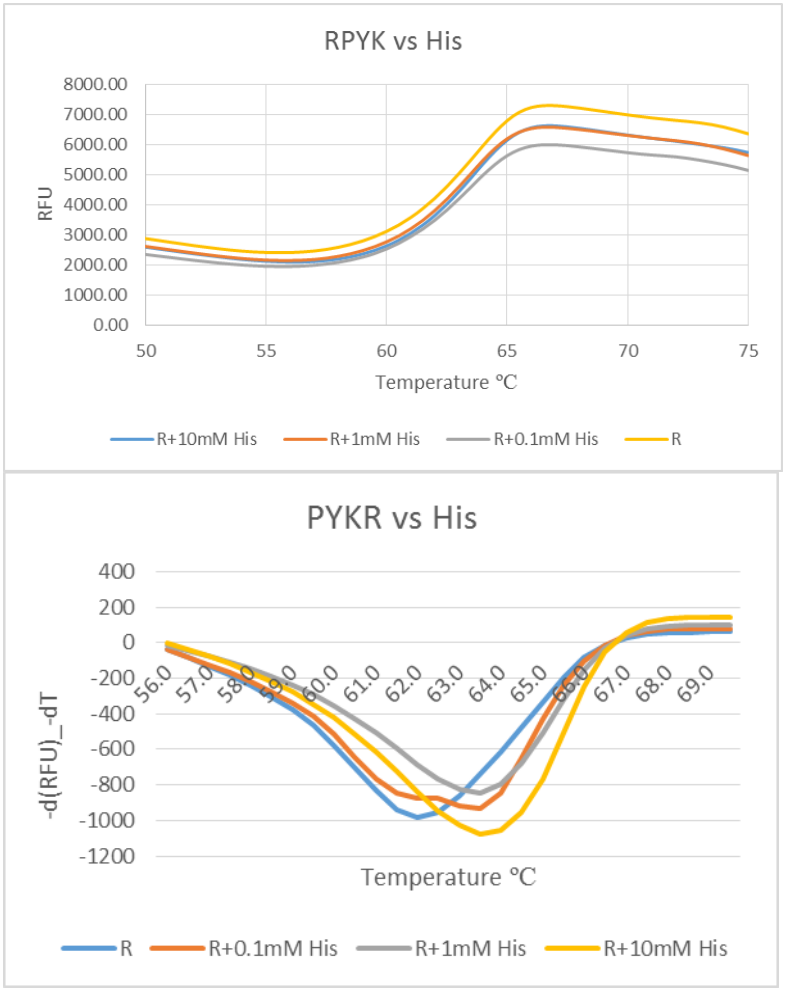

Figure 4-18. Thermal stability of RPYK and effects of His at 0.1mM, 1mM, 10mM. Interestingly, the melting temperature of RPYK increased from 62 ºC (RPYK) to 64 ºC (RPYK+His at 0.1mM, 1mM, 10mM).

4.5.3 T3 is an inhibitor of RPYK

T3 (triiodothyronine) is a thyroid hormone produced by thyroid gland in human body that is responsible for the regulation of metabolism. The inhibition of M2PYK activity by T3 has been reported (Morgan et al., 2013b). The inhibition of LPYK has been discussed previously (see Figure 4-15). We also carried out an assay to test the possible inhibition of RPYK by T3 and show (Figure 4-19) that RPYK activity was inhibited by 85% from 98.34 unit/mg. As with LPYK, we did not show the dose response curve of T3, because the solubility of T3 in aqueous buffer was low and the results were complicated.

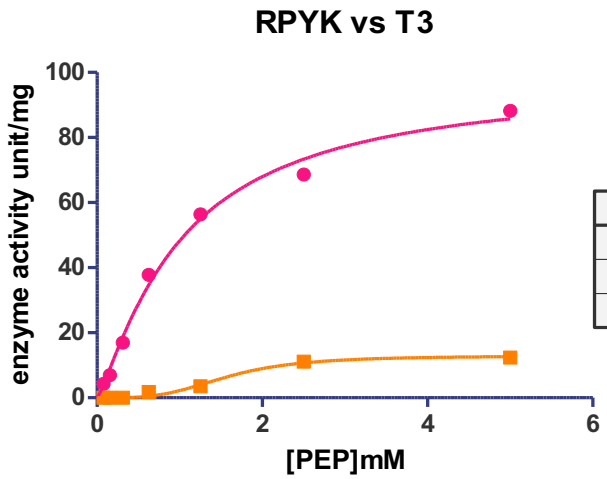

	R	R+T3
Vmax	98.34	12.88
h	1.213	3.468
Kprime	1.036	4.797

Figure 4-19. The T3 effect on RPYK. RPYK was diluted to 0.001mg/ml from 8.1mg/ml in to PBS solution and PBS solution with 20uM T3. After 10 minutes room temperature pre-incubation, the V_{max} of LPYK with T3 was reduced from 98.34 unit/mg to 12.88 unit/mg.

4.6 Discussion

4.6.1 Amino acids and metabolites screening

In this study, we screened a group of amino acids and metabolites and determined the specific activities of each PYK isoform and ligand combination (at a ligand concentration of 2 mM). Here we combine these results to calculate the relative activation or inhibition percentage in **Error! Reference source not found.**, using the following formula with M2PYK with F-1,6-BP as an example:

$$activation\ percentage = \frac{(activity\ of\ M2PYK + FBP) - (activity\ of\ M2PYK)}{(activity\ of\ M2PYK)} \times 100\%$$

From this table, we can conclude that M1PYK and LPYK are not very sensitive to amino acids and metabolite regulation. In contrast, M2PYK and RPYK are sensitive to amino acids and metabolites regulation, but in different ways. There are both activators and inhibitors for M2PYK, but only activators for RPYK except at high concentrations of cysteine.

	M1PYK	M2PYK	LPYK	RPYK
F1,6BP	0%	126%	92%	115%
oxalic acid	-75%	-70%	-74%	-78%
cysteine	-8%	-13%	6%	88%
histidine	-2%	119%	-6%	65%
tryptophan	-2%	-63%	-12%	53%
glutamine	-4%	7%	6%	45%
methionine	-8%	-56%	0%	46%
valine	0%	-70%	-12%	58%
serine	-2%	112%	-6%	53%
isoleucine	3%	-51%	-2%	20%
phenylalanine	-14%	-69%	6%	53%
alanine	6%	-63%	0%	50%
proline	-2%	-49%	-18%	53%
leucine	5%	-2%	0%	7%
tyrosine	0%	7%	-12%	13%
glycine	-5%	56%	0%	11%
threonine	0%	-55%	6%	0%
arginine	-3%	-3%	-2%	6%
glutamic acid	3%	-2%	-3%	11%
lysine	0%	7%	-6%	12%
F6P	-2%	0%	5%	7%
malic acid	-2%	7%	-6%	18%
alpha-ketoglutarate	-5%	-14%	6%	20%
succinic acid	3%	0%	-6%	12%
citric acid	-5%	-7%	-8%	7%
GMP	0%	-42%	-6%	0%
AMP	-2%	-49%	0%	5%
UMP	0%	7%	-6%	7%

Table 9. Summary of metabolites screening of four human PYK isoforms. Strong activation or inhibition was marked with red and green (more than 20%).

M2PYK is critical for regulating the synthesis and metabolism of serine. Knock-down and inactivation of M1 and M2 PYK have been shown to result in a build-up of metabolites in the glycolytic pathway enabling synthesis of serine from its precursor 3-phosphoglycerate (Chaneton et al., 2012). In a complementary experiment, cells treated with a synthetic M2PYK activator become dependent on serine for continued

cell proliferation (Kung et al., 2012). Together with the knowledge that binding of serine activates M2PYK, these results suggested that there is a feedback mechanism regulated by serine concentration, which provides a balance between glycolysis/ATP production (promoted by serine-bound active M2PYK) and cell proliferation (favoured by inactive M2PYK). A number of families of drug-like M2PYK activator molecules have been tested on cancer cell lines (Anastasiou et al., 2012; C. Guo et al., 2013; J. K. Jiang et al., 2010; Kung et al., 2012; Vander Heiden, Christofk, et al., 2010; Yacovan et al., 2012). Interestingly, M2PYK activators profoundly reduced cell proliferation only in models where nonessential amino acids (alanine, aspartic acid, asparagine, glutamic acid and serine) are removed from cell media (Kim et al., 2015; Kung et al., 2012; Parnell et al., 2013; Warner, Carpenter, & Bearss, 2014). This sensitivity is likely due to a lack of serine nutrient which cannot be synthesised by the cell when M2PYK is activated.

	concentration range	
	Lefauconnier et al. 1976	*Brodzki et al. 2005*
Ala in normal tissue	0.8-1.2 mM	0.4-0.6 mM
Ala in tumour tissue	1.6-2.2 mM	4.6-6.8 mM
His in normal tissue	around 0.1 mM	0.1-0.3 mM
His in tumour tissue	around 0.2 mM	0.2-0.6 mM
Phe in normal tissue	around 0.1 mM	0.1-0.3 mM
Phe in tumour tissue	0.2-0.3 mM	0.1-0.7 mM
Ser in normal tissue	0.4-0.5 mM	0.5-0.7 mM
Ser in tumour tissue	0.6-0.9 mM	1.2-1.8 mM

Figure 4-20. Intracellular concentrations of free amino acids in normal and tumour tissues. The concentration ranges of detected amino acids from two references (Brodzki, Tatara, Pasternak, Rózańska, & Szponder, 2005; Lefauconnier, Portemer, & Chatagner, 1976).

As shown in Figure 4-20, measured intracellular alanine concentrations from various cell types range from 0.4 mM to over 6.8 mM in Brodzki's study, which is in the range to inhibit M2PYK activity in vitro. However, in vivo the regulation depends not on a single ligand but on the combination effect of all regulators including the strong activator F-1,6-BP with low AC_{50}. The main biosynthetic route for alanine is via alanine transaminase (ALT) using pyruvate as a substrate (Chougule et al., 2008) and

elevated levels of ALT are indeed found in cancer patients. Pancreatic ductal adenocarcinoma tumour cells rely on alanine which is provided in millimolar concentrations by autophagous pancreatic stellate cells which feeds the tumour (Sousa et al., 2016). Labelling studies further show that pyruvate generated from the transaminase feeds the citric acid cycle. These observations suggest that alanine serves a double purpose of blocking glycolytic flux (allowing metabolite to build up the concentration of the PYK activator F-1,6-BP) and providing pyruvate for the TCA cycle.

Allostasis is the process of achieving equilibrium in a changing (nutrient) environment, and M2PYK provides an excellent example of an allostatic regulator in which the opposing effects of activating (alanine) and inhibiting (serine) amino acids provide a finely-balanced feed-back mechanism for tuning M2PYK activity over a wide range of absolute and relative concentrations. With high levels of serine (or F-1,6-BP), M2PYK will be turned on and the TCA cycle will be fuelled by pyruvate from the last step in glycolysis (Chaneton et al., 2012). With high levels of alanine (or phenylalanine or tryptophan), M2PYK is turned off and the TCA cycle may be fuelled by pyruvate produced by alanine transaminase (Sousa et al., 2016). Depending on the relative concentrations of serine (up to ~1 mM) and alanine (up to ~5 mM), M2PYK activity can be tuned to run from 5% to 100% of its maximum velocity Figure 4-4. The important regulatory factor is the ratio of activating and inhibiting 8 amino acids and other effectors such as F-1,6-BP, as well as post-translational modifications. Thus, M2PYK can act to regulate metabolism by sensing a range of concentrations and can use these inputs to control its enzyme activity by switching quickly (within seconds) between inactive T-state and active R-state conformations. At very low levels of amino acid concentration (less than their K_i values) and with enzyme concentration less than ~2 μM, M2PYK will dissociate into enzymatically inactive monomers. Monomeric M2PYK has been shown to enter the nucleus and promote transactivation of HIF-1 target genes (Lv et al., 2013), many of which are metabolic enzymes, thus providing another regulatory mechanism for M2PYK. Cellular biochemical networks that regulate metabolism, phagocytosis and transcription are composed of highly interconnected nodes which communicate by perturbing molecular concentrations and reaction rates. The structural and enzymatic results presented here provide a molecular

description of the M2PYK metabolic sensor mechanism which can react to widely fluctuating nutrient concentrations in the cell and deliver appropriate signal outputs to these biochemical pathways. RPYK, LPYK, and M1PYK are expressed in specific tissues which may go some way to explaining why their regulation by amino acids is different to that of M2PYK.

For LPYK and M1PYK, both enzymes are quite insensitive to amino acids concentration. The reason might be that their environments (in muscle and liver) are stable and are constantly exposed to higher metabolites concentrations. T3 regulates LPYK and RPYK

In 2013, T3 was reported to be strong inhibitor of M2PYK by stabilising an inactive monomeric form of M2PYK. Here we showed that T3 can also strongly inhibit LPYK and RPYK. M1PYK was also reported to be inhibited by T3 with an IC_{50} above 4 μM. However, from the analytical gel filtration results in section 2.4.2, M1PYK, LPYK, and RPYK do not dissociate at 0.1 mg/mg, which is the lowest concentration we could use in the size exclusion chromatography. We cannot confirm if the inhibition of LPYK and RPYK by T3 is caused by similar mechanism as M2PYK.

In future work, several possible experiments could further explore this inhibitory mechanism. For example, analytical gel filtration of LPYK and RPYK with T3 might show if T3 stabilises the monomeric form of both isoforms. Co-crystallisation of M2PYK, LPYK, and RPYK in complex with T3 would also be good targets and show if T3 could bind to the amino acid pocket.

CHAPTER 5. Biophysical assays on human pyruvate kinase isoforms

Introduction

In this chapter, we describe the use of NMR to study ligand binding by the different human isoforms of PYK. In Chapter 3, enzymatic studies were used to measure the inhibition and activation of metabolites of all four isoforms and these results were consistent with amino acids binding in an allosteric pocket and activating or inhibiting the M2PYK isoform. RPYK also showed enzymatic activation by 11 of the 20 amino acids tested. The NMR experiments described here show that even isoforms, for which metabolites have little inhibitory or activating effect, can also bind strongly to the conserved allosteric pocket.

5.1 STD-NMR assay for ligands binding

Nuclear magnetic resonance (NMR) is an excellent method for detecting ligand-protein binding directly. Saturation Transfer Difference nuclear magnetic resonance (STD-NMR) spectroscopy provides us with a powerful tool to monitor weak ligand-protein binding for K_D values in the mM to μM range (Venkitakrishnan, Benard, Max, Markley, & Assadi-Porter, 2012). As the name indicates, STD-NMR measures the NMR signal of the magnetization transferred from protein (the receptor) to the bound ligand. A selective radiofrequency radiation is applied to saturate protein NMR signals. Then, this saturation transfers to small ligands bound to the protein by intermolecular NOE (Nuclear Overhauser Effect) (Anderson & Freeman, 1962). The magnitude of such saturation transferred to the small molecule is related to the proximity of ligand

atoms to the protein binding pocket (Mayer & Meyer, 2001).

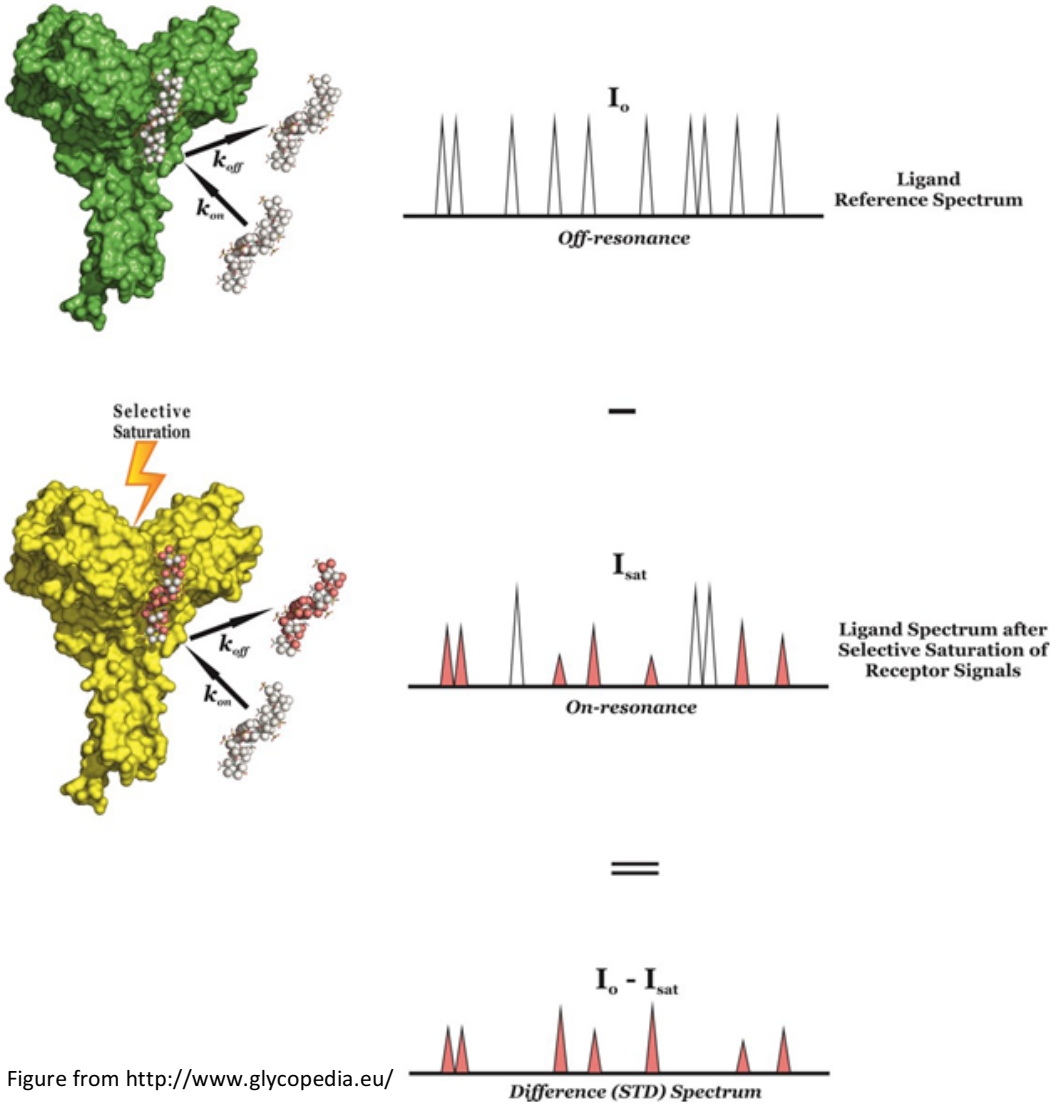

Figure 5-1. Basic theory of STD-NMR. I_0: signal intensities of the free ligand. I_{sat}: signal intensities of bound ligands. I_{STD}: signal intensities of bound ligands. The difference spectra show which signals have been affected by binding to the receptor. The size of the signal is proportional to the proximity of the ligand atom to the protein.

The figure shows the basic theory of STD-NMR: the STD spectrum I_{STD} is the difference between an off-resonance ligand reference proton spectra I_0 and an on-resonance ligand spectra I_{sat} after irradiating the protein only at a specific range. For a ligand bound to the protein, its protons which are close to the protein (less than 5 Å) receive saturation transfer from the protein and appear in the difference in spectra. The protons which are closer to the protein will show stronger signals in the I_{STD} spectra. As with all NOEs, the magnetization transferred from protein to ligand obeys an

inverse power law and is proportional to 1/d**6. In the STD spectra, only signals from hydrogen atoms from the ligand which are in close proximity to the protein will show up, as only for these atoms is there a difference between the on-resonance and off-resonance spectra. The differences in the NMR intensities are shown in the difference spectra: $I_{STD} = I_0 - I_{sat}$ where I_{STD} shows intensity of the binding.

The intensity of all NMR signals depends on the 'saturation time' which in these experiments can vary between 5 and 15 s. All results presented here were measured with a saturation time of 16 seconds. For a given saturation time an amplification factor can be determined and used to scale results from different experiments. If we choose one proton peak as a standard, the amplification factor (A_{std}) can be calculated from the equation below.

The STD amplification factor (A_{std}): A_{std} is determined by the relative STD effect $\frac{I_{STD}}{I_0}$ and the molar ratio of ligand to protein $\frac{[L]_T}{[P]}$. The average number of ligand molecules saturated per molecule of receptor. These A_{std} values for each peak in the STD-NMR spectra can be calculated by the equation below:

$$A_{STD} = \frac{I_{STD}}{I_0} \times \frac{[L]_T}{[P]} \qquad \text{Equation 5-1}$$

where

I_{STD}: is the signal intensity of a given peak of a bound ligand.

I_0: a given peak of signal intensities of the peak in the non-resonance spectrum, which is at the same position as the chosen I_{STD} peak

$[L]_T$: ligand concentration.

$[P]$: total protein concentration in the solution.

Protons which are closer to the receptor show higher A_{STD} values than other protons. At a given saturation time and ligand concentration, the amplification factor also could be depicted as the average number of small molecules that bind to one molecule of protein.

Mapping of the ligand binding moieties: These differences in A_{std} values can be used for 'Ligand Mapping' helping to identify which ligand moieties are important and bind closer to protein. If we set the peak in the STD spectra with highest intensity of ligand hydrogens to 100%, and calculate the percentage of all other hydrogen signals, a ligand binding moieties map may be generated. An illustration of binding mapping for a ligand shows the process of fast exchange between the pocket on the target protein and the ligand in Figure 5-2. The protein receives the selective saturation pulse and transfers the magnetization signal to hydrogen atoms on bound small ligand molecules. Protons, which are in close contact with the pocket, receive higher saturation signal. More remote ligand hydrogens receive less saturation. Atoms not in contact with the receptor at all do not receive a saturation signal. The mapping of ligand binding moieties reflects that the different proximities of each group on the ligand to the receptor surface.

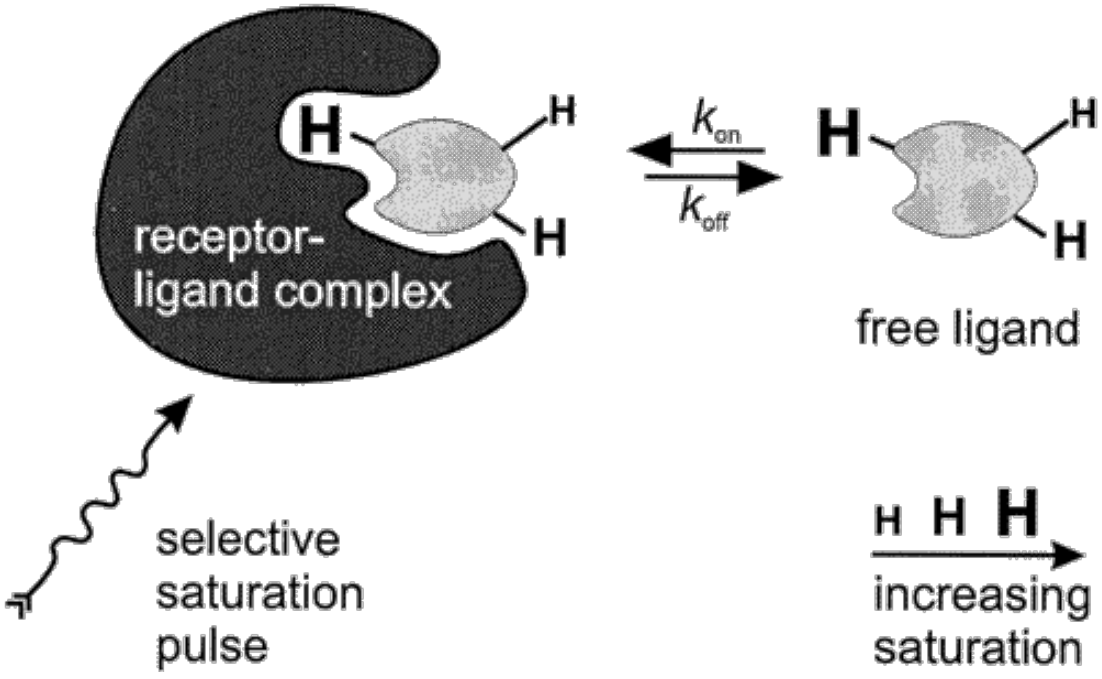

Figure 5-2. Illustration of how saturation may be transferred to a specific ligand. Larger-sized symbols represents a closer interaction with the target protein.

Determination of dissociation constant (K_D): K_D may also be measured by STD-NMR by titrating increasing ligand concentrations. An equation analogous to the Michaelis-Menten equation is used to analyse the STD-NMR data.

$v_0 = \frac{V_{MAX}[L]}{K_M + [L]}$ Equation 5-2, the Michaelis-Menten equation.

Where [L] = ligand concentration.

V_{max} = maximum rate reached in the enzyme reaction system.

Km = the substrate concentration at half V_{max}

$A_{STD} = \frac{\alpha_{std}[L]}{K_D + [L]}$ Equation 5-3 the analogous equation.

Where α_{std} is the maximum amplification factor.

[L] = ligand concentration.

K_D = the substrate concentration at half V_{max} point.

In this equation, when ligand concentration [L] is increasing, the ligand-protein binding will be saturated and the amplification A_{STD} will increase until it reaches the maximum value α_{std} (assuming that the ligand concentration is much higher than protein concentration ([L] >> [P])). The A_{STD} here can be any given peak in the STD-NMR spectrum.

5.2 Protocol and results

A 1D proton NMR (DPFGSE-Double Pulse Field Gradient Spin Echo) measurement on the protein-ligand mixture was carried out to measure the ligand spectra just before the STD-NMR measurement to determine the purity of the ligand solution. As the STD-NMR samples were prepared in 90% H_2O and 10% D_2O solution to investigate exchangeable protons, the concentration of small ligands is typically between 0.1 and1 mM, but water has a concentration of 55 M and the assay suffers from the H_2O signal masking all the other small ligand signals. To overcome this, a water suppression pulse sequence was used in these NMR assays.

Samples for NMR analysis were prepared in PBS with metals [66.7 mM KCl, 6.7 mM $MgCl_2$] containing 20 μM PYK (M1, M2, L, or R), 1 mM amino acid (His, Phe, Ala, Ser, or Cys), 80 mM potassium phosphate, 10 % D_2O at pH 7.4. 550 μl of the sample was placed into a Norell NMR tube (5 mm o.d). 1D NMR data were recorded at 25 ºC with a Bruker Advance 600 NMR spectrometer 10 minutes after adding 1 mM amino-acid ligand. All the data were processed using NMR data processing software-TopSpin 3.5pl 6.

The spectra for LPYK in complex with each of the ligands (1 mM L-serine, L-phenylalanine, L-histidine, L-cysteine, or L-alanine) are shown in Figure 5-3. There are some similar peaks at around 4.7 ppm and 3.5 ppm in all the spectra. Peaks at around 4.7 ppm are signals of hydrogen in water and peaks at around 3.5 ppm are assumed to be hydrogen in glycerol. The appearance of glycerol in the spectra was unexpected and we hypothesized that the glycerol was probably introduced during the protein purification step. This may explain the same peaks present at around 3.5 ppm in all the spectra. All the other peaks from each spectrum can be assigned to hydrogens of each L-amino acid (See Figure 5.3).

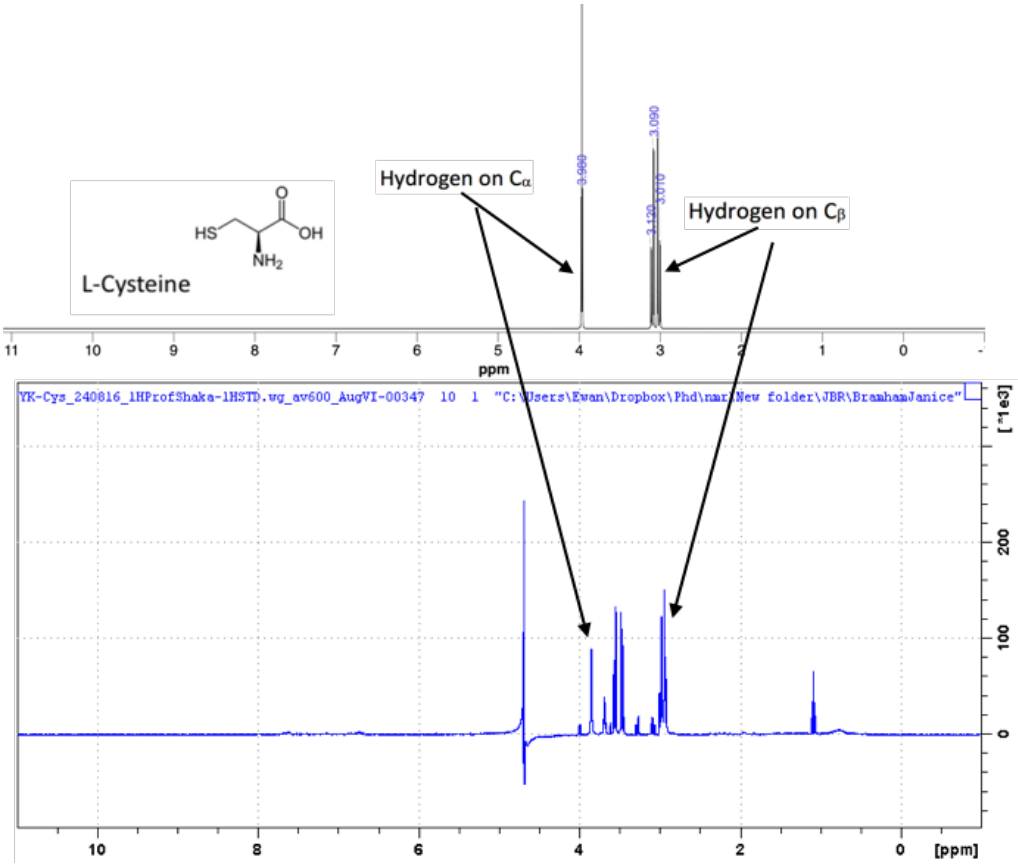

a

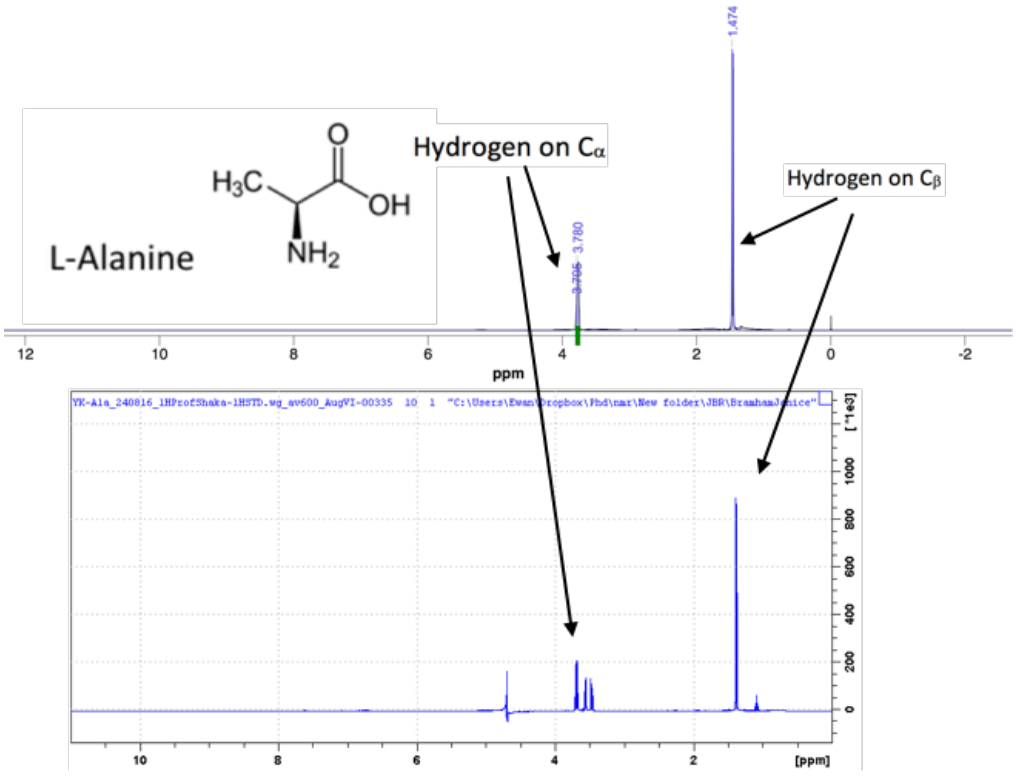
L-Alanine
Hydrogen on Cα
Hydrogen on Cβ
ppm
[ppm]

b

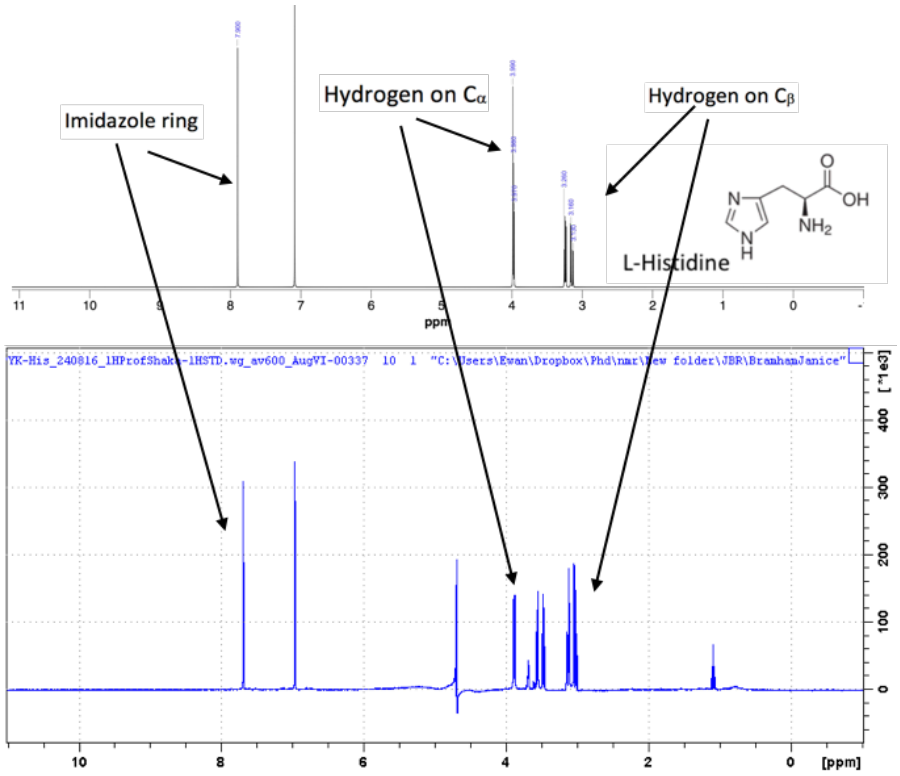
Imidazole ring
Hydrogen on Cα
Hydrogen on Cβ
L-Histidine
ppm
[ppm]

c

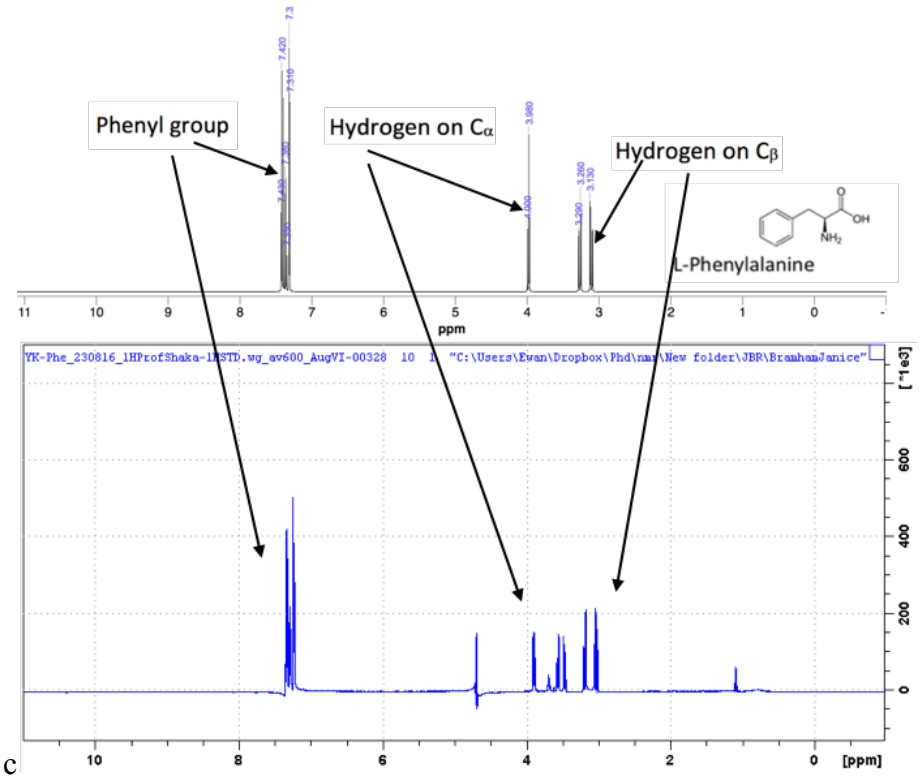
Phenyl group
Hydrogen on Cα
Hydrogen on Cβ
L-Phenylalanine
ppm
[ppm]
[*1e3]

c

d

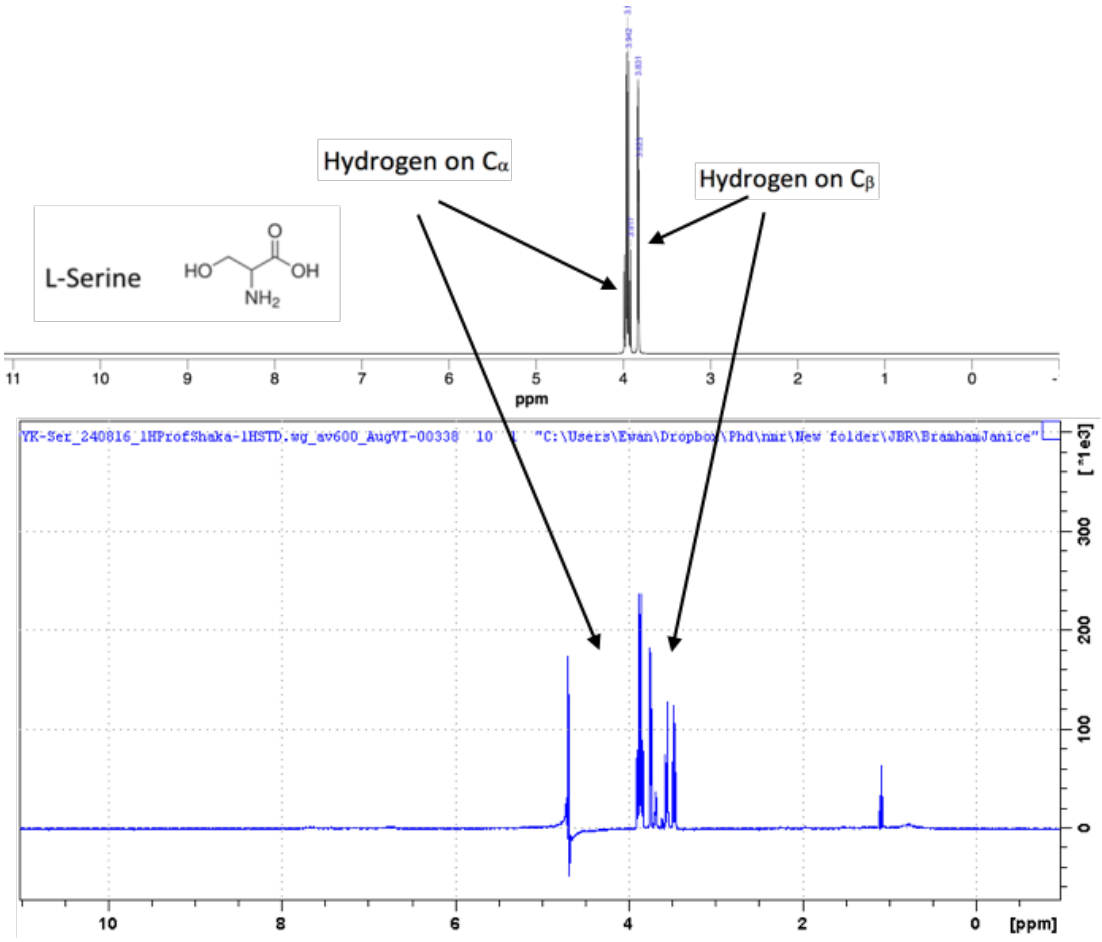

e

Figure 5-3. ^{1}H NMR spectra for L-phenylalanine, L-cysteine, L-histidine, L-serine, and L-alanine. The upper part of each figure is a standard spectrum from the Biological Magnetic Resonance Data Bank (http://www.bmrb.wisc.edu/ref_info/statful.htm) and the bottom part is the 1D protein NMR spectrum of the protein-ligand (LPYK-amino acids). Peaks of hydrogen atoms bonded to C_α and C_β have been assigned for each amino acid. a) LPYK-cysteine; b) LPYK-alanine; c) LPYK-histidine; d) LPYK-phenylalanine; e) LPYK-serine.

On-resonance spectra were obtained in Bruker Advance III by saturating the protein with a set of Gaussian-shaped pulses (saturation time 3 s, 50 ms for each pulse at 20 Hz) at -2 ppm, where the ligands do not have signals but the protein has. Off-resonance irradiation is set at around 50 ppm to obtain the ligand reference spectra. Data were collected through standard Bruker pulse programs at 25 °C. As shown in Figure 5-4, the spectrum in green is the ligand reference spectrum I_0, which contains the signals

of all ligands including ligands bound to LPYK and ligands not bound to protein. The spectrum in red is I_{sat}, which is the on-resonance spectrum containing only signals of ligand not bound to LPYK. The difference spectrum of I_{STD} (blue) between spectra of I_0 (Greenhall) and I_{sat} (red) has been processed in NMR data processing software-TopSpin 3.5pl 6. The I_{STD} spectrum is scaled up by 61.02-fold as the difference between I_0 and I_{STD} is relatively small. These three spectra show similar peaks at around 3.7 ppm, 1.4 ppm. This result suggests that these spectra could be consistent with signals of hydrogen from alanine however, some peaks were detected which do not exist in Figure 5-3 b, so alanine can be discounted. Peaks at around 4.7 ppm in the three spectra are believed to be signals from water and peaks at around 3.5 ppm only in I_0 and I_{STD} are estimated to be signals of contaminants.

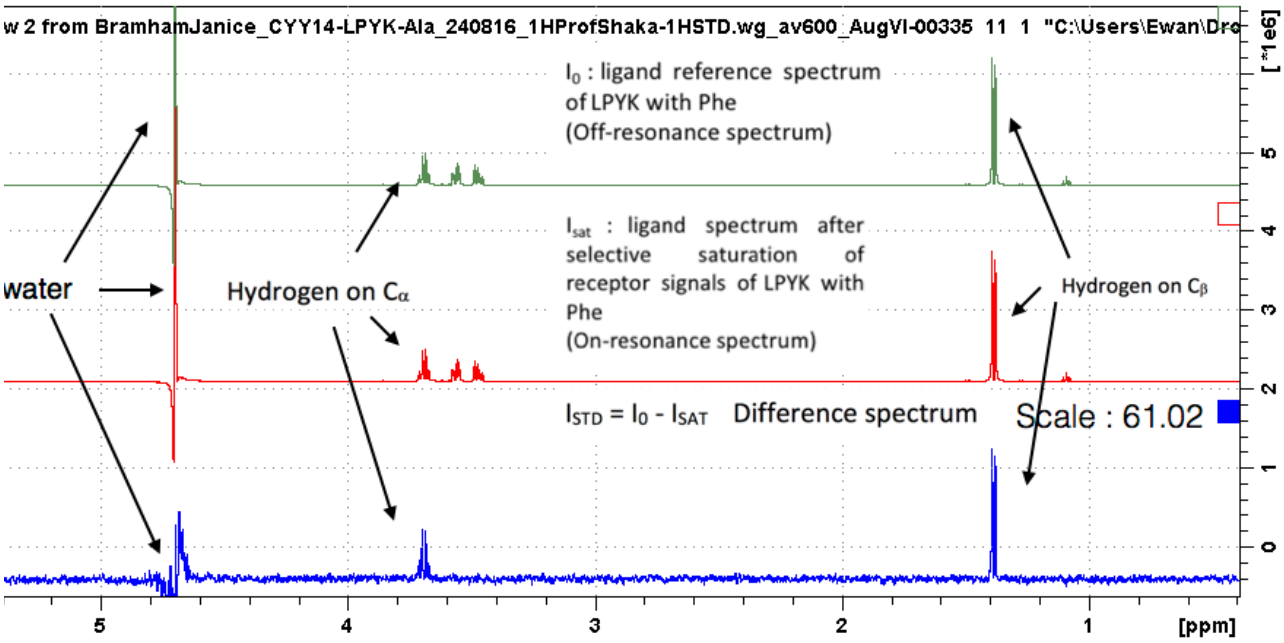

Figure 5-4. On-resonance spectrum I_{SAT}, Off-resonance irradiation $I_{0,}$ and difference spectrum of LPYK-alanine mixture.

5.2.1 STD-NMR of M1PYK, M2PYK, LPYK, and RPYK with Phe

NMR measurements for M1PYK with 1 mM Phe, M2PYK with 1 mM Phe and RPYK with 1 mM Phe and LPYK with 1 mM Phe were processed using same method described above and the results are shown in Figure 5-5. From this figure, three peaks at about 7 ppm show signals for Phe. Water molecules, which bind to the protein, also

show signals in the STD-NMR spectra and peaks around 4.7 ppm suggests that hydrogen from water are saturated by association with the protein. The signal of ^{1}H on Cα and ^{1}H Cβ of Phe have been pointed out in Figure 5-3. There are peaks in the spectra of M1PYK and M2PYK with Phe at 3.5 ppm in Figure 5-5, which are again from the contaminant.

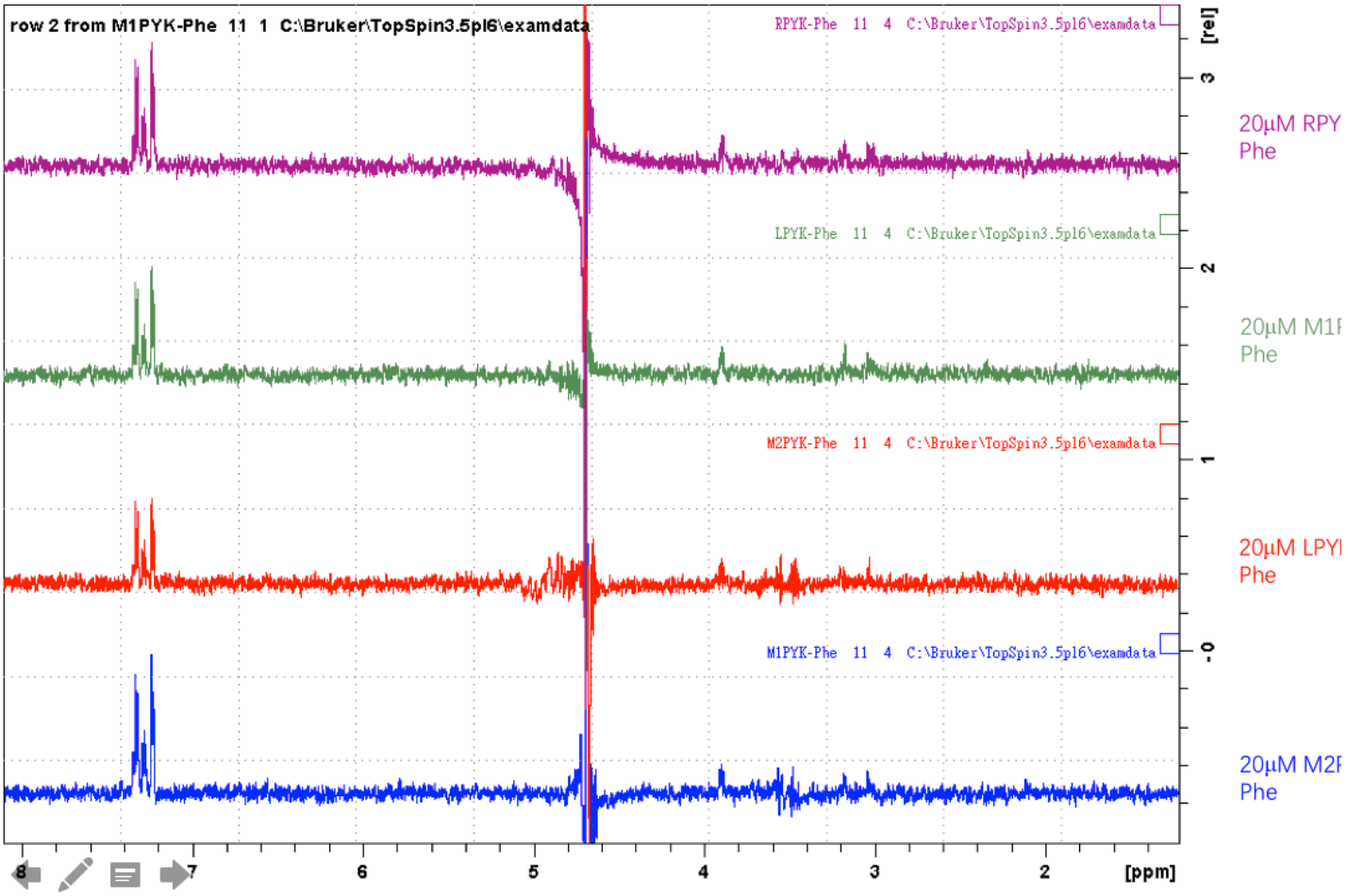

Figure 5-5. Comparison of peak intensities in the STD-NMR spectra. Purple curve represents STD-NMR spectrum of 20 μM RPYK with 1mM Phe; Green represents M1PYK; Red represents LPYK; Blue represents M2PYK.

To further analyse and compare the spectra between M1PYK-Phe, M2PYK-Phe, LPYK-Phe, and RPYK-Phe, we calculated the amplification factors of each peak on the four spectra using $A_{STD} = \frac{I_{STD}}{I_0} \times \frac{[L]_T}{[P]}$ Equation 5-1.

We chose the phenyl group peaks, which show the strongest signals in the STD-NMR data. The A_{STD} value of the phenyl group peaks are shown in Figure 5-6. The

amplification factor from the M1PYK-Phe spectrum is about 0.8. The amplification factors from the other three spectra are about 0.5. As ligand concentration and saturation time were the same in these four experiments and ASTD (M1PYK) > ASTD (M2PYK) > ASTD (LPYK) > ASTD (RPYK), it suggests the average number of Phe molecules binding to one M1PYK, M2PYK, LPYK, or RPYK molecule (monomer) are about 0.8, 0.4, 0.5, or 0.6, respectively. It also suggests that the affinity of M1PYK for Phe is higher than that of the other three isoforms. Interestingly, from our studies of amino acid regulation of enzymatic activity in Chapter 4, Phe enhances the activity of RPYK, exerts strong down-regulation on M2PYK, slight down-regulation on M1PYK, and has no effect on LPYK. This suggests that though the amino acids pockets in four isoforms are very conserved, the effects caused by amino acid binding are different.

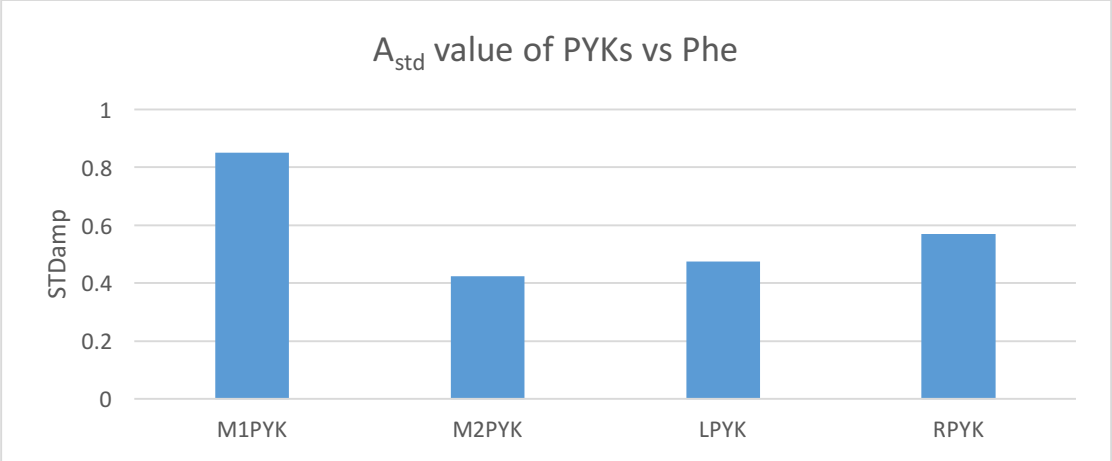

Figure 5-6. The Amplification factors of ^{1}H on the phenyl group of STD-NMR spectra.

To compare signals of hydrogen on different position of Phe, we calculated the amplification factor of all six peaks of all four human PYK isoform spectra in Figure 5-5. We set the highest amplification factor in each spectrum as 100% and calculated the relative percentage of other hydrogen amplification factors. The results are shown in Figure 5-7. From these mappings, hydrogens with the highest amplification factor are on the phenyl group in all four isoforms. Hydrogens on C_{β} show the lowest amplification factor. This kind of trend suggests that the phenyl group might be closer to the protein compared to C_{β} in the binding of all four isoforms of PYK.

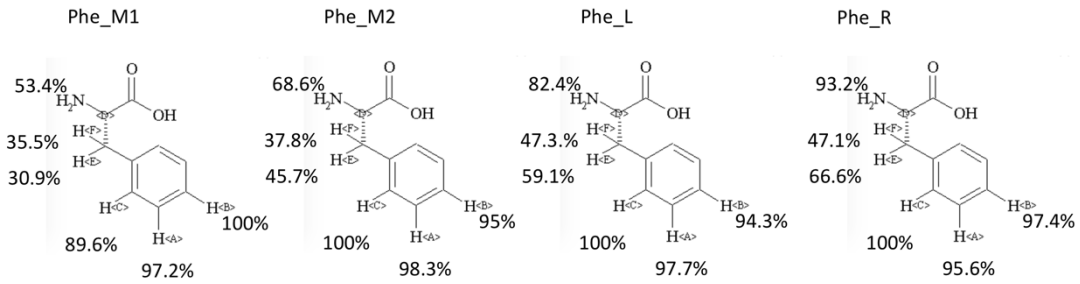

Figure 5-7. Mapping of ligand binding moieties of Phe in the STD-NMR spectra of all four human PYKs with Phe. H(A)-H(B)represent hydrogens on different position of Phe.

5.2.2 STD-NMR of M1PYK, M2PYK, LPYK, and RPYK with Ala

We processed the data to get the difference spectra (I_{STD}) of four STD-NMR measurements of hPYKs with 1 mM Ala. The results are shown in Figure 5-8. All four spectra of M1PYK with Ala, M2PYK with Ala, LPYK with Ala, and RPYK with Ala show peaks at 3.7 ppm and 1.4 ppm, which are same as peaks as in Figure 5-3. This result suggests that Ala binds to all human PYK isoforms. There are still peaks at around 3.5 ppm, which is estimated as signal from contaminating glycerol introduced in the purification step.

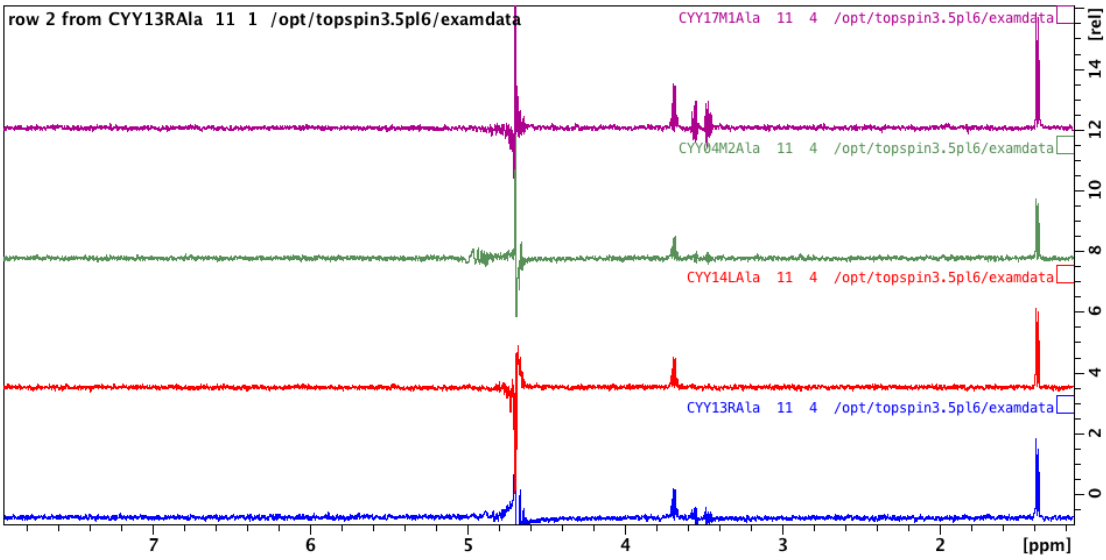

Figure 5-8. Comparison of peak intensities in the ^{1}H NMR spectra of Ala with human pyruvate kinases (Peaks in blue indicate Ala with M1PYK, M2PYK in red, LPYK in green, RPYK in purple).

To further investigate the binding affinities of four isoforms with Ala, we chose the amplification factors of the peak of hydrogen on C_β of Ala at 1.4 ppm to compare in Figure 5-8. Interestingly, this result shows the same trend as in the Phe assays in Figure 5-6. M1PYK shows highest amplification factor and it suggests that the affinity of Ala with M1PYK is higher than Ala with other isoforms. This also suggests that the average occupancy of Ala bound to each monomer of M1PYK is about 1, but that the occupancy of M2PYK monomer is just 0.5. Compared with the kinetic data of these enzymes in Chapter 4, only M2PYK and RPYK could be regulated by alanine. This again suggests that that alanine binds to the conserved amino acid binding pocket in all four isoforms of human PYKs, but only affects enzymatic activity of M2PYK and RPYK.

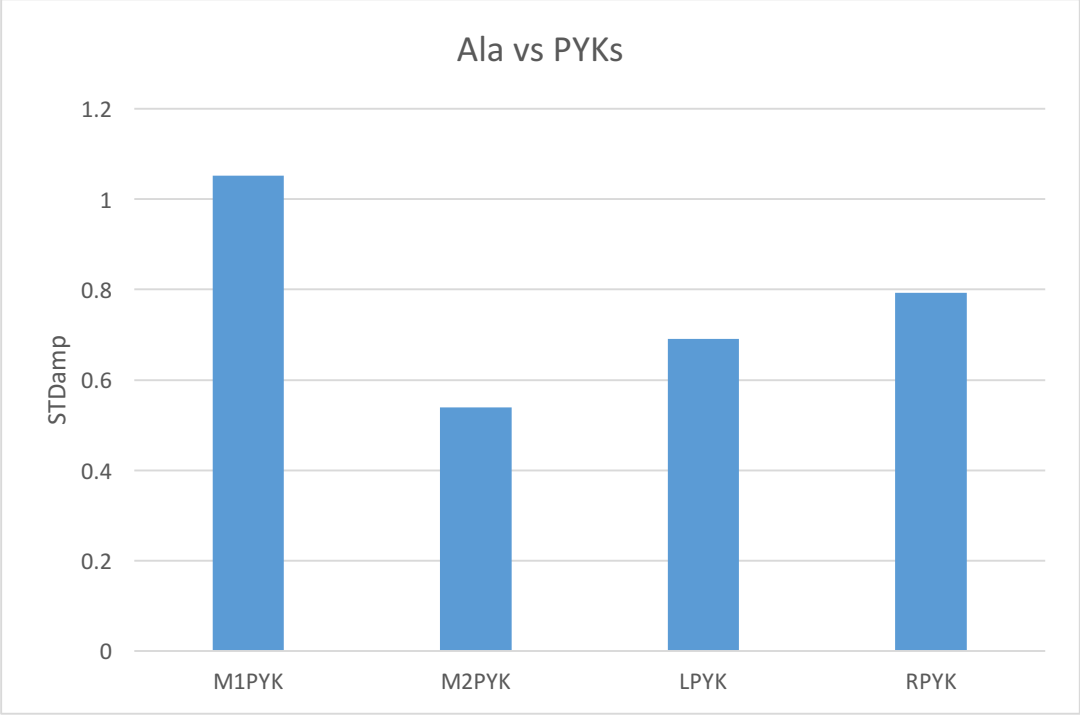

Figure 5-9. The Amplification factors of ^1H on C_β of Ala determined from STD-NMR spectra.

The mapping of ligand binding moieties of alanine in Figure 5-9 shows that the amplification factor of hydrogen on C_β of alanine is higher than that of hydrogen on

C_α in all four isoform assays. This result might suggest that alanine binds to the same pocket of four isoforms.

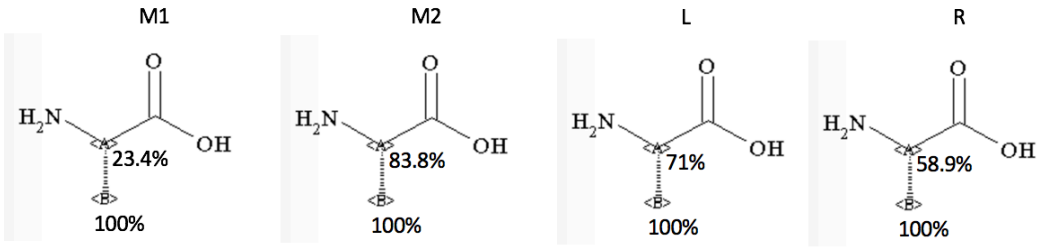

Figure 5-10. The mapping of ligand binding moieties of alanine in the STD-NMR spectra of all four human PYK isomers. H(A)-H(B) represent hydrogens on C_{alpha} and C_{beta}.

5.2.3 STD-NMR of M1PYK, M2PYK, LPYK, and RPYK with Cys

We processed the data to get the difference spectra (I_{STD}) for four STD-NMR measurements of hPYKs with 1 mM Cys. The results are shown in Figure 5-11. All four spectra contain peaks at around 3 ppm and 4 ppm, which are the same as peaks in Figure 5-3. As with Ala and Phe measurements, Cys STD-NMR results suggest that Cys binds to four isoforms of human PYKs as well.

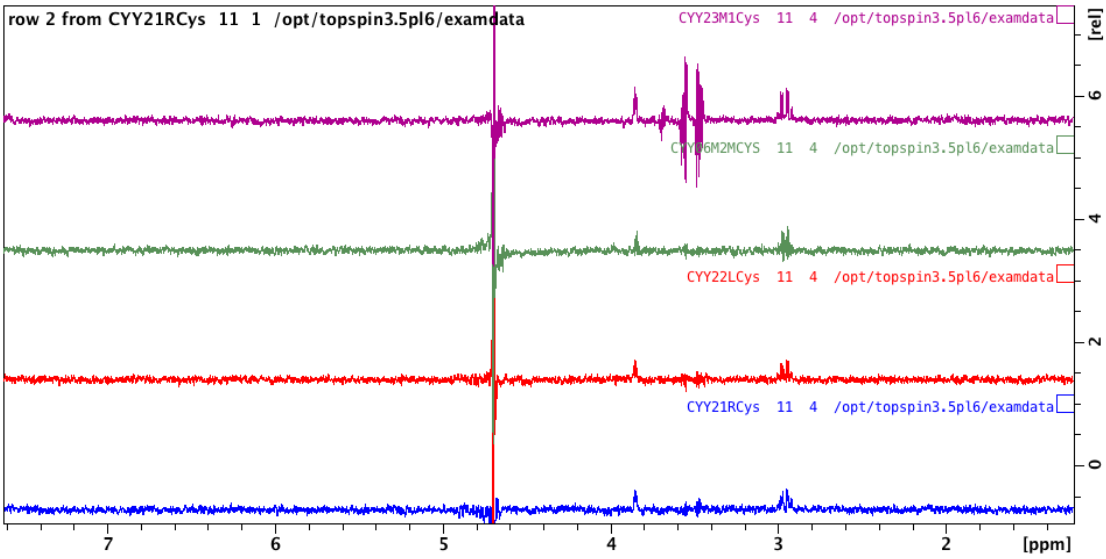

Figure 5-11. Comparison of peak intensities in the ^{1}H NMR spectra of Cys with human pyruvate kinases (M1PYK in purple, M2PYK in green, LPYK in red, and RPYK in blue).

To further investigate the binding affinities of four isoforms with Cys, we chose the amplification factors using a signal from a hydrogen atom on C_{β} of Ala which occurs at 3 ppm in Figure 5-11. Again, this result shows same trend as for Phe and Ala (Figure 5-6 and Figure 5-9). M2PYK shows a much lower amplification factor and it suggests that the affinity of Cys with M2PYK is weaker than Cys with other isoforms. But these results are not consistent with enzymatic assays as only RPYK could be activated by Cys.

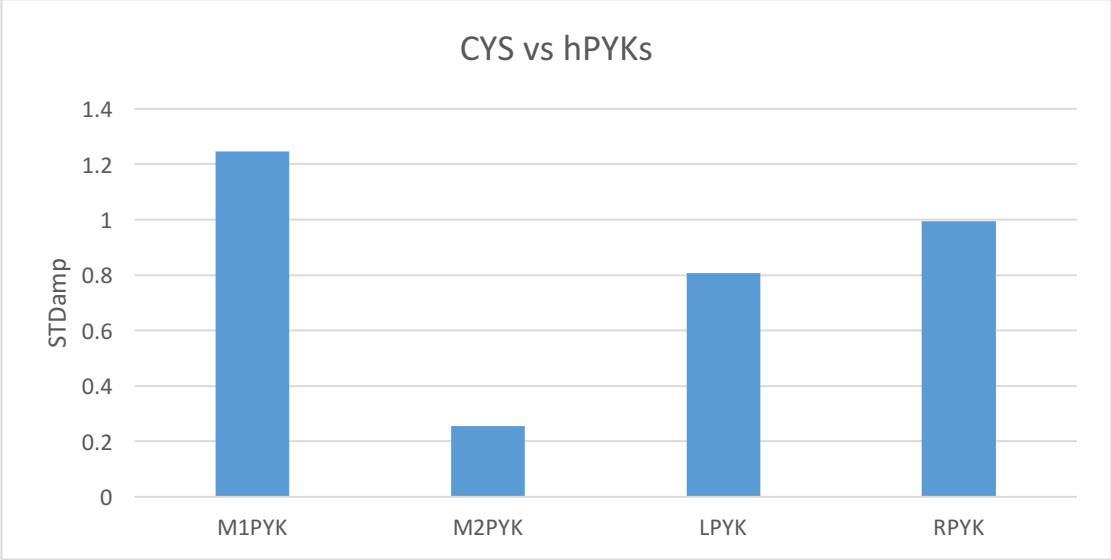

Figure 5-12. The Amplification factors of ^{1}H on C_{β} of Cys of STD-NMR spectra

The mapping of ligand binding moieties of cysteine is shown in Figure 5-13. The amplification factor of hydrogen on C_{β} of alanine is lower than that of hydrogen on C_{α} in all four isoform assays. This result might suggest that alanine binds to the same pocket of four isoforms.

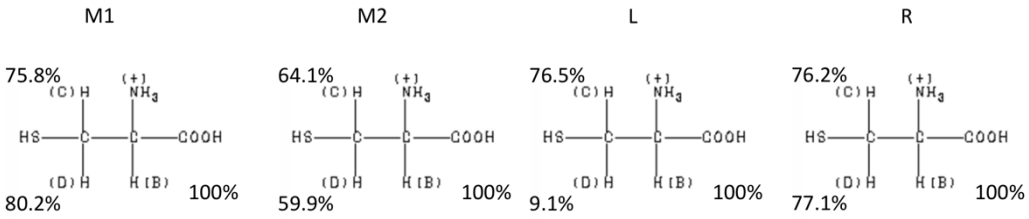

Figure 5-13. The mapping of ligand binding moieties of alanine in the STD-NMR spectra of all four human PYK isoforms with cysteine. H(A)-H(B) represent hydrogens on the C_{alpha} and C_{beta} carbon atoms of Cys.

5.2.4 STD-NMR results for M2PYK with increasing L-alanine concentration

To study the dissociation constant (K_d) of L-alanine binding with M2PYK, we carried out a series of STD-NMR assays with increasing alanine concentration from 111 nM to 3 mM. Spectra for off-resonance ^{1}H NMR data of four isoforms with alanine are shown at concentrations from 111 nM to 3 mM (Figure 5-14). We see there are three

different groups of peaks in each spectrum: water signals at 4.7 ppm, alanine signals at 3.7 ppm and 1.4 ppm, and contamination signals at about 3.5 ppm and 1.1 ppm. If we compare the magnitudes of peaks at the same position in the four spectra, we can easily see that the water and contamination signals remain at the same respective levels, but alanine signals increase with alanine concentration.

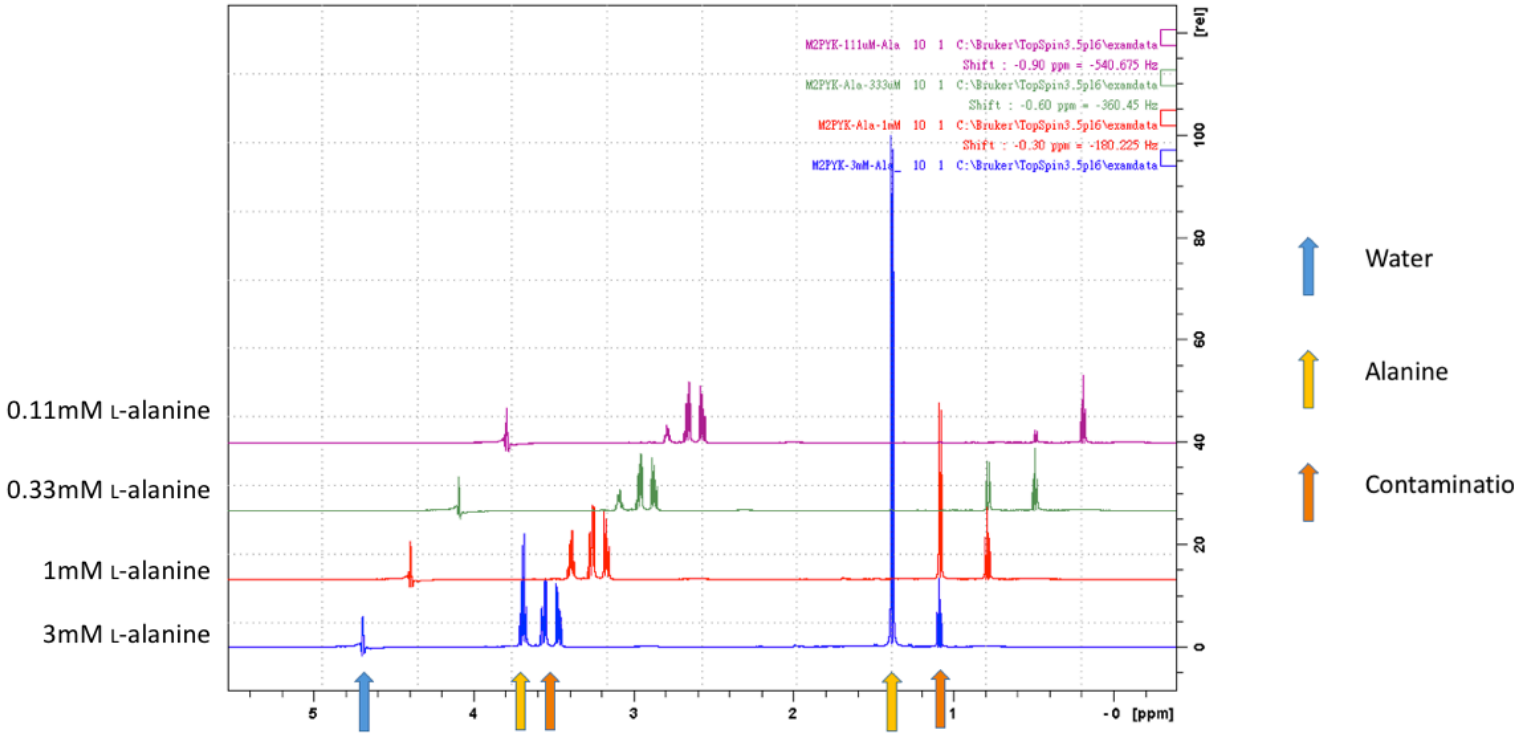

Figure 5-14. Stacked spectra of off-resonance NMR data of M2PYK with four L-alanine concentrations (0.11 mM_purple, 0.33 mM_green, 1mM_red, and 3mM_blue) confirming that signal magnitude of the alanine peaks increases with alanine concentration. Water signals are shown with blue arrow, alanine signals with yellow arrows, and contamination peaks with orange arrows.

The STD-NMR results in Figure 5-15 show that peaks at 3.7 ppm and 1.4 ppm are related to the alanine concentration (higher alanine concentrations show higher signals) confirming that the concentration of the M2PYK-alanine complex increases with the alanine concentration.

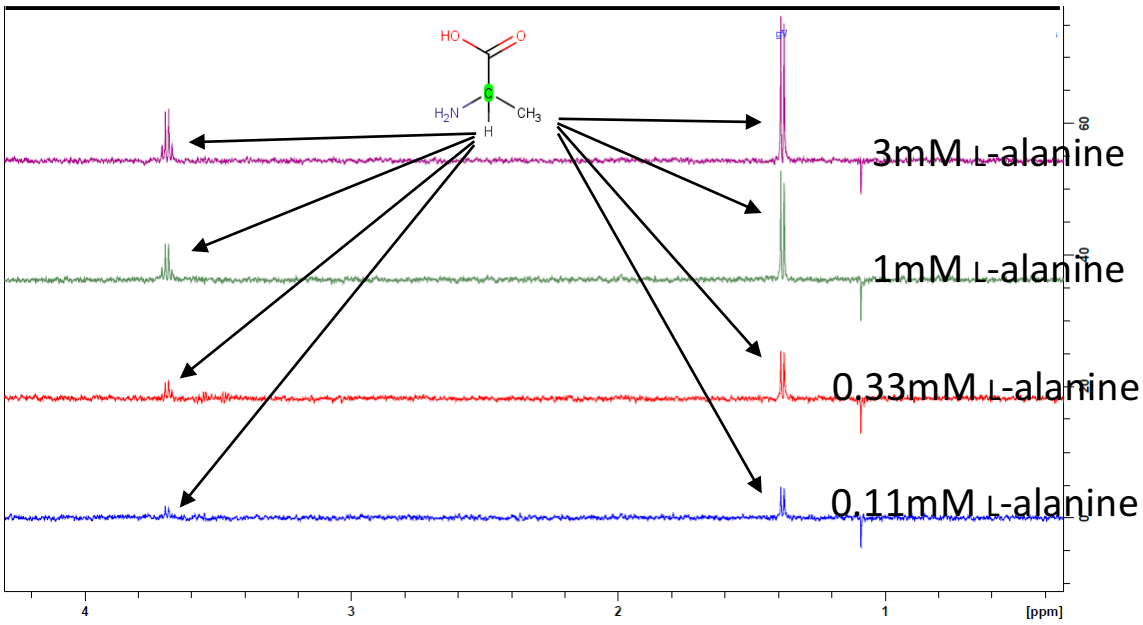

Figure 5-15. Comparison of peak intensities in the STD-NMR spectra of alanine with human pyruvate kinase M2 with four different alanine concentrations.

The STD amplification factor at 1.4 ppm for four spectra were calculated and plotted according to Equation 5-3 as shown in Figure 5-16:

$$A_{STD} = \frac{\alpha_{std}\,[L]}{K_D + [L]}$$ Equation 5-3

Figure 5-16 shows that amplification factor maximum is 0.4 and the estimated K_d is 231 μM. According to the previously determined enzyme assay data, $K_d[Ala]$ is 62 μM, which is about 4 times smaller than calculated from the STD-NMR results. The reason for this difference is still unknown.

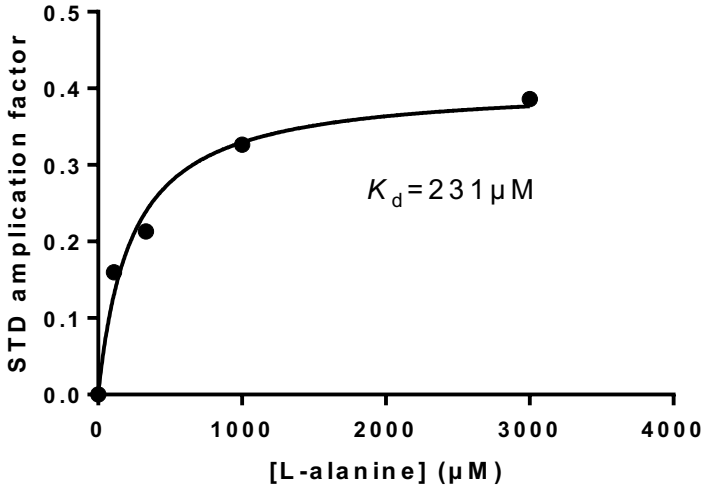

Figure 5-16. The alanine binding effect on M2PYK was detected by STD-NMR. STD amplification factor was plotted using equation 5-3 which has the same form as the Michaelis-Menten equation.

CHAPTER 6. SAXS studies on hPYKs

Attempts to crystallise full length hRPYK and hLPYK were unsuccessful. SAXS (Small-angle X-ray scattering) provides a way of obtaining protein structural information in solution rather than in a crystal (Dyer et al., 2014; Skou, Gillilan, & Ando, 2014).

As shown in Figure 6-1, an incident X-ray beam penetrates the protein solution/background solution and scatters on a 2D detector from which structural data can be derived. Unlike X-ray crystallography, the protein molecules in solution are randomly oriented and undergo Brownian motion, so the scattering pattern is an average over all orientations. The scattering vector is defined as $q = (4\pi\sin\theta) / \lambda$, where 2θ is the angle between incident X-ray and scattered X-ray, λ is the wavelength of the incident X-ray radiation. The 2D scattering image can be integrated into a 1D curve (the intensity plot in Figure 6-1), after a subtraction of buffer scattering intensity from protein sample scattering intensity, defined as scattering intensity / versus q with a unit of inverse angstroms. The curve of $log[I(q)]/q$ reveals information about oligomeric state, shape, and size of the sample protein. The Fourier transform of the curve provides the interatomic distance distribution function, $P(r)$.

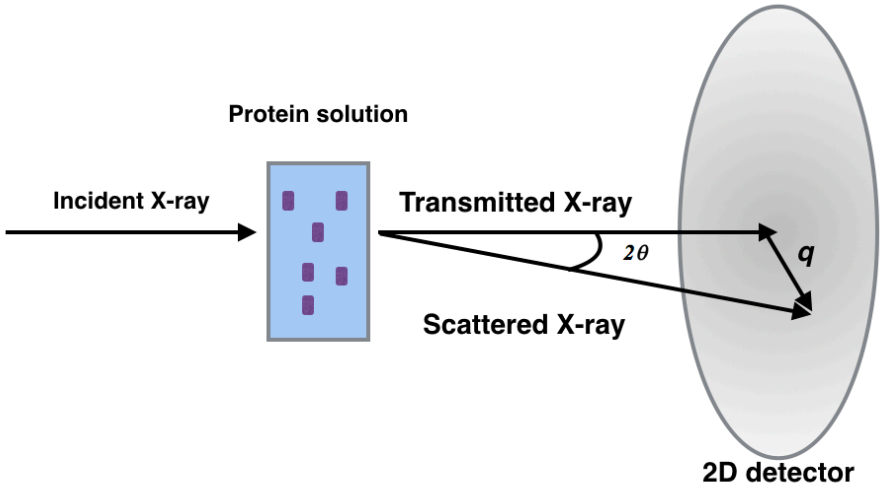

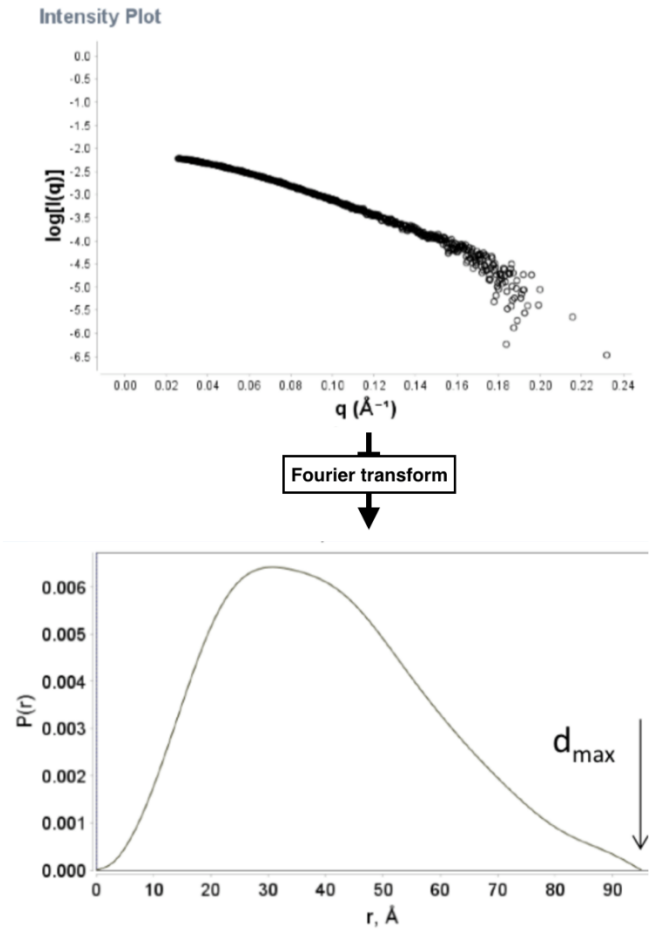

Figure 6-1. Schematic representation of SAXS experiment with protein in solution. The incident X-rays penetrate the protein solution and scatter at a low angle. A 2D detector is used to capture the scattered photons. The angle between incident beam and scattered photons is 2θ (generally <3°), q is the scattering vector, describing the change of scattered radiation. The upper part of the intensity plot is the *log[I(q)]/q* curve, where *I(q)* represents the scattering intensity. After the Fourier transform, the *P(r)* function is constrained between r = 0 and r = d_{max}.

More information such as *I(0)* (the zero angle scattered intensity when $2\theta = 0$) and R_g (radius of gyration) can also calculated (Jacques and Trewhella, 2010). As the I(0) cannot be distinguished from the unscattered radiation beam, we can calculate the value of *I(0)* by two methods.

One is the Guinier analysis when q is small:

$$I(q) = I(0)e^{\frac{-q^2R_g^2}{3}}$$

Equation 4

Using this equation a linear fit of ln[(I)q] versus q can be used to calculate I(0) and R_g, when $qR_g < 1.3$ Å (Jacques and Trewhella, 2010). A downturn or an upturn indicates interparticle interference or aggregation respectively when q is low (Mertens and Svergun, 2010).

The other calculation of *Rg* and *I(0)* is more accurate using the entire scattering profile with P(r) distribution function:

Rg is the second moment of P(r).

$$R_g^2 = \frac{\int P(r) r^2 dr}{2 \int P(r) dr}$$

Equation 5

I(0) is the zero[th] moment of P(r)

$$I(0) = 4\pi \int_0^{D_{max}} P(r) dr$$

Equation 6

Molecular weight can also be calculated through extrapolation of the relationship of I(0) and the particle volume.

$$M_w = \frac{I(0).N_A}{C(\Delta p.V)^2}$$

Equation 7

Where *N* is the number of scattering particles per unit volume, *V* is the particle volume, $\Delta\rho$ is the contrast (the difference between the electron densities of the buffer and protein molecule), *C* is the mass per unit volume, *u* is the partial specific volume, MW is the molecular weight, N_A is the Avogadro's number (Jacques & Trewhella, 2010).

SAXS experiments were carried out at the Diamond Light Source, Oxofordshire, UK at the B21 BioSAXS beamline. All samples were dissolved in PBS-CM buffer (9.33 mM potassium phosphate, 136 mM, NaCl, 2.7 mM, KCl, 0.6 mM, $MgCl_2$, 0.9 mM $CaCl_2$). The data were obtained at room temperature (25 °C). To check concentration dependant effects and amino acid binding effects on the protein structure, we used a series of protein concentrations in SAXS experiments:

1) For M1PYK: 0.87, 1.74, 3.48, 6.97 mg/ml
2) For M2PYK: 0.25, 0.5, 2.3 mg/ml

3) For LPYK: 1.39, 2.78, 5.55 mg/ml
4) For RPYK: 3.2 mg/ml
5) For M2PYK with 2.5 mM Phe: 0.25, 0.5, 1, 2.3 mg/ml
6) For M2PYK with 2.5 mM Ser: 0.25, 0.5, 1, 2.3 mg/ml

The data were analysed through Scatter 3.0H.

6.1.1 SAXS analysis of human M1PYK

SAXS data was generated from His-tagged human M1PYK at a series of concentrations. Guinier analysis of the data was used to determine parameters including $R_{g,}$ Porod volume mass, P(r) $R_{g,}$ and D_{max} (as described above) which are presented in **Error! Reference source not found.**. The Guinier analysis mass (between 215.24 kDa to 238.21 kDa) and R_g (between 44.0 to 45.3) remain constant as the protein concentration increases. The mass of M1PYK is 240.4 kDa which is in the range. If the I(0)/c or R_g increases with concentration, there might be concentration dependant protein aggregation or oligomeric state change. The lack of such a correlation suggests that there is no concentration dependant oligomerisation (or aggregation). The molecular weight (between 251.85 and 271.59 kDa) calculated from Porod volume (non-concentration dependant) is slightly higher than the Guinier analysis mass (from 215.24 to 238.21 kDa). The average calculated D_{max} is about 108.5 Å. Measurement of structure 3SRF, D_{max} is about 135.3 Å.

Protein concentrations (mg/ml)	Guinier Analysis Mass	Guinier analysis Rg (Å)	Porod volume Mass	P(r) Rg (Å)	Dmax (Å)	Oligomerisation state
0.87(14.45μM)	238.21	45.3	259.68	40.01	109	Tetramer
1.74(28.9μM)	221.20	44.8	271.59	37.16	110	Tetramer
3.48(57.8μM)	215.24	44.3	265.65	39.26	108	Tetramer

6.97(115.6μM)	219.32	44.0	251.85	40.10	107	Tetramer
Average	223.49	44.6	262.19	39.13	108.5	
Standard deviation	10.12	0.57	8.44	1.37	1.29	

Table 10. SAXS parameters of human M1PYK at a series of protein concentrations (0.87 – 6.97 mg/ml). The R_g of M1PYK is calculated to be 44.6 Å and 39.13 Å from Guinier analysis and real space analysis, respectively. From the estimated molecular weight of both analysis, the predicted assembly of the protein is tetramer.

The two plots in Figure 6-2A suggests that M1PYK at 0.87 mg/ml is not aggregated: the intensity plot of M1PYK does not show a sharp drop in intensity at low q; Guinier fitting shows a linear plot without up or downturns in Figure 6-2 B. The q x R_g ranges from 0.35 to 1.27 and an R_g of 45.3 Å was estimated. The P(r) distribution was calculated using a q ranging from 0 to 0.14 Å showing that D_{MAX} is about 96 Å.

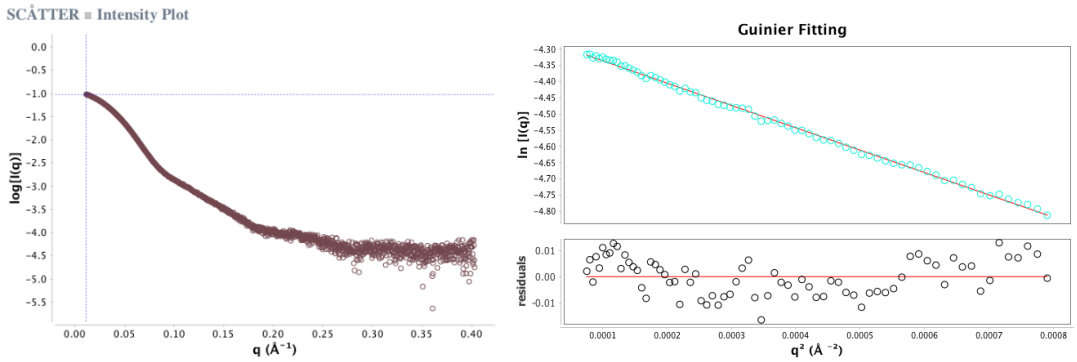

A B

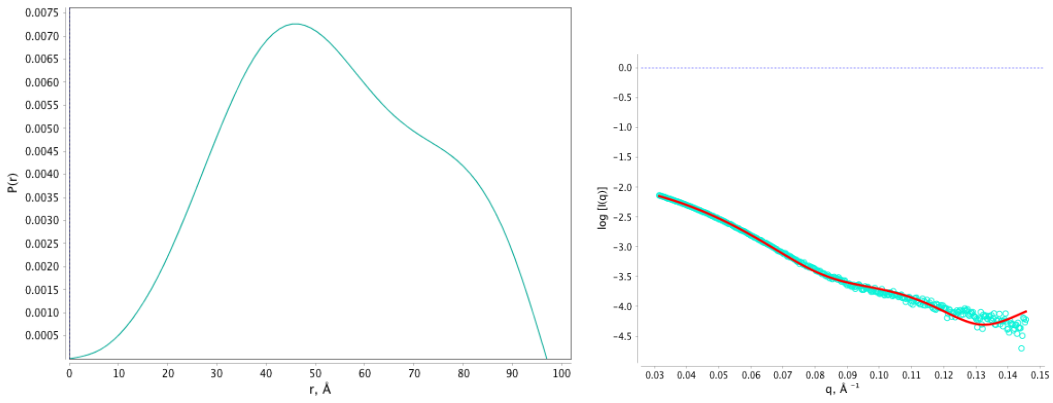

C D

Figure 6-2. SAXS scattering data of M1PYK at 0.87 mg/ml.

A intensity plot of M1PYK at 0.87 mg/ml.

B Guinier fitting of the intensity plot from A. The q x R_g ranges from 0.35 to 1.27. A R_g of 45.3 Å was estimated.

C P(r) distribution provides information including R_g, real space I(0), maximum dimension of particle, D_{max}. Multiple shoulders appearing after 60 Å indicate multiple domains in the protein.

D The estimated curve form P(r) fits well at q range from 0 to 0.14 $Å^{-1}$.

6.1.2 SAXS analysis of human M2PYK

SAXS data were generated from His-tagged human M2PYK at a series of concentrations from 0.5 to 2.3 mg/ml with/without amino acids regulators (2.5 mM Phe or 2.5 mM Ser), to investigate how natural activators phenylalanine and serine affect the structural status of M2PYK. Guinier analysis mass, R_g, Porod volume mass, P(r) R_g, and D_{max} are shown in **Error! Reference source not found.**. The Guinier analysis mass and R_g increase from 199.56 kDa to 712.04 kDa and from 41.3 to 43.7 as the protein concentration decreases. It is much higher than the real protein molecular weight of 240.9 kDa. But the estimated protein Mw from Porod volume data increases along the concentration changes, indicative of oa significant concentration dependant protein aggregation or oligomeric state change for M2PYK. According to the analytical gel filtration data in Chapter 3.4.7, 50% of M2PYK molecules in solution dissociates at 0.1 mg/ml. The Mw overestimation might be created by a concentration dependant protein aggregation. At 2.3 mg/ml M2PYK, Guinier analysis mass of M2 with Phe or Ser are 298.00 and 294.13 kDa, which is much higher than M2 alone (199.52 kDa). As protein was diluted to 1 mg/ml and 0.5 mg/ml, Guinier analysis mass of M2, M2 with Phe, or M2 with Ser are at same level (642.46 – 725.36 kDa).

Protein concentrations (mg/ml)	Guinier Analysis Mass	Guinier analysis Rg (Å)	Porod volume Mass	P(r) Rg (Å)	Dmax (Å)	Oligomerisation state
2.3 (38.3μM)	199.52	43.7	259.68	40.57	101	Tetramer
2.3(38.3μM) with Phe	298	44.4	274.04	31.46	111	Tetramer
2.3(38.3μM) with Ser	294.13	43.5	253.82	41.4	110	Tetramer
1.0(16.6μM)	712.04	42.2	413.39	39.89	105	-
1.0(16.6μM) with Phe	658.75	41.8	421.41	39.32	104	-
1.0(16.6μM) with Ser	725.36	42.1	407.73	39.67	107	-
0.5(8.3μM)	642.46	41.3	370.67	35.35	83	-
0.5(8.3μM) with Phe	676.27	42.3	338.67	35.54	85	-
0.5(8.3μM) with Ser	648.38	40.3	360.42	36.42	92	-
Average	539.43	42.40	344.43	37.74	99.78	
Standard deviation	210.30	1.28	67.09	3.24	10.54	

Table 11. SAXS parameters of human M2PYK at a series of protein concentrations (0.5 – 2.3 mg/ml). The R_g of M2PYK is calculated to be 42.4 Å and 37.74 Å from Guinier analysis and real space analysis, respectively. D_{max} is estimated to be 99.78 Å on average. Mass values from both analysis are with high standard deviations.

Two figures in Figure 6-3 suggest that M2PYK at 2.3 mg/ml shows no aggregation: M1PYK has no sharp drop close to zero in Figure 6-3 A, Guinier fitting shows a linear plot without up or downturns in Figure 6-3 B. The q x R_g ranges from 0.23 to 1.29. A R_g of 43.7 was estimated. The $P_{(r)}$ distribution was calculated using a q ranging from 0 to 0.14 Å.

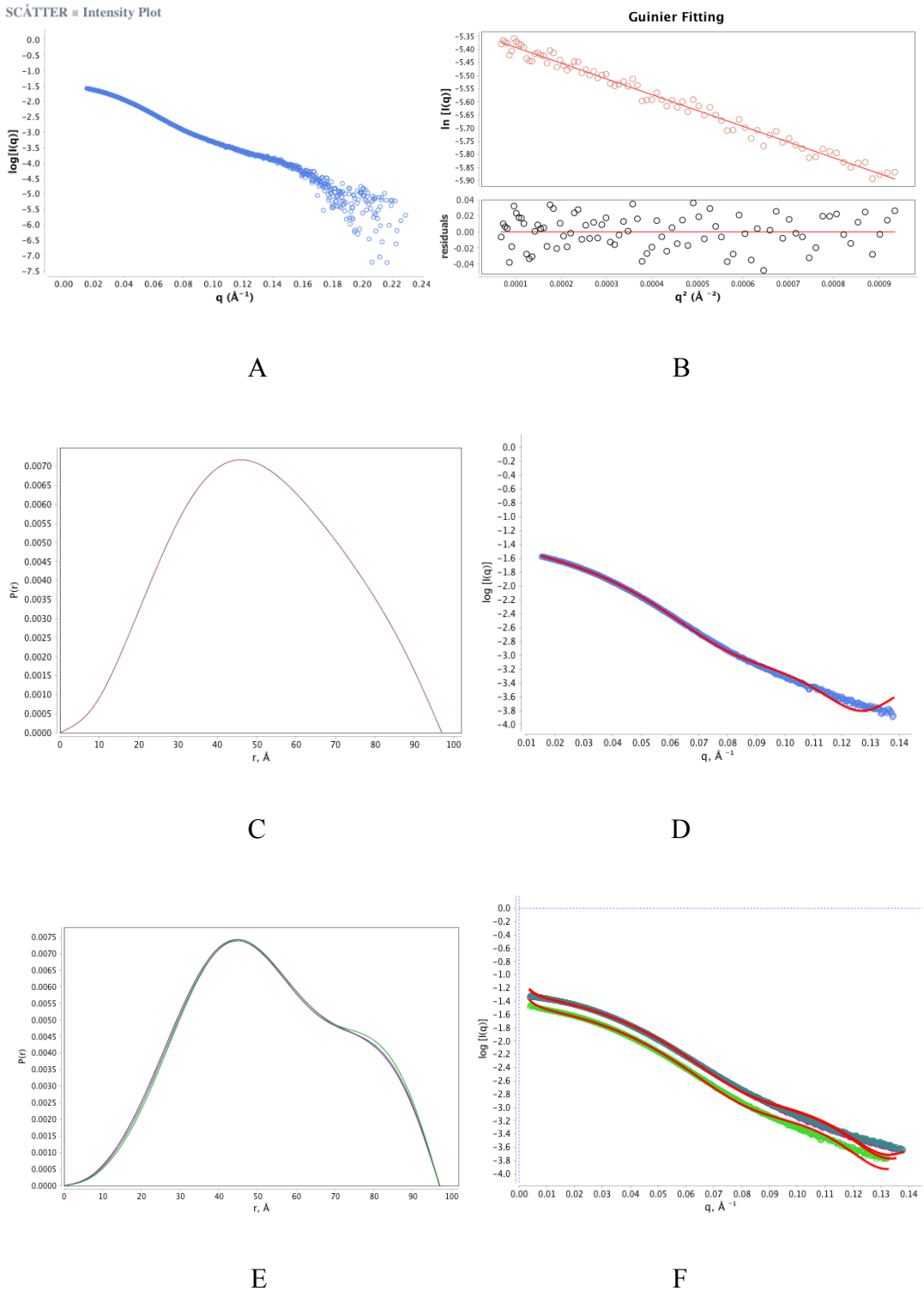

Figure 6-3. SAXS scattering data of M2PYK at 2.3 mg/ml.

A intensity plot.

B Guinier fitting of the intensity plot from A. The q x R_g ranges from 0.23 to 1.29. A R_g of 43.7 was estimated.

C $P_{(r)}$ distribution provides information including R_g , real space I(0), maximum dimension of particle, D_{max}.

D The estimated curve form $P_{(r)}$ fits well at q range from 0 to 0.14 $Å^{-1}$.

E $P_{(r)}$ distribution of M2PYK (green), M2PYK with 2.5 mM (purple), M2PYK with 2.5 mM Ser (blue) almost overlap each other. Value of R_g, and maximum dimension of particle, D_{max} for each are at same level.

F The estimated curves of M2PYK (green), M2PYK with 2.5 mM (purple), M2PYK with 2.5 mM Ser (blue) form $P_{(r)}$ fits well at q range from 0 to 0.14 Å.

6.1.3 SAXS analysis of human LPYK

SAXS data were generated from His-tagged human LPYK at a series of concentrations from 1.39 to 5.55 mg/ml. Guinier analysis mass, R_g, Porod volume mass, $P_{(r)}$ R_g, and D_{max} are shown in . The Guinier analysis mass (between 204.48 kDa to 215.51 kDa) and R_g (between 42.6 to 43.1) remain constant as the protein concentration increases. It is close to the real protein molecular weight of 242.7 kDa. The estimated protein Mw or R_g are stable as the concentration changes and it seems that there is not a concentration dependant protein aggregation or oligomeric state change for LPYK. A molecular weight (from 245.1 to 255.96 kDa) calculated from Porod volume (non-concentration dependant) is slightly higher than the mass calculated from the Guinier analysis. D_{max} is determined by the points from 0 to 0.15 Å as there is high noise ratio for higher q. D_{max} is about 104 Å.

Protein concentrations (mg/ml)	Guinier Analysis Mass	Guinier analysis Rg (Å)	Porod volume Mass	P(r) Rg (Å)	Dmax (Å)	Oligomerisation state

5.55 (91.45μM)	215.51	43.1	255.96	40.47	116	Tetramer
2.78 (45.73μM)	206.7	42.6	248.54	39.87	118	Tetramer
1.39 (22.86μM)	204.48	42.6	245.10	39.89	121	Tetramer
Average	208.90	42.77	249.87	40.08	118.33	
Standard deviation	5.83	0.29	5.55	0.34	2.52	

Table 12. SAXS parameters of human LPYK at a series of protein concentrations (1.39 – 5.55 mg/ml). The R_g of LPYK is calculated to be 42.77 Å and 40.08 Å from Guinier analysis and real space analysis, respectively. D_{max} is estimated to be 118.33 Å on average.

Two figures show that LPYK at 1.39 mg/ml is not aggregated: the intensity plot has no sharp drop close to zero in Figure 6-4 A, Guinier fitting shows a linear plot without up or downturns in Figure 6-4B. The q x R_g ranges from 0.17 to 1.27. A R_g of 42.8 was estimated. The $P_{()}$ distribution was calculated using a q ranging from 0 to 0.12 Å.

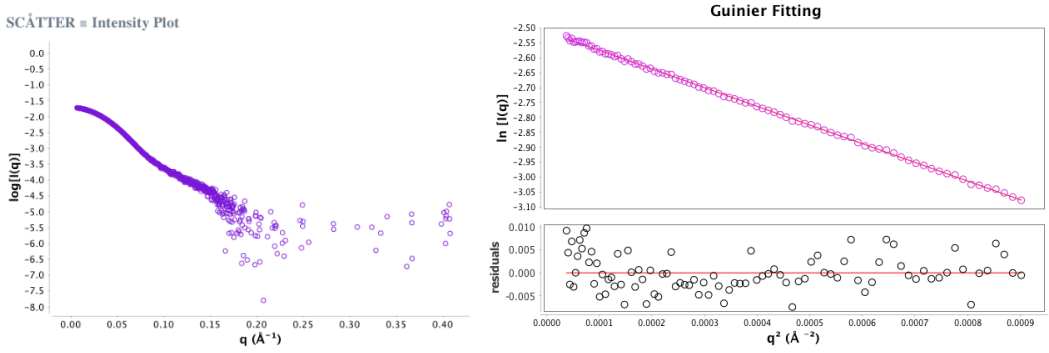

A B

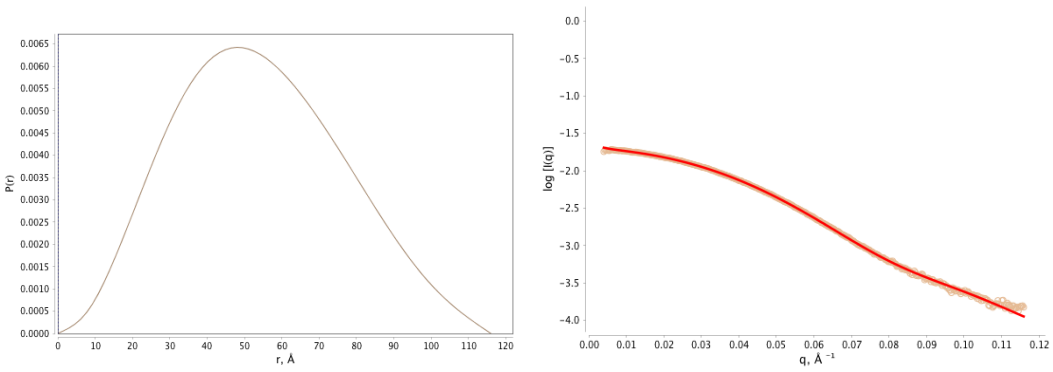

C D

Figure 6-4. SAXS scattering data of LPYK at 1.39 mg/ml.
A intensity plot.

B Guinier fitting of the intensity plot from A. The q x R_g ranges from 0.17 to 1.27. A R_g of 42.6 was estimated.

C $P_{(r)}$ distribution provides information including R_g, real space I(0), maximum dimension of particle, D_{max}. D_{max} is about 115 Å.

D The estimated curve form P(r) fits well at q range from 0 to 0.12 $Å^{-1}$.

6.1.4 SAXS analysis of human RPYK

SAXS data were generated from His-tagged human RPYK at 3.2 mg/ml. Guinier analysis mass, R_g, Porod volume mass, and D_{max} are shown in **Error! Reference source not found.**. Molecular weight (259.68 kDa) calculated from Porod volume (non-concentration dependant) is slightly higher than the Guinier analysis mass (223kDa) and is close to the calculated protein molecular weight of 256.0 kDa. D_{max} is 144 Å and determined by the points from 0 to 0.12 Å as there is high noise ratio for higher q. It is much higher than D_{max} of other isoforms (M1: 108.5 Å, M2: 99.78 Å, L 118.33 Å). Compared to the LPYK sequence in Chapter 1.1.1, RPYK has a N-terminal extension which may explain this difference.

Protein concentrations (mg/ml)	Guinier Analysis Mass	Guinier analysis Rg (Å)	Porod volume Mass	P(r) Rg (Å)	Dmax (Å)	Oligomerisation state
3.2 (50.00µM)	223.16	51	259.68	47.53	144	Tetramer

Table 13. SAXS parameters of human RPYK at 3.2 mg/ml. The R_g of RPYK is calculated to be 51 Å and 47.53 Å from Guinier analysis and real space analysis respectively. D_{max} is estimated to be 144 Å.

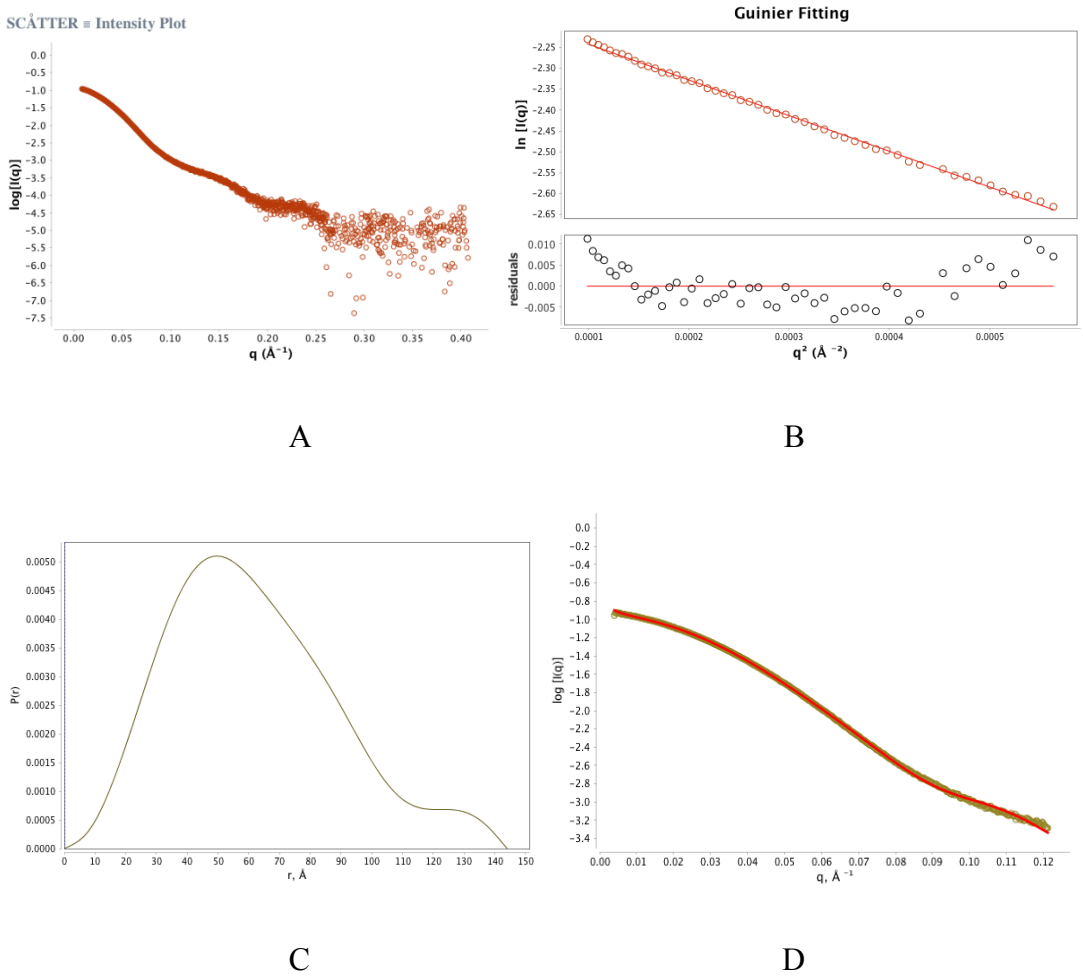

Figure 6-5. SAXS scattering data of RPYK at 3.2 mg/ml.

A. intensity plot.

B. Guinier fitting of the intensity plot from A. The q x R_g ranges from 0.12 to 1.07. A R_g of 51 was estimated.

C. $P_{(r)}$ distribution provides information including R_g, real space I(0), maximum dimension of particle, D_{max}.

D. The estimated curve for $P_{(r)}$ fits well at q range from 0 to 0.12 $Å^{-1}$.

6.1.5 Discussion

The major aim of the SAXS experiments was to obtain structural insights of the four His-tagged human pyruvate kinases. Data were collected for each protein over a range of protein concentrations. From the results of the whole set of STD-NMR data, apart from M2PYK at low protein concentrations (1.0, 0.5 mg/ml), the molecular weight data based on Guinier analysis are similar to the theoretical tetrameric PYK molecular weights. The mass predictions of all four isoforms using $P_{(r)}$ distribution are also in agreement with calculated values but slightly higher than Guinier analysis data. Taken together, these data would suggest that human pyruvate kinases are tetrameric in solution and do not differ much in overall structure from X-ray crystallography structures.

CHAPTER 7. Summary and forward look

This thesis has discussed biochemical and biophysical studies of all four human pyruvate kinase forms (M1PYK, M2PYK, LPYK, and RPYK) and provides a number of novel and interesting insights. Firstly, reducing environments were found to play an

important role in enzyme activity regulation, thermal stability, and oligomerisation states. Secondly, selected amino acids were identified as inhibitors or activators of enzyme activity. Thirdly, biophysical assays (STD-NMR and SAXS) were used to obtain new information about the interactions of human pyruvate kinases and free amino acids.

7.1 Summary of thesis

The biology and biochemistry of the four human pyruvate kinases were reviewed and the hypothesis was developed that regulation of the PYK isoforms was a result of the different biochemical environments of the various human cell types. (CHAPTER 1)

Four human pyruvate kinase isoforms (M1PYK, M2PYK, LPYK, and RPYK) were produced in stable and robust *E. coli* culture systems. The protein purification protocols were shown to be reproducible. Kinetic and biophysical properties of these proteins were characterised. (CHAPTER 2)

The analytical gel filtration assay shows that only M2PYK exists in an equilibrium between tetramers and monomers at 0.1 mg/ml, while the other three isoforms were only observed as tetramers. We also found that enzyme activity drops significantly after dilution to a low concentration (0.001mg/ml). M2PYK activity loss could be explained by monomerisation. However, the loss of activity for LPYK and RPYK might be due to another process such as oxidation. We also proved that reducing reagents prevent the loss of activity. (CHAPTER 3)

We identified some amino acid regulators of human pyruvate kinases, some being activators and some inhibitors. Each regulator can activate or inhibit one or more isoforms. For M2PYK, we also found that both inhibitor and activator amino acids are competitive. Certain amino acids like alanine, which neither inhibit nor activate M2PYK were also found to compete with other amino acid regulators. (CHAPTER 4)

STD-NMR data suggested that all amino acids have a universal binding mode with all human pyruvate kinase isoforms. (CHAPTER 5)

SAX study showed that hPYKs are tetrameric in solution. (CHAPTER 6)

7.2 Discussion

7.2.1 Cysteine oxidation regulation on hPYKs

According to the redox regulation tests on hPYKs, three of these (M2PYK, RPYK, and LPYK) are sensitive to the reducing reagent DTT. Moreover, RPYK lost its activity during long periods of incubation, while DTT could maintain activity from the beginning or even partially recover its activity. In the analytical gel-filtration assays, reducing reagent helped wild-type M2PYK to maintain a majority in tetrameric oligomeric states after 12 hours of incubation at 0.1 mg/ml protein concentration (in Dr Meng Yuan's thesis). However, RPYK and LPYK didn't show any dissociation from tetramers to monomers during the long incubation period as demonstrated by results in Chapter 3. Based on the sequence comparison in Chapter 1.1.2, we know both 358 and 326 residues of M2PYK are conserved at the same position of the other isoforms.

All these results suggest that RPYK and LPYK might be regulated by redox regulators via oxidation or reduction on cysteines present on the surface of the protein, just like in M2PYK but without dissociation. Anastasiou *et al.* demonstrated that the redox state regulates M2PYK enzymatic activity and oligomerisation state, and also suggested that Cys358 was the major residue in the structure to be oxidized (Anastasiou et al., 2011). In 2014, Dr Rosie Mitchell demonstrated that Cys326 could be regulated by redox state in her PhD thesis. Dr Meng Yuan also showed in his PhD thesis that Cys326 positions in the tetramer interface of M2PYK and a mutant, M2PYK-C326S (cysteine to serine), changes the M2PYK to monomeric form and with very low activity. The sequence and structure differences in the C-C interface of M1PYK and M2PYK might explain this phenomenon, as shown in Figure 7-1 (from Dr Meng Yuan's unpublished work). It is shown that the salt bond between residues Arg399 and Glu418 within the same subunit in a T-state tetramer changes to a new salt bond between Arg399 in one subunit and Glu418 in the adjacent subunit. But in the M1PYK structure, the 399 position is valine which cannot form the salt bond but remains close to maintain the R-state. According to the sequence information, the 399 position in RPYK and LPYK is identical to M2PYK. This might explain why RPYK and LPYK could be regulated

from T-state to R-state by the Arg399-Glu418 salt bond leading conformational change.

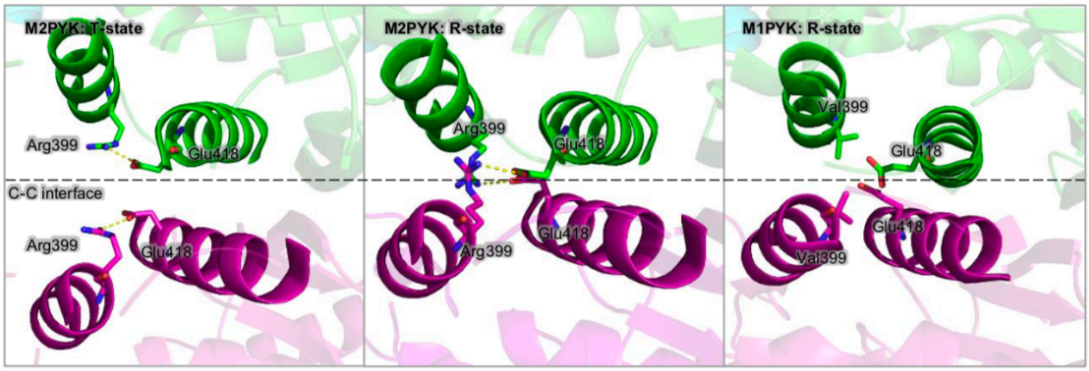

Figure 7-1. C-C interface of M2PYK, R-state and M1PYK R-state.

Future work to explore the function of C358 and other cysteine residues in LPYK and RPYK could involve the design of mutated proteins where the respective cysteine positions are replaced by stable residues like serine and to investigate their enzymatic activity and the structure change.

7.2.2 Metabolites binding and regulation in hPYKs

Among the metabolites we tested, there were a group of activators, inhibitors, and non-regulators detected, the results are summarized as follow:

For M1PYK, only Phe inhibits its enzymatic activity slightly by 14%, this was also shown in previous studies (Rozengurt, de Asúa, & Carminatti, 1970). Ala has been reported to have an inhibition effect on M1PYK (Williams, Holyoak, McDonald, Gui, & Fenton, 2006), however in this study we failed to demonstrate significant regulation of M1PYK. F-1,6-BP, the natural effector of the other three isoforms, didn't show any activation effect on M1PYK, which is consistent with previous literature (Jurica et al., 1998). Oxalic acid, an analogue of the substrate, inhibits M1PYK strongly by 75% confirming the previous report (Buc HA, 1981). Other amino acids and metabolites tested didn't show any enzymatic regulation of M1PYK.

For M2PYK enzymatic tests, F-1,6-BP, Ser, His and Gly showed a strong activation effect on enzyme activity. Oxalic acid, GMP, AMP and a group of amino acids (Tyr, Met, Val, Iso, Phe, Ala, Pro, Thr) were identified as strong inhibitors. This confirmed

the relative reports in literature: Cys and Phe were reported to have inhibitory effect on M2PYK (H. P. Morgan et al., 2013; Nakatsu et al., 2015), while Cys was reported to be an activator (Chaneton et al., 2012).

For LPYK, F-1,6-BP as effector and oxalic acid show an activation and inhibition effect, respectively. No regulatory effect of Ala on LPYK was detected during tests here, which is inconsistent with the published inhibition effect (Llorente, Marco, & Sols, 1970). All other metabolites are non-regulators for LPYK.

For RPYK, F-1,6-BP as effector and oxalic acid still show a strong activation and inhibition effect, respectively. Eleven amino acids and alpha-ketoglutarate were detected as activators for RPYK. Ala was reported as inhibitor in an early report (Marie, Buc, Simon, & Kahn, 1980), however in our study Ala is shown to be an activator.

Surprisingly, the STD-NMR study of hPYKs (M1PYK, M2PYK, LPYK, RPYK) with amino acids (His, Phe, Ala, Ser, Cys) in Figure 5-5 showed that each of the 1D protein NMR spectra of protein-ligand combinations we have tested gave binding signals, this includes the protein isoforms with both their regulators and non-regulators from the metabolite list we tested in activity assays as shown in **Error! Reference source not found.**. For example, Ala is an activator for RPYK, an inhibitor for M2PYK, and a non-regulator for M1PYK and LPYK. Although the biological and structural properties are different, this phenomenon suggests that there might be universal binding between amino acids and hPYKs. A conserved binding pocket for all amino acids is possible.

Based on my colleague Dr Meng Yuan's work on the human M2PYK crystal structures, human M2PYK co-crystallized with alanine, phenylalanine, serine and tryptophan without F-1,6-BP, shows that all four amino acids regulate the activity of M2PYK by stabilising the tetrameric structure in T or R state, shown in Figure 7-2. The hydrophobic amino acids (Ala, Phe, Trp) stabilise the M2PYK tetramer as T state and the hydrophilic amino acid stabilises the R state. The conformational transformation between two states is facilitated by a rigid-body rotation of 11° of each subunit.

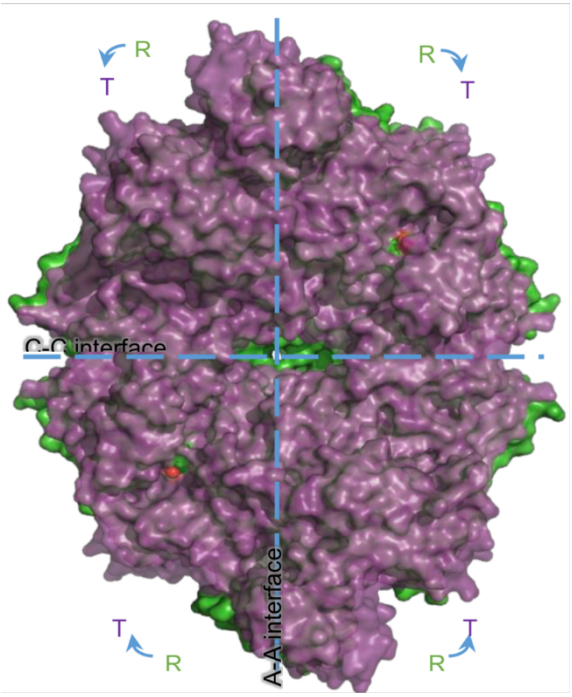

Figure 7-2. M2PYK tetramers equilibrate between R and T state. The active R state tetramer and the inactive T state tetramer are indicated by green and purple, respectively. The rotation direction is shown by arrows. The figure is provided by Dr Meng Yuan's unpublished work.

Furthermore, the binding pockets identified in these structures are identical, as shown in Figure 7-3. The same allosteric binding pocket is located between the A-domain and C-domain of each subunit of the tetramer. The binding locations of each amino acid is in the same direction. The carboxyl groups of the four amino acids are bound to the residues Asn70 and Arg106, and their amino groups to residues His464 and Ile469. In addition, the hydroxyl group of serine forms a hydrogen bond with Arg43 located on the N-terminal part, while other amino acids push the N-terminus away by approximately 6 Å, and thereby trigger the conformational transformation from the R to the T state.

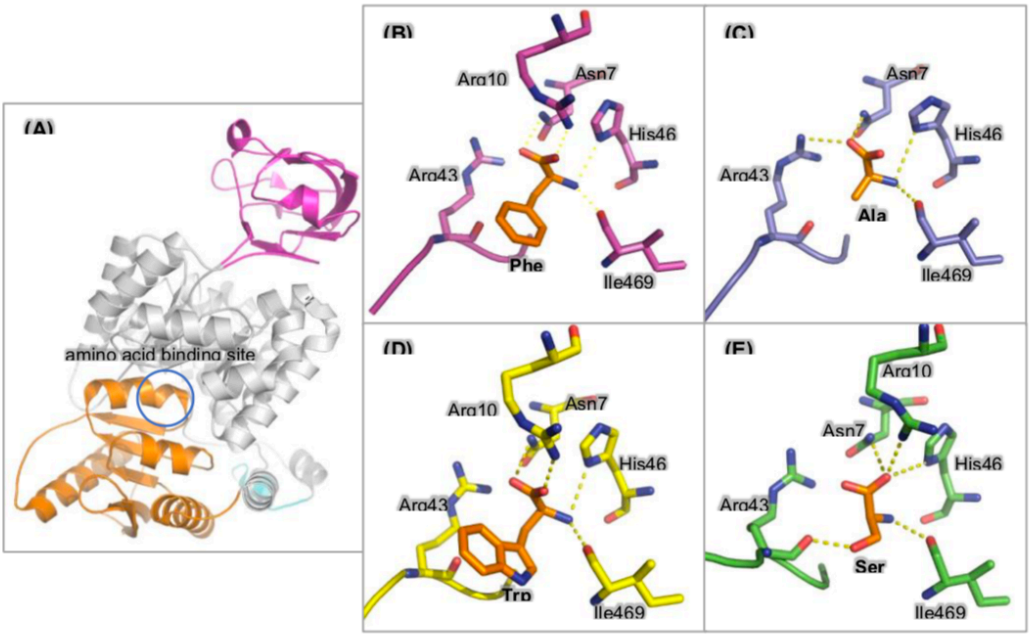

Figure 7-3. The binding of amino acids (Phe, Ala, Trp, Ser). (A) the architecture of one subunit of M2PYK. (B-E) structure of the amino acid binding site with four amino acids, respectively. The figure is provided by Dr Meng Yuan's unpublished work.

Compared with the structure from early reports shown in Figure 1-6, the **amino acid binding** pocket **identified in M2PYK is similar in the** other PYK isoforms and the residues in**volved in ligand binding** are identical. On the basis of the STD-NMR study and Dr Meng Yuan's structure information, we could hypothesi**ze** that the amino acid pocket**s** in all four PYK isoforms are conserved and might bind any amino acid. But the effect of the binding on **the** protein structure can change depending on the amino group interaction with the **residues in the** N-termin**al part**. Therefore the hypothesis of amino acid binding and regulation is that the conserved amino acid pocket is highly receptive to the binding of amino acids but the consequent new bond formation **at the C-C interface** and **con**forma**tional** change is more important in maintaining **the** oligomeric state. This also explains why one amino acids**'** (alanine as inhibitor) regulatory effect on M2PYK is changed **by** the presence of another amino acid (serine as activator).

There are many interesting aspects around the topic of the regulatory effects of metabolites on hPYKs which could be studied in future work. For example, the effect

of combinations of two activators (for example: serine and alanine with RPYK), one activator/inhibitor with one non-regulator (for example, serine with tyrosine on M2PYK) has not yet been studied. Because there are many amino acids and other metabolites present in cytosol, it is the combination effect of all regulators and non-regulators (they might also occupy the amino acid pocket) that will determine the enzymatic activity rather than any single amino acid. Secondly, the combination of amino acids (use phenylalanine as example) with the potent allosteric activator F-1,6-BP, binding in a different effector site, has not been studied so far. Phenylalanine pushes the tetrameric equilibrium from R state to the T state while F-1,6-BP leads to the opposite effect. The result might be that at certain F-1,6-BP concentration, amino acids (use phenylalanine as example) can up-regulate RPYK and down-regulate M2PYK but at a higher level of F-1,6-BP phenylalanine may lose its regulatory effects. Thirdly, attempts to generate crystal structures of RPYK co-crystalised with activators will be important to confirm the binding site and the mechanism of the regulations. Crystal structures of hPYKs with non-regulators will be useful to confirm if the universal binding exists.

7.2.3 Oligomeric structure of the PYK isoforms

Based on the study of analytical gel filtration, the oligomerisation states of M1PYK, RPYK, LPYK are predominantly tetramers in the PBS solution (also used in enzymatic tests) at low protein concentration (0.1 mg/ml). M2PYK solution contains both tetramers and monomers. The results of a related study by Dr Meng Yuan also suggested that M2PYK at certain protein concentration (0.1 mg/ml) equilibrates from tetramers to a mixture of monomer and tetramers. Here, we discuss the possible oligomeric states of each PYK isoform in the presence of different metabolites.

Based on the evidence from Chapter 3 and Chapter 4, M1PYK is always fully activated and was not regulated by the reducing reagent DTT, any of the metabolites listed in Table 9, or through long incubations at low concentration. The oligomeric state of M1PYK should be predominantly R-state tetramers in the presence of any ligand tested, reducing reagent, or at low concentration with long incubation time. The explanation to this phenomenon might be that M1PYK expressed in muscle cells with a constant high energy demand requires M1PYK's full activity under any condition. Although

the muscle cells always contain high amino acid concentration and alanine was reported to have an inhibitory effect on M1PYK (McCormack et al., 2017), the universal binding hypothesis suggests that alanine inhibition won't play an important role while in the presence of all other non-regulator binding amino acids.

For M2PYK, there might be three situations. It was shown that the protein is in R-state tetramers in the presence of F-1,6-BP, or other identified activators (Chapter 4) and in the presence of reducing reagent (Chapter 3). It is present as T-state tetramers in the presence of metabolites identified as inhibitors. It could also be seen to exist as monomers in the presence of T3 or at low protein concentration for a long incubation time.

For RPYK and LPYK, the oligomeric state of the protein is generally tetrameric. Activators and inhibitors push the equilibrium to one of R state and T state, respectively. Non-regulators might not lead to any conformational change.

7.2.4 The structure and physicochemical properties of the metabolites analysis

The amino acid regulation of PYKs might be related to their physiochemical properties such as hydrophobicity. In Figure 7-4, we demonstrated that a higher hydrophobicity value of the ligand has a higher inhibitory effect on M2PYK activity and strong activators have a low hydrophobicity value. As shown in Figure 1-6 and Figure 7-3, the amino acid pocket is conserved and the residues in the pocket at different isoforms are identical, but Phe with a high hydrophobicity pushes the N-terminus away and changes the conformational state of the tetramer, while serine with low hydrophobicity forms a hydrogen bond with Arg43 which has lowest hydrophobicity value in the table.

The observed relationship between hydrophobicity and enzymatic regulation is limited however as it cannot be applied to amino acids such as Leu and Arg and for RPYK. To expand this hypothesis, crystal structure information of other ligands with M2PYK or RPYK will be useful. Another factor in this ligand binding and regulation mechanism might be the size of the amino acid.

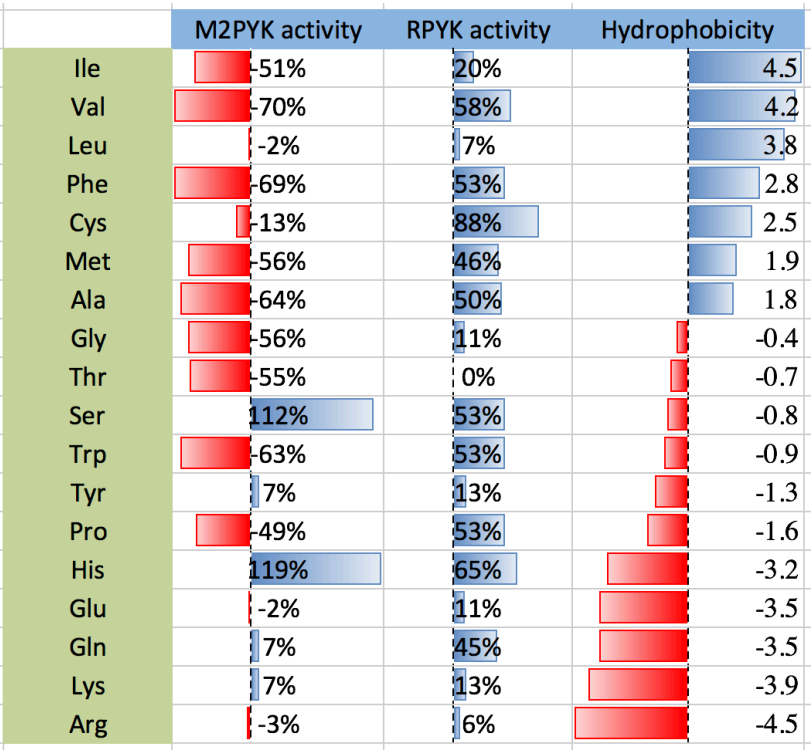

Figure 7-4. The amino acids hydrophobicity values compared with M2PYK and RPYK activities. The activity data are from Table 9. The hydrophobicity data are from the web: (https://www.cgl.ucsf.edu/chimera/docs/UsersGuide/midas/hydrophob.html#dnote)

7.2.5 Possible biological implications

M1PYK: The fully activated state of M1PYK exposed to any amino acid suggests that any change in amino acid concentrations won't affect its activity. The biological function of M1PYK is simple and always fully active.

M2PYK: The enzymatic regulation of M2PYK detected in Chapter 4 is summarized in Figure 7-5. Interestingly, all activators come from upstream – or upstream branches - in the pathway (F-1,6-BP, serine, glycine) or from uptake from outside the cytosol (histidine). The inhibitors come from downstream branches of the pathway (alanine) or from nutrient supply as dietary essential amino acids (proline, threonine, methionine, tryptophan, phenylalanine). In 2012, Chaneton demonstrated that in cancer cells serine is a natural regulator and described a rheostat-like mechanism between M2PYK regulation and the serine biosynthesis. Glycine is also derived from the serine

biosynthesis pathway and has an activation effect on M2PYK. The rheostat-like mechanism might be upregulated by a combination effect of serine and glycine. In the alanine biosynthesis pathway, alanine transaminase catalyses pyruvate to alanine, and its activity is normally elevated in tumour cells (Chougule, Hussain, & Agarwal, 2008). This phenomenon might form another rheostat-like mechanism between alanine biosynthesis and M2PYK regulation in normal cells but be rewired in tumour cell to a high alanine biosynthesis and low PYK activity state. Moreover, the explanation of the inhibition by GMP (guanosine monophosphate) and AMP (adenosine monophosphate) might be that the high DNA and RNA biosynthesis rates in fast proliferating cells result in suppression of M2PYK activity.

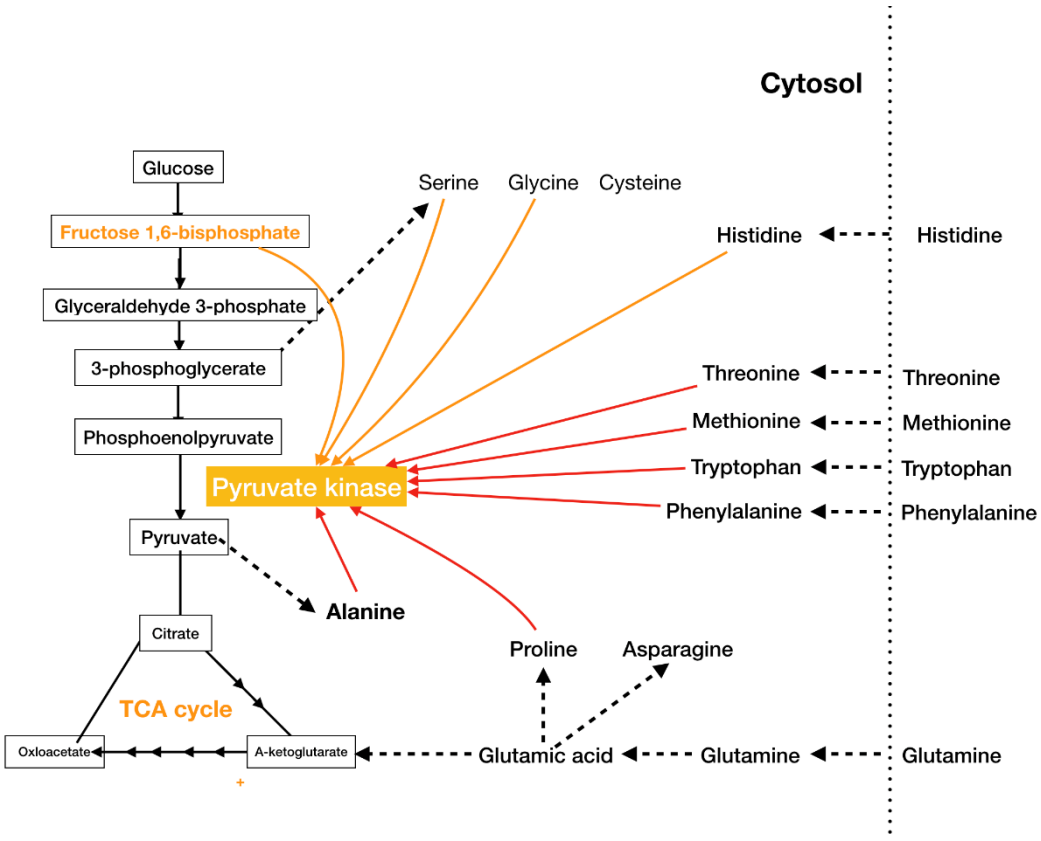

Figure 7-5. The regulation of M2PYK by metabolic amino acids in the cytosol.

LPYK: The liver type PYK is less active compared with M1PYK and is not strongly regulated by any amino acid or metabolites with only F-1,6-BP having an activation effect. The major functions of hepatic cells in glucose related biological processes are: glycogenesis when there are high blood glucose levels, glycogenosis when blood levels are low, gluconeogenesis when there are low blood glucose level and hepatic

glycogen reserves become exhausted. The gluconeogenesis pathway and glycolysis pathway are combined in Figure 7-6. The steps from pyruvate to PEP and F-1,6-BP to F6P are separate in both pathways, involving distinct enzymes, so it might be feasible that no F-1,6-BP accumulation occurs in gluconeogenesis. This could explain why LPYK could only be activated by F-1,6-BP as its activity could only be useful when the carbon flux follows glycolysis to generate ATP. Activity would remain low when gluconeogenesis occurs with possibly no F-1,6-BP accumulation in the cytosol.

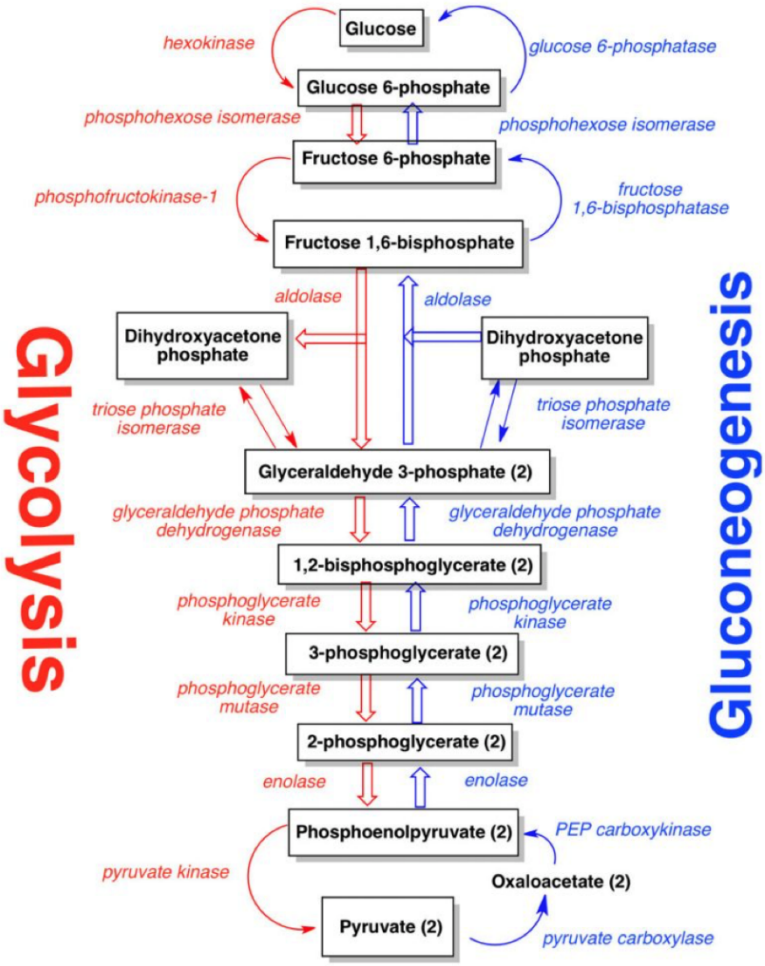

Figure 7-6. Combination diagram of the pathways of glycolysis and gluconeogenesis.

RPYK: RPYK normally has low activity levels and could be regulated by many amino acids and F-1,6-BP. This might be explained by the unique biological environment in erythrocytes. The uptake of amino acids by erythrocytes after intestinal absorption could elevate the activator concentrations including alanine (from 0.5-0.7 mM), histidine (from 0.08-0.15 mM), isoleucine (from 0.08-0.23 mM) with glutamine

maintaining higher concentration at 0.55 mM (Agli et al., 1998). Based on the results from Chapter Figure 4-17, the AC_{50} of alanine, histidine, isoleucine, glutamine is estimated to be 1.0 mM, 0.1mM, 1.0 mM, 10 mM. Only the AC_{50} of histidine fits into the erythrocyte amino acid concentration range. When erythrocytes absorb glucose or amino acids to reach a high intracellular concentration, RPYK is activated and generates more pyruvate, raising the ATP/ADP ratio. In other biological conditions, the enzyme activity remains low. Further work on amino acid regulation of RPYK activity and this regulatory effect on the biological function of erythrocytes might require further studies to test the glycolysis rate at different amino acid concentrations in erythrocytes.

References

Agli, A. N., Schaefer, A., Geny, B., Piquard, F., & Haberey, P. (1998). Erythrocytes participate significantly in blood transport of amino acids during the post absorptive state in normal humans. *European Journal of Applied Physiology and Occupational Physiology*. https://doi.org/10.1007/s004210050452

Alberghina, L., & Gaglio, D. (2014). Redox control of glutamine utilization in cancer. *Cell Death and Disease*. https://doi.org/10.1038/cddis.2014.513

Anastasiou, D., Poulogiannis, G., Asara, J. M., Boxer, M. B., Jiang, J. K., Shen, M., … Cantley, L. C. (2011). Inhibition of pyruvate kinase M2 by reactive oxygen species contributes to cellular antioxidant responses. *Science*. https://doi.org/10.1126/science.1211485

Anastasiou, D., Yu, Y., Israelsen, W. J., Jiang, J. K., Boxer, M. B., Hong, B. S., … Vander Heiden, M. G. (2012). Pyruvate kinase M2 activators promote tetramer formation and suppress tumorigenesis. *Nature Chemical Biology*. https://doi.org/10.1038/nchembio.1060

Anderson, W. A., & Freeman, R. (1962). Influence of a second radiofrequency field on high-resolution nuclear magnetic resonance spectra. *The Journal of Chemical Physics*. https://doi.org/10.1063/1.1732980

Ashizawa, K., McPhie, P., Lin, K.-H., & Cheng, S.-Y. (1991). An in Vitro Novel Mechanism of Regulating the Activity of Pyruvate Kinase M<inf>2</inf> by Thyroid Hormone and Fructose 1,6-Bisphosphate. *Biochemistry*. https://doi.org/10.1021/bi00243a010

Ayi, K., Min-Oo, G., Serghides, L., Crockett, M., Kirby-Allen, M., Quirt, I., … Kain, K. C. (2008). Pyruvate kinase deficiency and malaria. *N Engl J Med*.

https://doi.org/10.1056/NEJMoa072464

Bakker, B. M., Michels, P. A. M., Opperdoes, F. R., & Westerhoff, H. V. (1997). Glycolysis in bloodstream form Trypanosoma brucei can be understood in terms of the kinetics of the glycolytic enzymes. *Journal of Biological Chemistry*. https://doi.org/10.1074/jbc.272.6.3207

Benesch, R., & Benesch, R. E. (1967). The effect of organic phosphates from the human erythrocyte on the allosteric properties of hemoglobin. *Biochemical and Biophysical Research Communications*. https://doi.org/10.1016/0006-291X(67)90228-8

Bergström, J., Alvestrand, A., & Fürst, P. (1990). Plasma and muscle free amino acids in maintenance hemodialysis patients without protein malnutrition. *Kidney International*. https://doi.org/10.1038/ki.1990.174

Brimacombe, K. R., Anastasiou, D., Hong, B. S., Tempel, W., Dimov, S., Veith, H., … Boxer, M. B. (2010). ML285 affects reactive oxygen species' inhibition of pyruvate kinase M2. *Probe Reports from the NIH Molecular Libraries Program*.

Brodzki, A., Tatara, M. R., Pasternak, K., Rózańska, D., & Szponder, T. (2005). Free amino acids in skin neoplastic tissues and serum in dogs. *Bulletin of the Veterinary Institute in Pulawy*.

Butterfield, D. A., & Sultana, R. (2007). Redox proteomics identification of oxidatively modified brain proteins in Alzheimer's disease and mild cognitive impairment: Insights into the progression of this dementing disorder. In *Journal of Alzheimer's Disease*. https://doi.org/10.3233/JAD-2007-12107

Cairns, R. A., Harris, I. S., & Mak, T. W. (2011). Regulation of cancer cell metabolism. *Nature Reviews Cancer*. https://doi.org/10.1038/nrc2981

Canepa, A., Filho, J. C. D., Gutierrez, A., Carrea, A., Forsberg, A.-M., Nilsson, E., … Bergström, J. (2002). Free amino acids in plasma, red blood cells, polymorphonuclear leukocytes, and muscle in normal and uraemic children. *Nephrology, Dialysis, Transplantation : Official Publication of the European Dialysis and Transplant Association - European Renal Association*.

Carminatti, H., Jiménez de Asúa, L., Leiderman, B., & Rozengurt, E. (1971). Allosteric properties of skeletal muscle pyruvate kinase. *Journal of Biological Chemistry*.

Cesaratto, L., Vascotto, C., Calligaris, S., & Tell, G. (2004). The importance of redox state in liver damage. *Annals of Hepatology : Official Journal of the Mexican Association of Hepatology*.

Chaneton, B., & Gottlieb, E. (2012). Rocking cell metabolism: Revised functions of the key glycolytic regulator PKM2 in cancer. *Trends in Biochemical Sciences*. https://doi.org/10.1016/j.tibs.2012.04.003

Chaneton, B., Hillmann, P., Zheng, L., Martin, A. C. L., Maddocks, O. D. K., Chokkathukalam, A., … Gottlieb, E. (2012). Serine is a natural ligand and allosteric activator of pyruvate kinase M2. *Nature*. https://doi.org/10.1038/nature11540

Changou, C. A., Chen, Y.-R., Xing, L., Yen, Y., Chuang, F. Y. S., Cheng, R. H., … Kung, H.-J. (2014). Arginine starvation-associated atypical cellular death involves mitochondrial dysfunction, nuclear DNA leakage, and chromatin autophagy. *Proceedings of the National Academy of Sciences*. https://doi.org/10.1073/pnas.1404171111

Chen, J., Xie, J., Jiang, Z., Wang, B., Wang, Y., & Hu, X. (2011). Shikonin and its analogs inhibit cancer cell glycolysis by targeting tumor pyruvate kinase-M2. *Oncogene*. https://doi.org/10.1038/onc.2011.137

Cheng, F., Wang, Z., Huang, Y., Duan, Y., & Wang, X. (2015). Investigation of salivary free amino acid profile for early diagnosis of breast cancer with ultra performance liquid chromatography-mass spectrometry. *Clinica Chimica Acta*. https://doi.org/10.1016/j.cca.2015.05.008

Chiarugi, P., Fiaschi, T., Taddei, M. L., Talini, D., Giannoni, E., Raugei, G., & Ramponi, G. (2001). Two Vicinal Cysteines Confer a Peculiar Redox Regulation to Low Molecular Weight Protein Tyrosine Phosphatase in Response to Platelet-derived Growth Factor Receptor Stimulation. *Journal of Biological Chemistry*. https://doi.org/10.1074/jbc.M102302200

Chougule, A., Hussain, S., & Agarwal, D. (2008). Prognosis and diagnostic value of serum pseudocholinesterase, serum aspartate transaminase, and serum alinine transaminase in malignancies treated by radiotherapy. *Journal of Cancer Research Terapy*.

Christofk, H. R., Vander Heiden, M. G., Wu, N., Asara, J. M., & Cantley, L. C. (2008). Pyruvate kinase M2 is a phosphotyrosine-binding protein. *Nature*. https://doi.org/10.1038/nature06667

Crabtree, H. G. (1929). Observations on the carbohydrate metabolism of tumours. *The Biochemical Journal*. https://doi.org/10.1042/bj0230536

Cumming, R. C., Andon, N. L., Haynes, P. A., Park, M., Fischer, W. H., & Schubert, D. (2004). Protein disulfide bond formation in the cytoplasm during oxidative stress. *Journal of Biological Chemistry*. https://doi.org/10.1074/jbc.M312267200

David, C. J., Chen, M., Assanah, M., Canoll, P., & Manley, J. L. (2010). HnRNP proteins controlled by c-Myc deregulate pyruvate kinase mRNA splicing in cancer. *Nature*. https://doi.org/10.1038/nature08697

Dayton, T. L., Gocheva, V., Miller, K. M., Israelsen, W. J., Bhutkar, A., Clish, C. B., … Vander Heiden, M. G. (2016). Germline loss of PKM2 promotes

metabolic distress and hepatocellular carcinoma. *Genes and Development*. https://doi.org/10.1101/gad.278549.116

Desai, S., Ding, M., Wang, B., Lu, Z., Zhao, Q., Shaw, K., … Yao, J. (2013). Tissue-specific isoform switch and DNA hypomethylation of the pyruvate kinase PKM gene in human cancers. *Oncotarget*. https://doi.org/10.18632/oncotarget.1159

Discher, D. J., Bishopric, N. H., Wu, X., Peterson, C. A., & Webster, K. A. (1998). Hypoxia regulates β-enolase and pyruvate kinase-M promoters by modulating Sp1/Sp3 binding to a conserved GC element. *Journal of Biological Chemistry*. https://doi.org/10.1074/jbc.273.40.26087

Dombrauckas, J. D., Santarsiero, B. D., & Mesecar, A. D. (2005). Structural basis for tumor pyruvate kinase M2 allosteric regulation and catalysis. *Biochemistry*. https://doi.org/10.1021/bi0474923

Dyer, K. N., Hammel, M., Rambo, R. P., Tsutakawa, S. E., Rodic, I., Classen, S., … Hura, G. L. (2014). High-throughput SAXS for the characterization of biomolecules in solution: A practical approach. *Methods in Molecular Biology*. https://doi.org/10.1007/978-1-62703-691-7_18

Eigenbrodt, E., Reinacher, M., Scheefers-Borchel, U., Scheefers, H., & Friis, R. (1992). Double role for pyruvate kinase type M2 in the expansion of phosphometabolite pools found in tumor cells. *Critical Reviews in Oncogenesis*.

Erickson, J. W., & Cerione, R. a. (2010). Glutaminase: a hot spot for regulation of cancer cell metabolism? *Oncotarget*. https://doi.org/10.1016/j.bbi.2008.05.010

Fenton, A. W. (2012). Identification of allosteric-activating drug leads for human liver pyruvate kinase. *Methods in Molecular Biology*. https://doi.org/10.1007/978-1-61779-334-9_20

Fermo, E., Bianchi, P., Chiarelli, L. R., Cotton, F., Vercellati, C., Writzl, K., … Zanella, A. (2005). Red cell pyruvate kinase deficiency: 17 New mutations of the PK-LR gene. *British Journal of Haematology*. https://doi.org/10.1111/j.1365-2141.2005.05520.x

FRAME, E. G. (1958). The levels of individual free amino acids in the plasma of normal man at various intervals after a high-protein meal. *The Journal of Clinical Investigation*. https://doi.org/10.1172/JCI103763

Gaascht, F., Teiten, M. H., Cerella, C., Dicato, M., Bagrel, D., & Diederich, M. (2014). Plumbagin modulates leukemia cell redox status. *Molecules*. https://doi.org/10.3390/molecules190710011

Geck, R. C., & Toker, A. (2016). Nonessential amino acid metabolism in breast cancer. *Advances in Biological Regulation*. https://doi.org/10.1016/j.jbior.2016.01.001

Gravel, S. P., Hulea, L., Toban, N., Birman, E., Blouin, M. J., Zakikhani, M., …

Pollak, M. (2014). Serine deprivation enhances antineoplastic activity of biguanides. *Cancer Research*. https://doi.org/10.1158/0008-5472.CAN-14-2643-T

Guo, C., Linton, A., Jalaie, M., Kephart, S., Ornelas, M., Pairish, M., … Xie, Z. (2013). Discovery of 2-((1H-benzo[d]imidazol-1-yl)methyl)-4H-pyrido[1,2-a]pyrimidin-4-ones as novel PKM2 activators. *Bioorganic & Medicinal Chemistry Letters*. https://doi.org/10.1016/j.bmcl.2013.03.090

Guo, D., Gu, J., Jiang, H., Ahmed, A., Zhang, Z., & Gu, Y. (2016). Inhibition of pyruvate kinase M2 by reactive oxygen species contributes to the development of pulmonary arterial hypertension. *Journal of Molecular and Cellular Cardiology*. https://doi.org/10.1016/j.yjmcc.2016.01.009

Gupta, V., & Bamezai, R. N. K. (2010). Human pyruvate kinase M2: A multifunctional protein. *Protein Science*. https://doi.org/10.1002/pro.505

Hanahan, D., & Weinberg, R. A. (2011). Hallmarks of cancer: The next generation. *Cell*. https://doi.org/10.1016/j.cell.2011.02.013

Heiden, M. G. Vander, Cantley, L. C., & Thompson, C. B. (2009). Understanding the warburg effect: The metabolic requirements of cell proliferation. *Science*. https://doi.org/10.1126/science.1160809

Hitosugi, T., Kang, S., Vander Heiden, M. G., Chung, T. W., Elf, S., Lythgoe, K., … Chen, J. (2009). Tyrosine phosphorylation inhibits PKM2 to promote the warburg effect and tumor growth. *Science Signaling*. https://doi.org/10.1126/scisignal.2000431

Iovine, B., Oliviero, G., Garofalo, M., Orefice, M., Nocella, F., Borbone, N., … Bevilacqua, M. A. (2014). The anti-proliferative effect of L-carnosine correlates with a decreased expression of hypoxia inducible factor 1 alpha in human colon cancer cells. *PLoS ONE*. https://doi.org/10.1371/journal.pone.0096755

Iqbal, M. A., Siddiqui, F. A., Gupta, V., Chattopadhyay, S., Gopinath, P., Kumar, B., … Bamezai, R. N. K. (2013). Insulin enhances metabolic capacities of cancer cells by dual regulation of glycolytic enzyme pyruvate kinase M2. *Molecular Cancer*. https://doi.org/10.1186/1476-4598-12-72

Israelsen, W. J., & Vander Heiden, M. G. (2015). Pyruvate kinase: Function, regulation and role in cancer. *Seminars in Cell & Developmental Biology*. https://doi.org/10.1016/j.semcdb.2015.08.004

Jacques, D. A., & Trewhella, J. (2010). Small-angle scattering for structural biology - Expanding the frontier while avoiding the pitfalls. *Protein Science*. https://doi.org/10.1002/pro.351

Jain, M., Nilsson, R., Sharma, S., Madhusudhan, N., Kitami, T., Souza, A. L., … Laird, N. (2012). Metabolite profiling identifies a key role for glycine in rapid cancer cell proliferation. *Science (New York, N.Y.)*.

https://doi.org/10.1126/science.1218595

Jiang, J. K., Boxer, M. B., Heiden, M. G. Vander, Shen, M., Skoumbourdis, A. P., Southall, N., … Thomas, C. J. (2010). Evaluation of thieno[3,2-b]pyrrole[3,2-d]pyridazinones as activators of the tumor cell specific M2 isoform of pyruvate kinase. *Bioorg Med Chem Lett*. https://doi.org/10.1016/j.bmcl.2010.04.015

Jiang, Z. F., Wang, M., Xu, J. L., & Ning, Y. J. (2017). Hypoxia promotes mitochondrial glutamine metabolism through HIF1α-GDH pathway in human lung cancer cells. *Biochemical and Biophysical Research Communications*. https://doi.org/10.1016/j.bbrc.2017.01.015

Jurica, M. S., Mesecar, A., Heath, P. J., Shi, W., Nowak, T., & Stoddard, B. L. (1998). The allosteric regulation of pyruvate kinase by fructose-1,6-bisphosphate. *Structure*. https://doi.org/10.1016/S0969-2126(98)00021-5

Kato, H., Fukuda, T., Parkison, C., McPhie, P., & Cheng, S. Y. (1989). Cytosolic thyroid hormone-binding protein is a monomer of pyruvate kinase. *Proc. Natl. Acad. Sci. USA*. https://doi.org/10.1073/pnas.87.4.1625d

Keller, K. E., Tan, I. S., & Lee, Y. S. (2012). SAICAR stimulates pyruvate kinase isoform M2 and promotes cancer cell survival in glucose-limited conditions. *Science*. https://doi.org/10.1126/science.1224409

Kim, D. J., Park, Y. S., Kim, N. D., Min, S. H., You, Y.-M., Jung, Y., … Yeom, Y. Il. (2015). A novel pyruvate kinase M2 activator compound that suppresses lung cancer cell viability under hypoxia. *Molecules and Cells*. https://doi.org/10.14348/molcells.2015.2314

Koshland, D. E., Nemethy, J. G., & Filmer, D. (1966). Comparison of Experimental Binding Data and Theoretical Models in Proteins Containing Subunits. *Biochemistry*. https://doi.org/10.1021/bi00865a047

Kuhn, V., Diederich, L., Keller, T. C. S., Kramer, C. M., Lückstädt, W., Panknin, C., … Cortese-Krott, M. M. (2017). Red Blood Cell Function and Dysfunction: Redox Regulation, Nitric Oxide Metabolism, Anemia. *Antioxidants & Redox Signaling*. https://doi.org/10.1089/ars.2016.6954

Kung, C., Hixon, J., Choe, S., Marks, K., Gross, S., Murphy, E., … Dang, L. (2012). Small molecule activation of pkm2 in cancer cells induces serine auxotrophy. *Chemistry and Biology*. https://doi.org/10.1016/j.chembiol.2012.07.021

Larsen, T. M., Laughlin, L. T., Holden, H. M., Rayment, I., & Reed, G. H. (1994). Structure of Rabbit Muscle Pyruvate Kinase Complexed with Mn2+, K+, and Pyruvate. *Biochemistry*. https://doi.org/10.1021/bi00186a033

Lefauconnier, J. M., Portemer, C., & Chatagner, F. (1976). Free amino acids and related substances in human glial tumours and in fetal brain: comparison with normal adult brain. *Brain Research*. https://doi.org/10.1016/0006-8993(76)90559-X

Llorente, P., Marco, R., & Sols, A. (1970). Regulation of Liver Pyruvate Kinase and the Phosphoenolpyruvate Crossroads. *European Journal of Biochemistry*. https://doi.org/10.1111/j.1432-1033.1970.tb00897.x

Lunt, S. Y., Muralidhar, V., Hosios, A. M., Israelsen, W. J., Gui, D. Y., Newhouse, L., … Vander Heiden, M. G. (2015). Pyruvate kinase isoform expression alters nucleotide synthesis to impact cell proliferation. *Molecular Cell*. https://doi.org/10.1016/j.molcel.2014.10.027

Lv, L., Li, D., Zhao, D., Lin, R., Chu, Y., Zhang, H., … Lei, Q. Y. (2011). Acetylation Targets the M2 Isoform of Pyruvate Kinase for Degradation through Chaperone-Mediated Autophagy and Promotes Tumor Growth. *Molecular Cell*. https://doi.org/10.1016/j.molcel.2011.04.025

Maeba, P., & Sanwal, B. D. (1968). The regulation of pyruvate kinase of Escherichia coli by fructose diphosphate and adenylic acid. *Journal of Biological Chemistry*.

Marie, J., Buc, H., Simon, M. P., & Kahn, A. (1980). Phosphorylation of human erythrocyte pyruvate kinase by soluble cyclic-AMP-dependent protein kinases. Comparison with human liver L-type enzyme. *European Journal of Biochemistry / FEBS*. https://doi.org/10.1111/j.1432-1033.1980.tb04718.x

Mayer, M., & Meyer, B. (2001). Group epitope mapping by saturation transfer difference NMR to identify segments of a ligand in direct contact with a protein receptor. *Journal of the American Chemical Society*. https://doi.org/10.1021/ja0100120

Mazurek, S. (2011). Pyruvate kinase type M2: A key regulator of the metabolic budget system in tumor cells. *International Journal of Biochemistry and Cell Biology*. https://doi.org/10.1016/j.biocel.2010.02.005

McCormack, W. G., Cooke, J. P., O'Connor, W. T., & Jakeman, P. M. (2017). Dynamic measures of skeletal muscle dialysate and plasma amino acid concentration in response to exercise and nutrient ingestion in healthy adult males. *Amino Acids*. https://doi.org/10.1007/s00726-016-2343-8

Monod, J., Wyman, J., & Changeux, J. P. (1965). On the nature of allosteric transitions: A plausible model. *Journal of Molecular Biology*. https://doi.org/10.1016/S0022-2836(65)80285-6

Morgan, H. P., McNae, I. W., Nowicki, M. W., Hannaert, V., Michels, P. A. M., Fothergill-Gilmore, L. A., & Walkinshaw, M. D. (2010). Allosteric mechanism of pyruvate kinase from Leishmania mexicana uses a rock and lock model. *Journal of Biological Chemistry*. https://doi.org/10.1074/jbc.M109.079905

Morgan, H. P., O'Reilly, F. J., Wear, M. A., O'Neill, J. R., Fothergill-Gilmore, L. A., Hupp, T., & Walkinshaw, M. D. (2013). M2 pyruvate kinase provides a mechanism for nutrient sensing and regulation of cell proliferation. *Proceedings of the National Academy of Sciences*. https://doi.org/10.1073/pnas.1217157110

Morgan, H. P., O'Reilly, F. J., Wear, M. a, O'Neill, J. R., Fothergill-Gilmore, L. a, Hupp, T., & Walkinshaw, M. D. (2013). M2 pyruvate kinase provides a mechanism for nutrient sensing and regulation of cell proliferation. *Proceedings of the National Academy of Sciences of the United States of America*, *110*(15), 5881–5886. https://doi.org/10.1073/pnas.1217157110

Munnich, A., Marie, J., Reach, G., Vaulont, S., Simon, M. P., & Kahn, A. (1984). In vivo hormonal control of L-type pyruvate kinase gene expression. Effects of glucagon, cyclic AMP, insulin, cortisone, and thyroid hormones on the dietary induction of mRNAs in the liver. *Journal of Biological Chemistry*.

Nakatsu, D., Horiuchi, Y., Kano, F., Noguchi, Y., Sugawara, T., Takamoto, I., … Murata, M. (2015). l-cysteine reversibly inhibits glucose-induced biphasic insulin secretion and ATP production by inactivating PKM2. *Proceedings of the National Academy of Sciences*. https://doi.org/10.1073/pnas.1417197112

Noguchi, T., Inoue, H., & Tanaka, T. (1986). The M1- and M2-type isozymes of rat pyruvate kinase are produced from the same gene by alternative RNA splicing. *Journal of Biological Chemistry*.

Noguchi, T., Yamada, K., Inoue, H., Matsuda, T., & Tanaka, T. (1987). The L- and R-type isozymes of rat pyruvate kinase are produced from a single gene by use of different promoters. *Journal of Biological Chemistry*.

Parnell, K. M., Foulks, J. M., Nix, R. N., Clifford, A., Bullough, J., Luo, B., … Kanner, S. B. (2013). Pharmacologic Activation of PKM2 Slows Lung Tumor Xenograft Growth. *Molecular Cancer Therapeutics*. https://doi.org/10.1158/1535-7163.MCT-13-0026

Prasannan, C. B., Tang, Q., & Fenton, A. W. (2012). Allosteric regulation of human liver pyruvate kinase by peptides that mimic the phosphorylated/dephosphorylated N-terminus. *Methods in Molecular Biology*. https://doi.org/10.1007/978-1-61779-334-9_18

Rozengurt, E., de Asúa, L. J., & Carminatti, H. (1970). Allosteric inhibition of muscle pyruvate kinase by phenylalanine. *FEBS Letters*. https://doi.org/10.1016/0014-5793(70)80549-X

Skou, S., Gillilan, R. E., & Ando, N. (2014). Synchrotron-based small-angle X-ray scattering of proteins in solution. *Nature Protocols*. https://doi.org/10.1038/nprot.2014.116

Snyder, L. M., & Reddy, W. J. (1970). Mechanism of action of thyroid hormones on erythrocyte 2,3-diphosphoglyceric acid synthesis. *The Journal of Clinical Investigation*. https://doi.org/10.1172/JCI106419

Sun, Y., Zhao, X., Zhou, Y., & Hu, Y. (2012). MiR-124, miR-137 and miR-340 regulate colorectal cancer growth via inhibition of the Warburg effect. *Oncology Reports*. https://doi.org/10.3892/or.2012.1958

Tanaka, T., Harano, Y., Morimura, H., & Mori, R. (1965). Evidence for the presence of two types of pyruvate kinase in rat liver. *Biochemical and Biophysical Research Communications*. https://doi.org/10.1016/0006-291X(65)90425-0

Thiele, I., Swainston, N., Fleming, R. M. T., Hoppe, A., Sahoo, S., Aurich, M. K., … Palsson, B. O. (2013). A community-driven global reconstruction of human metabolism. *Nature Biotechnology*. https://doi.org/10.1038/nbt.2488

Tilton, W. M., Seaman, C., Carriero, D., & Piomelli, S. (1991). Regulation of glycolysis in the erythrocyte: role of the lactate/pyruvate and NAD/NADH ratios. *The Journal of Laboratory and Clinical Medicine*.

Trachootham, D., Lu, W., Ogasawara, M. A., Nilsa, R.-D. V., & Huang, P. (2008). Redox regulation of cell survival. *Antioxidants & Redox Signaling*. https://doi.org/10.1089/ars.2007.1957

Valentini, G., Chiarelli, L., Fortin, R., Speranza, M. L., Galizzi, A., & Mattevi, A. (2000). The allosteric regulation of pyruvate kinase. *The Journal of Biological Chemistry*. https://doi.org/10.1074/jbc.M001870200

Valentini, G., Chiarelli, L. R., Fortin, R., Dolzan, M., Galizzi, A., Abraham, D. J., … Mattevi, A. (2002). Structure and function of human erythrocyte pyruvate kinase. Molecular basis of nonspherocytic hemolytic anemia. *The Journal of Biological Chemistry*. https://doi.org/10.1074/jbc.M202107200

van Zwieten, R., van Oirschot, B. A., Veldthuis, M., Dobbe, J. G., Streekstra, G. J., van Solinge, W. W., … van Wijk, R. (2015). Partial pyruvate kinase deficiency aggravates the phenotypic expression of band 3 deficiency in a family with hereditary spherocytosis. *American Journal of Hematology*. https://doi.org/10.1002/ajh.23899

Vander Heiden, M. G., Christofk, H. R., Schuman, E., Subtelny, A. O., Sharfi, H., Harlow, E. E., … Cantley, L. C. (2010). Identification of small molecule inhibitors of pyruvate kinase M2. *Biochemical Pharmacology*. https://doi.org/10.1016/j.bcp.2009.12.003

Vander Heiden, M. G., Locasale, J. W., Swanson, K. D., Sharfi, H., Heffron, G. J., Amador-Noguez, D., … Cantley, L. C. (2010). Evidence for an alternative glycolytic pathway in rapidly proliferating cells. *Science*. https://doi.org/10.1126/science.1188015

Vaulont, S., Munnich, A., Decaux, J. F., & Kahn, A. (1986). Transcriptional and post-transcriptional regulation of L-type pyruvate kinase gene expression in rat liver. *Journal of Biological Chemistry*.

Venkitakrishnan, R. P., Benard, O., Max, M., Markley, J. L., & Assadi-Porter, F. M. (2012). Use of NMR Saturation Transfer Difference Spectroscopy to Study Ligand Binding to Membrane Proteins. In *Membrane Protein Structure and Dynamics*. https://doi.org/10.1007/978-1-62703-023-6_4

Wan, J., Ristenpart, W. D., & Stone, H. A. (2008). Dynamics of shear-induced ATP release from red blood cells. *Proceedings of the National Academy of Sciences*. https://doi.org/10.1073/pnas.0805779105

Wang, R., Tan, J., Zhang, G., Zheng, W., & Li, C. (2017). Risk factors of hepatic dysfunction in patients with Graves' hyperthyroidism and the efficacy of 131 iodine treatment. *Medicine (United States)*. https://doi.org/10.1097/MD.0000000000006035

Warburg, O., Wind, F., & Negelein, E. (1927). The metabolism of tumors in the body. English reprint. *The Journal of General Physiology*. https://doi.org/10.1097/00000441-193107000-00022

Warner, S. L., Carpenter, K. J., & Bearss, D. J. (2014). Activators of PKM2 in cancer metabolism. *Future Medicinal Chemistry*. https://doi.org/10.4155/fmc.14.70

Williams, R., Holyoak, T., McDonald, G., Gui, C., & Fenton, A. W. (2006). Differentiating a ligand's chemical requirements for allosteric interactions from those for protein binding. Phenylalanine inhibition of pyruvate kinase. *Biochemistry*. https://doi.org/10.1021/bi0524262

Wong, T. S., Liu, X. B., Ho, A. C. W., Yuen, A. P. W., Ng, R. W. M., & Wei, W. I. (2008). Identification of pyruvate kinase type M2 as potential oncoprotein in squamous cell carcinoma of tongue through microRNA profiling. *International Journal of Cancer*. https://doi.org/10.1002/ijc.23583

Yacovan, A., Ozeri, R., Kehat, T., Mirilashvili, S., Sherman, D., Aizikovich, A., … Becker, O. M. (2012). 1-(sulfonyl)-5-(arylsulfonyl)indoline as activators of the tumor cell specific M2 isoform of pyruvate kinase. *Bioorganic and Medicinal Chemistry Letters*. https://doi.org/10.1016/j.bmcl.2012.08.054

Yamada, K., Tanaka, T., Miyamoto, K., & Noguchi, T. (2000). Sp family members and nuclear factor-Y cooperatively stimulate transcription from the rat pyruvate kinase M gene distal promoter region via their direct interactions. *Journal of Biological Chemistry*. https://doi.org/10.1074/jbc.M001543200

Yang, W., & Lu, Z. (2013). Nuclear PKM2 regulates the Warburg effect. *Cell Cycle*. https://doi.org/10.4161/cc.26182

Zanella, A., & Bianchi, P. (2000). Red cell pyruvate kinase deficiency: from genetics to clinical manifestations. *Best Practice & Research Clinical Haematology*. https://doi.org/10.1053/beha.1999.0057

Zaroulis, C. G., Kourides, I. A., & Valeri, C. R. (1978). Red cell 2,3-diphosphoglycerate and oxygen affinity of hemoglobin in patients with thyroid disorders. *Blood*.

Zhang, J., Pavlova, N. N., & Thompson, C. B. (2017). Cancer cell metabolism: the essential role of the nonessential amino acid, glutamine. *The EMBO Journal*. https://doi.org/10.15252/embj.201696151